Energy conservation in aceticlastic methanogenic archaea and the human gut archaeon *Methanomassiliicoccus luminyensis*

Dissertation

zur

Erlangung des Doktorgrades (Dr. rer. nat.)
der
Mathematisch-Naturwissenschaftlichen Fakultät
der
Rheinischen Friedrich-Wilhelms-Universität Bonn

vorgelegt von

Stefanie Berger
aus Freising

Bonn, 26.02.2015

Angefertigt mit Genehmigung der Mathematisch-Naturwissenschaftlichen

Fakultät der Rheinischen Friedrich-Wilhelms-Universität Bonn

Erstgutachten: Prof. Dr. Uwe Deppenmeier
Zweitgutachten: apl. Prof. Dr. Christiane Dahl
Tag der mündlichen Prüfung: 12.06.2015
Erscheinungsjahr: 2015

Parts of this thesis have already been published:

Berger, S.; Welte, C.; Deppenmeier, U. (2012). Acetate activation in *Methanosaeta thermophila*: characterization of the key enzymes pyrophosphatase and acetyl-CoA synthetase. *Archaea* 2012: 315153

TABLE OF CONTENTS

ABBREVIATION LIST

Acetyl-CoA	Acetyl-coenzyme A
ACS	Acetyl-CoA synthetase
ADP	Adenosine diphosphate
AMP	Adenosine monophosphate
Amp	Ampicillin
APS	Ammonium persulfate
ATP	Adenosine triphosphate
BCA	Bicinchoninic acid
BLAST	Basic Local Alignment Search Tool
bp	Base pair(s)
BSA	Bovine serum albumin
BV	Benzyl viologen
°C	Degree Celsius
CBS	Cystathionine β-synthase
cDNA	Complementary DNA
CoA	Coenzyme A
CODH/ACS	CO dehydrogenase/acetyl-CoA synthase
C_t	Cycle threshold
CTAB	Cetyltrimethylammonium bromide
CV	Column volume
Da	Dalton
DMA	Dimethylamine
DSMZ	Deutsche Sammlung von Mikroorganismen und Zellkulturen

	(German Collection of Microorganisms and Cell Cultures)
DTNB	5,5'-dithiobis-2-nitrobenzoic acid
DMSO	Dimethylsulfoxid
DNA	Desoxyribonucleic acid
dNTP	Deoxyribonucleoside triphosphate
DOTAP	N-[1-(2,3-Dioleoyloxy)propyl]-N,N,N-trimethylammonium methyl sulfate
DTT	Dithiothreitol
EDTA	Ethylendiamintetraacetic acid
Et al.	*Et alii/et aliae* (and others)
F_{420}	(N-L-lactyl-γ-L-glutamyl)-L-glutamic acid phosphodiester of the 7,8-didemethyl-8-hydroxy-5-desazariboflavin-5´-phosphate
Fd	Ferredoxin
for	forward
Frh	F_{420}-reducing hydrogenase
g	Gravitation force
GAP-DH	Glyceraldehyde-3-phosphate dehydrogenase
h	hour
Hdr	Heterodisulfide reductase
IPTG	Isopropyl-β-D-thiogalactopyranosid
IOR	Indolepyruvate:ferredoxin oxidoreductase
H_2O_{dest}	demineralized H_2O
H_4MPT	Tetrahydromethanopterin
H_4SPT	Tetrahydrosarcinapterin
HABA	4-hydroxyazobenzen-2-carbonic acid
HEPES	2-(4-(2-Hydroxyethyl)-1-piperazinyl)-ethan-sulfonic acid

HS-CoB	7-Mercaptoheptanoylthreonine phosphate
HS-CoM	2-Mercaptoethansulfonate
kb	kilo base pairs
K_{cat}	Turnover number
KEGG	Kyoto Encyclopedia of Genes and Genomes
K_M	Michaelis Menten constant
LDH	Lactate dehydrogenase
LB	Lysogeny broth
M	Mol L^{-1}
mcrA	Methyl-CoM reductase subunit A
MF	Methanofuran
MI	Maximal induction
Min	Minute
MK	Myokinase
MMA	Monomethylamine
MOPS	3-(N-morpholino)-propansulfonic acid
MP	Methanophenazine
mRNA	Messenger RNA
Mtr	Methyl-H_4MPT:HS-CoM methyltransferase
MTZ	Metronidazol
MV	Methyl viologen
NAD(H)	Nicotinamide adenine dinucleotide
NADP(H)	Nicotinamide adenine dinucleotide phosphate
NCBI	National Center for Biotechnology Information

Neo	Neomycin
NMR	Nuclear magnetic resonance
PAGE	Polyacrylamide gel electrophoresis
PEP	Phosphoenolpyruvate
PFK	Phosphofructokinase
P_i	Orthophosphate
PK	Pyruvate kinase
PPase	Pyrophosphatase
PPDK	Pyruvate phosphate dikinase
PP_i	Pyrophosphate
pH	Negative decadic logarithm of proton concentration
rev	reverse
ddH_2O	double-demineralized H_2O
RNA	Ribonucleic acid
rRNA	Ribosomal RNA
RT-qPCR	Reverse transcription quantitative polymerase chain reaction
SDS	Sodium dodecyl sulfate
SOC	Super optimal broth with catabolite repression
sp./spp.	Species
TAE	Tris-acetate-EDTA
TEMED	*N*,*N*,*N*′,*N*′-tetramethylethylenediamine
Tris	Tris(hydroxymethyl)-aminomethan
TMA	Trimethylamine
TMAO	Trimethylamine oxide

TMAU	Trimethylaminuria
OD	Optical density
PCR	Polymerase chain reaction
U	Unit
v_{max}	Maximal reaction rate
v/v	Volume per volume
V	Volt
w/v	Weight per volume

1. INTRODUCTION

1.1 Introduction to methanogenic archaea

Methanogenic archaea are important players in nature: by producing methane from end products of anaerobic bacterial metabolism, they catalyze global carbon turnover. H_2+CO_2, methylated compounds or acetate can be converted and methane is produced as a major end product. Methane is then used as carbon and energy source by methylotrophic bacteria or it is chemically degraded to CO_2.

Methanogenic archaea are strictly anaerobic organisms. Nevertheless, they are very widespread in nature. Typical habitats include swamps, freshwater sediments and waterlogged soils such as paddy fields. Moreover, they thrive in the digestive tracts of ruminants and termites. They have great impact on global ecology not only because of their role in carbon cycling but also because methane is a potent greenhouse gas being 21-fold more active than CO_2. During the last 150 years the atmospheric methane concentration has increased more than twofold also due to anthropogenic methane emissions from the extensive use of agriculture, from the petrol industry and from landfills.

Another important habitat of methanogenic archaea are biogas plants. In such plants biomass is degraded in a process involving complex microbial consortia. Methanogenic archaea are involved in the last step of the process, which is conversion of H_2+CO_2 to methane and conversion of acetate to methane and CO_2. The resulting biogas is composed mainly of methane (48-65 %, (Rasi *et al.*, 2007)) and CO_2 (36-41 %, (Rasi *et al.*, 2007)). Since it is produced from renewable resources biogas is a clean form of energy.

Most methanogenic archaea depend on H_2+CO_2 for methanogenesis. However, in natural habitats, acetate-converting methanogens prevail (Ferry and Lessner, 2008). Methane from acetate accounts for about two-thirds of biologically produced methane.

Six orders of methanogenic archaea are well established, namely Methanobacteriales, Methanocellales, Methanococcales, Methanopyrales, Methanomicrobiales and Methanosarcinales (Liu and Whitman, 2008; Sakai *et al.*, 2008). Recently, a human-associated species was obtained in pure culture and named *Methanomassiliicoccus* (*Mm.*) *luminyensis* (Dridi *et al.*, 2012). The name was given after Marseilles, the place of isolation. This organism is grouped within a new order of methanogens proposed to be termed Methanomassiliicoccales (Iino *et al.*, 2013).

Altogether, a thorough understanding of methanogenesis is needed for such important and topical fields as energy supply, global carbon flux and climate change. This thesis will focus on energy conservation in the obligate aceticlastic methanogen *Methanosaeta* (*Mt.*) *thermoacetophila*, the versatile *Methanosarcina* (*Ms.*) *mazei* and the newly discovered

Mm. luminyensis.

1.2 Methanogenesis – the central pathway leading to energy conservation

The pathway of methanogenesis is common to all methanogenic archaea. Classically, three different types are distinguished. Hydrogenotrophic methanogens of the orders Methanobacteriales, Methanocellales, Methanococcales, Methanopyrales and Methanomicrobiales depend on H_2+CO_2 and/or formate as substrates for methanogenesis. One of the very few exceptions to this is *Methanosphaera* (*Mp*.) *stadtmanae*, which is a human gut commensal (Fricke *et al*., 2006). Phylogenetically it is a member of the Methanobacteriales, however, it grows only on methanol+H_2 and thus is clearly distinct from most other members of the above-named orders.

Members of the order Methanosarcinales are the most versatile methanogens. Different methylated compounds like methanol, methylated amines or methylsulfides can be converted. This methylotrophic methanogenesis results in the formation of methane and CO_2. Some members of the Methanosarcinales can additionally grow on H_2+CO_2.

The third pathway is the conversion of acetate to methane and CO_2 (aceticlastic methanogensis). Aceticlastic methanogens are also grouped within the order of Methanosarcinales. Although they are very widespread in nature there are only two genera of aceticlastic methanogens, namely *Methanosarcina* and *Methanosaeta*.

Several unusual cofactors are involved in methanogenesis (Deppenmeier, 2002a). The cytoplasmic electron carrier coenzyme F_{420} is a 5-deazaflavin derivative with an absorption maximum at 420 nm and a characteristic green fluorescence. A hydrophobic cofactor isolated from membranes of *Methanosarcina* spp. is methanophenazine (MP), a 2-hydroxy-phenazine derivative that serves as membrane-bound electron carrier. It is restricted to cytochrome-containing methanogens with membrane-bound electron transfer chains. Coenzyme M (HS-CoM), methanofuran (MF) and tetrahydromethanopterin (H_4MPT) are C_1 carrier molecules. In the order of Methanosarcinales H_4MPT is replaced by a slightly modified molecule termed tetrahydrosarcinapterin (H_4SPT). Finally, there is coenzyme B (HS-CoB), which provides electrons for the reduction of methyl groups to methane by the methyl-CoM reductase. The heterodisulfide from HS-CoM and HS-CoB (CoM-S-S-CoB) that is formed in the course of this reaction serves as terminal electron acceptor.

Biochemically, methanogens can be divided into two classes: In members of the order Methanosarcinales methanogenesis and energy conservation is based on cytochromes and involves redox driven ion translocation across the cytoplasmic membrane. In contrast, obligate hydrogenotrophic methanogens lack cytochromes and cannot couple membrane-bound electron transfer reactions with the extrusion of protons or sodium ions (Thauer *et al*., 2008).

In methanogenesis, carbon appears in its highest state of oxidation as CO_2 and in its most reduced form as methane. Different redox states enter the pathway depending on the substrate (Figure 1).

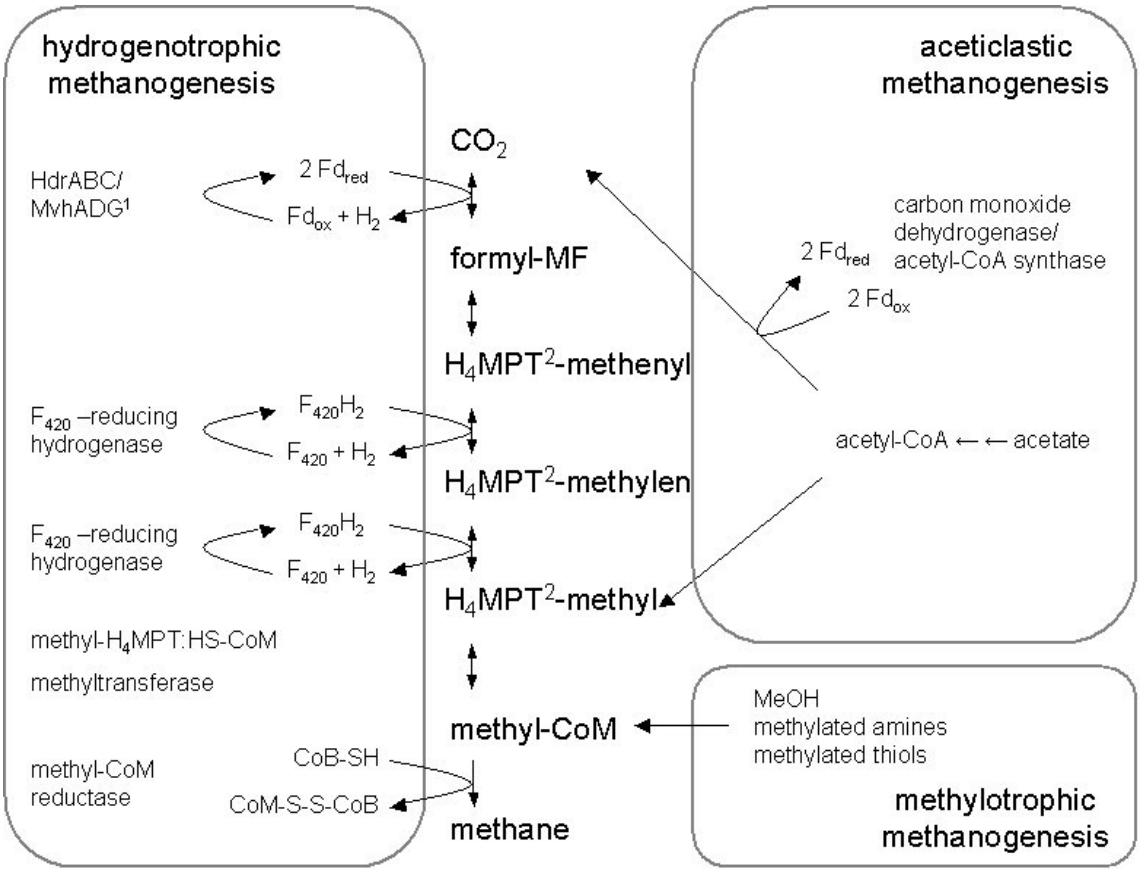

Figure 1: Methanogenesis from different substrates. Carbon enters the pathway in different oxidation states depending on the substrate and becomes either reduced or oxidized. In any case, methane is a final product. Fd – ferredoxin; H_4MPT – tetrahydromethanopterin; HdrABC/MvhADG – heterodisulfide reductase/Mvh hydrogenase; MF – methanofuran. [1]: In hydrogenotrophic methanogenesis in the genus *Methanosarcina* the Ech hydrogenase is employed for Fd reduction. [2]: In the order Methanosarcinales H_4MPT is replaced by H_4SPT (tetrahydrosarcinapterin).

In the CO_2-reducing pathway ferredoxin (Fd), which is a common electron carrier molecule in anaerobic metabolism, is used as electron donor for CO_2 reduction (Rouvière and Wolfe, 1989; Costa *et al.*, 2010; Kaster *et al.*, 2011). Different enzymes are employed for the reduction of Fd in the different groups of methanogens. In methanogens without cytochromes the reaction is catalyzed by the cytoplasmic heterodisulfide reductase (HdrABC), which forms a complex with the Mvh hydrogenase (MvhADG) (Kaster *et al.*, 2011). This enzyme complex couples the exergonic H_2-dependent reduction of CoM-S-S-CoB to the endergonic H_2-dependent reduction of Fd. Since the electrons deriving from H_2 oxidation are used for one exergonic and one endergonic reduction reaction, this process is called electron bifurcation.

Electron bifurcation was first described for the butyryl-CoA dehydrogenase/Etf complex from *Clostridium kluyveri* (Li *et al.*, 2008) and later also demonstrated for the HdrABC/MvhAGD complex from methanogenic archaea (Kaster *et al.*, 2011).

In contrast, methanogens with cytochromes found another way to overcome the energetic barrier of Fd reduction: H_2-dependent Fd reduction is coupled to the dissipation of an ion gradient by the membrane-bound Ech hydrogenase (Meuer *et al.*, 1999; Meuer *et al.*, 2002).

In either group, in the very first step of CO_2 reduction CO_2 is bound to MF. Subsequently, Fd-dependent reduction to formyl-MF as catalyzed by the formyl-MF dehydrogenase takes place. The formyl group is transferred to H_4MPT or H_4SPT, respectively. H_4MPT/H_4SPT-formyl is further reduced to methenyl-H_4MPT/H_4SPT and afterwards methyl-H_4MPT/H_4SPT. Electrons are derived from $F_{420}H_2$, which is reduced by the cytoplasmic F_{420}-reducing hydrogenase. The methyl group is transferred to HS-CoM and finally reduced by the methyl-CoM reductase using electrons from HS-CoB to yield methane and CoM-S-S-CoB. In methanogenesis from methylated compounds substrate-specific methyltransferases transfer methyl groups to HS-CoM and catalyze the generation of CH_3-S-CoM. One quarter of methyl groups is fed into the oxidative branch and is oxidized to CO_2 by the reverted pathway of CO_2 reduction. Reducing equivalents are used for the generation of $F_{420}H_2$ and reduced Fd. Three quarters of methyl groups are reduced with HS-CoB by the methyl-CoM reductase to form methane and the heterodisulfide CoM-S-S-CoB.

In aceticlastic methanogenesis, in the first step acetate is activated to acetyl-CoA at the expense of ATP. The acetyl-CoA molecule is cleaved by the action of a CO dehydrogenase / acetyl-CoA synthase (CODH/ACS) into its carbonyl and methyl moiety. The carbonyl moiety is oxidized to CO_2 and reducing equivalents are transferred to Fd. The methyl moiety is bound to H_4SPT, further transferred to HS-CoM and finally again methane and CoM-S-S-CoB are produced.

As was described above, methane and in the methylotrophic and aceticlastic pathway CO_2 are final products of methanogenesis. Another product is the heterodisulfide CoM-S-S-CoB, an oxidized compound that serves as terminal electron acceptor. In obligate hydrogenotrophic methanogens H_2 is the electron donor for the reduction of CoM-S-S-CoB. No membrane-bound electron transfer reactions are involved, instead reduction of CoM-S-S-CoB is catalyzed by the cytoplasmic HdrABC/MvhADG complex (Kaster *et al.*, 2011). However, for energy conservation an electrochemical ion gradient is needed that can be used by an A_oA_1-ATP synthase for ATP generation. The only enzyme that actively builds such a gradient in obligate hydrogenotrophic methanogens is the methyl-H_4MPT:HS-CoM methyltransferase (Mtr). It catalyzes the transfer of a methyl group from H_4MPT to HS-CoM during methanogenesis. Since this is an exergonic reaction and the Mtr is membrane-bound it can thus build an ion gradient. Most electrochemical gradients are built with protons, yet in

this case sodium ions are translocated across the cytoplasmic membrane.

The Mtr is also involved in energy conservation in aceticlastic and methylotrophic methanogenesis. However, here also membrane-bound electron transfer reaction occur. Reduced Fd and/or $F_{420}H_2$ from methanogenesis are oxidized by membrane-bound enzymes of an anaerobic respiratory chain. Hence, an ion gradient is generated, which can be used for ATP synthesis. The exact composition of methanogenic respiratory chains is discussed in the following chapters.

1.3 Acetate activation and respiratory chain of *Mt. thermoacetophila*

The genus *Methanosaeta* from the order of Methanosarcinales is specialized in using acetate as a substrate. The dependence on acetate is reflected in a very high affinity: only 7 - 70 μM are needed to sustain growth (Jetten *et al.*, 1992b). In this study, a thermophilic species with an optimal growth temperature of 55 °C was cultivated. It has been known under the name *Mt. thermophila*, which was recently placed on the list of rejected names (Tindall, 2014). The organism is now referred to as *Mt. thermoacetophila*. Cells are rod-shaped and form long filaments surrounded by a proteinaceous sheath.

Using acetate as sole substrate for methanogenesis, the change in free energy is only -36 kJ mol^{-1} CH_4 under standard conditions (Deppenmeier, 2002a). Therefore, efficient energy conservation systems are needed. The genome sequence of *Mt. thermoacetophila* is known since 2007 (Smith and Ingram-Smith, 2007) and revealed the presence of four acetyl-CoA synthetase (ACS) genes and a gene encoding a cytoplasmic pyrophosphatase (PPase). It was therefore assumed that for the first step of aceticlastic methanogenesis, acetate activation, *Mt. thermoacetophila* (similarly to *Mt. concilii* (Jetten *et al.*, 1989)) uses ACS enzymes. ACSs catalyze acetate activation according to Reaction (1).

Reaction (1) $\quad acetate + ATP + CoA \leftrightarrow acetyl\text{-}CoA + AMP + PP_i$

Pyrophosphate (PP_i) is thought to be hydrolyzed by the action of a PPase shifting the equilibrium of the reaction towards product formation. Thus, the expense for acetate activation is two ATP equivalents (Jetten *et al.*, 1992a). Therefore, in downstream processes at least two ATP equivalents have to be produced in order to compensate for the acetate activation reaction. Additionally, a net gain has to be made to sustain cells of *Mt. thermoacetophila*.

Being an obligate aceticlastic methanogen *Mt. thermoacetophila* shifts reducing equivalents to Fd during methanogenesis and Fd_{red} has to be re-oxidized by enzymes of the respiratory chain. However, any of the Fd_{red}-oxidizing enzymes from methanogens known to date, namely Ech hydrogenase and Rnf complex, are missing in *Mt. thermoacetophila* (Smith and

Ingram-Smith, 2007). It has been proposed that the $F_{420}H_2$ dehydrogenase, also known as Fpo complex is a potential candidate for Fd_{red}-oxidation (Figure 2). During methylotrophic methanogenesis the Fpo complex oxidizes $F_{420}H_2$ with subunit FpoF working as electron input module (Abken and Deppenmeier, 1997; Welte and Deppenmeier, 2011a). Yet, in *Mt. thermoacetophila* subunit FpoF is missing. It was shown that membranes of *Mt. thermoacetophila* indeed could not oxidize $F_{420}H_2$ (Welte and Deppenmeier, 2011b). It has been hypothesized that reduced Fd can interact with subunit FpoI from the Fpo complex in *Mt. thermoacetophila* and thus channels electrons from Fd_{red} into the respiratory chain (Welte and Deppenmeier, 2011b). Electrons would probably be transferred to the membrane-bound carrier molecule MP. They would be further transferred to a membrane-bound heterodisulfide reductase (HdrDE). HdrDE acts as terminal reductase and reduces CoM-S-S-CoB, regenerating HS-CoM and HS-CoB for methanogenesis. The last enzyme thought to be involved in the energy conserving system of *Mt. thermoacetophila* is the above-mentioned Mtr. During methanogenesis it catalyzes methyl group transfer and concomitantly translocates two sodium ions per acetate molecule. In analogy to HdrDE from *Ms. mazei* the *Mt. thermoacetophila* enzyme probabely translocates two protons per acetate molecule. For the Fpo complex the exact stoichiometry of ion translocation is still a matter of debate. However, for *Methanosarcina* spp. translocation of two protons per acetate molecule has been shown (Bäumer *et al.*, 2000).

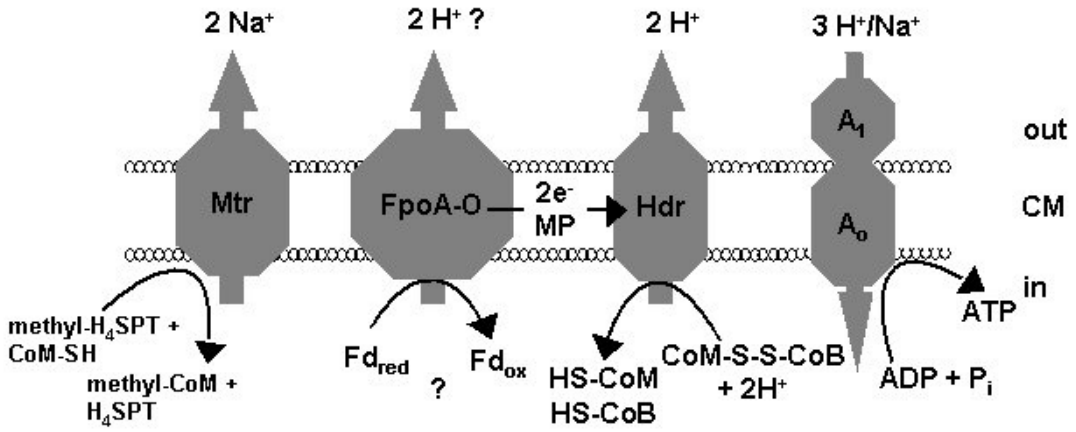

Figure 2: Proposed scheme of the respiratory chain in *Mt. thermoacetophila*. The translocation of six ions by membrane-bound enzymes would lead to the generation of two ATP molecules per acetate molecule. CM – cytoplasmic membrane; Fpo – $F_{420}H_2$ dehydrogenase, also known as Fpo complex; H_4SPT – tetrahydrosarcinapterin; Hdr – heterodisulfide reductase; MP – methanophenazine; Mtr – methyl-H_4MPT:HS-CoM methyltransferase.

Based on the assumption that the A_oA_1-ATP synthase uses three ions to phosphorylate one ADP molecule (Welte and Deppenmeier, 2014) ion translocation by the respiratory chain of

Mt. thermoacetophila as described above would account for the synthesis of two ATP molecules. Two ATP equivalents are consumed by ACS and PPase in the acetate activation reaction. Hence, for *Mt. thermoacetophila* growing on acetate there would be no ATP net gain.

In this study, ACS and PPase from *Mt. thermoacetophila* were examined in terms of gene expression and enzymatic activity. The question here was whether ATP equivalents were potentially being spared in the acetate activation reaction. If this would be the case, translocation of six ions would be sufficient for the survival of *Mt. thermoacetophila*.

1.4 Branched respiratory chain in *Ms. mazei*

Another organism used in this study was *Ms. mazei*. Compared to *Methanosaeta* spp. *Methanosarcina* spp. have a lower acetate affinity but can use an unusually broad spectrum of other substrates. *Ms. mazei* forms coccoid cells that can build the typical "sarcina" clusters. A single cell phenotype is observed under laboratory conditions. Having a broad substrate spectrum and reasonably fast doubling time, *Ms. mazei* is a well-established model organism. Its genome sequence has been known since 2002 (Deppenmeier *et al.*, 2002).

Compared to *Mt. thermoacetophila* its respiratory chain additionally contains two hydrogenases, namely the Ech and Vho hydrogenase (Figure 3). The Ech hydrogenase was shown to oxidize reduced Fd (Meuer *et al.*, 1999; Welte *et al.*, 2010b) and to translocate one

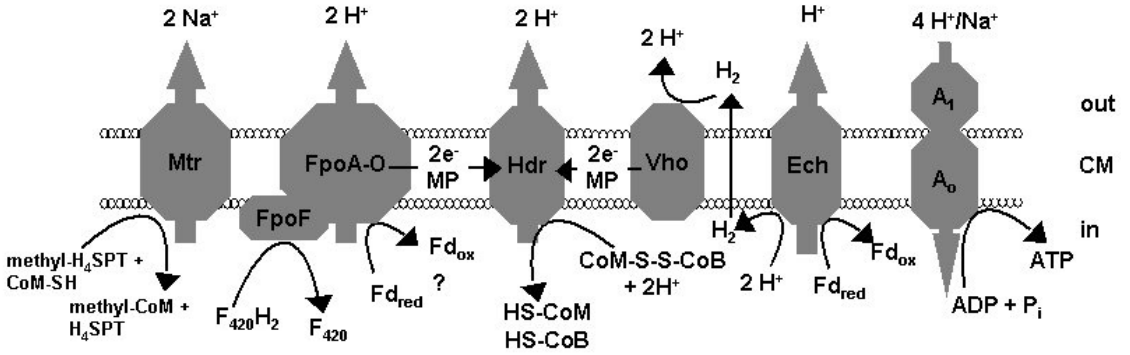

Figure 3: Respiratory chain in *Ms. mazei*. During aceticlastic methanogenesis, Fd_{red} is oxidized by the Ech hydrogenase and electrons are shifted to protons to yield H_2. H_2 is oxidized by the Vho hydrogenase and finally heterodisulfide is reduced. Seven ions are translocated and can be used for ATP synthesis. In methylotrophic methanogenesis, the Fpo complex translocates two additional protons. CM – cytoplasmic membrane; Ech – energy conserving hydrogenase; Fpo – $F_{420}H_2$ dehydrogenase, also known as Fpo complex; H_4SPT – tetrahydrosarcinapterin; Hdr – heterodisulfide reductase; MP – methanophenazine; Mtr – methyl-H_4MPT:HS-CoM methyltransferase; Vho – F_{420}-non-reducing hydrogenase.

proton across the cytoplasmic membrane (Welte *et al.*, 2010a). In the course of the reaction the protein transfers electrons to protons to yield H_2. H_2 diffuses across the membrane and is oxidized by the Vho hydrogenase at the outer phase of the cell thereby releasing two protons. The Vho hydrogenase donates electrons to the membrane-bound electron carrier MP that takes up two protons from the cytoplasm. Hence the overall reaction results in scalar proton translocation with a stoichiometry of $2H^+/2e^-$. Reduced MP is oxidized by the membrane-bound HdrDE and again two protons are translocated. The process described above depends on reduced Fd and therefore takes place in aceticlastic methanogenesis. With a total of seven ions translocated per acetate molecule, the balance in *Ms. mazei* is marginally better than in *Mt. thermoacetophila*. Yet, there is another difference between the two organisms concerning acetate activation. *Ms. mazei*, like other *Methanosarcina* strains, acquired an acetate activation system that originates from bacteria (Deppenmeier *et al.*, 2002). It consists of acetate kinase and phosphotransacetylase. These enzymes catalyze acetate activation according to Reactions (2) and (3).

Reaction (2) acetate + ATP ↔ acetyl-phosphate + ADP
Reaction (3) acetyl-phosphate + CoA ↔ acetyl-CoA + P_i

Since the acetate kinase catalyzes hydrolysis of ATP to ADP and exchange of the phosphate group against CoA is possible without further ATP consumption only one ATP equivalent is spent in the course of this reaction. Assuming that the ATP synthase uses four protons to phosphorylate one ADP molecule *Ms. mazei* growing on acetate achieves a net gain of three protons. This corresponds to 0.75 ATP molecules per acetate molecule.

The Fpo complex from *Ms. mazei* includes the subunit FpoF responsible for oxidation of $F_{420}H_2$ (Figure 3). It was therefore thought that the Fpo complex in *Ms. mazei* is important only during methylotrophic methanogenesis. Yet, the generation of a *Ms. mazei* Δ*ech* deletion mutant led to the finding that also without the Ech hydrogenase reduced Fd is still oxidized by membranes of *Ms. mazei* (Welte *et al.*, 2010b). Analogous to *Mt. thermoacetophila*, it is hypothesized that the Fpo complex without FpoF, which can dissociate from the complex, can accept electrons from reduced Fd that are channeled into the respiratory chain.

The subunit that could possibly accept electrons from Fd_{red} is FpoI. In this study, an antibody against subunit FpoI was generated and used to test the interaction between Fd and the Fpo complex. In another attempt to resolve the inquiry, knock-out vectors were cloned to generate double-mutants lacking both Ech hydrogenase and parts of or the whole Fpo complex. Additionally, to gain a deeper understanding of the Fpo complex, experiments were carried out specifically targeting FpoO using a *Ms. mazei* Δ*fpoO* knock-out mutant.

1.5 First approach towards an understanding of energy conservation in *Mm. luminyensis*

Mm. luminyensis was isolated from the human gut in 2012 (Dridi *et al.*, 2012). The vast majority of microorganisms in the human gut are bacteria, but methanogenic archaea are common inhabitants as well. Prominent examples are *Methanobrevibacter* (*Mb.*) *smithii* and *Methanosphaera* (*Mp.*) *stadtmanae* (Lin and Miller, 1998; Scanlan *et al.*, 2008; Dridi *et al.*, 2009). As mentioned before, *Mp. stadtmanae* consumes H_2 and methanol and *Mb. smithii* is an obligate hydrogenotrophic methanogen. Thus, they play an important role in preventing the accumulation of fermentation end products.

Recently, analyses of 16S rRNA and *mcrA* gene sequences have unraveled the presence of a Thermoplasmatales-related lineage of methanogenic archaea in the human gut (Mihajlovski *et al.*, 2008; Scanlan *et al.*, 2008; Mihajlovski *et al.*, 2010; Paul *et al.*, 2012; Borrel *et al.*, 2013). Several new species from that lineage have been isolated or enriched. *Mm. luminyensis* was obtained in pure culture and grows optimally at 37 °C with 40 mM methanol and 1 bar H_2+CO_2 (80:20) (Dridi *et al.*, 2012).

It was proposed that apart from the consumption of fermentation end products, there might be other benefits to be gained from methanogenic archaea in the human gut. Dietary ingredients like choline are converted to TMA by bacteria in the gut. In individuals suffering from trimethylaminuria or “fish-odor syndrome” TMA is taken up into the bloodstream and excreted via breath, sweat and urine. Due to the intense fishy odor of TMA this causes social stress to the patients (Brugère *et al.*, 2014). In healthy individuals about 95 % of TMA are converted to the odorless trimethylamine oxide (TMAO). However, enhanced levels of TMAO might result in an increased risk of cardiovascular disease. *Mm. luminyensis* was shown to deplete TMA by using it as a substrate. Therefore, it could help to control TMA concentration in the human gut and thus also TMAO concentration in the bloodstream in a process termed “archaebiotics” (Brugère *et al.*, 2014).

The genome sequence of *Mm. luminyensis* has been known since 2012 (Gorlas *et al.*, 2012). According to bioinformatic analyses, *hdrABC*/*mvhADG* genes are present. Additionally, a truncated Fpo complex missing subunits FpoF and FpoO can be found (Borrel *et al.*, 2014). It was speculated that the truncated Fpo complex accepts electrons from reduced Fd and generates a membrane potential used for ATP synthesis (Borrel *et al.*, 2014; Lang *et al.*, 2014). However, an Ech hydrogenase can also be found that could oxidize Fd as well and build a proton gradient (Borrel *et al.*, 2014). In this study, biochemical evidence for the activity of HdrABC/MvhADG and Ech hydrogenase is firstly demonstrated and a tentative model for energy conservation in *Mm. luminyensis* is presented.

2. MATERIALS AND METHODS

2.1 Chemicals and other materials

2.1.1 Chemicals

Chemicals used in this work had a least p.a. quality. Unless indicated otherwise chemicals were ordered from Merck KgaA (Darmstadt, Germany), Carl Roth GmbH (Karlsruhe, Germany), Sigma-Aldrich (Munich, Germany), Fluka (Sigma-Aldrich, Munich, Germany), Serva (Heidelberg, Germany) or VWR (Darmstadt, Germany).

2.1.2 Gases

CO_2 (99,9 %), H_2 (99,9 %), N_2 (99,9 %) and Argon (99,9 %) were supplied by Air Liquide, Düsseldorf, Germany.

2.1.3 Enzymes

The enzymes used in this study are summarized in Table 1.

Table 1: Enzymes used in this study

Enzyme	Supplier
Alkaline Phosphatase	Thermo Scientific (Schwerte, Germany)
DNAse I	Thermo Scientific (Schwerte, Germany)
DreamTaq polymerase	Thermo Scientific (Schwerte, Germany)
Ferredoxin:$NAPD^+$ oxidoreductase from *Spinacea oleracea*	Sigma-Aldrich (Munich, Germany)
Lactate dehydrogenase	Sigma-Aldrich (Munich, Germany)
Myokinase	Sigma-Aldrich (Munich, Germany)
Phusion® polymerase	Thermo Scientific (Schwerte, Germany)
Pyruvate kinase	Sigma-Aldrich (Munich, Germany)
Restriction enzymes	Thermo Scientific (Schwerte, Germany)
T4 DNA ligase	Thermo Scientific (Schwerte, Germany)

2.1.4 Antibiotics

Antibiotics used in this study, their solvents and concentrations are given in Table 2.

Table 2: Antibiotics used in this study

Antibiotic	Solvent	Concentration of stock solution
Ampicillin	50 % ethanol	100 mg mL^{-1}
Puromycin	ddH_2O	5 mg mL^{-1}
Neomycin	ddH_2O	15 mg mL^{-1}
Tetracyclin	70 % ethanol	10 mg mL^{-1}

2.1.5 Software

The software tools used in this study are summarized in Table 3.

Table 3: Software used in this study

Software	Purpose
Chromas Lite 2.01 (Technelysium Pty Ltd)	Analysis of DNA sequence data
Clone Manager 7.03 (Scientific and Educational Software)	Planning of cloning strategies, vector maps
GIMP 2	Image processing
Magellan 6.5 (Magellan Software)	Photometric assays
Microsoft Excel (Microsoft)	Data analysis
Primer D'Signer (IBA)	Primerdesign for pASK vectors
Spectra Manager 1.54.03 (Jasco Corporation)	Enzyme kinetics
iCycler	RT-qPCR
GraphPad Prism 6, GraphPad Software Inc., La Jolla, USA	Enzyme kinetics

2.2 Organisms, vectors, plasmids and primers

2.2.1 Primers

Primers used in this study were designed with the Primer D'Signer (IBA GmbH, Göttingen, Germany), with Primer 3 (http://bioinfo.ut.ee/primer3-0.4.0/primer3, 30.12.2014) or were developed manually. Manufacturing was done by Eurofins MWG Operon (Ebersberg, Germany). Sequences of primers are listed in Table 4.

Table 4: Sequences of primers used in this study

Function		Sequence (5' → 3')	Restriction enzyme
Colony PCR	pASK_for	GAGTTATTTTACCACTCCCT	n.a.
	pASK_rev	CGCAGTAGCGGTAAACG	n.a.
Cloning into expression vector	mthe0236_for	ATGGTAGGTCTCAAATGGCAGATAATA TCTATGTGGTCGGG	*Eco*31I
	mthe0236_rev	ATGGTAGGTCTCAGCGCTCTTCTTGA ATGCGGACTCGAGC	*Eco*31I
Cloning into expression vector	mthe1194_for	ATGGTAACCTGCATTAGCGCCGCTGA GACTGCAAAGACTGCTG	*Bve*I
	mthe1194_rev	ATGGTAACCTGCATTATATCAGACTAT GAGCGGGATGTTCTCG	*Bve*I
	mthe0236_for	GCCAGCATGTATGAGCTG	n.a.
	mthe0236_rev	CATGTGGGTGACTTGAAT	n.a.
RT-qPCR target genes	mthe1194_for	CCAGTGGATCATCGAGTA	n.a.
	mthe1194_rev	CAGAAATCGAGGTAGTTC	n.a.
	mthe1195_for	TAAGGAGCTTGCTGAGAA	n.a.
	mthe1195_rev	CAGAACTCTATGTAGTGG	n.a.
	mthe1196_for	TCGAAGGCGTATGCTGAC	n.a.
	mthe1196_rev	CGCCTCGTCAGCCTGCTT	n.a.
	mthe1413_for	CAGGCGCGCTCCGCGAG	n.a.
	mthe1413_rev	GGCCTTTATCGGGATAGG	n.a.
	mthe0554_for	TATCATTGGGGTTACAAG	n.a.
	mthe0554_rev	CAGAGATGGGTATTGATC	n.a.
RT-qPCR GAP-DH	mthe0701_for	CTATGCCGTTGCTGTGAA	n.a.
	mthe0701_rev	TTGGCGGTGCATTTATCT	n.a.
RT-qPCR ribosomal protein S3P	mthe1722_for	GTTCGTCATGATTGGCAC	n.a.
	mthe1722_rev	CCCCTTCTGGAGCTTATC	n.a.
RT-qPCR intergenic region	igr1_for	GCGGTCAACCTATTTTATTT	n.a.

between mthe_1194 and mthe_1195	igr1_rev	TTACATACCTCCATTCATCT	n.a.
RT-qPCR intergenic region between mthe_1195 and mthe_1196	igr2_for	AACGTCCGCAATTTTTATTT	n.a.
	igr2_rev	CTGCCTCCAGCCCATCCCG	n.a.
Cloning of vector for deletion of *fpoO* in *Ms. mazei* Δ*ech*	mm2479_ up_for	CCTTCTCGAGTTCGGGCTTTCCTTTG TTTA	*Xho*I
	mm2479_ up_rev	ATGAAGCTTCACAGGTCGCAATCTGT CAT	*Hin*dIII
	mm2479_ down_for	AACGCTGCAGGAACACGTACACCCG CATTA	*Pst*I
	mm2479_ down_rev	TACTACTAGTCCTCAGTTGGACGTTTA CTC	*Bcu*I
Cloning of vector for deletion of *fpoA-O* in *Ms. mazei* Δ*ech*	mm2491_ up_for	CCTTCTCGAGGCCCTCCAAGTCCTGC ACCT	*Xho*I
	mm2491_ up_rev	CATGAAGCTTAGTGCAGCAATCTGAAA TTGC	*Hin*dIII
	mm2479_ down_for	TACTACTAGTGAACACGTACACCCGCA TTA	*Bcu*I
	mm2479_ down_rev	TACTGCGGCCGCCCTCAGTTGGACGT TTACTC	*Not*I
Cloning of vector for deletion of *fpoF* in *Ms. mazei* Δ*ech*	mm0627_ up_for	CCGGCTCGAGTGCAATTAACATCTATT GTA	*Xho*I
	mm0627_ up_rev	CCTTGATATCTCAGTTACCTCCACTGC CT	*Eco*RV
	mm0627_ down_for	GTAACTAGTCAGTATGAAGTCCGAAAC TT	*Bcu*I
	mm0627_ down_rev	AGCGCGGCCGCGGAAAGTGGTCTAC CTTA	*Not*I

2.2.2 Organisms

Organisms used in this work were *Clostridium* (*Cl.*) *pasteurianum*, *Escherichia* (*E.*) *coli* strains DH5α and BL21 (DE3), *Methanosaeta* (*Mt.*) *thermoacetophila, Methanosarcina (Ms.) mazei* and *Methanomassiliicoccus* (*Mm.*) *luminyensis*. Their genotypes can be found in Table 5.

Table 5: Organisms used in this thesis and their genotypes

Organism	Genotype	Reference
Clostridium (Cl.) pasteurianum	Wild type	DSM 525^{T}
Escherichia (E.) coli		
E. coli DH5α	F–, Φ80*lacZ*ΔM15, Δ(l*ac-ZYA-argF*)U169, *deoR*, *recA*1,*endA*1, *hsdR*17(rk-, mk+),*phoA*, *supE*44, *λ*-, *thi*-1,*gyrA*96, *relA*1	(Hanahan, 1983)
E.coli BL21 (DE3)	F–*, omp*T, *had*S*B* (r*B*-m*B*-), *gal*, *dcm* (DE3)	Invitrogen (Carlsbad,USA)
Methanosarcina (Ms.) mazei Gö1		
Ms. mazei Gö1	Wild type	DSM 7222
Ms. mazei ΔfpoO	Puro^{R} Δ*mm2479* deletion mutant of *Ms. mazei* Gö1	Cornelia Welte (Radboud Universiteit, The Netherlands)
Methanosaeta (Mt.) thermoacetophila	Wild type	DSM 6194
Methanomassiliicoccus (Mm.) luminyensis	Wild type	DSM 25720

2.2.3 Vectors and plasmids

Vectors and plasmids used in this study are summarized in Table 6.

Table 6: Vectors and plasmids used in this thesis

Name	**Function**	**Source**
pASK-mm2486	Production of recombinant FpoI from *Ms. mazei*	Sarah Refai, personal communication

pASK-mthe0236	Production of recombinant PPase from *Mt. thermoacetophila*	This thesis
pASK-mthe1194	Production of recombinant ACS from from *Mt. thermoacetophila*	This thesis
pPR-mm2093+4	Production of recombinant IOR from *Ms. mazei*	Cornelia Welte, personal communication
pPR-mm1619	Production of recombinant ferredoxin Mm1619 from *Ms. mazei*	(Welte and Deppenmeier, 2011b)
pRKISC	Production of iron-sulfur cluster containing proteins in *E. coli*	(Yamamoto *et al.*, 1997)
pJK3-neoR-ΔfpoA-O	Deletion of *fpoA-O* in the *Ms. mazei* Δ*ech* mutant	This thesis
pJK3-neoR-ΔfpoF	Deletion of *fpoF* in the *Ms. mazei* Δ*ech* mutant	This thesis
pJK3-neoR-ΔfpoO	Deletion of *fpoO* in the *Ms. mazei* Δ*ech* mutant	This thesis
pASK-IBA3	Cloning of pASK-mthe0236	IBA (Göttingen, Germany)
pASK-IBA3	Cloning of pASK-mthe1194	IBA (Göttingen, Germany)

2.3 Microbiological methods

2.3.1 Cultivation of *Cl. pasteurianum*

Cl. pasteurianum is cultivated anaerobically in glucose yeast extract medium (DSMZ medium 54) with 30 °C incubation temperature.

Glucose yeast extract medium (DSMZ medium 54)

Glucose	20 g
Yeast extract	10 g
$CaCO_3$	20 g
H_2O_{dest}	ad 1000 mL

The medium was sparged with N_2 to make it anoxic and afterwards autoclaved. For isolation of Fd, iron and sulfur compounds are added as sterile filtered solutions: 4 mL L^{-1} $FeCl_3$ (5 % [w/v] in EtOH), 0.5 mL L^{-1} $FeNH_4$ citrate (30 mM) and 0.5 mL L^{-1} L-cysteine (100 mM).

2.3.2 Cultivation of *E. coli*

E. coli is routinely cultivated at 37 °C in lysogeny broth (LB). For agar plates 1.5 % agar is

added.

LB for cultivation of *E. coli*

Tryptone	10 g
Yeast extract	5 g
NaCl	10 g
H_2O_{dest}	ad 1000 mL
pH 7.5	

For protein overproduction maximal induction (MI) medium is used. M9 salts are autoclaved separately and added prior to inoculation. Additionally, $CaCl_2$ is added to a final concentration of 100 μM, $MgSO_4$ to a final concentration of 1 mM and $FeNH_4$ citrate to a final concentration of 1 μM.

MI medium for protein overproduction in *E. coli*

Tryptone	32 g
Yeast extract	20 g
20 × M9 salts	50 mL
H_2O_{dest}	ad 1000 mL

20 × M9-solution

$Na_2HPO_4 \times 2\ H_2O$	120 g
KH_2PO_4	60 g
NaCl	10 g
NH_4Cl	20 g
H_2O_{dest}	ad 1000 mL

For all media, the appropriate antibiotics were added after autoclaving. For regeneration after transformation, SOC medium is used that was supplied by New England Biolabs (Frankfurt am Main, Germany).

2.3.3 Vitamin solution

Vitamin solution was prepared 10 stock solution. The solution could be stored at -20 °C.

Vitamin solution 10 □

Biotin	0.02 g
Folic acid	0.02 g
Pyridoxin × HCl	0.1 g
Thiamin × HCl	0.05 g
Riboflavin	0.05 g
Nicotinic acid	0.05 g
Ca-Pantothenate	0.05 g
Vitamin B12	0.001 g
p-Aminobenzoic acid	0.05 g
α-Lipoic acid	0.05 g
H_2O_{dest}	ad 1000 ml

2.3.4 Trace element solutions

Trace element solutions were prepared for the cultivation of *Ms. mazei*, *Mt. thermoacetophila* and *Mm. luminyensis*. All solutions could be stored at 4 °C.

Trace element solution SL6 for the cultivation of *Ms. mazei*

$ZnSO_4$	0.1 g
$MnCl_2 \times 4\ H_2O$	0.03 g
H_3BO_3	0.3 g
$CoCl_2 \times 6\ H_2O$	0.2 g
$CuCl_2 \times 2\ H_2O$	0.01 g
$NiCl_2 \times 6\ H_2O$	0.02 g
$Na_2MoO_4 \times 2\ H_2O$	0.03 g
H_2O_{dest}	ad 1000 mL

Methanogenium medium trace element solution for the cultivation of *Mt. thermoacetophila*

Nitrilotriacetic acid	1.5 g
$MgSO_4 \times 7\ H_2O$	3 g

$MnSO_4 \times H_2O$	0.5 g
NaCl	1 g
$FeSO_4 \times 7\ H_2O$	0.1 g
$CoSO_4 \times 7\ H_2O$	0.18 g
$CaCl_2 \times 2\ H_2O$	0.1 g
$ZnSO_4 \times 7\ H_2O$	0.18 g
$CuSO_4 \times 5\ H_2O$	0.01 g
$KAl(SO_4)_2 \times 12\ H_2O$	0.02 g
H_3BO_3	0.01 g
$Na_2MoO_4 \times 2\ H_2O$	0.01 g
$NiCl_2 \times 6\ H_2O$	0.025 g
$Na_2SeO_3 \times 5\ H_2O$	0.3 mg
H_2O_{dest}	ad 1000 mL

Modified trace element solution SL10 for the cultivation of *Mm. luminyensis*

EDTA	15 mM
$FeCl_2 \times 4\ H_2O$	1.5 g
$ZnCl_2$	0.07 g
$MnCl_2 \times 4\ H_2O$	0.1 g
H_3BO_3	0.006 g
$CoCl_2 \times 6\ H_2O$	0.19 g
$CuCl_2 \times 2\ H_2O$	0.002 g
$NiCl_2 \times 6\ H_2O$	0.024 g
$Na_2MoO_4 \times 2\ H_2O$	0.036 g
H_2O_{dest}	ad 1000 mL
pH 7 with NaOH	

2.3.5 Cultivation of *Ms. mazei*

Ms. mazei was cultivated anaerobically at 37 °C either in 16 mL Hungate tubes (Bellco Glass Inc., Vineland, New Jersey, USA) or in Müller-Krempel serum flasks (Ochs Glasgerätebau, Bovenden, Germany). The medium was complex or minimal medium modified after DSMZ

medium 120 with the following components. For minimal medium complex components were omitted.

DSMZ medium 120 for cultivation of *Ms. mazei*

K_2HPO_4	0.348 g
KH_2PO_4	0.227 g
NH_4Cl	0.5 g
$MgSO_4 \times 7\ H_2O$	0.5 g
$CaCl_2 \times 2\ H_2O$	0.25 g
NaCl	2.25 g
$FeSO_4 \times 7\ H_2O$	0.002 g
Na-acetate $\times 3\ H_2O$	1 g
Yeast extract	2 g
Casein hydrolysate	2 g
$NaHCO_3$	0.85 g
Resazurin	0.001 g
Trace element solution SL6	1 mL
Vitamin solution 10 ×	1 mL
H_2O_{dest}	ad 1000 mL

If acetate was used as a substrate the amount of $NaHCO_3$ was doubled to have a stronger carbonate buffer. After addition of all components the pH was brought to 8.5 by addition of 6 M NaOH. At pH 8.5 the medium becomes turbid. By sparging with N_2+CO_2 (80:20) oxygen is removed and the pH is brought to 7 and the medium becomes clear again. Anaerobic flasks were closed with airtight rubber stoppers and autoclaved. For inoculation a 2 % inoculum was used. Prior to inoculation substrates were added. Since *Ms. mazei* reaches the lowest doubling time using TMA as a substrate, TMA was routinely used with a final concentration of 50 mM. Other substrates were methanol (final concentration 150 mM) or acetate (final concentration 100 mM). For complete reduction of the medium prior to inoculation cysteine-HCl and Na_2S were added to a final concentration of 1.5 mg mL^{-1}. To avoid bacterial contamination Amp was routinely used with a final concentration of 100 μg mL^{-1}. If mutant strains were cultivated, puromycin (5 μg mL^{-1}) was added.

2.3.6 Cultivation of *Mt. thermoacetophila*

DSMZ medium 387 for cultivation of *Mt. thermoacetophila*

NH_4Cl	0.5 g
K_2HPO_4	0.4 g
$MgCl_2 \times 6\ H_2O$	0.1 g
Resazurin	0.001 g
Methanogenium trace element solution	10 mL
H_2O_{dest}	ad 940 mL

Anoxic compounds added to DSMZ medium 387 prior to inoculation

$NaHCO_3$ 5 % [w/v]	20 mL L^{-1}
$CaCl_2 \times 2\ H_2O$ 1 % [w/v]	10 mL L^{-1}
10 × vitamin solution	10 mL L^{-1}
Coenzyme M 1.42 % [w/v]	10 mL L^{-1}
$Na_2S \times 9\ H_2O$ 5 % [w/v]	5 mL L^{-1}
Amp 100 mg mL^{-1}	Final concentration 100 μg mL^{-1}

For cultivation of *Mt. thermoacetophila* DSMZ medium 387 was used. The basic medium is boiled and cooled under N_2+CO_2 (80:20) until a pH of 5.8 is reached. Serum flasks are sealed with gas tight rubber stoppers and autoclaved. Prior to inoculation sterile, anoxic compounds are added. 50 mM acetate are used as substrate and 2 % of culture are used as inoculum. Since *Mt. thermoacetophila* is a thermophilic species cultures are incubated at 55 °C.

2.3.7 Cultivation of *Mm. luminyensis*

Mm. luminyensis was cultivated in two different basic media with different additives. The basic media are *Methanobrevibacter* medium according to (Dridi *et al.*, 2012) and DSMZ medium 119. As additives tungstate/selenite solution, a fatty acid mixture and sludge fluid were used. Furthermore, *Ms. mazei* extract was prepared as described in the following.

Methanobrevibacter medium for cultivation of *Mm. luminyensis*

KH_2PO_4	0.5 g
$MgSO_4 \times 7\ H_2O$	0.4 g

NaCl	5 g
NH_4Cl	1 g
$CaCl_2 \times 2\ H_2O$	0.05 g
Trace element solution SL10	1 mL
WO_4^{2-}/SeO_3^{2-} solution	2 mL
Yeast extract	1 g
Na-acetate $\times 3\ H_2O$	2.7 g
Resazurin	0.001 g
Peptone	1 g
Cysteine HCl $\times\ H_2O$	0.5 g
Sludge fluid	50 mL
H_2O_{dest}	ad 830 mL

Compounds added to *Methanobrevibacter* medium prior to inoculation

$NaHCO_3$ 5 % [w/v]	80 mL L^{-1}
Na-formate 5 % [w/v]	40 mL L^{-1}
10 × vitamin solution	10 mL L^{-1}
$Na_2S \times 9\ H_2O$ 7.5 g/50 mL	3.2 mL L^{-1}
Amp 100 mg mL^{-1}	Final concentration 100 μg mL^{-1}

The pH of *Methanobrevibacter* medium is adjusted to 7.5 by addition of 6 M KOH. The medium is sparged with N_2+CO_2 (80:20) and afterwards autoclaved. Prior to inoculation $NaHCO_3$ is added as buffering agent together with vitamins and Na_2S as reductant. 75 mM methanol were routinely used as substrate, together with H_2 in the gas phase. Therefore, inoculated cultures are sparged with H_2+CO_2 (80:20) through a sterile filter (0.2 μm) and after sparging 1 bar overpressure is added. Cultures are inoculated with 16 % inoculum and incubated at 37 °C.

DSMZ medium 119 for cultivation of *Mm. luminyensis*

KH_2PO_4	0.5 g
$MgSO_4 \times 7\ H_2O$	0.4 g
NaCl	0.4 g
NH_4Cl	0.4 g
$CaCl_2 \times 2\ H_2O$	0.05 g
$FeSO_4 \times 7\ H_2O$	0.002 g
Trace element solution SL10	1 mL
Yeast extract	1 g

Na-acetate × 3 H_2O	2.7 g
Na-formate	1 g
Sludge fluid	50 mL
Fatty acid mixture	20 mL
Resazurin	0.001 g
H_2O_{dest}	ad 930 mL

The medium is sparged with N_2+CO_2 (80:20) to make it anoxic and furthermore it adjusts the pH to 6.8-7.0. The medium is autoclaved and prior to inoculation $NaHCO_3$ (4 g L^{-1}), cysteine-HCl × H_2O (0.5 g L^{-1}) and Na_2S × 9 H_2O (0.5 g L^{-1}) are added. 75 mM methanol are used as substrate, with H_2+CO_2 (80:20) at 1 bar overpressure in the gas phase. Cultures are inoculated with 16 % inoculum and incubated at 37 °C.

Fatty acid mixture for cultivation of *Mm. luminyensis*

Valeric acid	0.5 g
Isovaleric acid	0.5 g
2-Methylbutyric acid	0.5 g
Isobutyric acid	0.5 g
H_2O_{dest}	ad 20 mL
pH 7.5 with NaOH	

Tungstate/selenite solution for cultivation of *Mm. luminyensis*

Na_2SeO_3	0.002 g
Na_2WO_4 × 5 H_2O	0.004 g
NaOH	0.4 g
H_2O_{dest}	ad 1000 mL

Sludge fluid is prepared from biogas sludge. Therefore, sludge from a mesophilic biogas plant (operating temperature 40 °C, fed with cow dung, dried poultry dung and maize silage), which had been stored at 4 °C is aerobically filtered with a 100 μm sieve and centrifuged (65000 × *g*, 30 min, 4 °C). The clear supernatant is transferred to serum flasks, sparged with N_2 and autoclaved. It can be stored at room temperature in the dark.

For the preparation of *Ms. mazei* extract *Ms. mazei* is cultivated to the mid-exponential growth phase. Cells are harvested by centrifugation (6000 × *g*, 20 min, 4 °C) and re-suspended in 10 mL modified *Methanobrevibacter* medium. Cells are lysed with sonication (5 min, 75 % power, 4 °C) using a Bandelin Sonoplus sonicator (Bandelin Electronic, Berlin, Germany). The lysate is centrifuged (15 min, 9000 × *g*, 4 °C) and the supernatant added to a *Mm. luminyensis* culture.

2.3.8 Preparation of frozen stocks

For the preparation of frozen stocks of *E. coli* an over night culture is mixed with DMSO (final concentration 15 % [v/v]) and frozen at -70 °C. For frozen stocks of methanogens a sterile, anaerobic 9 mL serum flask is filled with 2 mL of culture and 2 mL of anaerobic sucrose solution (50 % [w/v]). The mixture can be stored at -70 °C under a 100 % H_2 gas phase.

2.3.9 Measurement of growth parameters

Growth of cultures was followed by measuring the optical density at 600 nm (OD_{600}). Therefore, samples were taken and measured against a blank consisting of the respective medium (Helios Epsilon Photometer, Thermo Scientific, Waltham, USA). Anaerobic medium containing resazurin was reduced with sodium dithionite prior to the measurement. If OD_{600} values were above 0.3, dilutions with the appropriate medium were made.

Before recording a growth curve cultures of *Ms. mazei* were passed at least two times in the medium used for the actual measurement. To calculate the growth rate μ and doubling time t_d OD_{600} values were logarithmized and plotted against time. From the slope of the curve resulting from the exponential growth phase (Equation 1), the growth rate μ (Equation 2) and the doubling time t_d (Equation 3) were calculated.

Equation 1: $m = (\ln x_t - \ln x_o) / (t-t_0)$
Equation 2: $\mu = m / \ln$
Equation 3: $t_d = \ln 2 / \mu$

2.4 Molecular biology methods

2.4.1 Isolation of chromosomal DNA from *Ms. mazei*

For the isolation of genomic DNA from *Ms. mazei* 1 mL of culture was centrifuged (25000 × *g*, 4 °C, 1 min) and the supernatant discarded. The pellet was re-suspended in sterile ddH_2O. Cells lysed upon addition of ddH_2O. Cell debris was removed by centrifugation (25000 × *g*, 4 °C, 10 min) and the supernatant was used for PCR. The preparation was always made directly before PCR.

2.4.2 Isolation of chromosomal DNA using CTAB (Ausubel *et al.*, 1987)

TE buffer (10 mM Tris pH 8, 1 mM EDTA)
SDS solution (SDS 10 % [w/v])
NaCl solution (5 M NaCl)
CTAB/NaCl solution (4.1 g NaCl solved in 80 mL H_2O_{dest}, 10 g CTAB added after warming to 50 °C, final volume 100 mL)

This method was used to extract genomic DNA from cells of *Mt. thermoacetophila*. Due to the proteinaceous sheath, which is on top of the normal cell envelope, DNA extraction with simpler methods led to low DNA yield or poor DNA quality. The method is based on the fact that DNA and CTAB precipitate at low concentrations of NaCl and can thus be separated from proteins and carbohydrates by centrifugation. CTAB can be removed by increasing the NaCl concentration, which renders DNA soluble again.

DNA was isolated from a 50 mL culture of *Mt. thermoacetophila.* Cells were harvested by centrifugation (15 min, 9000 × *g*). The pellet was re-suspended in 570 µL TE buffer. 40 µL 10% SDS solution and 5 µL proteinase K (20 mg mL^{-1}) were added and incubated for 30 min at 37 °C. Subsequently, 200 µL 5 M NaCl were included and the mixture was gently stirred. After addition of 80 µL CTAB/NaCl solution incubation for 10 min at 65 °C followed. 1.3 mL of chloroform were added prior to centrifugation (15 min, 14000 × *g*). The uppermost phase was passed into a new 1.5 mL Eppendorf cup and mixed with the same volume of phenol:chloroform 1:1. After centrifugation (15 min, 14000 × *g*) the upper phase was transferred into a new cup and mixed with 2-propanol. Another centrifugation (15 min, 14000 × *g*) was performed, 2-propanol was removed and the pellet was washed with 300 µL of ice-cold 70 % ethanol and dried at 60 °C. The purified DNA was re-suspended in ddH_2O and stored at 4 °C.

2.4.3 RNA extraction

Total RNA from *Mt. thermoacetophila* DSM 6194 was isolated by TRI Reagent® extraction. 250 mL cultures were grown to the mid- to late- exponential growth phase. The cultures were quick-chilled by shaking in a –70 °C ethanol bath for 5 min. Afterwards, cells were harvested under anaerobic conditions by centrifugation (11000 × *g*, 25 min, 4 °C). Cell pellets were re-suspended in 5 mL TRI Reagent®. Total RNA was extracted according to the manufacturer's instructions (Ambion, Darmstadt, Germany). All consumables were autoclaved twice to inactivate RNAses. Preparations were treated with DNAse I (Thermo Scientific, Schwerte, Germany) to reduce DNA contaminations. Cleaning and concentration of RNA were achieved using the SurePrep RNA Cleanup and Concentration Kit (Fisher Scientific, Schwerte, Germany). RNA preparations were checked for DNA contamination by PCR and denaturing agarose gel electrophoresis.

2.4.4 Isolation of plasmid DNA

For the preparation of plasmid DNA from *E. coli* the GeneJet™ Plasmid Miniprep Kit (Thermo Scientific, Schwerte, Germany) was used according to the manufacturer's instructions. For the preparation of high copy plasmids 2 ml of an over night culture were used, for the

preparation of low copy plasmids 10 mL of culture. The isolated plasmids were stored at 4 °C for short-term and at -20 °C for long-term.

2.4.5 Determination of DNA and RNA concentration

DNA/RNA concentrations were measured photometrically at 260 nm. Concentrations were calculated according to Equation 4 and Equation 5.

Equation 4: DNA μg mL^{-1} = A_{260} × dilution factor × 50
Equation 5: RNA μg mL^{-1} = A_{260} × dilution factor × 40

By measuring the 260 nm/280 nm ratio DNA/RNA could also be checked for protein contamination. Pure DNA has a 260 nm/280 nm ratio of 1.8 and for pure RNA the ratio is 2.

2.4.6 Polymerase chain reaction (PCR)

The polymerase chain reaction (PCR) is used for the amplification of DNA molecules *in vitro* (Mullis *et al.*, 1986). Gen-specific oligonucleotides were used as primers for the DNA polymerase (Table 4). The annealing temperature was set approximately 5 °C lower than the melting temperature of primers. Different polymerases were utilized in the course of this study. For cloning the Phusion® polymerase (Thermo Scientific, Schwerte, Germany) was used due to its high fidelity (reaction mix according to Table 7). For analytical purposes like colony PCR the Dream Taq DNA polymerase was employed (reaction mix according to Table 8). The elongation time was adjusted according to the length of the fragment and to the polymerase (Dream Taq polymerase 60 s/1000 bp, Phusion® polymerase 15 s/1000 bp).

Colony PCR was used to check plasmids for the insertion of DNA fragments after ligation and transformation. Colonies were picked in 10 µL of sterile ddH_2O. LB medium was inoculated with 5 µL of the mixture and the other 5 µL were used for PCR. For colony PCR with pASK-vectors (IBA, Göttingen, Germany) primers pASK_for and pASK_rev were employed. They were binding to the vector backbone thus amplification was independent from the insert that was cloned into the vector.

Table 7: Contents of PCR for DNA amplification with the Phusion® polymerase

Component	Final concentration
Buffer HF	1 ×
dNTPs	0.25 mM
forward primer	0.5 μM
reverse primer	0.5 μM

DMSO	5 %
Phusion® polymerase	0.5 U
DNA	0.5 µL
ddH_2O	ad 50 µL

Table 8: Contents of PCR for DNA amplification with the Dream Taq polymerase

Component	Final concentration
DreamTaq Green buffer	1 ×
dNTPs	0.125 mM
DMSO	4 %
forward primer	0.25 µM
reverse primer	0.25 µM
Taq polymerase	1.25 U
ddH_2O	ad 25 µL

2.4.7 RT-qPCR

Reverse transcription quantitative polymerase chain reaction (RT-qPCR) assays were performed to assess the relative amount of mRNA for a certain gene of interest in relation to a constitutively transcribed reference gene. RNA extraction was performed as described. Primers were designed with Primer3 (bioinfo.ut.ee/primer3/, 12.01.2015) and yielded PCR products in the range of 150 bp, except for the intergenic region between different ACS encoding genes, where products were around 300 bp. Assays routinely contained 200 ng RNA and the Quanti Tect RT-PCR SYBR® Green Mastermix (Qiagen, Hilden, Germany) was used according to the manufacturer's instructions. Primers were added to a final concentration of 1 pmol μL^{-1}. Reverse transcriptase (RT) was added according to the manufacturer's instructions. For every RNA preparation control assays without RT were performed to exclude DNA contaminations. As reference genes *mthe_0701* encoding the glyceraldehyde-3-phosphate dehydrogenase and *mthe_1722* encoding ribosomal protein S3P were utilized. The iCycler (Bio-Rad, Munich, Germany) was used for PCR with concomitant quantification of SYBR® Green fluorescence. The PCR program consisted of four cycles (Table 9). In the first cycle, RNA was translated to DNA. Afterwards the DNA polymerase was heat-activated, cycle three was a normal PCR reaction and in the end, a melting curve was recorded to assure specific product generation.

Table 9: Program for RT qPCR

Cycle	Temperature [° C]	Time [min]	Repeats
1	50	30:00	1
2	95	15:00	1
3	95	00:15	
	50	00:30	40
	72	00:30	
4	35 + 1 every cycle	00:10	60

With the iCycler software the C_t value (cycle threshold) was calculated, which was the threshold for the detection of a fluorescence signal. Values of the reference genes were subtracted from values for the genes of interest (ΔC_t = C_t (gene of interest) – C_t (reference gene)) to yield ΔC_t values. From those values the fold change in relation to the reference gene could be calculated (fold change = $2^{-\Delta Ct}$) or $\Delta\Delta C_t$ values were calculated ($\Delta\Delta C_t$ = ΔC_t (gene of interest) – ΔC_t (gene)) to evaluate the fold change in relation to another gene.

2.4.8 Restriction digest

Restriction endonucleases were employed to specifically cut DNA molecules. This led to the formation of short, single stranded overhangs called sticky ends. Complementary sticky ends could be used for the generation of new DNA molecules via ligation as catalyzed by DNA ligase.

In the course of this study among others the type IIS restriction enzyme *Eco*31I was used. It cuts in a certain distance to the site of recognition generating sticky ends with a sequence that is distinct from that of the recognition site. With this type of enzyme directional cloning with only one enzyme is made possible. The components of digestion reactions can be found below:

Plasmid DNA or PCR product	1 µL or 10 µL
Buffer according to the manufacturer's instructions	to 1 ×
Restriction endonuclease	1 µL
ddH_2O	ad 10 µL

Samples were incubated at 37 °C for at least 1 h. For plasmids alkaline phosphatase was added 30 min prior to the end of the reaction. This led to the removal of phosphate groups in order to prevent religation of the plasmid. After restriction digestion DNA fragments were

purified with the GeneJet™ PCR Clean Up Kit (Thermo Scientific, Schwerte, Germany).

2.4.9 Ligation

Ligation was used to fuse DNA fragments that were digested with restriction endonucleases. The composition of ligation reactions is summarized below:

Plasmid DNA	2 µL
PCR product	15 µL
Ligation Buffer	2 µL
T4 DNA ligase	1 µL

The mixture was incubated for 1 h at room temperature and transformed into *E. coli* DH5α (New England Biolabs, Frankfurt am Main, Germany). Plasmids carrying the correct inserts were identified with colony PCR.

2.4.10 Agarose gel electrophoresis

TAE Puffer (40 mM Tris; 20 mM acetic acid; 10 mM EDTA, pH 8.5)
6 × loading dye (bromophenol blue 0.125 % [w/v], sucrose 20 % [w/v])

Agarose gel electrophoresis was used to separate DNA fragments according to their sizes. A marker with fragments of defined length was used for calibration. Depending on the size of the fragment either the 1 kb DNA ladder (diluted according to the manufacturer's instructions) or the Low range DNA ladder (Thermo Scientific, Schwerte, Germany) were employed. Likewise depending on the size of the fragments 1-2 % agarose were solved in TAE buffer by heating. DNA samples were mixed with loading dye in a 1:6 ratio and loaded onto the gel. TAE buffer was used as running buffer and a voltage of 80 V was applied for approximately one hour.

2.4.11 Staining of agarose gels

DNA or RNA separated by agarose gel electrophoresis was stained with GelRed solution (Biotium, Hayward, USA) for approximately 10 min at room temperature. GelRed intercalates in DNA and RNA molecules and changes its absorption spectrum. Upon excitation with UV-light (wave length of 254 nm) orange fluorescent bands become visible on the gel. The fluorescence is proportional to the amount of DNA or RNA.

2.4.12 DNA sequencing

DNA sequencing was performed by StarSeq (StarSeq GmbH, Mainz, Germany). According to the manufacturer's instructions 1 μL of DNA was mixed with 1 μL of primer (10 pmol μL^{-1}) and

5 µL of ddH_2O. Analysis of sequencing data was done with Chromas Lite 2.01 (Technelysium Pty Ltd, South Brisbane, Australia).

2.4.13 Denaturing agarose gel electrophoresis

10 × MOPS buffer (0.4 M MOPS, pH 7; 0.1 M sodium acetate; 10 mM EDTA)
Loading dye (formamide 95 %, EDTA 18 mM, SDS 0.025 %, xylene cyanol 0.02 %, bromophenol blue 0.02 %)

Denaturing agarose gel electrophoresis was used to evaluate the quality of RNA preparations. In high quality RNA preparations two bands corresponding to ribosomal 23S RNA and 16S RNA are visible. 1 % agarose gels were prepared in 72 mL of H_2O_{dest}, 10 mL 10 × MOPS buffer and 18 mL 37 % formaldehyde. 1 µg of RNA were mixed with 2 × loading dye, heated for 10 min at 65 °C and loaded while still hot. 1 × MOPS was used as running buffer at 80 V. RNA was be stained with GelRed.

2.4.14 Heat shock transformation of *E. coli*

To 50 µL of supercompetent cells (New England Biolabs, Frankfurt am Main, Germany) 5 µL ligation mixture were added. After 30 min incubation on ice a heat shock was performed by incubating at 42 °C for 30 s. Cells were placed on ice for another 5 min. 950 µL SOC medium were added and than cells were incubated at 37 °C for 30-45 min. Plating was done on selective LB agar plates which were incubated over night at 37 °C.

2.4.15 Liposome mediated transformation of *Ms. mazei*

Bicarbonate/sucrose solution (sucrose 0.85 M, Na_2CO_3 4.2 g L^{-1}, DTT 5 mM, resazurin 1 µg ml^{-1})

All steps were performed anaerobically in an anaerobic chamber (Coy Laboratory Products, Grass Lake, USA). Cultures were grown to the mid-exponential growth phase. 10 mL were harvested by centrifugation (5000 × *g*, 10 min). The supernatant was discarded and cell pellets were re-suspended in 0.5 mL bicarbonate/sucrose solution. 30 µL of linearized plasmid DNA were mixed with 20 µL of bicarbonate/sucrose solution. 30 µL of DOTAP reagent (Carl Roth GmbH, Karlsruhe, Germany) were solved in 70 µL of bicarbonate/sucrose solution. The mixtures were put together and incubated for 15 min at room temperature for the formation of DNA-liposome complexes. Afterwards, the mixture was added to the harvested cells and everything was incubated for six hours. The preparation was used to inoculate 5 mL of *Ms. mazei* medium additionally containing 0.5 M sucrose. After incubation over night the culture was passed into fresh medium and incubated at 37 °C until visible

growth.

2.5 Biochemical methods

2.5.1 Aerobic protein overproduction

Proteins without oxygen-sensitive cofactors (ACS (Mthe1194) and soluble PPase (Mthe0236)) were aerobically produced in *E. coli* BL21 (DE3) containing the respective plasmids (Table 6). 100 mL of complemented MI medium were inoculated with 1 % pre-culture and incubated at 37 °C and 180 rpm until an OD_{600} of 0.6-0.7 was reached. Cultures were induced by the addition of anhydrotetracyclin (200 ng mL^{-1}) and incubated for several hours at 37 °C or over night at 25 °C. Cells were harvested by centrifugation (10 min, 4 °C, 6000 × *g*) and could be stored at -20 °C.

2.5.2 Anaerobic protein overproduction

Proteins that contain oxygen-sensitive cofactors iron sulfur clusters (Mm2093+Mm2094, Mm1619) were produced anaerobically in *E. coli* BL21 (DE3) with the respective plasmids (Table 6). The pRKISC plasmid was used to facilitate correct assembly of iron sulfur clusters. To 100 mL of complemented MI medium 1 mM cysteine, 0.1 mM $FeSO_4$ and 0.1 mM Na_2S were added and the medium was inoculated with 1 % pre-culture. The culture was incubated at 37 °C and 180 rpm until an OD_{600} of 0.8-1 was reached. Protein production was induced by the addition of IPTG, the medium was supplied with 1 mM $FeSO_4$ and 1 mM Na_2S. For IOR, additionally 0.1 mM thiamine were added. The induced cultures were incubated over night at 25 °C. Cells were harvested by centrifugation (10 min, 4 °C, 6000 × *g*) and could be stored at -20 °C.

2.5.3 Cell lysis

Cells were routinely lysed with sonication. Prior to cell lysis cultures were harvested by centrifugation (Beckman Coulter Avanti J-20XP centrifuge, JA-25.50 rotor). If necessary, DNAse I was added for DNA digestion. For the isolation of heterologously produced proteins, *E. coli* cells were suspended in buffer W (100 mM Tris-HCl, 150 mM NaCl, pH 8; 1 mL per 100 mL culture). Cells of *Mm. luminyensis* were suspended in potassium phosphate buffer (40 mM, pH 7). Cells of *Cl. pasteurianum* were suspended in water. Suspensions were treated with sonication (Bandelin Sonoplus sonicator, Bandelin Electronic, Berlin, Germany) at 4 °C for 1 min mL^{-1} at half maximal intensity.

2.5.4 Protein purification with Strep-tag affinity chromatography

Streptactin Superflow® (IBA, Göttingen, Germany)

buffer W (100 mM Tris-HCl, 150 mM NaCl, pH 8)
buffer E (buffer W + 2.5 mM desthiobiotin)
buffer R (buffer W + 1 mM HABA)

Strep-tag affinity chromatography was used to isolate heterologously overproduced proteins from cell lysate. Proteins without oxygen-labile cofactors were purified aerobically, if iron sulfur clusters were present, the whole procedure was performed in an anaerobic chamber (Coy laboratory products, USA) under a N_2+H_2 (98:2) atmosphere. For anaerobic protein purification 5 mM DTT were added to every buffer. Cells were lysed and the lysate was centrifuged (9000 × *g*, 4 °C, 15 min) and applied to the pre-equilibrated Streptactin column. The loaded column was washed with 5 × 1 CV buffer W and afterwards the purified protein was eluted with 6 × 0.5 mL buffer E. Regeneration was performed using 2 × 4 CV buffer R which was removed again with buffer W. Protein contents were measured as described and purified proteins were stored at -70 °C.

2.5.5 Determination of protein concentration

Protein concentrations were routinely measured according to Bradford (Bradford, 1976). Therefore, 980 µL of Bradford reagent obtained from Sigma-Aldrich (Munich, Germany) were mixed with 20 µL of sample. After incubation for 10 min at room temperature in the dark absorption at 595 nm was measured. Protein concentrations were determined according to a BSA calibration curve.

The concentration of ferredoxin from *Cl. pasteurianum* and ferredoxin Mm1619 heterologously from *Ms. mazei* produced in *E. coli* could not reliably be quantified with the Bradford assay. Therefore, ferredoxin concentrations were measured with the BCA assay which is a modified Biuret assay. The assay is very sensitive because Cu^{1+} ions complexed with protein are additionally chelated by BCA resulting in a deep violet staining. In this study the BCA Protein Assay Kit (Novagen, Merck KgaA, Darmstadt, Germany) was utilized according to the manufacturer's instructions. 10-20 µL sample were mixed with 200 µL BCA reagent, incubated 30 min at 37 °C and measured in the Nano Quant Infinite M200 plate reader (Tecan, Crailsheim, Germany) at 562 nm. The protein concentration was determined according to a BSA calibration curve.

2.5.6 Sodium dodecyl sulfate polyacrylamide gel electrophoresis (SDS-PAGE)

Loading buffer (bromophenol blue 0.01 % [w/v], β-mercaptoethanol 0.05% [v/v], glycerol 50 % [v/v])
Collecting buffer (600 mM Tris, pH 6.8)
Separation buffer (1,8 M Tris, pH 8.8)

SDS solution (SDS 0.5% [w/v]
APS solution (APS 10 % [w/v])
Electrode buffer (20 mM Tris, 190 mM Glycin, SDS 0.1 % [w/v], pH 8.3)

SDS-PAGE according to Laemmli (Laemmli, 1970) was used to separate proteins according to their molecular mass in a polyacrylamide gel matrix (composition according to Table 11). For molecular mass determination the PageRuler prestained protein ladder (Thermo Scientific, Schwerte, Germany) was used. Gels were run in vertical mini-chambers purchased from Bio-Rad (Munich, Germany). Prior to loading, samples were mixed with loading buffer in a 1:1 ratio and denatured by heating for 5 min at 95 °C. Gel runs were performed with 20 mA in the collecting gel and 30 mA in the separating gel.

Table 11: Composition of SDS polyacrylamide gels used in this study

Component	Collecting gel 5 %	Separating gel 10 %	Separating gel 12.5 %
Acrylamide solution (Rotiphorese Gel 40)	250 µL	1.5 mL	2 mL
Separation buffer	-	1.2 mL	1.2 mL
Collecting buffer	400 µL	-	-
SDS solution	400 µL	1.2 mL	1.2 mL
ddH_2O	950 µL	2.1 mL	1.6 mL
TEMED	5 µL	5 µL	5 µL
APS	30 µL	30 µL	30 µL

2.5.7 Silver stain

Fixing solution (methanol 50 % [v/v], acetic acid 12 % [v/v], formaldehyde 0.05 % [v/v])
Thiosulfate solution (thiosulfate 0.02 % [w/v])
Silver nitrate solution (silver nitrate 0.1 % [w/v])
Developing solution (Na_2CO_3 3 % [w/v], formaldehyde 0.1 % [v/v])

Silver staining was used to visualize proteins, which were separated by SDS-PAGE. Divalent silver ions bind to the proteins in the gel matrix, which become visible upon silver ion reduction. The detection limit of this method is approximately 1 ng per protein band. Gels are incubated in fixing solution for at least 20 min, followed by 10 min incubation in 50 % methanol and afterwards 10 min ddH_2O. The gel is neutralized by thiosulfate solution (1 min)

and rinsed with ddH_2O (1 min). Afterwards, it is incubated with silver nitrate solution (4 °C in the dark) and subsequently incubated with developer solution until bands become visible.

2.5.8 Fast protein liquid chromatography

For the determination of the molecular mass of Mthe0236 from *Mt. thermoacetophila* gel filtration chromatography was performed with an Äkta system (GE Healthcare, Munich, Germany). Gel filtration chromatography is based on the fact that smaller proteins are retained on the column while larger ones elute earlier. For calibration the Kit for Protein Molecular Weights, 29,000–700,000 (Sigma-Aldrich, Munich, Germany) was employed. It contains the carbonic anhydrase (29 kDa), bovine serum albumine (66 kDa), alcohole dehydrogenase (150 kDa), β-amylase (200 kDa), apoferritin (443 kDa) and thyroglobulin (669 kDa). For determination of the void volume v_0 Blue Dextran was employed. The void volume was 44.5 mL and the column volume v_c was 120.6 mL. The elution volume v_e of proteins used for calibration was measured and K_{av} values were determined according to Equation 6.

Equation 6: $K_{av} = (v_e – v_0) / (v_t - v_0)$

K_{av} was plotted against the decadal logarithm of the molecular mass of the proteins used for calibration, and the resulting curve was used for molecular mass determination. For the determination of the molecular mass of the native Mthe0236 enzyme, a Hi Load 16/60 Superdex 75 prep grade column was equilibrated with 40 mM Tris-HCl pH 8 with 150 mM NaCl and 1 mM $MnCl_2$. Mthe0236 was produced in *E. coli* and purified as described. 1.5 mg protein were loaded onto in the pre-equilibrated column. The run was performed with the above-mentioned buffer at a flow rate of 0.5 mL min^{-1}. V_e was determined for Mthe0236 and the molecular mass was determined according to the calibration curve.

2.5.9 Generation and purification of the FpoI antibody

Phosphate buffer saline (PBS buffer; 8 g NaCl, 0.2 g KCl, 0.5 g $Na_2HPO_4 \times 7\ H_2O$, 0.2 g KH_2PO_4 ad 1 L H_2O_{dest})

An antibody directed against subunit FpoI from the Fpo complex from *Ms. mazei* was obtained by immunization of a rabbit and subsequent purification of the antibody from blood serum. Recombinant FpoI protein for antibody generation was supplied by Sarah Refai (Rheinische-Friedrich-Wilhelms Universität Bonn, Germany). Antibody production was performed by Seqlab (Göttingen, Germany).

FpoI from *Ms. mazei* was produced and purified as described. Affi-Gel 10 (Bio-Rad, Munich, Germany) was centrifuged (4500 × *g*, 1 min) until 0.5 mL of column material were obtained.

The material was washed in 100 mM $NaHCO_3$ pH 8.5 for three times. 7 mg of recombinant FpoI protein in 100 mM $NaHCO_3$ pH 8.5 were added to the column material and incubated at 4 °C for 1 h with shaking at 500 rpm. Afterwards, the column material was collected by centrifugation (5000 × *g*, 1 min). Unreacted esters were blocked by addition of 333 mM ethanolamine in 100 mM $NaHCO_3$ pH 8.5 and incubation for 1 h at 4 °C.

The ready-made Affi-Gel was filled into a chromatography column and washed ten times with 0.5 mL PBS buffer with 1 M NaCl. Blood serum was stored at -20 °C. Prior to purification it was thawed and 1 mL of serum was centrifuged (5000 × *g*, 10 min). The supernatant was applied to the column. The loaded column was washed ten times with 0.5 mL Tris-HCl 10 mM, pH 7.5 and ten times with 0.5 mL Tris-HCl 10 mM, 0.5 M NaCl, pH 7.5. For elution 1.5 mL Eppendorf cups were filled with 0.25 mL Tris-HCl pH 8. Elution was done with 0.5 mL glycine 100 mM pH 2.5. The fractions were collected in the above-mentioned cups for immediate neutralization. The column was washed with 10 mM Tris-HCl pH 8.8 and stored in 0.2 [w/v] sodium azide. The purified antibody could be stored at -70 °C.

2.5.10 Isolation of Fd from *Cl. pasteurianum*

Ferredoxins are small, acidic proteins and act as important electron carriers in anaerobic metabolism. Therefore, they are an essential component for many experiments. Different ferredoxins exist which are often functionally interchangeable. In this study, *Clostridium* (*Cl.*) *pasteurianum* was used as a source for ferredoxin used to analyse the soluble heterodisulfide reductase from *Mm. luminyensis*.

For ferredoxin isolation 4 L of *Cl. pasteurianum* culture were grown anaerobically, cells were harvested aerobically for 20 min at 8000 × *g* and lysed by sonication. All proteins except flavins and ferredoxin were precipitated by addition of an equal volume of ice-cold aceton. After centrifugation (10000 × *g*, 15 min, 4 °C) the supernatant was applied to a DEAE cellulose column for anion exchange chromatography. A dark-brown ring representing ferredoxin appeared at the upper part of the column. By washing with 200 mM Tris-HCl buffer pH 8 flavins were removed from the column. Accordingly a yellowish washing fraction was collected. For elution of ferredoxin 500 mM Tris-HCl buffer pH 8 was employed. 5 mL fractions were collected and ferredoxin eluted in a narrow peak as judged by the brown colour of the respective fractions. Fractions were pooled and concentrated by ultrafiltration with Centricon ultrafiltrators (cut-off 5 kDa, Merck Millipore, Schwalbach, Germany) until a final concentration of 14 mg mL^{-1}. Aliquots were stored aerobically at -70 °C.

2.5.11 Preparation of membrane fractions

Potassium phosphate buffer (potassium phosphate 40 mM, pH 7)

The whole preparation was performed anaerobically in an anaerobic chamber (Coy laboratory products, USA). Cultures of *Ms. mazei* and *Mm. luminyensis* were grown to the exponential growth phase. Cells were harvested by centrifugation (6000 × *g*, 20 min, 4 °C) and were re-suspended in potassium phosphate buffer (40 mM, pH 7). Cells of *Ms. mazei* lysed upon the addition of buffer, whereas cells of *Mm. luminyensis* were lysed with sonication. The lysate was ultracentrifuged at 150000 × *g* (1.5 h, 4 °C). After that, two fraction were obtained: the supernatant, which contained the cytoplasmic compounds and a pellet, which consisted mainly of membranes. For tests with the cytoplasmic fraction, the supernatant was used. For tests with the membrane fraction as an additional washing step, the pellet was suspended in potassium phosphate buffer (40 mM, pH 7) and again centrifuged (150000 × *g,* 1.5 h, 4 °C). Membrane fractions of *Mm. luminyensis* and *Ms. mazei* could be stored at -70 °C under an H_2 atmosphere.

2.5.12 Purification of the cofactor F_{420} from *Methanotorris igneus*

The cofactor F_{420} is an electron carrier molecule and due to its absorbance at 420 nm it can be used for various photometric assays. In the course of this study it was purified from the methanogenic archaeon *Methanotorris igneus*.

200 g cell mass were kindly provided by Harald Huber (Universität Regensburg, Germany). Cells were thawed in an anaerobic chamber and re-suspended with anaerobic Tris-HCl buffer (150 mL, 50 mM Tris-HCl pH 7.5, 0.3 M NaCl). DNAse I was added for DNA digestion. Afterwards, F_{420} was extracted with acetone (50 % v/v). The extract had a bright reddish colour with a yellow-greenish glimmer. In the following, steps were carried out under aerobic conditions. The extract was applied to a pre-equilibrated QAE-Sephadex A50 column (10 × 3 cm). F_{420} possesses multiple glutamate side chains that bound to this anion exchange material. Hence, a dark green ring representing the concentrated F_{420} appeared at the upper part of the column. The flow-through still had a bright red colour but had lost its yellow-greenish glimmer. After a washing step with 50 mM Tris-HCl pH 7.5 and 50 mM NaCl the F_{420} was eluted with a NaCl gradient (0-1 M in 50 mM Tris-HCl pH 7.5). The elution fractions (10 mL) were tested for absorbance at 420 nm and high absorbance of up to 2.4 was measured. Fractions with an absorbance higher than 0.7 were pooled, diluted with H_2O to a NaCl concentration of 50 mM and again applied to a QAE-Sephadex column pre-equilibrated with 10 mM HCl. Since F_{420} becomes colourless under acidic conditions only a slight greenish glimmer was retained when the elution fractions were applied to the column. After washing with 10 mM HCl F_{420} was eluted with 150 mL of 30 mM HCl. The elution fraction was adjusted to pH 7 and turned from slightly greenish to a bright yellow-green colour. The solution was lyophilized and a final volume of 13.5 mL was obtained. Photometrically a concentration of 2 mM F_{420} was determined. This was sufficient for approximately 1000

enzymatic assays. The purity of the compound was assayed by recording a spectrum between 200 and 650 nm (Figure 4). A major peak could be observed at 420 nm, which is known to be the absorption maximum. Several minor peaks were observed around 250 nm, which were all in accordance with previous records of the pure compound. Hence, the electron carrier molecule F_{420} was isolated in considerable amounts and to high purity.

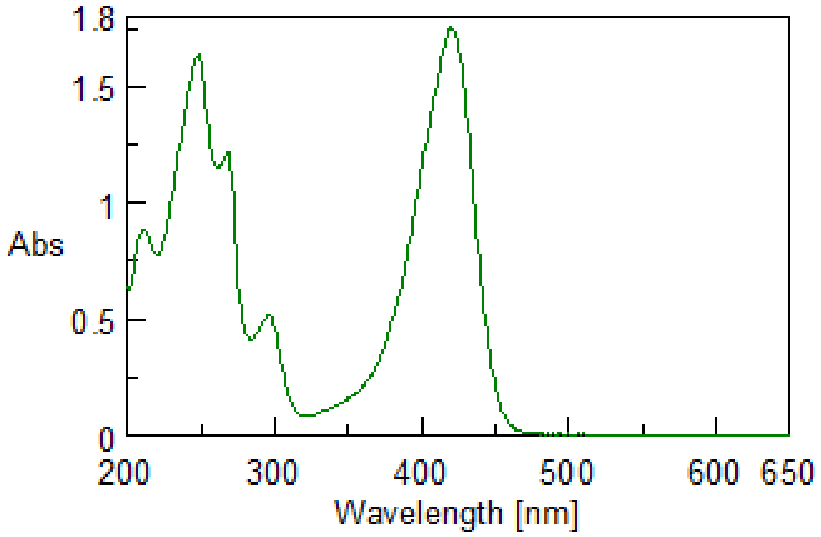

Figure 4: Spectrum of the purified cofactor F_{420} – a major peak could be observed at 420 nm, which is known to be the absorption maximum.

2.5.13 Reduced F_{420}

If F_{420} should be used as electron donor it had to be reduced with $NaBH_4$. Therefore, 200 µL of 2 mM F_{420} were filled into a glass vial. $NaBH_4$ was added under N_2 until the preparation became colourless. The pH was titrated to pH = 0 with 1 M anaerobic HCl to remove excess $NaBH_4$. The pH was brought to pH = 7 with 1 M anaerobic NaOH. The vial was sealed with a gas-tight rubber stopper and $F_{420}H_2$ was used immediately.

2.6 Analytical techniques

2.6.1 Chemical detection of DMA and MMA

Cu^{2+} solution (ammonium acetate (20 g), $CuSO_4$ (0.2 g), NaOH (10 g), NH_4OH (20 mL), ad 100 mL H_2O_{dest})

Acetylacetone/formaldehyde solution (4 mL acetylacetone, 10 mL formaldehyde (30 %) ad 150 mL H_2O_{dest})

DMA and MMA can be used as methanogenic substrates. In the course of this study breakdown of DMA and MMA by *Mm. luminyensis* was tested. Therefore, 1 mL samples were anaerobically taken from cultures growing with 75 mM MMA or 37.5 mM DMA. Samples were centrifuged for 5 min at 10000 × *g*, the cell-free supernatant was transferred to a 1.5 mL Eppendorf cup and could be stored at -70 °C. DMA concentrations were measured by the copper dithiocarbamate method. Samples were thawed and to 100 µL of sample 400 µL of H_2O_{dest} were added. The sample was mixed with 50 µL of Cu^{2+} solution. After that 500 µL of carbon disulfide in benzene (5% [v/v]) and 50 µL acetic acid (30% [v/v]) were added and the solution was centrifuged for 1 min at 10000 × *g*. Finally, absorption at 430 nm could be measured. For MMA determination 50 µL samples were mixed with 200 µL Na-acetate buffer (100 mM, pH 5.6). 300 µL acetylacetone/formaldehyde solution and 450 µL acetone were added and the mixture was incubated for 5 min at 95 °C. After cooling on ice the absorption at 410 nm was measured. Calibration curves were recorded using solutions with known concentrations of MMA and DMA in the same medium that was used for cultivation of *Mm. luminyensis* (*Methanobrevibacter* medium with 5 % sludge fluid [v/v]). For MMA, concentrations between 0 and 100 mM were used and for DMA concentrations ranged between 0 and 50 mM.

2.7 Enzyme activity assays

In the course of this study the reaction rate of different enzymatic systems was investigated. Firstly, the heterologously produced ACS and PPase enzymes from *Mt. thermoacetophila* have been characterized. Secondly, activity of different membrane-bound enzymes was measured in membrane fractions of *Ms. mazei* and *Mm. luminyensis.* Lastly, soluble heterodisulfide reductase activity was measured in the cytoplasmic fraction of *Mm. luminyensis*.

Product formation was measured photometrically, either directly or after chemical detection of the desired product. One unit is defined as one µmol substrate min^{-1}. Reaction rates were calculated according to Equation 7.

Equation 7: $U/mg = ((\Delta E/min * d_f)/(d * \varepsilon * v)) / c$

$\Delta E/min$ = change in extinction min^{-1}
ε = molar extinction coefficient [mM^{-1} cm^{-1}]
c = protein concentration [mg mL^{-1}]
d = layer thickness of the cuvette [cm]
d_f = dilution factor

2.7.1 Acetyl-CoA synthetase: enzyme assay with auxiliary enzymes

Two different assays were used for the characterization of the ACS. In an assay with auxiliary enzymes the reaction of the ACS was coupled to the reactions of myokinase (MK), pyruvate kinase (PK) and lactate dehydrogenase (LDH) (Figure 11, modified after (Meng *et al.*, 2010)). Enzymes were obtained from Sigma-Aldrich (Munich, Germany) and were used in non-limiting amounts (5.7 U MK, 2.3 U PK and 2.1 U LDH). Furthermore, the assay contained 50 mM HEPES pH 7.5, 5 mM $MgCl_2$, 3 mM PEP, 1 mM CoA, 2.5 mM ATP, 1 mM DTT, 20 mM Na-acetate and 0.15 mM NADH. The reaction was started by the addition of the ACS. Since 55 °C is the optimal growth temperature of *Mt. thermoacetophila*, assays were performed at this temperature. The decrease in absorption at 340 nm was measured with the Jasco V-650 UV/VIS spectrophotometer (Jasco, Groß-Umstadt, Germany). The method was used to determine the K_M value for acetate. The acetate concentration was varied between 5 μM and 20 mM. For calculation of enzymatic activity according to Equation 7, a molar extinction coefficient of 6.2 mM^{-1} cm^{-1} was used.

2.7.2 Acetyl-CoA synthetase: enzyme assay with pyrophosphate detection method

β-mercaptoethanol (0.5 M)
Ammoniumtetramolybdate solution (2.5 % [w/v] in 5 N H_2SO_4)
Eikonogen reagent (0.25 g sodium sulfite, 14.65 g potassium disulfate and 0.25 g 1-amino-2-naphthol-4-sulfonic acid dissolved in 80 mL 80 °C hot H_2O_{dest}, cooled to room temperature, filled to 100 mL and filtered)
Trichloroacetic acid (12 % [w/v])

Detection of PP_i was modified after (Kuang *et al.*, 2007). The method is specific for PP_i and is not disturbed by a 10-fold excess of P_i. A molybdate complex is formed, which upon reduction develops an intense blue color. K_M values for ATP and CoA were determined with this method. The assay contained 50 mM HEPES pH 7.5, 5 mM $MgCl_2$, 1 mM DTT and 1 mM CoA. The reaction temperature was set to 55 °C. ATP concentrations were varied between 7.5 μM and 1 mM; CoA concentrations were varied between 10 to 150 μM. 380 μL samples were taken at different time points and the reaction was stopped with 380 μL trichloroacetic acid. Afterwards, 100 µL of ammoniumtetramolybdate solution, 100 µL of 0.5 M β-mercaptoethanol and 40 µL of the Eikonogen reagent were added. Samples were incubated for 15 min at 37 °C and the absorption at 580 nm was measured. PP_i concentrations were determined according to a standard curve (0-0.5 mM PP_i). The specific enzyme activity was calculated according to Equation 7. $(\Delta E/min)/\varepsilon$ was replaced by $\Delta c/min$ (change of concentration of product per min).

2.7.3 Pyrophosphatase enzyme activity assay

Molybdate reagent (15 mM ammonium tetramolybdate, 100 mM zinc acetate, pH 5 with HCl)
Ascorbic acid (10 % [w/v], pH 5 with NaOH)
Trichloroacetic acid (10 % [w/v])

PPase activity was measured in a discontinuous assay. Samples were taken at different time points and P_i was measured as blue molybdate complex (method modified after (Saheki *et al.*, 1985)). Prior to the measurement the enzyme was activated with Mn^{2+}. Therefore, it was incubated in 40 mM Tris buffer pH 8 with 1 mM $MnCl_2$ for 5 min at room temperature (protein concentration 0.5 mg mL^{-1}). The reaction buffer contained 40 mM Tris pH 8, 5 mM $MgCl_2$ and 1 mM PP_i. The reaction was started by the addition of 1.25 µg of PPase. For K_M value determination, the concentration of PP_i was varied between 0.125 mM and 3 mM. 25 µL of sample were taken at different time points and the reaction was stopped by the addition of 5 µL of trichloroacetic acid. 750 µL and 250 µL of molybdate reagent were added. Samples were incubated at 30 °C for 15 min and the extinction at 850 nm was measured photometrically (HeliosEpsilon, Thermo Scientific, Schwerte, Germany). P_i concentrations were calculated according to a calibration curve. The specific enzyme activity was calculated according to Equation 7. (ΔE/min)/ε was replaced by Δc/min (change of concentration of product per min).

2.7.4 Ellman assay

The Ellman assay (Ellman, 1958) is used to determine free thiol groups, e.g. of the thiols HS-CoM and HS-CoB. In enzymatic assays, 20 µL of sample were mixed with 950 µL 150 mM Tris-HCl pH 8.1 and 100 µL DTNB (5 mM in 50 mM Na-acetate, pH 5.0). The absorption of the sample was immediately measured at 412 nm. During the synthesis of the heterodisulfide, 100 µL sample were mixed with 950 µL 150 mM Tris-HCl pH 8.1 and a small amount $NaBH_4$ to reduce disulfides to thiols. Then 100 µL acetone were added to remove the excess $NaBH_4$. Then thiols were photometrically detected at 412 nm after addition of 100 µL DTNB (5 mM in 50 mM Na-acetate, pH 5.0).

2.7.5 Membrane-bound Ferredoxin: heterodisulfide oxidoreductase enzyme assay

Ferredoxin-dependent heterodisulfide reduction was measured using indolpyruvate: ferredoxin oxidoreductase (IOR, (Bock *et al.*, 1996)) for ferredoxin reduction and the Ellman's assay for the quantification of CoM and CoB thiols. The assay was performed in rubber-stoppered glass vials under an N_2 atmosphere in 200 µL potassium phosphate buffer (40 mM, pH 7.0, 1 µg mL^{-1} resazurin, reduced with Ti(III)-citrate), 1 mM CoA, 0.5 mM thiamine pyrophosphate, 4 mM phenylpyruvate, 1.25 mM heterodisulfide, 150 µg IOR,

100 µg Fd Mm1619, and 250 µg membrane fraction. Enzymatic activity was calculated according to Equation 7.

2.7.6 Membrane-bound H_2: heterodisulfide oxidoreductase enzyme assay

Hydrogen-dependent heterodisulfide reduction was measured in rubber-stoppered glass vials under an H_2 atmosphere in 200 µL potassium phosphate buffer (40 mM, pH 7.0, 1 µg mL^{-1} resazurin, reduced with Ti(III)-citrate) with 1.25 mM heterodisulfide and 100 µg membrane fraction. Enzymatic activity was calculated according to Equation 7.

2.7.7 Membrane-bound $F_{420}H_2$ dehydrogenase enzyme activity assay

The activitiy of the $F_{420}H_2$ dehydrogenase was determined photometrically at 420 nm, the absorbance maximum of cofactor F_{420}.The assay was performed anaerobically in a rubber-stoppered glass cuvettes under an N_2 atmosphere in 600 µL potassium phosphate buffer (40 mM, pH 7.0, 1 µg mL^{-1} resazurin, 5 mM DTT). The assay contained 70 µM $F_{420}H_2$ (ε = 40 mM^{-1} cm^{-1}), 50 µg membrane fraction and MV (0.3 mM) as electron mediator and MTZ (0.5 mM) as terminal electron acceptor. Specific enzyme activity was calculated according to Equation 7.

2.7.8 Membrane-bound $F_{420}H_2$: heterodisulfide oxidoreductase enzyme assay

Activity of the $F_{420}H_2$ dehydrogenase coupled to heterodisulfide reduction was measured photometrically at 420 nm essentially as described for measuring enzyme activity for $F_{420}H_2$ dehydrogenase with the exception that MV/MTZ were replaced by 50 µM heterodisulfide. Specific enzyme activity was calculated according to Equation 7.

2.7.9 BV-mediated heterodisulfide oxidoreductase enzyme assay

Heterodisulfide reductase individually was measured with BV as electron donor and heterodisulfide as electron acceptor. The assay was performed in an anaerobic rubber-stoppered glass cuvette under an N_2 atmosphere in 600 µL potassium phosphate buffer (40 mM, pH 7.0, 1 µg mL^{-1} resazurin, 5 mM DTT) with cytoplasmic or membrane fraction as indicated in the respective results part and 1 mM BV that was reduced to an absorption at 575 nm of 1-1.5 with a freshly prepared 100 mM dithionite solution. The activity was followed photometrically at 575 nm and the specific enzyme activity was calculated according to Equation 7with a molar extinction coefficient of 8.9 mM^{-1} cm^{-1} for BV.

2.7.10 MV-coupled hydrogenase enzyme assay

Hydrogenase enzyme activity was determined in rubber-stoppered anaerobic glass cuvettes under an H_2 atmosphere. The assays contained 600 µL potassium phosphate buffer (40 mM,

pH 7.0, 1 μg mL^{-1} resazurin, 5 mM DTT), cytoplasmic or membrane fraction as indicated in the respective results part and MV (ε = 13.6 mM^{-1} cm^{-1}, 8 mM) as final electron acceptor. The activity was followed photometrically at 604 nm. Specific enzyme activity was calculated according to Equation 7.

2.7.11 Enzyme activity measurement of Ech hydrogenase

Activity of Ech hydrogenase was measured in rubber-stoppered glass vials under an N_2 atmosphere. Evolution of hydrogen dependent on ferredoxin oxidation was followed by gas chromatography (GC-14A, Shimadzu, Japan) coupled to a thermal conductivity detector (current 50 mA). Carrier gas was argon, injector temperature was 120 °C, detector temperature 100 °C and column temperature 40 °C. The hydrogen peak was observed with a retention time of 0.9 min with an argon flow of 30 mL min^{-1}. The assay contained 200 μL potassium phosphate buffer (40 mM, pH 7.0, 1 μg mL^{-1} resazurin, 5 mM DTT), 1 mM CoA, 0.5 mM thiamine pyrophosphate, 4 mM phenylpyruvate, 150 μg IOR, 100 μg Fd Mm1619, and 250 μg membrane fraction. Enzymatic activity was calculated according to an H_2 calibration curve.

2.7.12 Enzyme activity measurement of the soluble bifurcating HdrABC/MvhADG complex

Enzyme activity of the soluble HdrABC/MvhADG complex was performed in rubber-stoppered anaerobic glass cuvettes under an H_2 atmosphere. The assay contained 300 μL potassium phosphate buffer (40 mM, pH 7.0, 1 μg mL^{-1} resazurin, 5 mM DTT), 300 μL cytoplasmic fraction, 40 μM NADP$^+$, 10 μg clostridial ferredoxin, 0.125 mM heterodisulfide and 10 U spinach ferredoxin: NADP$^+$ reductase (Sigma-Aldrich, Munich, Germany). In this assay, hydrogen was oxidized and the electrons transferred to heterodisulfide and ferredoxin in a bifurcation mechanism; ferredoxin was subsequently oxidized by spinach ferredoxin: NADP$^+$ reductase to yield NADPH that was photometrically measured at 340 nm (ε = 6.2 mM^{-1} cm^{-1}).

2.8 Organic chemistry

2.8.1 Chemical synthesis of the heterodisulfide

The heterodisulfide from CoM-SH and CoB-SH, CoM-S-S-CoB, is the terminal electron acceptor of the methanogenic respiratory chain. Therefore, for many experiments it is an indispensable component. Since it is not commercially available, it was chemically synthesized in the course of this study according to (Welte and Deppenmeier, 2011c). CoB-SH was synthesized from the commercially available precursor bromoheptanoic acid ethyl

ester and coupled to the likewise purchasable CoM-SH. The scheme of the chemical synthesis can be viewed in Figure 5. First, the bromine group of the bromoheptanoic acid ethyl ester (reaction mixture contained 17.8 g) was replaced by thiourea yielding a thiuronium salt. This compound was saponified by boiling in an alkaline solution to produce thioheptanoic acid. After repeated extraction with chloroform at pH < 1 and 1 M Na_2CO_3 production of a thiol was proven in an Ellman's assay. In the next step dithioheptanoic acid was produced through oxidation by I (10 % w/v) / KI (20 % w/v) solution. The yield was about 2 g. Dithioheptanoic acid reacted with N-hydroxysuccinimide and dicyclohexylcarbodiimide to N-hydrosuccinimide ester. After washing the N-hydroxysuccinimide ester with isopropanol, L-threonine phosphate was added and replaced the imide group. The product of the reaction was 7-mercapto-heptanoyl-threonine phosphate also termed CoB-SH. CoB-SH was fully reduced by addition of $NaBH_4$. The reduced compound was combined with fivefold excess CoM-SH and the mixture exposed to air. Incubation for 16 h led to production of the heterodisulfide CoM-S-S-CoB which was subsequently purified by hydrophobic interaction chromatography. Dithioheptanoic acid and N-hydroxysuccinimide ester were solved in deuterized DMSO and subjected to ^{1}H and ^{13}C NMR analysis and synthesis of the respective products was confirmed. Both compounds were pure. The NMR analyses (Bruker Avance dpx400, Bruker, Leiderdorp, The Netherlands) were performed with the settings 300 Mhz, RT, δ [ppm]. The spectra for dithioheptanoic acid can be viewed in Figure 6 and for N-hydroxysuccinimide ester in Figure 7. The biological activity of heterodisulfide was tested with *Ms. mazei* membrane fraction in a photometric assay. From the change in absorption it was calculated that 100 μmol of CoM-S-S-CoB were produced, which was sufficient for approximately 250 enzymatic assays.

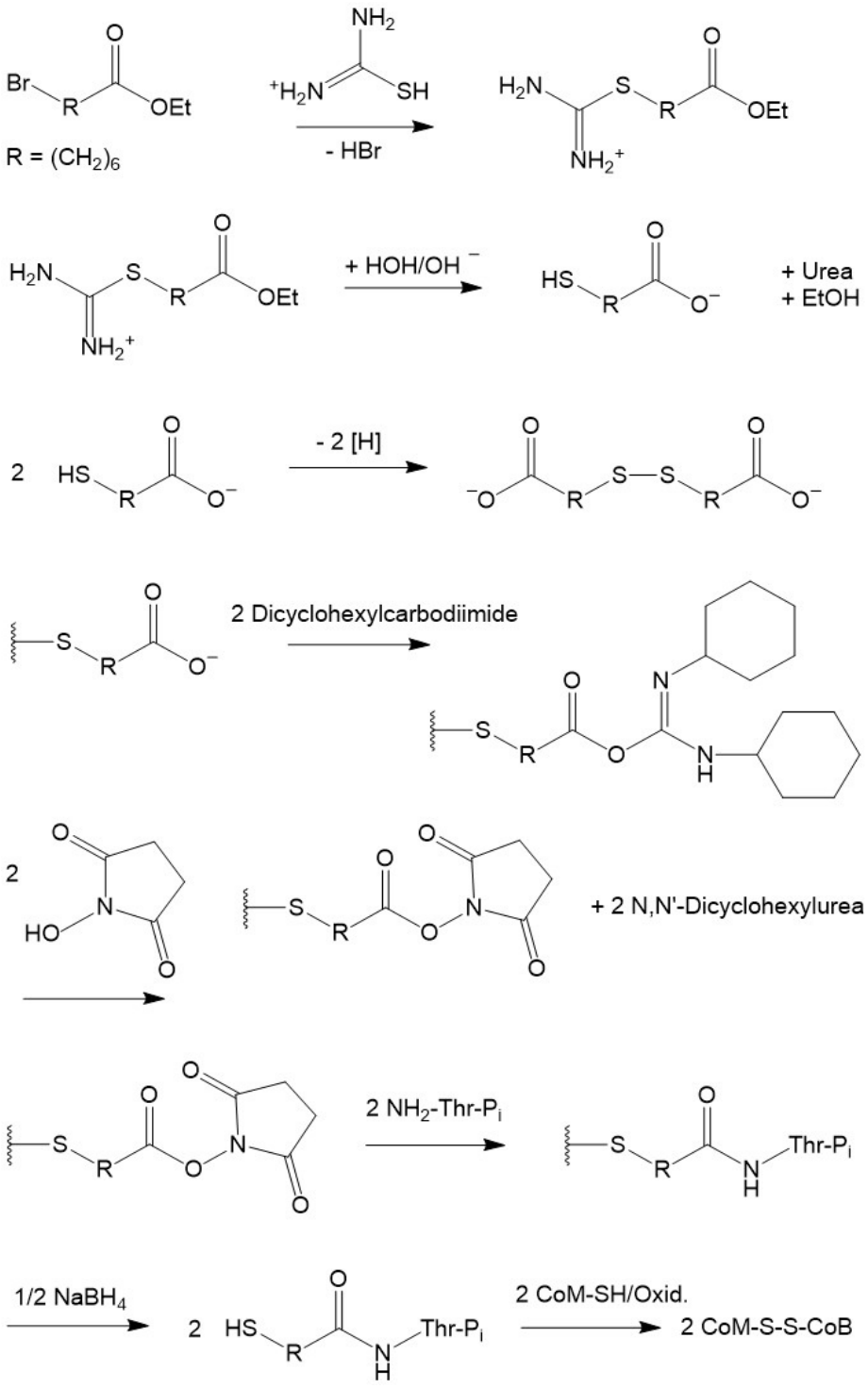

Figure 5: Chemical synthesis of the heterodisulfide. Bromo heptanoic acid ethyl ester was used as a precursor for the synthesis of CoB-SH. After various steps the ready-made CoB-SH was coupled to CoM-SH through oxidation by aerial oxygen. The product of this reaction was the heterodisulfide CoM-S-S-CoB.

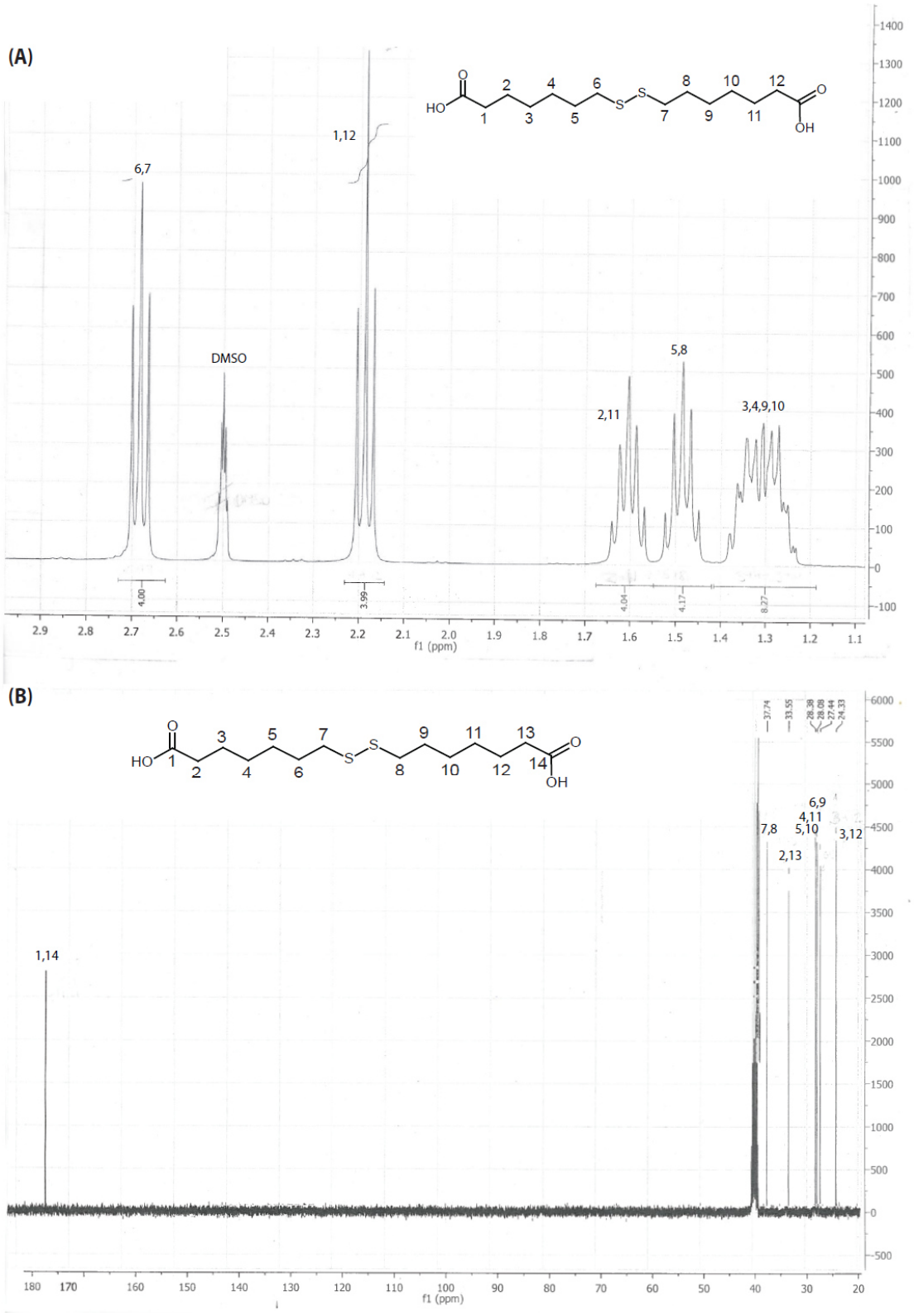

Figure 6: NMR spectra of dithioheptanoic acid. Dithioheptanoic acid was subjected to ^{1}H-NMR (A) and ^{13}C-NMR (B) to check the purity of the compound after synthesis from bromoheptanoic acid ethyl ester. A Bruker Avance dpx400, (Bruker, Leiderdorp, The Netherlands) was used (300 Mhz, RT, δ [ppm]). Since all peaks were matching with the molecule, only dithioheptanoic acid was produced.

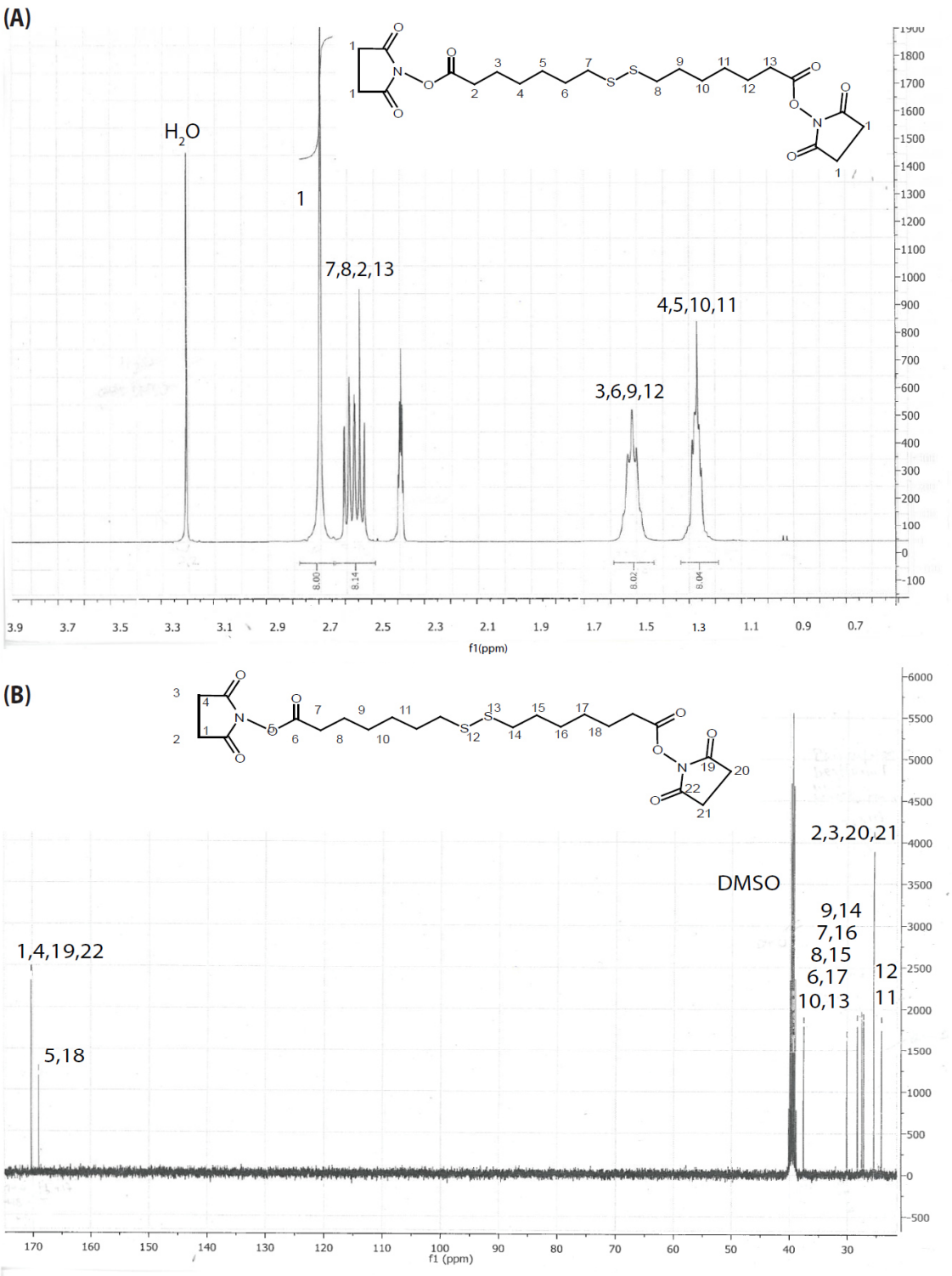

Figure 7: NMR spectra of N-hydroxysuccinimide ester. N-hydroxysuccinimide ester was analyzed with ^{1}H-NMR (A) and ^{13}C-NMR (B) with a Bruker Avance dpx400, (Bruker, Leiderdorp, The Netherlands; 300 Mhz, RT, δ [ppm]) to check generation of the right product from dithioheptanoic acid, N-hydroxysuccinimide and dicyclohexylcarbodiimide. Since all peaks could be assigned to the structure of the molecule, N-hydroxysuccinimide ester was produced.

2.9 Bioinformatic methods

Genomes were browsed in KEGG (http://www.genome.jp/kegg/) or NCBI (http://www.ncbi.nlm.nih.gov/).

For genome analysis of *M. luminyensis*, the BLAST (Basic Local Alignment Search Tool) from NCBI (http://blast.ncbi.nlm.nih.gov/Blast.cgi) was used. Accession numbers of queries and hits are noted in the results part of this thesis.

Alignments of protein or gene sequences were performed with ClustalW2 (http://www.ebi.ac.uk/Tools/msa/clustalw2/).

Prosite (http://prosite.expasy.org/) was used to investigate putative functions and prosthetic groups of proteins of unknown function, e.g. FpoO.

3. RESULTS

In this study, different aspects of energy metabolism in three different methanogenic archaea were analyzed. In the first part, acetate metabolism in the obligate aceticlastic *Mt. thermoacetophila* was investigated. Acetate has to be activated at the expense of ATP before it is metabolized. Thus, in the first part of this work, genes and the respective enzymes probably involved in the acetate activation reaction were examined.

In the second part, a closer look was taken at the Fpo complex from *Ms. mazei*. In methylotrophic methanogenesis, the Fpo complex catalyzes oxidation of $F_{420}H_2$. However, it was proposed that it could also be involved in methanogenesis from acetate (Welte and Deppenmeier, 2011a). In this pathway reducing equivalents are transferred to Fd, which was shown to be re-oxidized by the Ech hydrogenase. Nevertheless, membranes of a *Ms. mazei* Δ*ech* deletion mutant could still perform Fd_{red} oxidation (Welte *et al.*, 2010b). It was concluded that another enzyme besides the Ech hydrogenase was able to catalyze the reaction. The Fpo complex is considered as a potential candidate. In the course of this study, an antibody against subunit FpoI was generated and used for inhibition studies. Fd_{red} oxidation by the Fpo complex would also have an impact on energy metabolism in *Mt. thermoacetophila*, which is missing all Fd_{red} oxidizing respiratory enzymes that are known to date. However, an *fpo* operon could be found in the genome (Smith and Ingram-Smith, 2007).

The last part of this thesis deals with *Mm. luminyensis*, a newly discovered methanogen isolated from the human gut (Dridi *et al.*, 2012). It is only distantly related to the above-mentioned methanogens, yet is closely related to the euryarchaeotic lineage of Thermoplasmatales. Substrates for methanogenesis are methylated compounds and H_2. This raises the question how this unusual combination of substrates is metabolized. According to genome sequence data, a comparably unusual set of genes encoding enzymes probably involved in methanogenesis and energy conservation is present. A comprehensive genome analysis and first biochemical data will be presented.

3.1 Acetate activation in *Mt. thermoacetophila*

For *Mt. thermoacetophila* as obligate aceticlastic methanogen acetate is the only substrate for methanogenesis. This makes energy conservation especially challenging. The change in free energy for conversion of acetate to methane and CO_2 is only –36 kJ mol^{-1} CH_4 under standard conditions. Furthermore, ATP equivalents are spent for acetate activation. It is thought that acetate activation in *Mt. thermoacetophila* is catalyzed by an acetyl-CoA synthetase (ACS) (Jetten *et al.*, 1989). Four genes encoding putative ACS enzymes are annotated in the genome (Smith and Ingram-Smith, 2007). ACS enzymes catalyze the

conversion of acetate, ATP and CoA to acetyl-CoA, AMP and pyrophosphate (PP_i). The intracellular accumulation of PP_i has to be prevented, because excess PP_i inhibits biosynthesis of macromolecules. Sequence data revealed the presence of a gene probably encoding a soluble pyrophosphatase (PPase) (Smith and Ingram-Smith, 2007). Together with subsequent hydrolysis of PP_i by a PPase, acetate activation in *Mt. thermoacetophila* would consume two ATP equivalents per acetate molecule. Yet, ion translocation by the respiratory chain of *Mt. thermoacetophila* is thought to be sufficient for the generation of two ATP molecules per acetate molecule. In this scenario there would be no ATP net gain and thus survival of *Mt. thermoacetophila* would not be possible. Therefore, in the first part of this study, four different ACS genes and the gene encoding a soluble PPase from the genome of *Mt. thermoacetophila* were examined with regard to gene expression level and enzymatic activity.

3.1.1 Relative transcript abundance of acetyl-CoA-synthetases and soluble pyrophosphatase genes

According to genome sequence data, *Mt. thermoacetophila* possesses four genes encoding ACS enzymes (Smith and Ingram-Smith, 2007). Three of them are tandemly organized (*mthe_1194*/*95*/*96*). A fourth ACS is encoded elsewhere on the chromosome (*mthe_1413*). In contrast to *Ms. mazei*, there is no evidence for genes encoding acetate kinase and phosphotransacetylase in *Mt. thermoacetophila*.

RT-qPCR experiments were performed to investigate the expression level of the different ACS encoding genes. High expression levels would point to an important role in acetate metabolism. Likewise, the PPase gene expression level was evaluated. For RT-qPCR, highly specific primers were needed, since the four ACS genes were highly homologous (at least 71 % identity). An alignment was made to identify the least homologous parts of the genes. Primers were designed that could bind specifically to these parts as shown in Figure 8. To further confirm specificity of primers designed for different genes, they were recombined in every possible way. RT-qPCR assays were performed with mthe_1194_for + mthe_1195_rev, mthe_1194_for + mthe_1196_rev and accordingly for the other combinations. With every combination, products were generated in very low amounts, if at all. Therefore, primers were considered to bind specifically to their target genes.

Total RNA was extracted from exponentially-growing cultures by TRI reagent with subsequent purification steps as described (2.4.3). Samples were checked for DNA by omitting the reverse transcriptase. DNA contaminations were found to be negligible. The transcript abundance of ACS and PPase-encoding genes was measured in relation to genes encoding glyceraldehyde-3-phosphate dehydrogenase (GAP-DH) and the ribosomal protein S3P. The GAP-DH has been shown to be constitutively expressed in methanogens (Hovey *et*

al., 2005; Veit *et al.*, 2006; Pflüger *et al.*, 2007). Similarly, ribosomal genes have high expression levels to allow efficient synthesis of ribosomes.

```
mthe_1194    CACCCCCCAGTGGATCATCGAGTACTCGAACTCCTACCAGTGGATGAAGAAGAAGGGCTTCAA 113
mthe_1195    TCCCCCTAAGGAGCTTGCTGAGAACTCAAATGTCATGCAGTGGATGAAGAAGAAGGGATTCAC 119
mthe_1196    TCCCCCGAAGGAGCTGGTTGAGAACTCAAATGTGATGCAGTGGATGAAGAAGAAGGGCTTCAA 116
mthe_1413    GCCGGCAAGCGACCTGGTGGAGAACTCCAATGTGATGCAGTGGATGAAGAGAAAGGGATTCAG 107
               *  *        *    *** **** **       *************  ***** ****

mthe_1194    GACAGAGAAGGAGATGCGCGAGTGGTGTGCCCAGAACTACCTCGATTTCTGGGATGATTGTCT 173
mthe_1195    AAGCGAGCGGGAGATGCGCGCCTGGACCGGCCAGCACTACATAGAGTTCTGGGACGATGGTAT 179
mthe_1196    GACAGAGAAAGAGATGCGGGAATGGTGCTCAAAGAACTATGTTGAGTTCTGGGACGATTGTCT 176
mthe_1413    GAGTGAGAAAGAGCTGCGGGCCTGGTGTTCCGAGAACTACGTTGAGTTCTGGGACGATAGTCT 167
              *  ***   *** **** *  ***       ** ****  * ** ******** *** ** *

mthe_1194    TCTCGGGATTCAGCGCTGGAGGCCT--GCAGAGCAGGGTCACGGATGCAGAGGCTAAGGTCGT 584
mthe_1195    TCTCCGGATTCAGCGCTGGAGGCCT--CCAGAGCAGGGTTCTCGATGCAGAGGCGAAGGTTGT 593
mthe_1196    TCTCAGGATTCAGCTC-GAAGGCGTATGCTGA-CAGGGTTATCGATGCGGAGTCGAAGAT-AT 587
mthe_1413    TCTCCGGATTCAGCGCAGGCGCGCTCCGCGAG--AGGATTAACGATGCTGGGGCCAGAGTC-C 578
             **** ********* * *  *   *   *     *** *    ***** * * * *   *

mthe_1194    CG-TGACATCTGATGGCTTCTACAGGCGTGGCAAGCCGCTCCCGCTCAAGCCGAACGTCGATG 643
mthe_1195    CG-TCACAACCGATGGATTCTACAGGCGCGGCAAGCCGCTCCCGCTCAAGCCGAACGTCGATG 652
mthe_1196    CGATCACCGTTGATGGATTCTGGAGGCGCGGAAAGATTGTGGAGCTCAAAAAGCAGGCTGACG 646
mthe_1413    TGATAACATGTGATGGATCATACAGAAGGGGCAAGCCTATCCCGATAAAGGCCCAAGCGGATG 637
              * * **    ***** *  *  **  * ** ***    *   * * **     * *  ** *

mthe_1194    AGGCAGTCCAGAACGCCCCGAGCGTTGAGAAGGTCGTCGTGGTCAAGA 703
mthe_1195    AGGCAGTCCAGAACGCCCCGAGCGTTGAGAAGGTCGTCGTGGTCAAGA 712
mthe_1196    AGGCGATTCAGGATGCTCCAACAGTAAAGCATCAGATCGTTTACAAGA 706
mthe_1413    AGGCCCTTCAGGACGCGCCCTCTGTCGAACGCCAGATTGTTTACAGAC 697
             ****  * *** * ** **    **  *        * **   **
```

Figure 8: Alignment of the four genes encoding putative AMP-forming ACS enzymes from the genome of *Mt. thermoacetophila*. Parts highlighted in gray are sequences of forward primers used in RT-qPCR experiments; parts highlighted in black indicate the respective reverse primers. The least homologous parts of the sequences were used for primer design to guarantee specific primer binding.

The transcript level of *mthe_1194* was 2.6- and 2.0-fold higher than those of the GAP-DH gene and the gene encoding the S3P protein, respectively (Figure 9). This was a strong indication for an important role in acetate metabolism. In contrast, transcripts of *mthe_1195* and *mthe_1196* were less abundant. In comparison to *mthe_1194,* transcript concentrations for *mthe_1195* and *mthe_1196* were 23- and 37-fold reduced. Expression of the single gene *mthe_1413* was slightly lower than expression of *mthe_1194*.

Since *mthe_1194*/*95*/*96* are tandemly positioned, the question arose whether they are organized in one operon. A close inspection revealed separation of genes by inserts of at least 300 bp that contain potential transcriptional starting elements (TATA and BRE boxes). RT-qPCR primers were designed, which bound to the beginning and the end of these intergenic regions. The results of RT-qPCR clearly showed that the intergenic region between *mthe_1195* and *mthe_1196* was transcribed to the same extent as the genes themselves. This strongly indicated that *mthe_1195* and *mthe_1196* were transcribed together (Figure 9). For the intergenic region between *mthe_1194* and *mthe_1195,* no transcript could be detected. Therefore, *mthe_1194* most likely represented a single transcriptional unit.

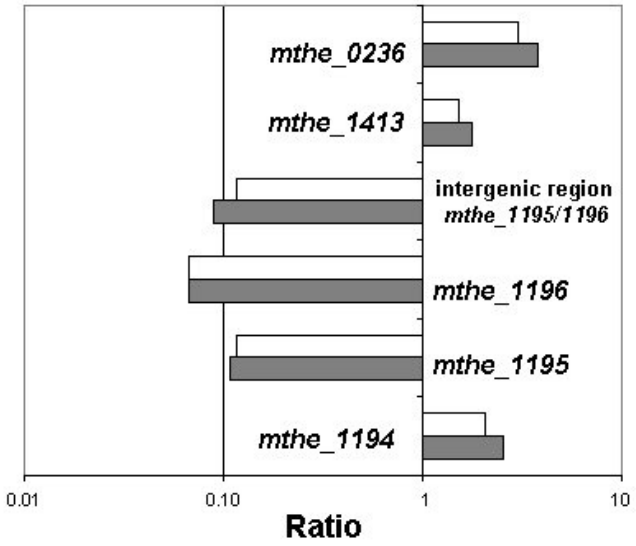

Figure 9: Relative transcript abundance of genes encoding ACSs (*mthe_1194*/*95*/*96*; *mthe_1413*) and PPase (*mthe_0236*) from *Mt. thermoacetophila*. Additionally, the transcript level of the intergenic region between *mthe_1195*/*96* is shown. The PPase gene was highly expressed and of all ACS genes, *mthe_1194* seemed to be most important. *Mthe_1195*/*96* most likely represents a single transcriptional unit. Gray boxes: transcript ratio of indicated gene or region versus gene encoding the glyceraldehyde-3-phosphate dehydrogenase; white boxes: transcript ratio of indicated gene versus gene encoding ribosomal protein S3P. Modified after (Berger *et al.*, 2012).

In addition to genes encoding the putative AMP-forming ACS enzymes, one gene encoding a putative ADP-forming ACS could be identified (*mthe_0554*). The corresponding enzyme acts like AMP-forming ACS enzymes described above, but forms ADP instead of AMP. ADP-forming ACS enzymes are known to catalyze acetate formation, but due to the energetic benefit to *Mt. thermoacetophila*, the enzyme's possible involvement in the reverse reaction, which is acetyl-CoA formation, was considered. However, the transcript concentration level of the gene encoding the putative ADP-forming ACS *mthe_0554* was about 4000-fold lower

than transcript concentration of the reference genes. Hence, under the chosen conditions, it most likely does not have a role in acetate metabolism.

As mentioned above, PP_i is a byproduct of acetyl-CoA formation by AMP-forming ACS enzymes. Hydrolysis of PP_i is essential to shift the equilibrium of important biosynthetic reactions like DNA synthesis towards product formation. Soluble PPases dissipate the energy stored in the phosphoanhydride bond as heat. However, theoretically at least part of the energy could be conserved. Therefore, it was interesting to evaluate the expression level of *mthe_0236* encoding a putative soluble PPase. RT-qPCR experiments were performed as already described for genes encoding putative ACS enzymes. The transcript levels of *mthe_0236* were found to be 3- to 4-fold higher than those of the reference genes encoding GAP-DH and ribosomal protein S3P (Figure 9). Thus, mRNA encoding a soluble PPase is highly abundant in cells of *Mt. thermoacetophila*, indicating an important role of the corresponding enzyme.

In summary, RT-qPCR revealed that of four genes encoding putative ACS enzymes, *mthe_1194* was most highly expressed during the exponential growth phase. In comparison to *mthe_1194,* transcript levels of *mthe_1413* were slightly lower and those of *mthe_1195* and *mthe_1196* were significantly reduced. Of the three genes that were tandemly positioned, the highly expressed *mthe_1194* represented a single transcriptional unit and *mthe_1195/96* were transcribed together. *Mthe_0236,* potentially coding for a soluble PPase, was transcribed to a higher degree than the reference genes encoding GAP-DH and ribosomal protein S3P. To further investigate their role in acetate metabolism, Mthe1194 and Mthe0236 were produced and tested for kinetic parameters.

3.1.2 Characterization of the acetyl-CoA-synthetase Mthe1194

Mthe_1194 encoding a putative AMP-forming ACS was cloned into an expression vector to yield pASK-*mthe1194*-5. Recombinant protein was produced in *E. coli* and purified by Strep-tactin affinity chromatography. The theoretical subunit molecular mass of Mthe1194 was 75 kDa, which was in accordance with SDS-PAGE analysis (Figure 10A). The enzymatic activity of Mthe1194 was tested with two different assays. In the first assay auxiliary enzymes were employed (Figure 11). The first reaction was catalyzed by Mthe1194 to yield acetyl-CoA, AMP and PP_i. Secondly, myokinase (MK) catalyzed the conversion of AMP and ATP to ADP, which together with phosphoenolpyruvate (PEP) was further converted to pyruvate and ATP by pyruvate kinase (PK). In the final step, pyruvate was reduced with NADH by lactate dehydrogenase (LDH), which led to a decrease in absorption at 340 nm. One important question to be answered was whether Mthe1194 in fact produced AMP and PP_i from ATP. If so, it would be clearly distinct from ADP-forming ACS enzymes. To address the question, the MK was omitted from the coupled enzymatic assay. If Mthe1194 would form ADP instead of

AMP, the reaction would have been able to proceed directly to conversion of PEP by PK, bypassing the step catalyzed by MK. It could be demonstrated here that the whole cascade was dependent on the presence of MK, meaning that MK was essential for the formation of ADP (Figure 12). Therefore, Mthe1194 indeed formed AMP and PP_i from ATP.

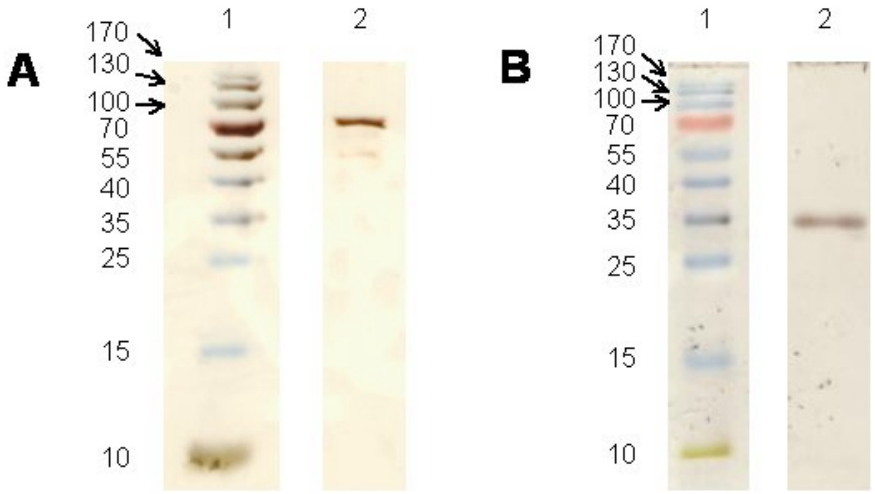

Figure 10: The ACS enzyme Mthe1194 (A, 75 kDa) and the soluble PPase Mthe0236 (B, 35 kDa) were heterologously produced in *E. coli* and analyzed by SDS-PAGE. Both proved to be pure and sizes were in agreement with theoretical molecular masses. 1(A)/(B): PAGE ruler prestained protein ladder; 2 (A): Mthe1194; 2 (B) Mthe0236. Modified after (Berger *et al.*, 2012).

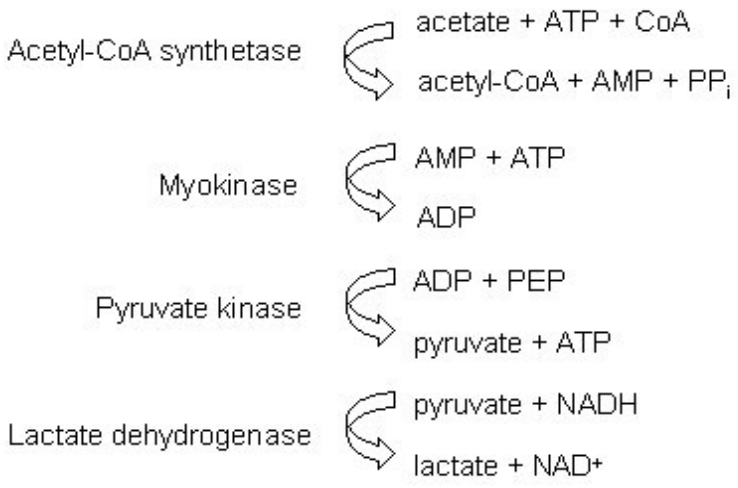

Figure 11: Coupled enzymatic assay to measure the activity of the AMP-forming ACS Mthe1194. The first reaction was catalyzed by the ACS enzyme Mthe1194. The next reactions were catalyzed by myokinase and pyruvate kinase. In the last step, NADH was oxidized to NAD^+ by lactate dehydrogenase, which was measured photometrically. PEP: Phosphoenolpyruvate.

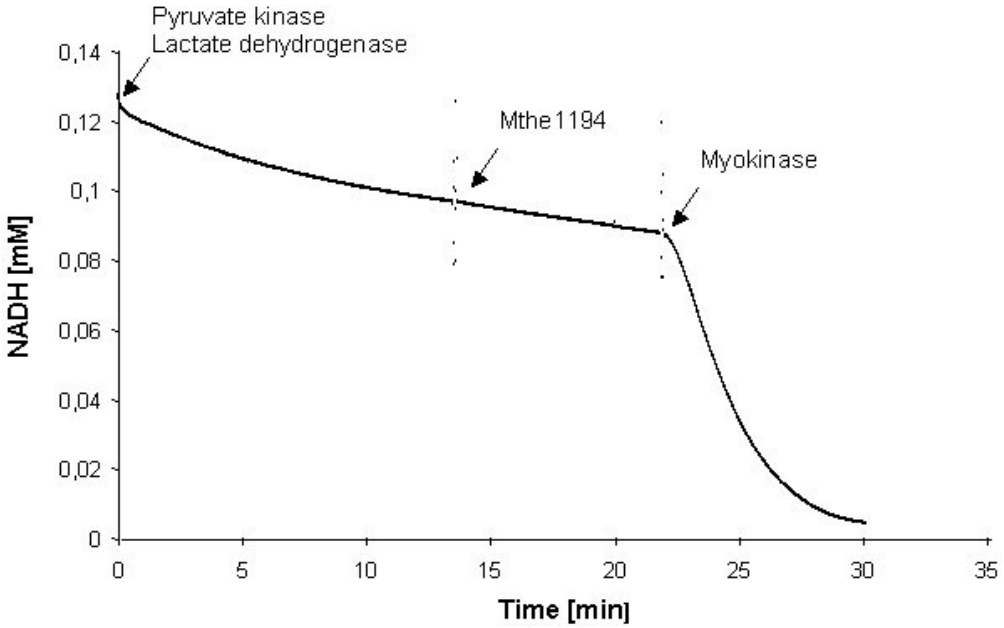

Figure 12: Enzymatic assay for the ACS enzyme Mthe1194 with auxiliary enzymes. NADH oxidation started only after addition of myokinase, hence Mthe1194 produces AMP and PP_i from ATP. The assay was performed at room temperature with non-limiting amounts of auxiliary enzymes. Oxidation of NADH was recorded photometrically at 340 nm.

Another aspect was the affinity of the enzyme for its substrates. If *Mt. thermoacetophila* relies on Mthe1194 for acetate activation the enzyme has to bind acetate, ATP and CoA effectively for efficient formation of acetyl-CoA. The assay that employed auxiliary enzymes was used to measure the K_M value for acetate (Figure 13A). ACS activity was measured with acetate concentrations between 5 μM and 20 mM. Data analysis with linear regression resulted in a K_M value for acetate of 0.4 mM with a v_{max} of 21.7 U mg^{-1} (Figure 13A). Using non-linear regression (GraphPad Prism 6, GraphPad Software Inc., La Jolla, USA), values were in the same range with a K_M value of 0.6 mM and v_{max} of 16.1 U mg^{-1}. These values were in accordance with literature data (Kohler and Zehnder, 1984; Jetten *et al.*, 1989; Teh and Zinder, 1992). Furthermore, a K_M value of 0.4-0.6 mM seemed low enough to allow efficient acetyl-CoA formation in natural habitats of *Mt. thermoacetophila*.

Since ATP and CoA concentrations in the cell are probably low, K_M values for these substrates were expected to be in the micromolar range. Therefore, in another assay PP_i was detected with a colorimetric approach (2.7.2). In a solution with ammoniumtetramolybdate, the addition of PP_i and the subsequent reduction led to the formation of a blue molybdate complex that could be measured at 580 nm. With this method, PP_i concentrations as low as 1 μM could be detected. In the enzyme activity assay, a v_{max} of

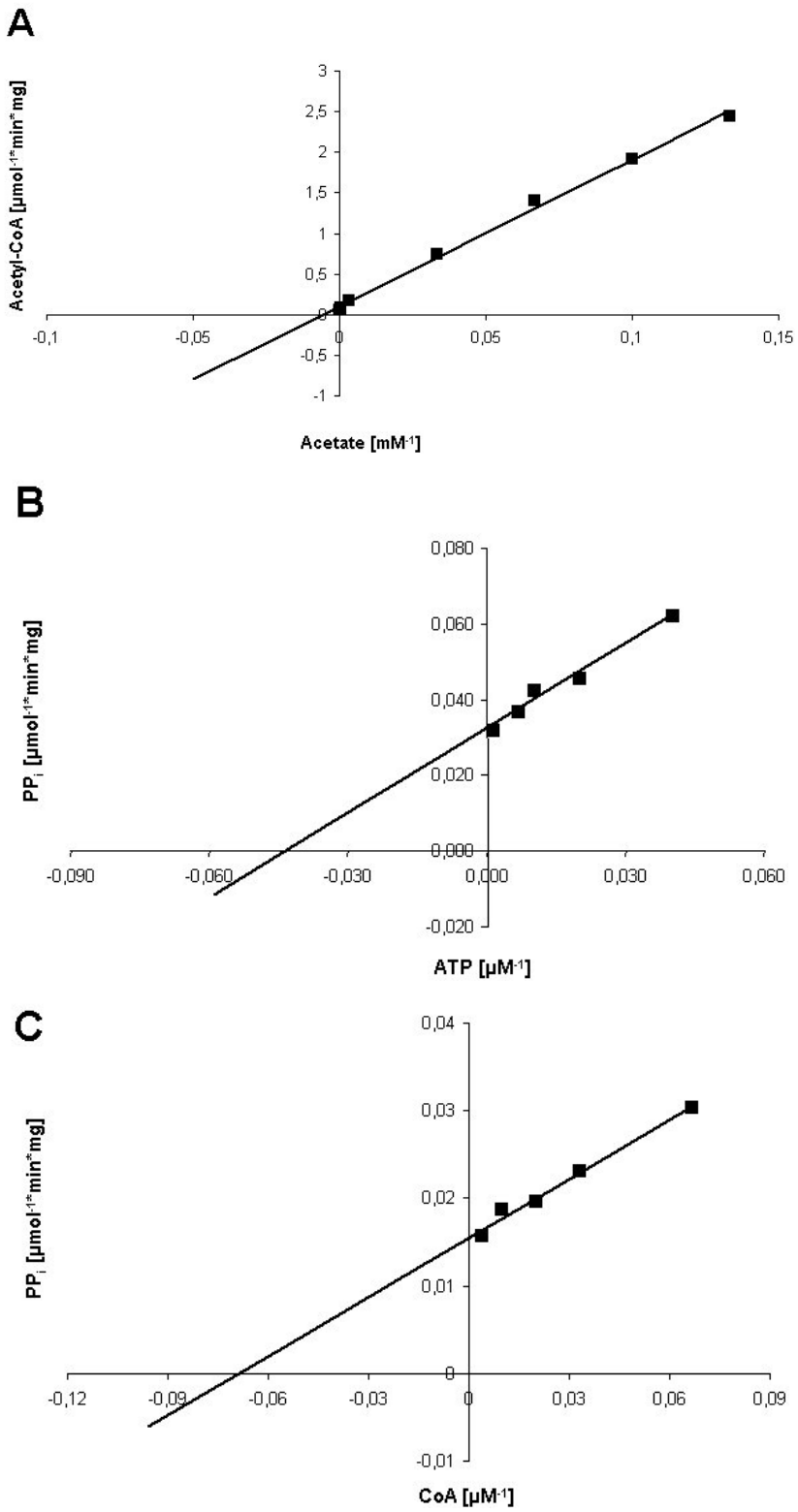

Figure 13: Determination of kinetic parameters of the ACS Mthe1194 according to Lineweaver Burk. A: Kinetic parameters for acetate as measured in an assay employing auxiliary enzymes. K_M was 0.4 mM and v_{max} was 21.7 U mg^{-1}. B: Kinetic parameters for ATP as measured by detection of PP_i. A K_M value of 20 µM and v_{max} of 28 U mg^{-1} were determined. C: K_M value for CoA measured as in B. K_M was 14.5 µM.

28 U mg^{-1} was measured for Mthe1194 by linear regression. The result of non-linear regression was 31 U mg^{-1} (GraphPad Prism 6, GraphPad Software Inc., La Jolla, USA). Hence, values measured with the PP_i detection method were in the same range as values determined by coupling ACS activity to auxiliary enzymes. K_M values for ATP and CoA were, respectively, 20 μM and 14.5 μM with linear regression (Figure 13B and 13C) and 24 µM and 20.5 µM with non-linear regression. Hence, both cofactors were efficiently bound to the enzyme. Even at low energy charge status of the cell with low ATP concentrations, ATP can still be used for acetyl-CoA formation.

To sum up, it could be demonstrated that Mthe1194 produces AMP and PP_i from ATP during acetyl-CoA formation and is thus distinct from ADP-forming ACS enzymes. Enzymatic activity and kinetic parameters were in accordance with literature data and seemed suitable to efficiently generate acetyl-CoA for methanogenesis (Kohler and Zehnder, 1984; Jetten *et al.*, 1989; Teh and Zinder, 1992).

3.1.3 Characterization of the soluble pyrophosphatase Mthe0236

Besides the ACS enzyme Mthe1194, a soluble PPase is thought to be involved in the acetate activation reaction in *Mt. thermoacetophila* (Mthe0236), catalyzing breakdown of PP_i formed by Mthe1194. There are two families of soluble PPases that are distinguished according to sequence homology. Family or type I PPases share a highly conserved active site structure and have similar catalytic properties (Cooperman *et al.*, 1992; Kankare *et al.*, 1994). They depend on Mg^{2+} for catalytic activity (Parfenyev *et al.*, 2001). Type I PPases are further divided into the prokaryotic type A with a subunit molecular mass of about 20 kDa and eukaryotic type B with a subunit molecular mass of about 28–35 kDa (Young *et al.*, 1998). Family or type II PPases share no sequence homology with type I PPases but are well conserved among themselves. They have been characterized primarily from bacteria. For full enzymatic activity, type II soluble PPases require Mn^{2+} as metal ion in the catalytic center. Usage of Mn^{2+} instead of Mg^{2+} facilitates removal of orthophosphate (P_i) from the active site after PP_i hydrolysis (Fabrichniy *et al.*, 2007). Therefore, the catalytic activity of type II soluble PPases is 10 to 20- fold higher than that of type I PPases (Parfenyev *et al.*, 2001).

The amino acid sequence of Mthe0236 from *Mt. thermoacetophila* annotated as type II soluble PPase was blasted against the NCBI protein data bank (pdb). Homologous enzymes are type II soluble PPases, as found in *B. subtilis* (42 % identity, bit score 265, E-value $3e^{-86}$), *Streptococcus* (*S.*) *gordonii* (37 % identity, bit score 223, E-value $6e^{-70}$) and *Methanocaldococcus* (*Mc.*) *jannaschii* (45 % identity, bit score 268, E-value $2e^{-87}$). An alignment of Mthe0236 with the respective sequences of the other enzymes is shown in Figure 14. A blast search revealed no significant similarity to any other type of enzyme. Thus, according to sequence homology Mthe0236 was classified as soluble PPase of the type II.

```
B.subtilis          -MEKILIFGHQNPDTDTICSAIAYADLK-NKLGFNAEPVRLGQVNGETQYALDYFKQESP 58
S.gordonii          --SKILVFGHQNPDSDAIGSSYAFAYLAREAYGLDTEAVALGEPNEETAFVLDYFGVAAP 58
Mt.thermoacetoph.   MADNIYVVGHKSPDTDSVTSAITYANLKNQLGMKDVVPAAAGEINNETKYVLEYFKIAPP 60
Mc.jannaschii       MR---YVVGHKNPDTDSIASAIVLAYFL------DCYPARLGDINPETEFVLRKFGVMEP 51
                          :.**:.**:*:: *: . * :       :  ..  *: * ** :.*  *    *

B.subtilis          RLVETAANE-VNGVILVDHNERQQSIKDIEEVQVLEVIDHQRIANFETAEPLYYRAEPVG 117
S.gordonii          RVITSAKAEGAEQVILTDHNEFQQSVADIAEVEVYGVVDHHRVANFETANPLYMRLEPVG 118
Mt.thermoacetoph.   VVLNDATDK---KVILVDHNEVGQAVDNIMKADILEIIDHHKIGDIQTGKPIFFHNEPVG 117
Mc.jannaschii       ELIESAKGK---EIILVDHSEKSQSFDDLEEGKLIAIIDHHKVG-LTTTEPILYYAKPVG 107
                   ::  *  :    :**.**.*  *:. :: : .:  ::**:::. : * :*:    :***

B.subtilis          CTATILNKMYKENNVKIE--------KEIAGLMLSAIISDSLLFKSPTCTDQDVAAAKEL 169
S.gordonii          SASSIVYRMFKEHSVAVS--------KEIAGLMLSGLISDTLLLKSPTTHPTDKAIAPEL 170
Mt.thermoacetoph.   ATGTIIASMYELNGVAIS--------KEMAGLMMAAILSDTVLFKSPTCTDKDKATVEKL 169
Mc.jannaschii       STATVIAELYFKDAIDLIGGKKKELKPDLAGLLLSAIISDTVLFKSPTTTDLDKEMAKKL 167
                    .:.:::  ::  . : :          ::***:::.::**::*:****    *   . :*

B.subtilis          AEIAGV-DAEEYGLNMLKAGADLSKKTVEELISLDAKEFTLGSKKVEIAQVNTVDIEDVK 228
S.gordonii          AELAGV-NLEEYGLAMLKAGTNLASKSAEELIDIDAKTFELNGNNVRVAQVNTVDIAEVL 229
Mt.thermoacetoph.   SKICGE-DPQKFGMEMLKAKSDIKSKTAKDILFGDFKKFDFSGVKAGVGQIEVMDLADLA 228
Mc.jannaschii       AEIAGISNIEEFGMEILKAKSVVGKLKPEEIINMDFKNFDFNGKKVGIGQVEVIDVSEVE 227
                    :::.*  : :::*: :*** : : . . ::::  * * * :.. :. :.*::.:*: ::

B.subtilis          KRQAELEAVISKVVAEKNLDLFLLVITDILENDSLALAIG--NEAAKVEKAFNVTLENNT 286
S.gordonii          ERQAEIEAAIEKAIADNGYSDFVLMITDIINSNSEILAIG--SNMDKVEAAFNFVLENNH 287
Mt.thermoacetoph.   PKREEILAEMRKALESEKLDMIVLMLTDVIKEASDLLFVGTAAAKEGFEKAFGGKVTNNS 288
Mc.jannaschii       SKKEDIYKLLEEKLKNEGYDLIVFLITDIMKEGSEALVVG---NKEMFEKAFNVKVEGNS 284
                     :: ::   : : : .:  . :::::**:::. *  * :*       .* **.  : .*

B.subtilis          ALLKGVVSRKKQVVPVLTDAMAE 309
S.gordonii          AFLAGAVSRKKQVVPQLTESFNA 310
Mt.thermoacetoph.   IYKEKVLSRKKQVIPPLESAFKK 311
Mc.jannaschii       VFLEGVMSRKKQVVPPLERAYNG 307
                         .:******:* *  :
```

Figure 14: Alignment of amino acid sequences of biochemically characterized type II soluble PPases with Mthe0236 from *Mt. thermoacetophila*. Greatest similarity was shared with the *Mc. jannaschii* type II soluble PPase (45 % identity), furthermore Mthe0236 was homologous to the respective enzymes from *B. subtilis* (42 % identity) and from *S. gordonii* (37 % identity).

In type II soluble PPases, the molecular mass of subunits is typically around 35 kDa (Young *et al.*, 1998). This was also the case with Mthe0236: the theoretical molecular mass of a monomer of Mthe0236 including Strep-tag was 34.9 kDa. Mthe0236 was heterologously produced in *E. coli* and purified by Strep-tactin affinity chromatography. The subunit molecular mass was investigated by SDS-PAGE analysis. As can be seen in (Figure 10B),

the subunit molecular mass of Mthe0236 was 35 kDa, which accords with the theoretical value. Furthermore, the preparation proved to be pure.

In most cases, the quaternary structure of native type II PPases from bacteria is a homodimer (Ahn *et al.*, 2001; Merckel *et al.*, 2001; Halonen *et al.*, 2005; Rantanen *et al.*, 2007). For type II soluble PPases from archaea, less data exists and the picture is not that clear. To investigate the subunit composition of the heterologously produced Mthe0236, the native enzyme was examined by size exclusion chromatography. Therefore, about 1.5 mg of purified Mthe0236 was applied to a Hi Load 16/60 Superdex 75 prep grade column in 40 mM Tris-HCl pH 8 with 150 mM NaCl and 1 mM $MnCl_2$. The molecular mass was calculated from a standard curve with proteins of known molecular masses (Figure 15). 71.4 ± 5 kDa were measured for Mthe0236. Thus, in its native form, Mthe0236 was present as a homodimer.

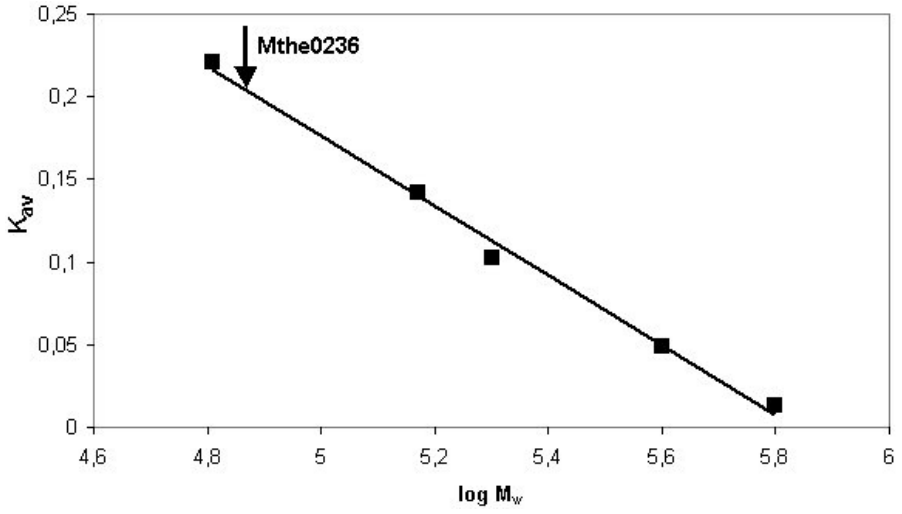

Figure 15: Determination of the molecular mass of the native PPase enzyme (Mthe0236, indicated by arrow). The calibration curve for size exclusion chromatography was calculated using the Kit for Protein Molecular Weights, 29,000–700,000 (Sigma-Aldrich, Munich, Germany) containing carbonic anhydrase (29 kDa), bovine serum albumine (66 kDa), alcohole dehydrogenase (150 kDa), β-amylase (200 kDa), apoferritin (443 kDa) and thyroglobulin (669 kDa). By measuring the K_{av} value of the native PPase enzyme, a molecular mass of 71.4 ± 5 kDa could be determined.

Another characteristic of soluble type II PPases is their high enzymatic activity. K_{cat} values of 1700-3300 s^{-1} are reported in the literature (Ahn *et al.*, 2001; Fabrichniy *et al.*, 2007). In this study the enzymatic activity was measured by detecting P_i in an assay modified after (Saheki *et al.*, 1985). Prior to enzyme activity assays, Mthe0236 was incubated with 1 mM $MnCl_2$, as Mn^{2+} is required as a metal ion in the catalytic center for full enzymatic activity. A v_{max} of 726 ± 40 U mg^{-1} was measured with linear regression according to Lineweaver Burk (Figure 16). The corresponding k_{cat} was 1728 s^{-1}. Non-linear regression resulted in a v_{max} of 1067 U mg^{-1} (GraphPad Prism 6, GraphPad Software Inc., La Jolla, USA) with a

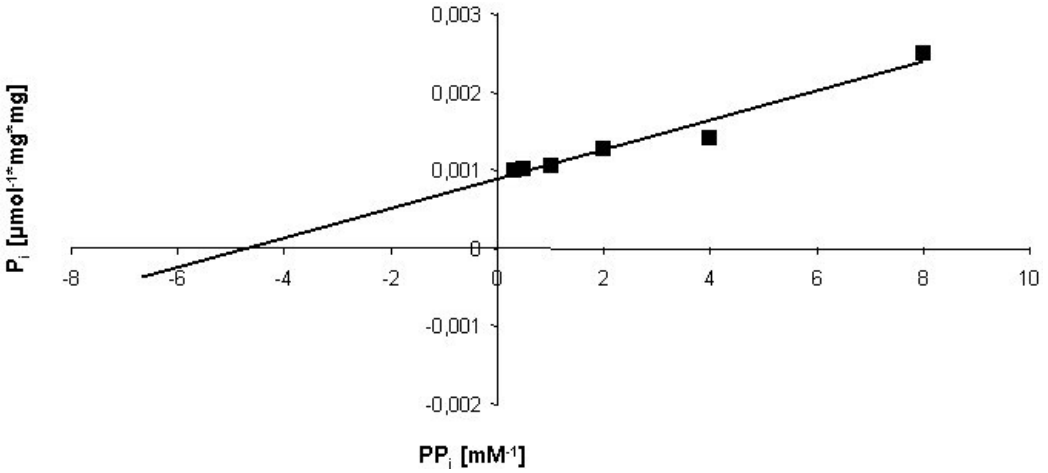

Figure 16: Determination of kinetic parameters of the soluble PPase Mthe0236, according to Lineweaver Burk. PPase activity was measured by detection of P_i. A v_{max} of 726 ± 40 U mg^{-1} and K_M value of 0.27 ± 0.05 mM was determined.

corresponding k_{cat} of 2540 s^{-1}. Likewise, the K_M value of Mthe0236 for PP_i was determined and found to be 0.27 ± 0.05 mM (linear regression, Figure 16) or 0.16 mM (non-linear regression (GraphPad Prism 6, GraphPad Software Inc., La Jolla, USA)). Both values were in accordance with data from literature (Ahn *et al.*, 2001; Fabrichniy *et al.*, 2007). It is known that the PP_i concentration in prokaryotic cells is in the millimolar range. Hence, the kinetic parameters of Mthe0236 are suitable to effectively degrade PP_i in cells of *Mt. thermoacetophila*.

In summary, Mthe0236 is a homodimeric, highly active and thus typical type II soluble PPase. Due to the high specific activity and a relatively low K_M value for PP_i, the major part of PP_i built by Mthe1194 or in biosynthetic reactions will be hydrolyzed. Therefore, the costs of acetate activation in *Mt. thermoacetophila* sum up to two ATP equivalents. Since ion translocation by membrane-bound enzymes of the respiratory chain is thought to be sufficient for synthesis of two ATP molecules per acetate molecule, the question is raised how *Mt. thermoacetophila* achieves an ATP net gain. This intriguing puzzle is going to be further addressed in the discussion part of this thesis.

3.2 The Fpo complex from *Ms. mazei*

The $F_{420}H_2$ dehydrogenase, also termed Fpo complex (F_{420}:phenazine oxidoreductase), can be found in the order Methanosarcinales but is absent in obligate hydrogenotrophic methanogens.

In methylotrophic methanogenesis the Fpo complex oxidizes $F_{420}H_2$ and concomitantly translocates two protons (Bäumer *et al.*, 2000). Thus, it contributes to the formation of an electrochemical proton gradient used for ATP synthesis. Genome sequencing revealed that it

is highly homologous to bacterial and eukaryotic NADH:quinone oxidoreductases (Welte and Deppenmeier, 2014), which can be also termed complex I or Nuo complex. Another homolog can be found in the euryarchaeon *Archaeoglobus fulgidus*, the F_{420}:quinone oxidoreductase, also known as Fqo complex (Brüggemann *et al.*, 2000).

In the model organism *Ms. mazei* the Fpo complex consists of 14 subunits FpoABCDFHIJ1J2KLMNO. The respective genes are organized in one operon except for the gene encoding subunit FpoF, which is located elsewhere on the chromosome (Figure 17, (Deppenmeier *et al.*, 2002)).

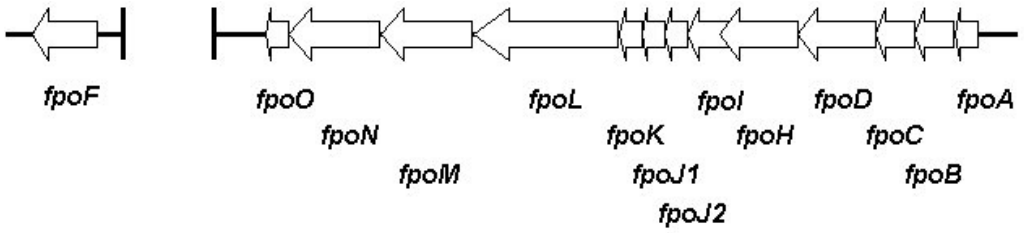

Figure 17: Structure of the *fpo* operon. Genes encoding FpoA-FpoO are clustered together in one operon of approximately 10 kb size. The gene encoding the $F_{420}H_2$-oxidizing subunit FpoF is separated from the rest of the operon.

Subunits FpoAHJ1J2KLMN are membrane-integral, whereas subunits FpoBCDI are associated to the membrane (Welte and Deppenmeier, 2014). For subunit FpoO, neither an exact localization nor function is known. In this study a *Ms. mazei* Δ*fpoO* mutant was employed to gain insight into the role of FpoO in energy metabolism.

Recently it has been proposed that besides its role in methylotrophic methanogenesis the Fpo complex could also be involved in methanogenesis from acetate (Welte and Deppenmeier, 2011b). FpoF that acts as an electron input module in methylotrophic methanogenesis is able to dissociate from the complex and can also be found in the cytoplasm. The “headless” Fpo complex is thought to interact with Fd_{red} and to channel electrons into the respiratory chain (Welte and Deppenmeier, 2011a). First experimental evidence to support this theory is presented in the following chapters.

3.2.1 Analysis of a *Ms. mazei* Δ*fpoO* mutant

Subunit FpoO of the Fpo complex in *Ms. mazei* is a small, hydrophilic 15 kDa protein encoded by the last gene in the *fpo* operon (Figure 17). FpoO can also be found in the close relatives *Ms. acetivorans* and *Ms. barkeri* and other members of the Methanosarcinales like *Methanohalobium evestigatum*, *Methanolobus tindarius* or *Methanococcoides burtonii*.

However, FpoO does not have a counterpart in the well-studied Nuo or the Fqo complex. Furthermore, protein blast analysis revealed no homology to any other protein characterized so far. Therefore, the function of FpoO in the Fpo complex is unclear. One [2Fe2S] cluster is predicted with Prosite, which is in accordance with the fact that 1.5 nmol of non-heme iron and 1.6 nmol of acid labile sulfur per nmol protein were detected in a purified, recombinant FpoO protein (Hofmann, 2003). This points to a possible involvement in electron transport processes. The Fpo complex is distinguished from homologous protein complexes by the fact that it transfers electrons to methanophenazine (MP), which is a membrane-integral cofactor specific for methanogens. Therefore, FpoO might be involved in electron transfer from $F_{420}H_2$ to MP.

As a first approach to evaluate the role of FpoO in the metabolism of *Ms. mazei*, growth experiments were performed with a mutant lacking *fpoO* (mutant constructed by Cornelia Welte, Radboud Universiteit Nijmegen, The Netherlands). In this mutant, the gene encoding FpoO is replaced by a puromycin resistance cassette (Figure 18).

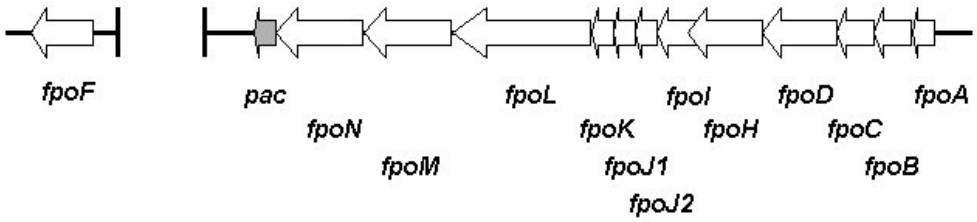

Figure 18: Structure of the *fpo* operon in the *Ms. mazei* Δ*fpoO* mutant. The gene encoding *fpoO* was substituted by a puromycin resistance cassette (*pac*).

It has to be mentioned here, that in *Ms. barkeri* the Fpo complex was demonstrated to play a minor role in $F_{420}H_2$ oxidation. Mutants lacking the *fpo* operon did not show a phenotype when they were cultivated with methanol as a substrate. It was found that instead of the Fpo complex, the F_{420}-reducing hydrogenase is used to produce H_2 from $F_{420}H_2$. H_2 is re-oxidized by the Vho hydrogenase and electrons are channeled into the respiratory chain (Kulkarni *et al.*, 2009). However, in *Ms. mazei* the Fpo complex is much more important. It was demonstrated that in mutants lacking the whole Fpo complex or subunit FpoF, $F_{420}H_2$ oxidation was severely impaired. In growth experiments with TMA as a substrate, the wild type had a doubling time of 7.7 h and mutants missing the whole complex or subunit FpoF showed a prolonged doubling time of 11.1 h and 11.3 h, respectively (Welte and Deppenmeier, 2011a). Hence, in a *Ms. mazei* mutant missing FpoO, a severe growth deficiency should be measurable if the loss of FpoO had consequences for energy conservation in methylotrophic methanogenesis.

To follow the growth of *Ms. mazei* Δ*fpoO,* the strain was cultivated in complex medium with

TMA or acetate, and the optical density at 600 nm (OD_{600}) was measured. As a control, the wild type strain was used. Growing on complex medium with TMA, the wild type had a doubling time of 6.5 ± 0.5 h. The doubling time of the *Ms. mazei* Δ*fpoO* mutant was 6.7 ± 0.7 h (Figure 19). Hence, the difference between mutant and wild type was in the range of standard deviation. Another aspect of growth experiments is the final OD_{600}. If a mutant reaches a lower final OD_{600} than the wild type but consumes the same amount of substrate, this points to less efficient energy conservation. However, in this experiment the final OD_{600} reached by *Ms. mazei* wt and Δ*fpoO* mutant was similar (Figure 19). Thus, the same amount of biomass was produced from the same amount of substrate and there was no evidence for an impaired energy conservation system in the mutant.

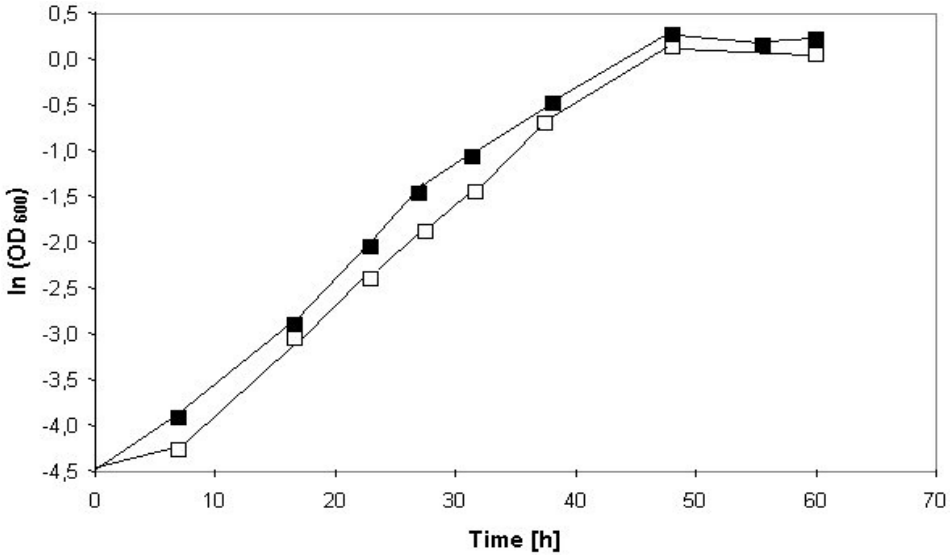

Figure 19: Growth curves for *Ms. mazei* wild type (■) and *Ms. mazei* Δ*fpoO* mutant (□). TMA was used as a substrate. There were no significant differences in doubling time and final OD_{600} between the mutant and wild type.

To exclude the possibility that a slight defect in the mutant was overlooked due to rich nutrient supply in the complex medium, growth experiments were performed in minimal medium. Again, TMA was used as a substrate. Doubling time in the wild type and mutant was slightly increased (8.6 h for the mutant, 7.9 h for the wild type), probably due to limited supply of biosynthetic precursors. Yet, again no significant difference in doubling time between *Ms. mazei* Δ*fpoO* mutant and wild type could be observed. Thus, using TMA as a substrate, growth of *Ms. mazei* was not impaired by the lack of FpoO.

In contrast to methylotrophic methanogenesis where reducing equivalents are transferred to F_{420} and Fd, in aceticlastic methanogenesis only Fd_{red} is generated. It has been proposed that the Fpo complex might not only interact with $F_{420}H_2$ but also with Fd_{red} (Welte and

Deppenmeier, 2011a, b, 2014). Therefore, acetate was used as substrate to investigate a possible role of FpoO in Fd_{red} oxidation without interference of $F_{420}H_2$. As already mentioned above, the $F_{420}H_2$-oxidizing subunit FpoF can dissociate from the complex and is active in the cytoplasm as F_{420}:Fd oxidoreductase. One hypothesis was that FpoO might be responsible for the interaction between FpoF and the membrane-associated subunits FpoBCDI. FpoO could serve as redox sensor to recognize the level of Fd_{red}. Thus, if the Fd pool becomes fully reduced in aceticlastic methanogenesis, FpoO could mediate dissociation of FpoF from the Fpo complex. Subsequently, other subunits of the Fpo complex would be accessible for Fd_{red} and the complex could thus contribute to Fd_{red} oxidation. Moreover, cytoplasmic FpoF could transfer electrons to F_{420} and $F_{420}H_2$ would act as a temporary electron sink. These two mechanisms would guarantee a steady supply of Fd for methanogenesis and allow a higher acetate turnover rate and thus faster growth. Therefore, if FpoO indeed acts as a trigger for the dissociation of FpoF, a phenotype with decreased doubling time could be expected for the *Ms. mazei* Δ*fpoO* mutant.

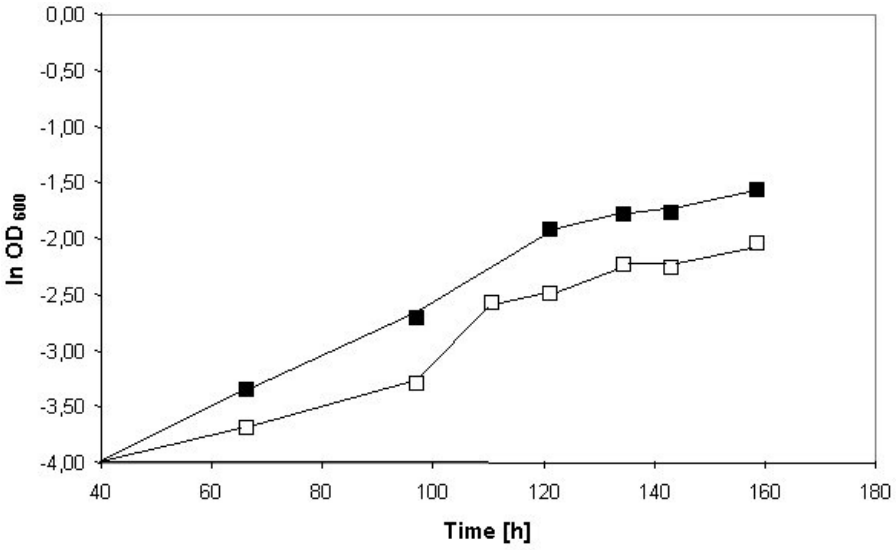

Figure 20: Growth curves for *Ms. mazei* wild type (■) and *Ms. mazei* Δ*fpoO* mutant (□). Acetate was used as a substrate. There was no significant difference in doubling time for mutant and wild type.

Using acetate as substrate, doubling time increased to 35.4 h for the wild type and 36.5 h for the mutant. The overall increase in doubling time is due to the fact that acetate is a poor substrate for methanogenesis. Yet, again there was no difference in doubling time between the *Ms. mazei* Δ*fpoO* mutant and the wild type (Figure 20).

The lack of a phenotype in the growth experiments led to the conclusion that subunit FpoO does not have an important role in energy conservation in methylotrophic or aceticlastic methanogenesis. However, to gain deeper insight into electron transport in the

Ms. mazei Δ*fpoO* mutant, enzymatic assays were performed with membrane fractions of the mutant and the wild type. The functionality of the Fpo complex itself was measured in a test with $F_{420}H_2$ as electron donor and the artificial electron acceptors methylviologen (MV)/metronidazol (MTZ). MV/MTZ can accept electrons directly from the Fpo complex and thus no other membrane-bound enzymes are involved in the respective assay. The enzymatic activity of membrane fractions was 40 mU mg^{-1} for the mutant, which is in the range of literature values for the wild type ((Welte and Deppenmeier, 2011c), Table 12). Thus, the Fpo complex was functional without subunit FpoO.

Table 12: Activity of membrane fractions of *Ms. mazei* wt and the Δ*fpoO* mutant.

Electron acceptor	*Ms. mazei* wt	*Ms. mazei* Δ*fpoO*
MV/MTZ[1]	50 mU/mg[2]	40 mU/mg
Heterodisulfide	65 mU/mg	60 mU/mg

$F_{420}H_2$ was used as electron donor. Electrons were transferred either to MV/MTZ[1] or to the heterodisulfide. [1]: Methylviologen / metronidazol; [2]: (Welte and Deppenmeier, 2011c)

Another test was performed using $F_{420}H_2$ as electron donor and the heterodisulfide as electron acceptor. In this test electrons are transferred from the Fpo complex to the membrane-bound heterodisulfide reductase (Hdr). The electron transfer is mediated by MP, therefore in this experiment the possible role of FpoO in electron transfer to MP was tested. Yet, similar enzymatic activities were measured in the wild type and in the mutant strain (65 mU mg^{-1} in the wild type, 60 mU mg^{-1} for the mutant, Table 12). Hence, it could be shown that subunit FpoO most likely is not involved in electron transfer to MP.

To sum up, a *Ms. mazei* Δ*fpoO* mutant was employed to investigate the role of subunit FpoO from the Fpo complex. Due to the presence of one [2Fe2S] cluster it was feasible that FpoO is involved in electron transfer to MP. In growth experiments, the mutant did not show a clear phenotype in comparison to the wild type. Additionally, electron transfer to MP was tested with enzymatic activity assays in membrane fractions of mutant and wild type. Again, no phenotype was observed. It was concluded that electron transfer processes are not impaired by the lack of FpoO. It was furthermore conceivable that FpoO might serve as a redox sensor that facilitates dissociation of subunit FpoF from the Fpo complex, making other subunits accessible for Fd_{red}. Growth experiments were performed with acetate as a substrate, as in aceticlastic methanogenesis, reducing equivalents are transferred solely to Fd. However, no phenotype was observed in growth experiments performed with acetate as a substrate.

3.2.2 Oxidation of Fd_{red} by the Fpo complex from *Ms. mazei*

In *Methanosarcina* spp. growing on acetate, reducing equivalents are transferred to Fd upon cleavage of acetyl-CoA and concomitant oxidation of the carbonyl moiety by a CODH/ACS enzyme. Fd_{red} is re-oxidized by membrane-bound enzymes of the respiratory chain. In *Ms. mazei* the Ech hydrogenase was shown to be responsible for Fd_{red} oxidation (Welte *et al.*, 2010b). However, the Ech hydrogenase is not conserved among all methanogenic archaea that are able to use acetate as a substrate. No Ech hydrogenase could be identified in the marine isolate *Ms. acetivorans*. There was evidence that another enzyme, namely the Rnf (*Rhodobacter* nitrogen fixation) complex, substitutes for the Ech hydrogenase (Li *et al.*, 2006).

The Rnf complex was originally identified in *Rhodobacter capsulatus* (Schmehl *et al.*, 1993) and homologs can be found in many bacteria and in some archaea, like *Ms. acetivorans*. The Rnf complex from *Acetobacterium* (*A.*) *woodii* was shown to accept electrons from Fd_{red} and to reduce NAD^+. It builds up a sodium ion gradient and thus participates in an anaerobic caffeate respiration in *A. woodii* (Biegel and Müller, 2010). For *Ms. acetivorans* it was demonstrated that Fd_{red} donates electrons to washed membrane fractions. Electrons could be further transferred via a multi-heme cytochrome *c* to the MP analogue 2-hydroxyphenazine or to the heterodisulfide (Wang *et al.*, 2011a). The Fd_{red}-dependent translocation of sodium ions by the Rnf complex from *Ms. acetivorans* was demonstrated in 2012 (Schlegel *et al.*, 2012) and thus in *Ms. acetivorans* the Rnf complex functions in analogy to the Ech hydrogenase.

The methanogenic archaeon *Mt. thermoacetophila* strictly depends on acetate as substrate for methanogenesis and hence needs Fd_{red}-oxidizing enzymes. Yet, according to genome sequencing data, neither Ech hydrogenase nor Rnf complex are present. Only genes encoding a membrane-bound heterodisulfide reductase and, surprisingly, genes encoding the Fpo complex, could be identified.

In another study a *Ms. mazei* Δ*ech* mutant was employed to demonstrate Fd_{red} oxidation catalyzed by the Ech hydrogenase (Welte *et al.*, 2010b). Indeed, in the mutant Fd_{red}-oxidation rates were decreased by about 50 % compared to the wild type. Since 50 % of the activity were retained, it was concluded that another enzyme was probably involved in Fd_{red} oxidation (Welte *et al.*, 2010b). Later it was shown that membrane fractions of *Mt. thermoacetophila* exhibited high Fd:heterodisulfide oxidoreductase activity, even though Ech hydrogenase and Rnf complex were absent (Welte and Deppenmeier, 2011b). It was speculated that in both organisms the Fpo complex could be responsible for Fd_{red} oxidation (Welte and Deppenmeier, 2014).

A comparison with the highly homologous complex I helped to identify the putative site of

Fd_{red}-oxidation in the Fpo complex (Figure 21). In 2010, complex I from *Thermus* (*T.*) *thermophilus* was successfully crystallized and the structure resolved to 3.9 Å resolution (Efremov *et al.*, 2010). Later, the membrane-bound part of the complex from *E. coli* could be resolved to 3.0 Å (Efremov and Sazanov, 2011). Different nomenclatures apply to the different complex I isoenzymes and other homologs. In this study, the *E. coli* complex I designations will be used (Nuo nomenclature).

In complex I, electrons are derived from NADH via NuoEFG. No NuoEFG homolog is present in *Ms. mazei* or *Mt. thermoacetophila* and NADH cannot serve as electron donor (Welte and Deppenmeier, 2014). In *Ms. mazei,* the hydrophilic subunit FpoF acts as electron input

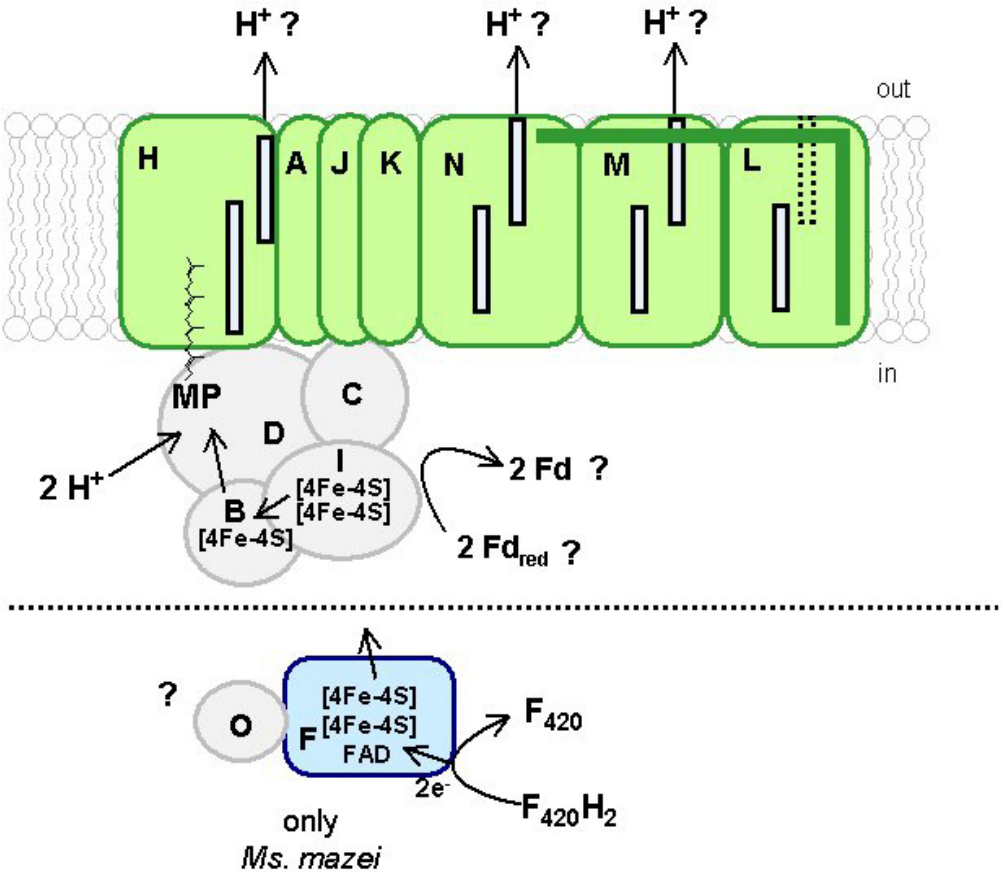

Figure 21: The Fpo complex as found in *Mt. thermoacetophila* and below the dotted line with additional subunits found in *Ms. mazei*. The structure was reconstructed according to the structure of complex I from *Thermus thermophilus* and *E. coli* (Efremov *et al.*, 2010; Efremov and Sazanov, 2011; Welte and Deppenmeier, 2014). The transversal helix found in subunit L that is thought to mediate conformational changes leading to proton translocation is marked in dark blue. Furthermore, in comparison to *T. thermophilus* and *E. coli,* subunit L from *Ms. mazei* contains an insertion that probably prohibits proton translocation at one coupling site (dotted line). In contrast, in *Mt. thermoacetophila* the insertion is missing and proton translocation should be possible. MP: methanophenazine. Modified after (Welte and Deppenmeier, 2014).

module and oxidizes the cytoplasmic electron carrier $F_{420}H_2$ (Abken and Deppenmeier, 1997). However, FpoF is known to be able to dissociate from the complex, granting access to the membrane-associated subunits FpoBCDI (Welte and Deppenmeier, 2011a). The exact localization of hydrophilic FpoO is unclear at present since there is no homologous counterpart in complex I, but it could be involved in the dissociation of FpoF. In *Mt. thermoacetophila,* the gene encoding FpoF is missing (Smith and Ingram-Smith, 2007) and consequently $F_{420}H_2$ cannot serve as electron donor for the respiratory chain, but is replaced by Fd_{red}. In complex I, electrons derived from NADH are transferred via the [4Fe4S] clusters N6a and N6b in NuoI to the terminal cluster N2 in NuoB (Efremov and Sazanov, 2011). Binding motives for [4Fe4S] clusters can be found in FpoI, which is homologous to NuoI and in FpoB, which is homologous to NuoB. It is thought that Fd_{red} is able to directly interact with subunit FpoI and that electrons from Fd_{red} can be transferred to [4Fe4S] clusters in FpoI and further to FpoB (Welte and Deppenmeier, 2011b, 2014).

This is substantiated by the fact that the FpoI polypeptide from *Mt. thermoacetophila* is longer than that of *Ms. mazei* and contains a C-terminal extension with an unusually high amount of lysine residues. This positively-charged amino acid could facilitate interaction with negatively-charged Fd (Welte and Deppenmeier, 2014). The modification of subunit FpoI from *Mt. thermoacetophila* could mirror the dependency of the organism on the Fpo complex for Fd_{red}-oxidation.

Oxidation of reduced cofactors is coupled to the concomitant translocation of protons across the cytoplasmic membrane, which is mediated by membrane-integral subunits. According to hydropathy plots, subunits FpoA, H, J, K, L, M and N form more than 50 transmembrane helices and are thus membrane-integral. So-called half-channels formed by transmembrane helices are responsible for proton translocation. In *Ms. mazei* two protons are translocated per two electrons (Bäumer *et al.*, 2000). Interestingly, in *Ms. mazei* one of the half-channels is thought to be dysfunctional due to an insertion in one of the transmembrane helices (Welte and Deppenmeier, 2014). The insertion cannot be found in *Mt. thermoacetophila* and thus, in comparison with *Ms. mazei,* the Fpo complex from *Mt. thermoacetophila* might contain an additional coupling site. Another important structural element is a transversal helix that belongs to subunit FpoL. It is thought to confer conformational changes, resulting from the reduction of MP to the half-channels, as a trigger for the translocation of protons (Efremov and Sazanov, 2011; Welte and Deppenmeier, 2014).

In this study the question of Fd_{red}-oxidation by the Fpo complex was addressed by the attempt to generate *Ms. mazei* double knock-out mutants. In such a mutant, two genes or operons are replaced by antibiotic resistance cassettes. Generation of single knock-outs in *Ms. mazei* is a routine procedure (Ehlers *et al.*, 2005). In this method, the gene of interest is

exchanged via homologous recombination with a puromycin resistance cassette. Mutants are resistant to puromycin and can be selected from the wild type, in which puromycin acts as inhibitor of protein biosynthesis. With this method, a mutant lacking the Ech hydrogenase was generated (Welte *et al.*, 2010b).

The construction of double mutants has long been hampered by the fact that only one selective antibiotic was available. Due to differences in cell wall architecture and translational machinery, most antibacterial antibiotics cannot be used for archaea. Yet, recently a system based on neomycin was established (Mondorf *et al.*, 2012). Neomycin is also an inhibitor of protein biosynthesis but no cross-resistance with puromycin could be observed (Mondorf *et al.*, 2012). Therefore, puromycin and neomycin act independently and can be used together.

A knock-out mutant, where the gene encoding the Ech hydrogenase was replaced by the puromycin resistance cassette (Welte *et al.*, 2010b), was used for the construction of a double mutant. The double mutant should be missing *fpoA-fpoO,* which would result in a *Ms. mazei* Δ*ech* Δ*fpo* mutant, still harboring *fpoF*. It has already been shown that in the membrane fraction of the *Ms. mazei* Δ*ech* mutant, the Fd_{red}-oxidation rate is decreased by about 50 % (Welte *et al.*, 2010b). The Fpo complex is thought to be responsible for the residual activity. If this residual activity was abolished in a double mutant missing Ech hydrogenase as well as the Fpo complex, it would become clear that the Fpo complex indeed catalyzes Fd_{red}-oxidation.

Furthermore, in a similar approach the generation of double knock-out mutants missing the Ech hydrogenase and either subunit FpoF or FpoO was attempted. With a *Ms. mazei* Δ*ech* Δ*fpoF* mutant, the role of FpoF in Fd_{red}-oxidation could be investigated, which is important especially since FpoF acts as F_{420}:Fd oxidoreductase (Welte and Deppenmeier, 2011a). Similarly, the role of FpoO could be investigated in a *Ms. mazei* Δ*ech* Δ*fpoO* mutant.

Knock-out vectors based on the pJK3 plasmid were generated. The vector could replicate in *E. coli* but was a suicide vector in *Ms. mazei*. Fragments of approximately 1 kb from the upstream region of *fpoA* and the downstream region of *fpoO* were cloned around the neomycin resistance cassette yielding pJK3-*neoR*-Δ*fpoA-O*. The same was done with the up- and downstream region of the *fpoF* and *fpoO* genes.

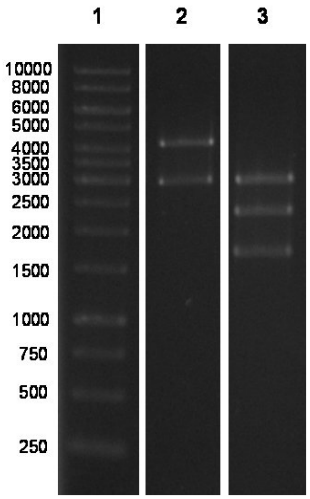

Figure 22: Restriction digestion of vectors used for double knock-outs in *Ms. mazei* Δ*ech*. (1) 1 kb DNA ladder; (2) pJK3-*neoR*-*fpo*Δ*A*-*O* digested in fragments of 2919 bp and 4154 bp with *Bsa*I; (3) pJK3-*neoR*-Δ*fpoO* split in fragments of 1662, 2267 and 2931 bp by digestion with *Bsa*I. Sizes of fragments were as expected.

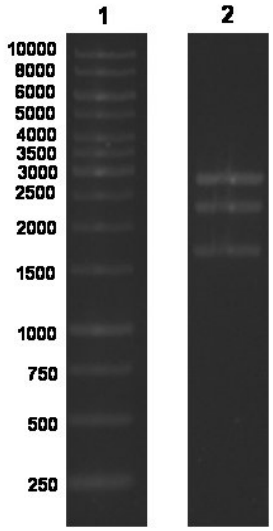

Figure 23: Restriction digest of pJK3-*neoR*-Δ*fpoF* used to knock-out *fpoF* in *Ms. mazei* Δ*ech*. (1) 1 kb DNA ladder; (2) pJK3-*neoR*-Δ*fpoF* digested with *Bsa*I. Fragments of the expected sizes (2362, 1761 and 2902 bp) could be obtained.

Those regions should promote homologous recombination between the vector and the chromosomal DNA, thereby integrating the resistance cassette into the chromosome replacing the *fpo* operon, *fpoF* or *fpoO*. Since the vector was not able to replicate in *Ms. mazei,* only cells with a chromosomal copy of the neomycin resistance cassette were able to grow when neomycin was added with a concentration of 15 μg mL^{-1}. Vectors containing the up- and downstream fragments were checked with restriction digestion with *Bsa*I.

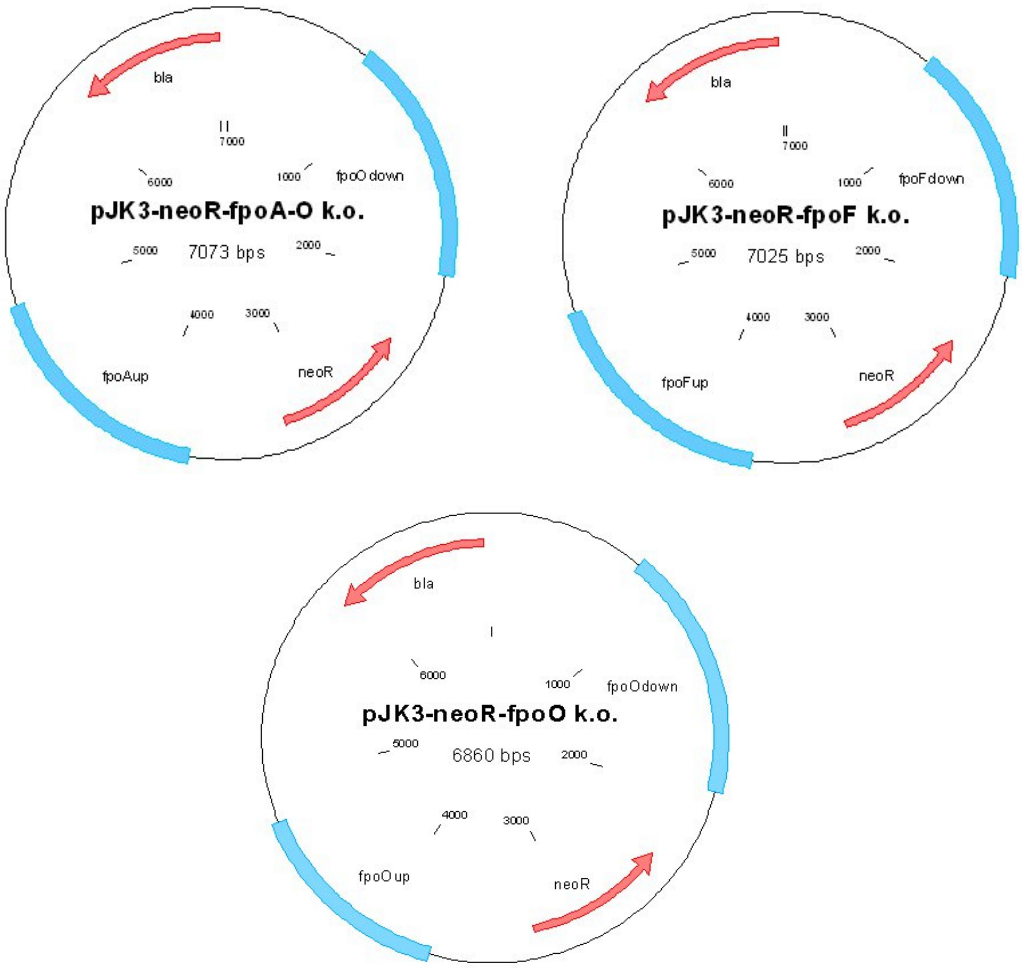

Figure 24: Knock-out vectors for the construction of a *Ms. mazei* double mutant. Vectors were transformed into the *Ms. mazei* Δ*ech* mutant via lipofection. The neomycin resistance cassette should be integrated into the chromosome via homologous recombination replacing the *fpo* operon, *fpoF* or *fpoO*. Bla – beta lactamase gene; neoR – neomycin resistance cassette.

Agarose gel electrophoresis confirmed the generation of DNA fragments of the expected sizes (2919 bp and 4154 bp for pJK3-*neoR*-Δ*fpoA-O*, Figure 22). Additionally, the presence of the *fpoA* upstream fragment and the *fpoO* downstream fragment was confirmed by DNA sequencing. Generation of fragments of the expected sizes was likewise confirmed for pJK3-*neoR*-Δ*fpoO* (1662, 2267 and 2931 bp, Figure 22) and for pJK3-*neoR*-Δ*fpoF* (2362, 1761 and 2902 bp, Figure 23). The vector maps can be viewed in Figure 24. Vectors were linearized and transformed into *Ms. mazei* Δ*ech* via lipofection (2.4.15). After regeneration overnight, puromycin (5 μg mL^{-1}) was added to the cultures to maintain the Δ*ech* mutant, and neomycin (15 μg mL^{-1}) was added to select for mutants missing the *fpo* operon, *fpoF* or *fpoO*. For the

potential *Ms. mazei* Δ*ech* Δ*fpo* double mutant, methanol was used as substrate and TMA was used for *Ms. mazei* Δ*ech* Δ*fpoF* and *Ms. mazei* Δ*ech* Δ*fpoO* double mutants.

In a mutant missing the Ech hydrogenase and the whole Fpo complex, electrons need to be channeled into the respiratory chain via the Vho hydrogenase. In a complete respiratory chain, the Vho hydrogenase oxidizes H_2 that is built by the Ech hydrogenase and donates electrons to the membrane-bound heterodisulfide reductase. However, H_2 can also be formed by the F_{420}-reducing hydrogenase from $F_{420}H_2$ as already explained in chapter 3.2.1. Therefore, growth should be slow but still possible. In the *Ms. mazei* Δ*ech* Δ*fpoF* mutant the Fd_{red}-oxidizing capacities of the Ech hydrogenase and $F_{420}H_2$ oxidation via FpoF are missing. H_2-oxidation by the Vho hydrogenase can be used as a rescue pathway, as already mentioned above, and furthermore the Fpo complex should support generation of a membrane potential by oxidizing Fd_{red}. Hence, such a mutant should be viable. *Ms. mazei Δech* Δ*fpoO* double mutants are missing subunit FpoO but contain the rest of the Fpo complex, including the $F_{420}H_2$-oxidizing subunit FpoF. It was shown in this study that $F_{420}H_2$-oxidation and electron transfer to MP do not depend on the presence of FpoO. Therefore, the *Ms. mazei Δech* Δ*fpoO* double mutant should be able to grow with methylated substrates such as methanol or TMA. Successful generation of a mutant is indicated by growth in cultures containing the selective antibiotics as mentioned above. Yet, after transformation no growth could be observed, even after several months of incubation time.

It was concluded that if Ech hydrogenase and Fpo complex are missing, cells are not viable and such a mutant cannot be obtained. This is in agreement with the finding that *Ms. mazei* growing on methylated substrates relies on the Fpo complex instead of the F_{420}-reducing hydrogenase (Welte and Deppenmeier, 2011a). A growth experiment with a *Ms. mazei* Δ*fpo* mutant revealed that while cultures are still able to grow, the doubling time is prolonged and thus the F_{420}-reducing hydrogenase cannot fully substitute for the loss of the Fpo complex (Welte and Deppenmeier, 2011a). Obviously, the loss of Ech hydrogenase and Fpo complex at the same time cannot be compensated for. The same is probably true for the *Ms. mazei Δech* Δ*fpoF* double mutant. It would still contain a headless Fpo complex, but obviously this cannot substitute for the lack of Ech hydrogenase and FpoF. For *Ms. mazei Δech* Δ*fpoO,* this seems unlikely because it was shown in this thesis that $F_{420}H_2$-oxidation by the Fpo complex was not impaired if subunit FpoO was missing. Therefore, double mutants should have been able to grow as was the case for a *Ms. mazei* Δ*fpoO* single mutant. Yet, the additional lack of the Ech hydrogenase in a potential double mutant might contribute to significantly decreased fitness, as is the case for the *Ms. mazei* Δ*ech* single mutant (Welte *et al.*, 2010b).

Therefore, a different approach was chosen to show Fd_{red}-oxidation by the Fpo complex. An antibody against subunit FpoI from the Fpo complex of *Ms. mazei* was produced and used to inhibit electron transfer from Fd_{red} to the Fpo complex. Subunit FpoI is homologous to subunit

NuoI from complex I that contains [4Fe4S] clusters N6a and N6b (Welte and Deppenmeier, 2014). From those clusters, electrons are further transferred to the terminal cluster N2 in NuoB. A homologous cluster is potentially harbored by FpoB. Electrons from Fd_{red} could be directly transferred to [4Fe4S] clusters in FpoI and further to MP via FpoB. This is supported by the fact that FpoI from *Mt. thermoacetophila*, where reducing equivalents are always transferred to Fd, contains a C-terminal extension which could facilitate interaction with Fd_{red} (Welte and Deppenmeier, 2014). An antibody binding to FpoI should interrupt Fd_{red} oxidation by shielding it against interactions.

Recombinant FpoI from *Ms. mazei* for production of the antibody was kindly provided by Sarah Refai (Rheinische-Friedrich-Wilhelms Universität, Bonn, Germany). Antibody generation was carried out by Seqlab (Göttingen, Germany). For purification from rabbit serum, affinity chromatography was performed. Therefore, FpoI was heterologously produced in *E. coli*. 7 mg of the FpoI protein were isolated via Strep-tag affinity chromatography and afterwards were coupled to Affi-Gel obtained from Bio-Rad (Munich, Germany). The Affi-Gel matrix consisted of a derivatized agarose gel bead support with N-hydroxysuccinimide esters as functional groups. N-hydroxysuccinimide esters react spontaneously with primary amino groups and can thus covalently bind proteins. Coupling of FpoI to the matrix and blocking of unreacted esters was carried out as described in the materials and methods part (2.5.9).

Rabbit serum was applied to the column, and after several washing steps the FpoI antibody was eluted with 100 mM glycine pH 2.5. Elution fractions were neutralized immediately with 1 M Tris-HCl buffer pH 8. The antibody eluted in fractions one, two and three. Fractions were pooled and the protein concentration, as determined by Bradford assay, was 26 μg mL^{-1}. The antibody solution was checked by SDS-PAGE. Two bands were detected by silver staining, which represented the heavy and the light chain of the FpoI antibody (Figure 25). There were no contaminations by other proteins.

The purified antibody was used in an enzymatic assay that measured the Fd_{red}-dependent reduction of the heterodisulfide and hence thiol production. For quantification of thiols, the so-called Ellman's reagent (5,5'-dithiobis-2-nitrobenzoic acid (DTNB)) was employed. This compound reacts with thiol groups to give a yellow color at neutral or alkaline pH.

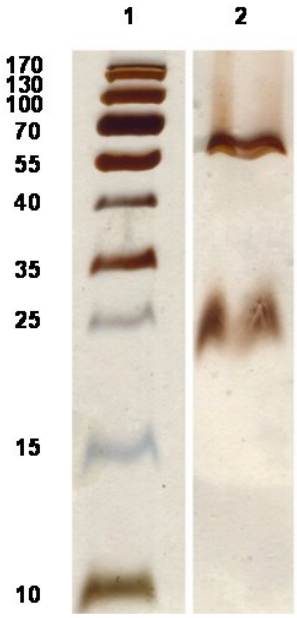

Figure 25: Heavy and light chain of the purified antibody against subunit FpoI from the Fpo complex of *Ms. mazei*. Isolation from rabbit serum was done by affinity chromatography using Affi-Gel according to the manufacturer's instructions. 0.26 µg of the antibody were loaded prior to silver staining. No contamination by other proteins was detected. 1: PAGE ruler prestained protein ladder; 2: FpoI antibody.

With this assay, membrane fractions of the *Ms. mazei* Δ*ech* mutant were already shown to catalyze Fd_{red}-dependent thiol production with a rate of 40-50 nmol min^{-1} mg^{-1}. The Fpo complex is thought to be responsible for the activity measured in the *Ms. mazei* Δ*ech* mutant (Welte and Deppenmeier, 2011a). If this is the case, Fd_{red}-dependent thiol production should be inhibited by the purified antibody that specifically binds to subunit FpoI from the Fpo complex.

Tests were performed anaerobically in rubber-stoppered glass vials with a N_2 atmosphere. Vials contained 200 µL potassium phosphate buffer (40 mM, pH 7) and were reduced with titanium (III) citrate. Firstly, it had to be excluded that the FpoI antibody unspecifically targeted the heterodisulfide reductase. If this were the case, a potential inhibitory effect on the Fpo complex would not have been measurable in this assay. Therefore, hydrogen was added as electron donor for the Vho hydrogenase. The aim of the hydrogen addition was to transfer electrons from the Vho hydrogenase to the heterodisulfide reductase and finally to the heterodisulfide. The Fpo complex was not involved in this electron transport chain, therefore thiol production rates should be the same with and without addition of the antibody (Figure 26).

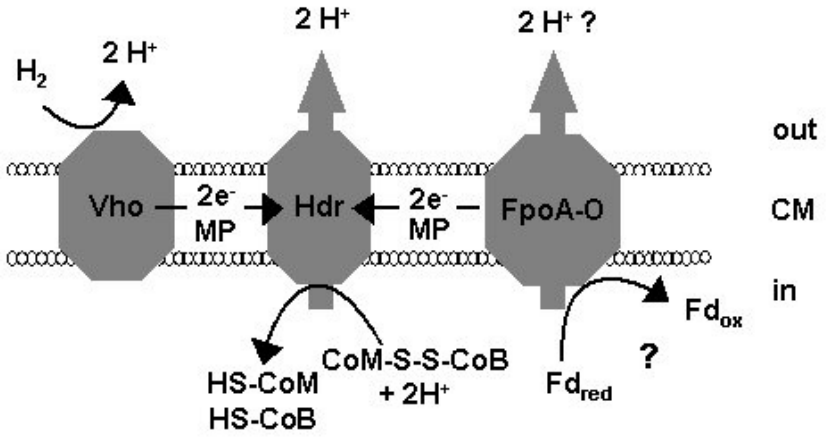

Figure 26: Simplified model of the respiratory chain of *Ms. mazei*. Electrons for the reduction of heterodisulfide are either derived from H_2 or from Fd_{red}. The Vho hydrogenase is used for H_2 oxidation. Fd_{red}-oxidation by the Fpo complex was investigated in the course of this study.

The assay contained 100 µg of *Ms. mazei* Δ*ech* membrane protein, 1.25 mM heterodisulfide and a 100 % H_2 atmosphere. In the positive control without addition of the FpoI antibody, the thiol production rate was 314 nmol min^{-1} mg^{-1}. Addition of 0.5 µg of antibody led to a thiol production rate of 392 nmol min^{-1} mg^{-1} (Table 13). It was concluded that the FpoI antibody had no unspecific interactions with the heterodisulfide reductase. Hence, the assay was suitable to measure a potential inhibition of the Fpo complex by the FpoI antibody.
Since Fd_{red}-dependent thiol production should be measured, Fd_{red} needed to be supplied. A system for enzymatic reduction of Fd was developed by Cornelia Welte (Radboud Universiteit Nijmegen, The Netherlands). It is based on the indolpyruvate:ferredoxin oxidoreductase (IOR) from *Ms. mazei*. This enzyme catalyzes oxidation of phenylpyruvate and concomitant reduction of Fd as shown in Reaction (4).

Reaction (4): Phenylpyruvate + CoA + 2 Fd_{ox} → Phenylacetyl-CoA + 2 Fd_{red} + CO_2 + 2 H^+

The IOR was produced in *E. coli* and purified anaerobically via Strep-tactin affinity chromatography. The enzyme consists of two subunits encoded by *mm_2093* and *mm_2094* that can be easily co-purified and stored at -70 °C. Thiamine pyrophosphate is needed as a cofactor and was therefore supplied in the enzymatic assay. Fd used in the assay was Mm1619 from *Ms. mazei*. Like the IOR it was recombinantly produced in *E. coli* and isolated with Strep-tactin affinity chromatography. Vectors for protein overproduction were provided by Cornelia Welte (Radboud Universiteit Nijmegen, The Netherlands).

Fd_{red}-dependent Ellman's assays routinely contained 150 µg IOR, 100 µg Fd Mm1619, 250 µg *Ms. mazei* Δ*ech* membrane fraction, 1.25 mM heterodisulfide, 4 mM phenylpyruvate, 1 mM CoA and 0.5 mM thiamine pyrophosphate. The reaction was started by the addition of Fd. Samples were taken every three minutes, DTNB was added and absorption at 412 nm

was measured immediately. In the positive control the FpoI antibody was omitted. The negative control contained all components except Fd and the antibody. For the positive control, the thiol production rate was 52 ± 6 nmol min^{-1} mg^{-1}, which is in the range of literature values (Welte *et al.*, 2010b). The addition of 0.5 µg of the FpoI antibody decreased the thiol production rate by about half and only 31 ± 6 nmol min^{-1} mg^{-1} were measured (Figure 27, Table 13).

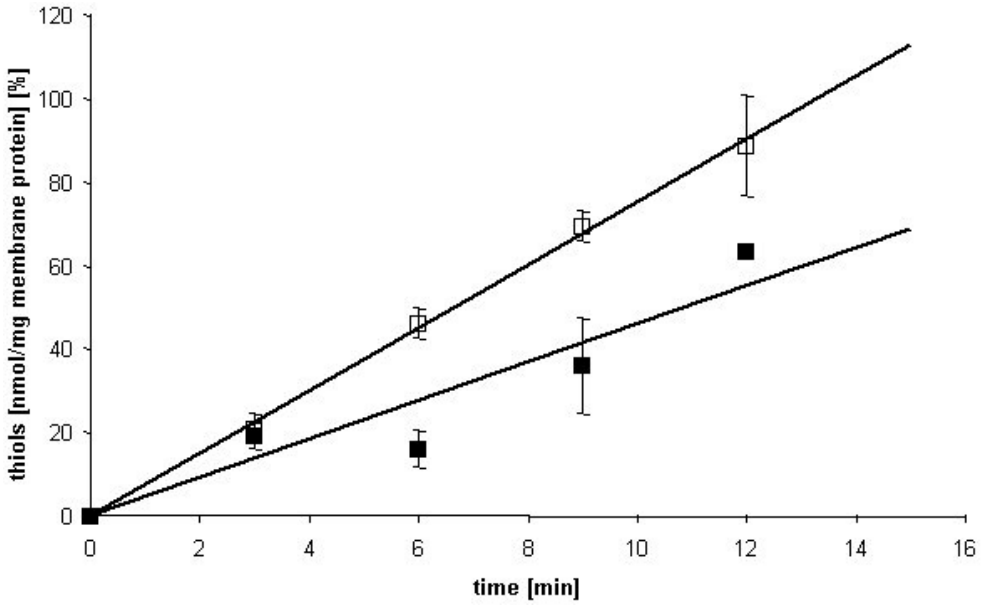

Figure 27: Thiol production rate of *Ms. mazei* Δ*ech* membranes with and without addition of an antibody binding to subunit FpoI. (□) Without antibody: 52 ± 6 nmol min^{-1} mg^{-1}; (■) With antibody: 31 ± 6 nmol min^{-1} mg^{-1} (addition of 0.5 µg of the FpoI antibody in 200 µL potassium phosphate buffer containing 250 µg *Ms. mazei* Δ*ech* membrane fraction).

This indicated clearly that Fd_{red} oxidation was inhibited by masking subunit FpoI with a specific antibody. It should be confirmed by using different amounts of antibody in the same test system. The addition of 0.13 µg of the antibody did not have an effect on the thiol production rate, 0.5 µg had the above-described effect and with the addition of 1.3 µg, no thiol production could be detected anymore (Figure 28).

The FpoI antibody solution therefore most certainly had an inhibitory effect on Fd_{red}-dependent thiol production by membranes of a *Ms. mazei* Δ*ech* mutant. Hence, it seems likely that subunit FpoI can accept electrons from reduced Fd that are channeled into the respiratory chain.

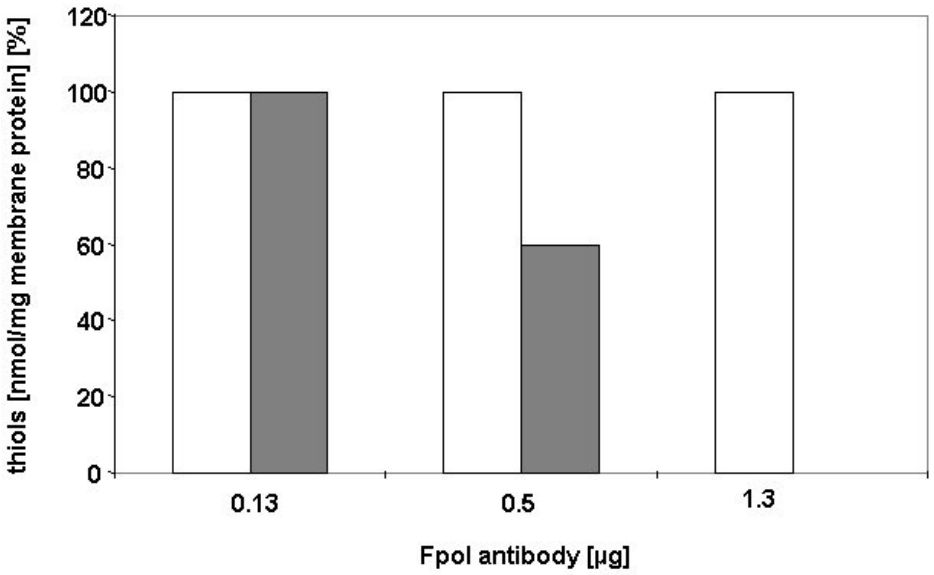

Figure 28: Relative thiol production rate of *Ms. mazei* Δ*ech* membranes with different amounts of an antibody binding to subunit FpoI. 0.13 µg of the antibody in a 200 µL assay containing 250 µg membrane protein did not have an effect on thiol production rate, addition of 0.5 µg decreased the thiol production rate by 40 % and addition of 1.3 µg abolished thiol production. White bars: positive control without antibody; gray bars: assay containing indicated amount of FpoI antibody.

As a control, the FpoI antibody was denatured by boiling for 10' at 100 °C. In its denatured form the antibody should not have an inhibitory effect on the thiol production rate because it cannot bind to the Fpo complex. In the assay containing the denatured antibody, a thiol production rate of 51 nmol min^{-1} mg^{-1} was measured. The control assay without addition of the antibody showed a thiol production rate of 44 nmol min^{-1} mg^{-1} (Table 13). Hence, the inhibitory effect of the FpoI antibody could be effectively abolished by heat denaturation.

Table 13: Thiol production rate of the membrane fraction of the *Ms. mazei* Δ*ech* mutant with and without FpoI antibody.

Electron donor	Thiol production rate [nmol min^{-1} mg^{-1}]	
	- FpoI antibody	+ FpoI antibody (0.5 µg)
H_2	314	392
Fd_{red}	52 ± 6	31 ± 6
	- FpoI antibody	+ FpoI antibody, denatured (0.5 µg)
Fd_{red}	44	51

Altogether, the evidence presented here demonstrated that Fd_{red}-dependent reduction of the heterodisulfide can be successfully inhibited by masking subunit FpoI with a specific antibody. This inhibitory effect was not due to unspecific interactions with other enzymes of the respiratory chain and could be abolished by heat denaturation of the antibody. Thus, the Fpo complex can accept electrons from reduced Fd, most likely via subunit FpoI. Since thiol production in the *Ms. mazei* Δ*ech* mutant was completely ceased with addition of 1.3 µg of the FpoI antibody, it can be concluded that there are no other membrane-bound enzymes that accept electrons from Fd_{red}.

It is tempting to speculate that the oxidation of Fd_{red} is an original trait of the Fpo complex, which was used before other electron carriers like F_{420} and their respective electron input modules evolved. Further, it seems that this ability has been retained in *Mt. thermoacetophila,* which produces only Fd_{red} during methanogenesis and contains none of the typical Fd_{red}-oxidizing enzymes (Rnf complex or Ech hydrogenase).

3.3 First insights into the energy metabolism of *Mm. luminyensis*

Mm. luminyensis is a member of a recently discovered, Thermoplasmatales-related lineage of methanogens. It was isolated with H_2 and methanol as substrates (Dridi *et al.*, 2012). After sequencing of the genome in 2012 (Gorlas *et al.*, 2012), it became obvious that the composition of proteins possibly involved in methanogenesis and energy conservation is quite unique. In the course of this study, utilization of methylated substrates other than methanol was investigated as well as enzymatic activity of soluble heterodisulfide reductase and Ech hydrogenase.

3.3.1 Bioinformatic analysis of *Mm. luminyensis*

To gain first insights into the metabolism of *Mm. luminyensis,* bioinformatic analyses were performed. The results that were obtained in the meantime were confirmed by (Borrel *et al.*, 2013; Poulsen *et al.*, 2013; Borrel *et al.*, 2014). Most methanogenic archaea depend on H_2+CO_2 for methanogenesis, which are the substrates with the highest change in free energy under standard conditions ($\Delta G^{0'}$ = –130 kJ mol^{-1} CH_4, (Deppenmeier, 2002b)). Electrons from H_2 are used to generate Fd_{red} and $F_{420}H_2$. Using these electron carrier molecules CO_2 is stepwise reduced via formyl-MF, methyl-H_4MPT and finally with HS-CoB to methane.

However, genes encoding enzymes catalyzing the above-mentioned reactions (formyl-MF dehydrogenase, Eha or Ehb, formylmethanofuran-H_4MPT formyltransferase, methenyl-H_4MPT cyclohydrolase, methylene-H_4MPT dehydrogenase and reductase, F_{420}-reducing hydrogenase) could not be found in the genome of *Mm. luminyensis*. Therefore, CO_2 reduction is not possible and H_2+CO_2 is not used as substrate. This was confirmed upon

isolation of the organism, which was achieved using H_2 and methanol (Dridi *et al.*, 2012).

Growth with methylated substrates such as methanol and methylated amines requires substrate-specific enzymes that catalyze uptake of substrates and transfer of methyl groups (Bose *et al.*, 2006; Pritchett and Metcalf, 2005, Krätzer *et al.*, 2009). Permeases facilitate uptake of trimethylamine (TMA), dimethylamine (DMA) and monomethylamine (MMA). After uptake, substrate-specific methyltransferases shift methyl groups to cognate corrinoid proteins (Figure 29). This is the first of two methyl transfer reactions. In the course of the reaction, the Co-containing cobalamin cofactor of the corrinoid protein changes between a methyl-Co(III) and Co(I) state (Rother and Krzycki, 2010).

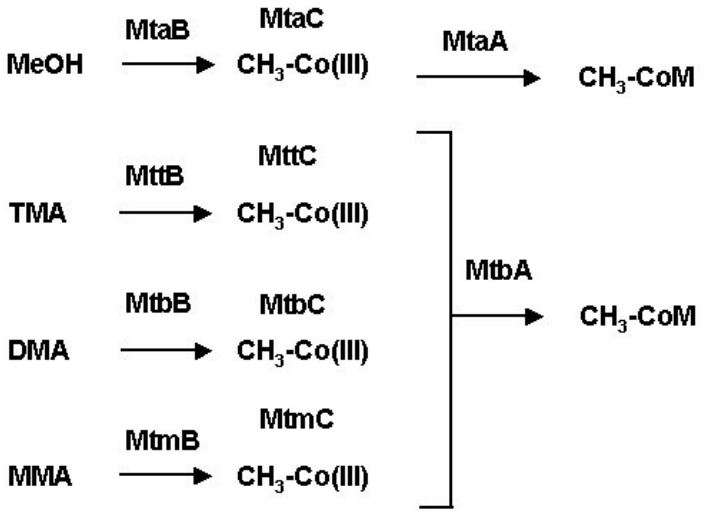

Figure 29: Methyl group transfer from methanol, TMA, DMA and MMA. Methyl groups are transferred by substrate specific methyltransferases to cognate corrinoid proteins and further to coenzyme M. MeOH: methanol.

Subsequently, in a second methyl transfer reaction, corrinoid proteins are demethylated by a methylcobamide:CoM methyltransferase (MtbA for methylamines and MtaA for methanol) that forms methyl-CoM. Finally, methyl-CoM is reductively demethylated by the methyl-CoM reductase to yield methane. Proteins probably involved in the degradation of methylated substrates were identified in *Mm. luminyensis* by comparison with the model organism *Ms. mazei*. For the respective function, homology and accession number in *Mm. luminyensis,* the reader is referred to Table 14.

In *Ms. mazei* most methyltransferases catalyzing the first methyl transfer reaction and also the corresponding corrinoid proteins exist in two or even three copies (Krätzer *et al.*, 2009). MtaA catalyzing the second methyl transfer of methyl groups derived from methanol exists in two copies, but the MtaA1 protein encoded by *mm_1070* seems to be the principal enzyme (Bose *et al.*, 2008). However, methyltransferases that catalyze the same reaction are highly

homologous and therefore in this study representative methyltransferases were used for sequence comparison. Gene numbers and sequences for comparison were derived from (Krätzer *et al.*, 2009) and from the NCBI and KEGG databases.

Permeases specific for TMA, DMA and MMA have been identified in *Ms. mazei* (Deppenmeier *et al.*, 2002). For the TMA permease Mm1691/1692, homologous counterparts with 63 and 60 % identity on the protein level could be found in *Mm. luminyensis* (accession numbers WP_019178521.1, WP_019178523.1). Blast search analysis with a second TMA permease from *Ms. mazei* (Mm2045/2046) retrieved the same hits in *Mm. luminyensis*. The only DMA permease from *Ms. mazei* Mm2964 is less well conserved in *Mm. luminyensis*. A rather unspecific hit was found in the NCBI database with 25 % identity and an E-value of $1e^{-13}$ (accession number WP_019176434.1). The same is true for the MMA permease from *Ms. mazei* (Mm1435). One weakly homologous proteins could be identified in *Mm. luminyensis* (accession number WP_019177909.1, 26 % $6e^{-11}$) that could be a MMA permease.

After uptake, substrate-specific methyltransferases transfer methyl groups to corresponding corrinoid proteins. Blast search analysis with a methanol-specific methyltransferase (methanol:corrinoid protein Co-methyltransferase, MtaB) from *Ms. mazei* (Mm1647), and with phylogenetically related methanol-specific methyltransferase sequences from an environmental sample (KF302411-KF302419, (Borrel *et al.*, 2013)), revealed three homologous proteins in *Mm. luminyensis* (accession numbers WP_019177726.1, WP_019176360.1, WP_019178088.1). Likewise, for the cognate corrinoid protein (methyl-Co(III) methanol-specific corrinoid protein, MtaC) from *Ms. mazei* (Mm1648) and the respective environmental sequences (KF302420-KF302421, (Borrel *et al.*, 2013)), three significantly homologous sequences could be identified (accession numbers WP_019177725.1, WP_019176359.1, WP_019178087.1). Furthermore, in *Mm. luminyensis* a protein homologous to the methanol-specific methylcobamide:CoM methyltransferase MtaA1 that transfers methyl groups to HS-CoM could be found. There is 35 % identity on the protein level with MtaA1 from *Ms. mazei* (Mm1070). Thus a methanol-specific methylcobamide:CoM methyltransferase probably exists in *Mm. luminyensis* (accession number WP_026068914.1). Therefore, *Mm. luminyensis* should be able to metabolize methanol.

For TMA the situtation is similar: *Mm. luminyensis* contains a putative TMA-specific methyltransferase (trimethylamine:corrinoid protein Co-methyltransferase, MttB, accession number WP_019178519.1) with 72 % identity with the respective protein from *Ms. mazei* (Mm1688, E-value $4e^{-176}$). The corresponding corrinoid protein (MttC, Mm1689 in *Ms. mazei*) had one homolog in *Mm. luminyensis* (accession number WP_019178520.1, 68 % identity, E-value $7e^{-70}$). The methylamine-specific MtbA from *Ms. mazei* catalyzing the second methyl

transfer reaction also had a counterpart in *Mm. luminyensis* (accession number WP_026068761.1). There was 38 % identity with MtbA from *Ms. mazei* and it is therefore most likely that a methylamine-specific methylcobamide:CoM methyltransferase is also present. Thus, all requirements for growth with methanol and TMA are fulfilled. Consequently, growth with H_2 and methanol or TMA has already been reported (Dridi *et al.*, 2012; Brugère *et al.*, 2014).

Currently, there is no data about growth with the methylated substrates DMA and MMA. As already mentioned above, the respective permeases are weakly conserved in *Mm. luminyensis*.

Table 14: Enzymes catalyzing breakdown of the methylated substrates methanol, TMA, DMA and MMA.

Function	Synonym	Accession number in *Mm. luminyensis*	Homolog in *Ms. mazei*	Identity [%]	E-value
Methanol:corrinoid protein Co-methyltransferase	MtaB1	WP_019177726.1		52	$3e^{-164}$
		WP_019176360.1	Mm1647	53	$1e^{-172}$
		WP_019178088.1		52	$4e^{-165}$
Methyl-Co(III) methanol-specific corrinoid protein	MtaC1	WP_019177725.1		45	$1e^{-63}$
		WP_019176359.1	Mm1648	45	$4e^{-64}$
		WP_019178087.1		47	$1e^{-68}$
Methanol-specific methylcobamide:CoM methyltransferase	MtaA1	WP_026068914.1	Mm1070	35	$5e^{-63}$
TMA permease	MttP	WP_019178521.1	Mm1691	63	$4e^{-161}$
		WP_019178523.1	Mm1692	60	$5e^{-40}$
Trimethylamine:corrinoid protein Co-methyltransferase	MttB1	WP_019178519.1	Mm1688	72	$4e^{-176}$
Methyl-Co(III) trimethylamine-specific corrinoid protein	MttC1	WP_019178520.1	Mm1689	68	$7e^{-70}$
DMA permease	MtbP	WP_019176434.1	Mm2964	25	$1e^{-13}$
Dimethylamine:corrinoid protein Co-methyltransferase	MtbB1	WP_019178526.1	Mm1693	77	0.0
		WP_019178527.1	Mm1694	72	$3e^{-49}$
Methyl-Co(III) dimethylamine-specific corrinoid protein	MtbC1	WP_019178525.1	Mm1687	71	$1e^{-54}$
MMA permease	MtmP	WP_019177909.1	Mm1435	26	$6e^{-11}$
Monomethylamine:corrinoid	MtmB1	WP_019178516.1	Mm1436	64	$1e^{-102}$

protein Co-methyltransferase		WP_019178553.1		62	$2e^{-99}$
		WP_019176315.1		66	$5e^{-107}$
Methyl-Co(III)		WP_019178518.1		37	$2e^{-41}$
monomethylamine-specific	MtmC1	WP_019178555.1	Mm1438	36	$1e^{-34}$
corrinoid protein		WP_019176313.1		35	$2e^{-41}$
Methylamine-specific methylcobamide:CoM methyltransferase	MtbA	WP_026068761.1	Mm1439	38	$2e^{-58}$

Furthermore, methyltransferase and corrinoid protein specific for dimethylamine (DMA) could be identified in *Mm. luminyensis*. Homologs for the DMA-specific methyltransferase represented by Mm1693/1694 in *Ms. mazei* (MtbB) could be identified (accession number WP_019178526.1, WP_019178527.1). The identity was 77 % with an E-value of 0.0 and 72 % with an E-value of $3e^{-49}$. For the cognate corrinoid protein MtbC (Mm1687 in *Ms. mazei*) there is one homolog in *Mm. luminyensis* (WP_019178525.1). The identity with Mm1687 was 71 % with a corresponding E-value of $1e^{-54}$.

Likewise, homologs of MtmB, the methyltransferase specific for monomethylamine (MMA) and respective corrinoid protein, MtmC, were present. Three homologs could be identified which were 64, 62 and 66 % identical with MtmB from *Ms. mazei* (Mm1436, E-values $1e^{-102}$, $2e^{-99}$, $5e^{-107}$ and accession numbers WP_019178516.1, WP_019178553.1, WP_019176315.1). For the corresponding corrinoid protein (Mm1438 in *Ms. mazei*) three homologs were detected (accession numbers WP_019178518.1, WP_019178555.1, WP_019176313.1), which shared 37, 36 and 35 % identity with E-values of $2e^{-41}$, $1e^{-34}$ and $2e^{-41}$.

The genome of *Mm. luminyensis* is sequenced except for a small part of ~17 kb (Borrel *et al.*, 2014). At present the collected sequencing information is assembled in contigs and a continuous sequence is not available. Yet, from annotated sequences available in NCBI it could be deduced that some methyltransferases were clustering together (Figure 30). The corresponding genes could potentially form operons, as is common for methyltransferase genes (Pritchett and Metcalf, 2005; Bose *et al.*, 2006; Krätzer *et al.*, 2009).

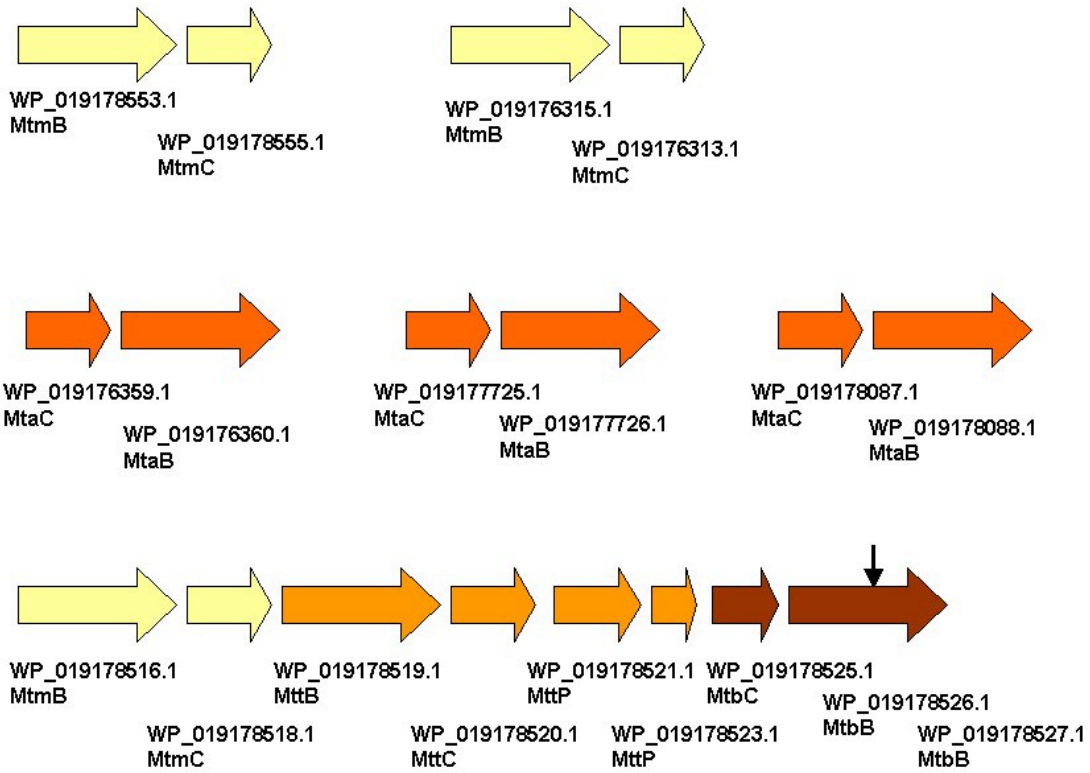

Figure 30: Clusters of methyltransferases from *Mm. luminyensis*. Yellow/Mtm: MMA metabolism, dark orange/Mta: methanol metabolism, bright orange/Mtt: TMA metabolism, red-brown/Mtb: DMA metabolism. The arrow indicates an *amber* codon for incorporation of pyrrolysine.

There were several small clusters containing MMA and methanol-specific methyltransferases and one big cluster with MMA, DMA and TMA-specific proteins (Figure 30). MtmB and MtmC proteins clustered together in two separate locations and three clusters could be identified for MtaB and MtaC proteins. The biggest cluster contained a full set of methyltransferases involved in MMA, DMA and TMA degradation, including a putative TMA permease (MttP). Potential MMA and DMA permeases as well as methylcobamide:CoM methyltransferases (MtaA and MtbA) had a different location.

To sum up, bioinformatic analyses of *Mm. luminyensis* revealed that homologs of all enzymes that are necessary for growth with H_2 and methanol or TMA are present. Accordingly, it was demonstrated that these substrates can be used for growth (Dridi *et al.*, 2012; Brugère *et al.*, 2014). Furthermore, enzymes catalyzing conversion of DMA and MMA could be identified. Therefore, growth with these substrates should be possible as well and was thus tested in the course of this study (3.3.2).

Methylamine-specific methyltransferases usually contain the rare amino acid pyrrolysine (Pyl, (Krzycki, 2004)). It is synthesized by PylBCD from two lysine molecules and bound to a Pyl-specific tRNA by the tRNA synthetase PylS for incorporation via the so-called *amber* codon (UAG, (Gaston *et al.*, 2011)). Since the *amber* codon normally is used as stop codon, a

suppressor tRNA (pylT) is needed to continue biosynthesis of methyltransferases. PylBCD, the tRNA synthetase PylS and the suppressor tRNA pylT could be identified in *Mm. luminyensis* as was also confirmed by Borrel (Borrel *et al.*, 2014). Therefore, correct biosynthesis of methyltransferases is guaranteed.

The final product of methyl group transfer reactions is methyl-CoM, which is a substrate for the methyl-CoM reductase. Using electrons from HS-CoB, it catalyzes reduction of the methyl moiety to methane. The other product of the reaction is the heterodisulfide CoM-S-S-CoB. The heterodisulfide is known to be reduced by the heterodisulfide reductase (Hdr). There is a membrane-bound HdrDE, which can be found in methanogenic archaea of the order Methanosarcinales (Heiden *et al.*, 1993). Yet, the majority of methanogens employ a soluble HdrABC. It is associated with the MvhADG hydrogenase that catalyzes H_2 oxidation. Electrons are transferred to the flavin-containing subunit HdrA, where electron bifurcation takes place. The exergonic reduction of the heterodisulfide is coupled to the endergonic reduction of Fd (Kaster *et al.*, 2011). In *Mm. luminyensis* the soluble HdrABC/MvhADG complex could be identified (accession numbers WP_019177460.1, WP_019177711.1, WP_019177712.1, WP_019177457.1, WP_019177459.1, WP_019177458.1; Table 15).

Table 15: Proteins possibly involved in energy conservation reactions in *Mm. luminyensis*

Function	Accession number in *Mm. luminyensis*	Homolog	Identity [%]	E-value
HdrA	WP_019177460.1	Msp1476	45	$3e^{-120}$
HdrB	WP_019177711.1	Msp1013	54	$5e^{-110}$
HdrC	WP_019177712.1	Msp1014	48	$8e^{-55}$
HdrD	WP_019178460.1	Mm1844	39	$6e^{-93}$
MvhA	WP_019177457.1	Msp0316	37	$2e^{-95}$
MvhD	WP_019177459.1	Msp0314	53	$6e^{-51}$
MvhG	WP_019177458.1	Msp0315	38	$8e^{-71}$
EchA1	WP_019176386.1[1]	Mm2320	n.a.[2]	n.a.[2]
EchA2	WP_019178471.1[1]			
EchB1	WP_019176385.1	Mm2321	32	$2e^{-42}$
EchB2	WP_019178472.1		41	$1e^{-51}$
EchC1	WP_019176384.1	Mm2322	63	$1e^{-60}$
EchC2	WP_019178473.1		53	$5e^{-55}$
EchD1	WP_019176383.1	Mm2323	36	$9e^{-10}$

EchD2	WP_019178474.1	Mm2324	32	$6e^{-12}$
EchE1	WP_019176382.1		44	$1e^{-111}$
EchE2	WP_019178475.1		43	$2e^{-106}$
EchF1	WP_019176381.1[1]	Mm2325	n.a.[2]	n.a.[2]
EchF2	WP_019178476.1[1]			
FpoA	WP_019176183.1	Mm2491	40	$2e^{-24}$
FpoB	WP_019176182.1	Mm2490	42	$4e^{-51}$
FpoC	WP_019176181.1	Mm2489	38	$8e^{-31}$
FpoD	WP_019176180.1	Mm2488	43	$3e^{-103}$
FpoH	WP_019176179.1[1]	Mm2487	n.a.[2]	n.a.[2]
FpoI	WP_019176178.1	Mm2486	31	$3e^{-14}$
FpoJ1	WP_019176177.1	Mm2485	48	$5e^{-18}$
FpoJ2	WP_019176176.1	Mm2484	30	0.002
FpoK	WP_019176175.1	Mm2483	61	$1e-^{34}$
FpoL	WP_019176174.1	Mm2482	43	$3e^{-147}$
FpoM	WP_019176173.1	Mm2481	44	$7e^{-130}$
FpoN	WP_019176172.1	Mm2480	48	$8e^{-128}$

[1]: WP numbers according to (Borrel *et al.*, 2014)

[2]: No data available because records of corresponding sequences were removed from the NCBI database.

Mm: *Ms. mazei*, Msp: *Mp. stadtmanae*

Thus, the enzyme is probably used for H_2 oxidation and concomitant reduction of the heterodisulfide and Fd. In this way, the cofactors HS-CoM and HS-CoB are regenerated. Additionally, subunit HdrD of the membrane-bound Hdr enzyme was identified (accession number WP_019178460.1). HdrD is the subunit catalyzing reduction of the heterodisulfide in members of the order Methanosarcinales. Normally, it is attached to the membrane via HdrE, which transfers electrons from MPH_2 to HdrD (Abken *et al.*, 1998). Yet, this membrane-integral subunit is missing from *Mm. luminyensis*. Therefore, the role of HdrD is not clear.

However, the fate of Fd_{red} that is generated by the soluble Hdr is also quite ambiguous. In hydrogenotrophic methanogens, Fd_{red} is used for CO_2 reduction by the formyl-MF dehydrogenase (Rouvière and Wolfe, 1989; Costa *et al.*, 2010; Kaster *et al.*, 2011). But since the CO_2 reducing pathway is not present in *Mm. luminyensis,* Fd_{red} has to be otherwise re-oxidized. One possible candidate is the Ech hydrogenase. This enzyme belongs to the multisubunit [NiFe] hydrogenases and is able to oxidize Fd_{red} with concomitant ion

translocation across the cytoplasmic membrane (Welte *et al.*, 2010b). The Ech hydrogenases from *Ms. mazei* and *Ms. barkeri* consist of subunits EchABCDEF. Homologs for all of these subunits were present in *Mm. luminyensis*. Interestingly, for each subunit there were two copies indicating the presence of two Ech hydrogenase isoenzymes (Table 15).

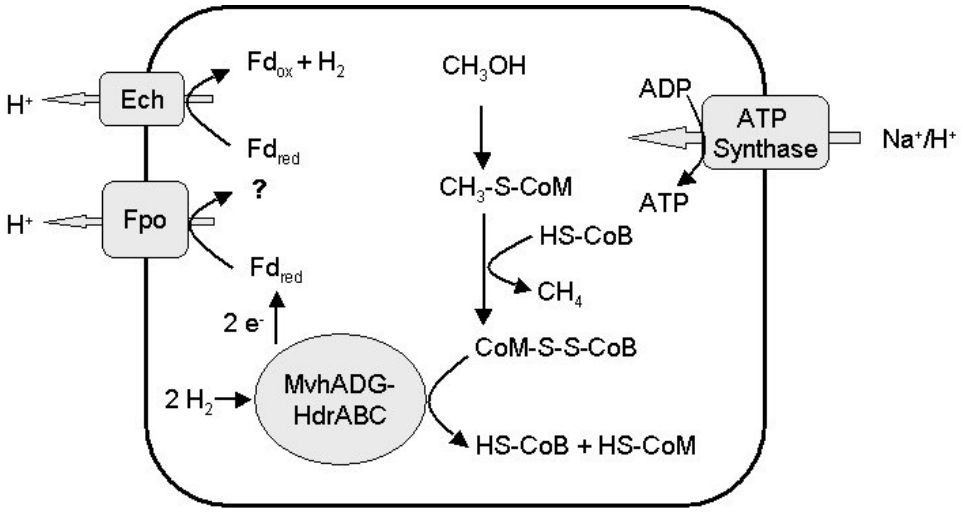

Figure 31: Tentative model of energy conservation mechanisms in *Mm. luminyensis*. Methyl groups are transferred to HS-CoM and reduced to methane with HS-CoB. Electrons are derived from H_2 via the HdrABC/MvhADG complex and transferred to the heterodisulfide and Fd. Fd_{red} could be re-oxidized by the Fpo complex, however, it is unclear which electron acceptor could be used in this reaction. Therefore, the Ech hydrogenase seems to be a better candidate for Fd_{red} oxidation. In this reaction H_2 is formed and furthermore the Ech hydrogenase is able to build a proton gradient, which can be used for ATP synthesis.

Additionally, a $F_{420}H_2$ dehydrogenase, also termed Fpo complex, could be detected (Table 15). This was surprising since the Fpo complex was formerly found only in the Methanosarcinales. In comparison to the Fpo complex from *Ms. mazei,* subunits FpoF and FpoO are missing from *Mm. luminyensis*. The lack of the $F_{420}H_2$-oxidizing subunit FpoF seemed reasonable since F_{420} is most likely not used as electron carrier molecule in *Mm. luminyensis*. Furthermore, in the course of this study, the Fpo complex was shown to be functional without subunit FpoO (3.2.1). Therefore, it is conceivable that the Fpo complex from *Mm. luminyensis* is used for oxidation of Fd_{red} formed by HdrABC/MvhADG. However, in the Methanosarcinales, upon oxidation of $F_{420}H_2$ or Fd_{red} the membrane-bound electron carrier MP is reduced and electrons are further transferred to HdrDE. Yet, the presence of such a membrane-bound electron transport chain in *Mm. luminyensis* is highly speculative. In contrast, Fd_{red}-oxidation via the Ech hydrogenase seemed feasible.

To sum it up, according to the current model of the energy conservation mechanism in

Mm. luminyensis, electrons are derived from H_2 via HdrABC/MvhADG and are delivered to the heterodisulfide yielding HS-CoB and HS-CoM and to Fd producing Fd_{red} (Figure 31). Methyl groups are transferred to HS-CoM via substrate-specific methyltranferases and reduced to methane with HS-CoB. Fd_{red} could be re-oxidized by the membrane-bound Ech hydrogenase. The Ech hydrogenase is able to translocate protons across the cytoplasmic membrane to build an electrochemical ion gradient for ATP synthesis. This is especially important since there was no evidence for a membrane-bound methyltransferase that is known to generate a sodium ion gradient in obligate hydrogenotrophic methanogens.

The enzymatic set found in *Mm. luminyensis* was unusual due to the presence of the soluble HdrABC/MvhADG typical of hydrogenotrophic methanogens on the one hand and the Fpo complex, so far only found in the Methanosarcinales, on the other. This makes *Mm. luminyensis* a very particular methanogenic archaeon.

3.3.2 Cultivation of *Mm. luminyensis*

Despite the fact that the human body is colonized by a huge number of microorganisms, until now very few archaeal species were shown to be associated with humans. However, metagenome analyses revealed the presence of uncharacterized archaea in the human gut (Mihajlovski *et al.*, 2008; Scanlan *et al.*, 2008). Since *mcrA* gene sequences were found, the presence of methanogenic species was presumed. *Mm. luminyensis* was isolated from the stool sample of an 86 year old healthy man using *Methanobrevibacter* medium (Dridi *et al.*, 2012). Cultures produced methane with methanol and H_2 as growth substrates. It was found that *Mm. luminyensis* grew best at 37 °C and pH 7.6. Furthermore, growth depended on the presence of tungstate and selenite. In another study, *Mm. luminyensis* was cultivated in DSMZ medium 119 with rumen fluid (Brugère *et al.*, 2014). The addition of rumen fluid was the main difference in cultivation conditions compared to the use of *Methanobrevibacter* medium. The rumen is colonized by methanogenic archaea and therefore rumen fluid can be used to support their growth. Likewise, sludge fluid can be prepared from biogas sludge and used for cultivation.

In this study, *Mm. luminyensis* was obtained from the DSMZ in medium 119 with 5 % [v/v] sludge fluid. Since isolation in *Methanobrevibacter* medium was achieved without the addition of rumen or sludge fluid it was attempted to grow *Mm. luminyensis* without the respective components. Therefore, *Methanobrevibacter* medium was employed as described (Dridi *et al.*, 2012). Furthermore, cultivation in modified DSMZ medium 119 was attempted. In the original recipe, medium 119 contains sludge fluid, a mixture of fatty acids like valeric acid and isobutyric acid, but no extra tungstate or selenite. Medium 119 was prepared in three different ways, without sludge fluid, without fatty acids and without tungstate/selenite; without sludge fluid, without tungstate/selenite but with fatty acids; and thirdly, without sludge fluid,

without fatty acids but with extra tungstate/selenite solution. Additionally, cultivation in DSMZ medium 120, a complex medium also used for cultivation of *Ms. mazei*, was attempted. In all cases, cultures of *Mm. luminyensis* were growing, but the final OD_{600} decreased with every passage and finally cultures were not growing at all. This led to the assumption that rumen and sludge fluid contained a component essential for growth of *Mm. luminyensis*. This might be, for example, a methanogenic cofactor, which cannot be synthesized by *Mm. luminyensis,* but is present in the fluid. For the methanogenic cofactor HS-CoM, auxotrophy has been reported (Taylor *et al.*, 1974). Therefore, HS-CoM was used as additive to a final concentration of 0.1 %. Yet, the addition of HS-CoM could not restore growth of cultures. Therefore, sludge fluid was prepared by ultracentrifugation of biogas sludge as described. It was added to medium 119 without fatty acids and without tungstate and selenite in a final concentration of 5 % [v/v]. Methanol (75 mM) and H_2 were used as substrates for growth. With the addition of sludge fluid, cultures were growing. Hence, sludge fluid contained a component, which was necessary for growth of *Mm. luminyensis*. Accordingly, cultures were also growing, when sludge fluid was added to *Methanobrevibacter* medium to a final concentration of 5 % [v/v]. Hence, *Methanobrevibacter* medium, containing tungstate and selenite and 5 % [v/v] sludge fluid, was routinely used to cultivate *Mm. luminyensis*. A growth curve was recorded by measuring the optical density at 600 nm (OD_{600}).

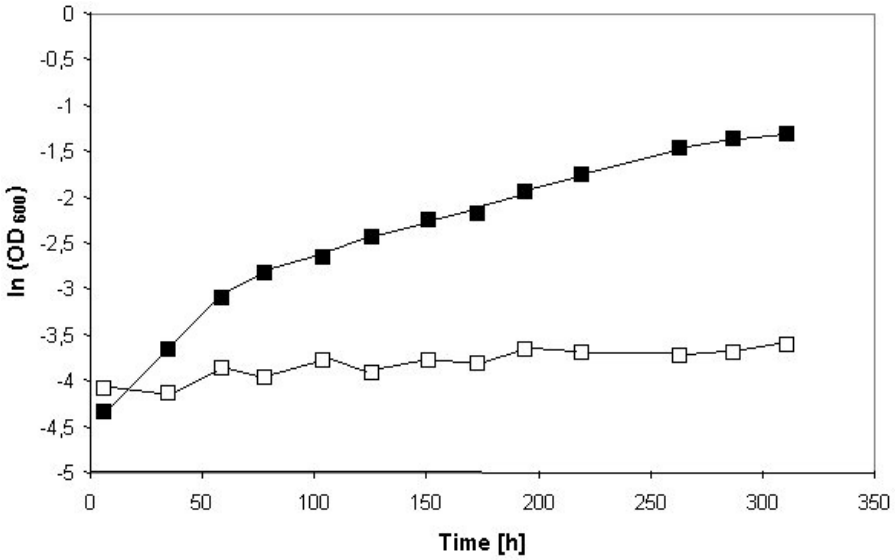

Figure 32: *Mm. luminyensis* growing in *Methanobrevibacter* medium with and without sludge fluid (other components were tungstate, selenite, MeOH (75 mM) and H_2+CO_2 (80:20, 1 bar)). Sludge fluid was added to a final concentration of 5 % [v/v] (■) and a control was performed without sludge fluid (□). Cultures with sludge fluid were growing, whereas cultures without sludge fluid did not. Doubling time as calculated from the exponential growth phase was 32 h. The exponential phase ended long before the final OD_{600} was reached.

As can be seen in Figure 32, cultures grew only with the addition of sludge fluid. A final OD_{600} of 0.27 was reached. However, exponential growth was possible only during the first 72 h. The doubling time was 32 h in this phase. After that, growth of the culture slowed down but still proceeded for another 10 days. This led to the conclusion that the component which was missing if no sludge fluid was added to the medium became a limiting factor during the exponential growth phase. Hence, the missing compound is contained in sludge fluid but the concentration is too low to fully support growth of *Mm. luminyensis*. Since sludge fluid is an undefined mixture containing various salts and a broad variety of organic components, *Ms. mazei* extract was prepared to more specifically test if the missing component could be a methanogenic cofactor or a comparable compound. *Ms. mazei* extract was added in addition to sludge fluid and was expected to support growth of *Mm. luminyensis*.

500 mL of a mid-exponential *Ms. mazei* culture were harvested and the cell pellet was re-suspended in *Mm. luminyensis* growth medium prior to lysis by sonication. The lysate was centrifuged and the supernatant added to a 250 mL culture of *Mm. luminyensis*. A growth curve was recorded (Figure 33). It can be seen that addition of *Ms. mazei* extract led to the same growth behavior, characterized by exponential growth only during the first 72 hours, as observed when only sludge fluid was added. Hence, the addition of *Ms. mazei* extract could not improve growth of *Mm. luminyensis*. Therefore, the missing compound seemed to occur only in sludge fluid and not in the cell extract and thus is not a methanogenic cofactor.

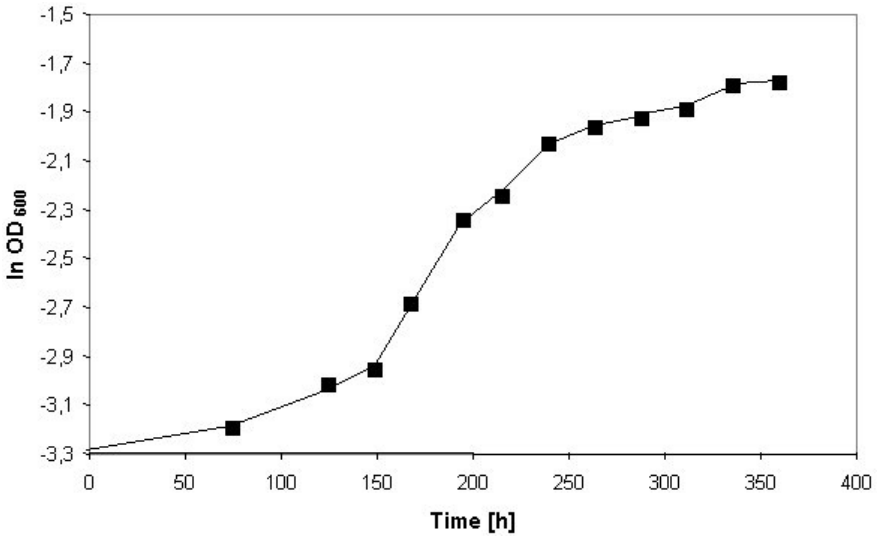

Figure 33: *Mm. luminyensis* was cultivated in *Methanobrevibacter* medium with *Ms. mazei* extract. In addition, the medium contained tungstate, selenite, MeOH (75 mM), H_2+CO_2 (80:20, 1 bar) and 5 % [v/v] sludge fluid. Exponential growth was only observed during the first doublings and afterwards decelerated. It was concluded that synthesis of methanogenic cofactors was not impaired in *Mm. luminyensis*.

Cultivation conditions were not optimal for *Mm. luminyensis*, yet with the addition of sludge fluid to a final concentration of 5 % [v/v], it was still able to grow. Therefore, *Methanobrevibacter* medium with sludge fluid (5 % [v/v]) and with tungstate/selenite solution was used to investigate growth with the methylated amines dimethylamine (DMA) and monomethylamine (MMA).

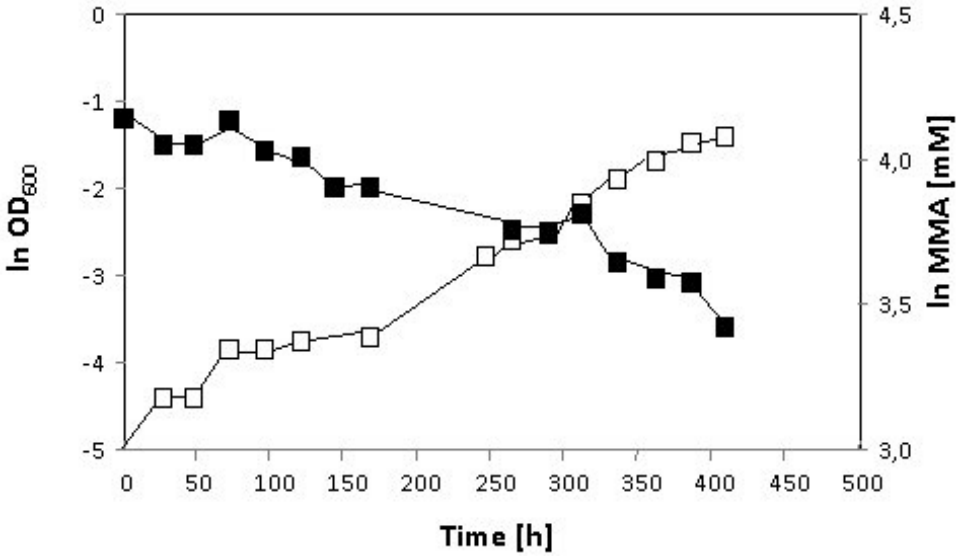

Figure 34: *Mm. luminyensis* growing in *Methanobrevibacter* medium with sludge fluid (5 % [v/v]), tungstate/selenite solution, 1 bar H_2+CO_2 (80:20) and 75 mM MMA. The culture grew to a final OD_{600} of 0.23 with a doubling time of 70 h. 37 mM MMA rested in the medium and were not consumed. (□) ln OD_{600}; (■) ln MMA concentration [mM].

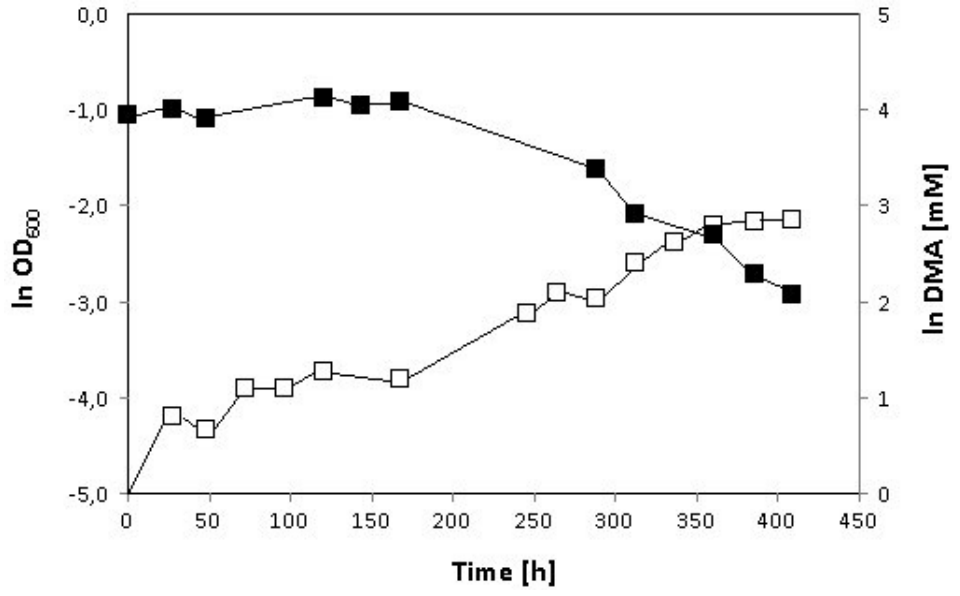

Figure 35: *Mm. luminyensis* growing in *Methanobrevibacter* medium with sludge fluid (5 % [v/v]), tungstate/selenite solution, 1 bar H_2+CO_2 (80:20) and 37.5 mM DMA. The culture grew to a final OD_{600} of 0.12 with a doubling time of 86 h. After reaching the final OD, no more DMA could be detected in the medium and only low amounts of MMA. (□) ln OD_{600}; (■) ln DMA concentration [mM].

Since it was found that the respective methyltransferases are encoded in the genome, growth with these substrates should be possible. *Mm. luminyensis* was cultivated anaerobically at 37 °C in *Methanobrevibacter* medium with sludge fluid (5 % [v/v]), tungstate/selenite solution and H_2 and either MMA or DMA as substrates. Growth was followed by measuring the optical density at 600 nm. For MMA and DMA determination, samples were taken from their respective cultures, centrifuged and the supernatant stored at -70 °C until the end of the experiment. MMA and DMA determination was performed as described (2.6.1). MMA was added to a final concentration of 75 mM. With this substrate, the doubling time was 70 h. When the culture reached its final OD_{600} of 0.23, the MMA concentration had decreased to 37 mM (Figure 34). DMA, which possesses two methyl groups, was added to a concentration of 37.5 mM. The final OD_{600} was 0.12 and the doubling time was 86 h. When the final OD was reached no more DMA and only low amounts of MMA could be detected (Figure 35).

Thus, it could be shown, that *Mm. luminyensis* cannot only use methanol for methanogenesis but also MMA and DMA. In comparison to methanol, the doubling time in cultures growing on MMA and DMA was increased. Nevertheless, both substrates are suitable for cultivation of the organism.

3.3.3 Soluble heterodisulfide reductase and Ech hydrogenase from *Mm. luminyensis*

After bioinformatic analyses, mechanisms of energy conservation in *Mm. luminyensis* were investigated with biochemical tests. A homolog of the cytoplasmic HdrABC/MvhADG was identified and is thought to catalyze H_2-oxidation and reduction of heterodisulfide and Fd. Furthermore, the Ech hydrogenase is probably present in membranes of *Mm. luminyensis*. To firstly test for activity of HdrABC/MvhADG and the Ech hydrogenase, a general hydrogenase assay was performed.

Therefore, cultures were grown to the mid-exponential phase, harvested and the cytoplasm and membrane fraction were separated by ultracentrifugation. While membranes could be stored at -70 °C, the cytoplasm had to be tested directly after preparation. Tests were performed photometrically with rubber-stoppered glass cuvettes. The gas atmosphere was 100 % H_2 and methylviologen (MV) was added as electron acceptor. Since methylviologen becomes violet upon reduction, the reaction could be followed at 604 nm. In the *Mm. luminyensis* membrane fraction, MV-dependent hydrogenase activity of 90 mU mg^{-1} protein was observed. With the same test, hydrogenase activity in the cytoplasmic fraction was measured and determined to be 780 mU mg^{-1} protein. Thus, initial evidence for the presence of hydrogenases possibly involved in energy conservation was given.

Table 16: Hydrogenase and heterodisulfide reductase activity in membrane fractions and cytoplasm of *Mm. luminyensis*

Fraction	Electron donor	Electron acceptor	Enzymatic activity [mU mg^{-1}]
Membrane	H_2	MV_{ox}	90
Cytoplasm	H_2	MV_{ox}	780
Membrane	BV_{red}	Heterodisulfide	-
Cytoplasm	BV_{red}	Heterodisulfide	2500
Cytoplasm	H_2	Heterodisulfide, Fd	4

MV_{ox}: oxidized methylviologen, BV_{red}: reduced benzylviologen

To examine the HdrABC/MvhADG complex in more detail, the natural electron acceptor heterodisulfide was added to the cytoplasmic fraction. Reduced benzylviologen (BV_{red}) with a maximal absorption at 575 nm served as artificial electron donor. The heterodisulfide was reduced at a rate of 2500 mU mg^{-1} (Table 16). Therefore, the HdrABC/MvhADG complex most likely is active in cells of *Mm. luminyensis*. Since subunit HdrD from the membrane-bound Hdr enzyme is encoded in the genome of *Mm. luminyensis,* and since reduction of the heterodisulfide by the membrane fraction of *Mm. luminyensis* would be a hint for the potential existence of a membrane-bound electron transport chain, the same test was performed with the membrane fraction of *Mm. luminyensis*. Yet, no BV_{red}-dependent heterodisulfide reduction could be measured. Thus, Hdr activity in *Mm. luminyensis* could only be found in the

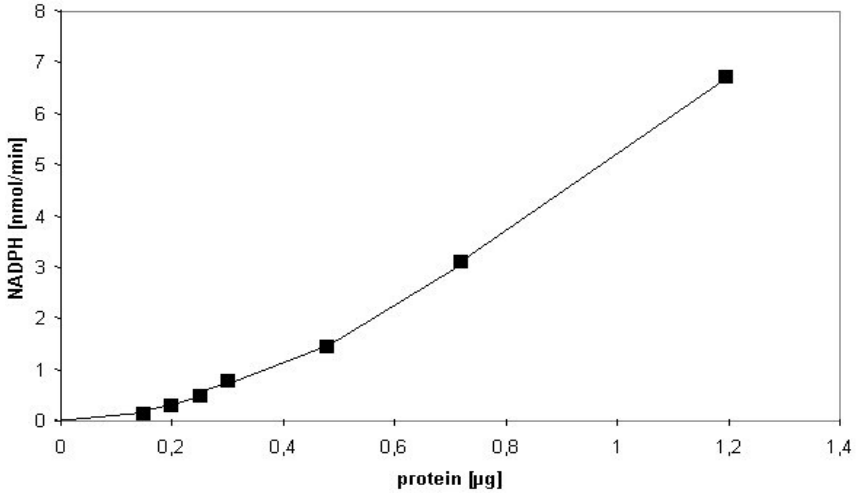

Figure 36: Soluble heterodisulfide reductase from *Mm. luminyensis*. Activity in the cytoplasmic fraction was measured with H_2 as electron donor, heterodisulfide and ferredoxin:$NADP^+$ reductase to report formation of reduced Fd. The NADPH formation rate increased with increasing protein concentration. Enhanced protein levels increased enzyme activity exponentially and a minimal amount of 0.5 µg is necessary for linear dependence.

cytoplasm. The catalytically active subunit HdrD from the membrane-bound heterodisulfide reductase seemed not to be present or dysfunctional due to the lack of HdrE. After heterodisulfide reduction could be shown in the cytoplasm of *Mm. luminyensis,* the dependence of the reaction on the natural electron donor H_2 was expected to be demonstrated. Electrons from H_2 are split in a bifurcation mechanism and are further transferred to the heterodisulfide and to Fd (Kaster *et al.*, 2011). To report enzymatic activity in a photometric assay, the ferredoxin:$NADP^+$ reductase was used that catalyzes electron transfer from Fd_{red} to $NADP^+$ which could be measured at 340 nm. Tests were performed in rubber-stoppered glass cuvettes with a 100 % H_2 atmosphere. The reaction was started by the addition of 100 µM heterodisulfide. Low but significant activity in the range of 4 mU mg^{-1} was detected. The addition of clostridial Fd stimulated the reaction but amounts naturally occurring in the cytoplasm were high enough to let the reaction proceed.

In Figure 36 it is shown that the NADPH formation rate increased with increasing amounts of protein. At low protein amounts, the slope was slightly exponential indicating that enhanced protein levels improved enzymatic activity. A minimal amount of 0.5 µg in the assay was necessary for linear dependence. Altogether, activity of the soluble heterodisulfide reductase typical of obligate hydrogenotrophic methanogens could be demonstrated.

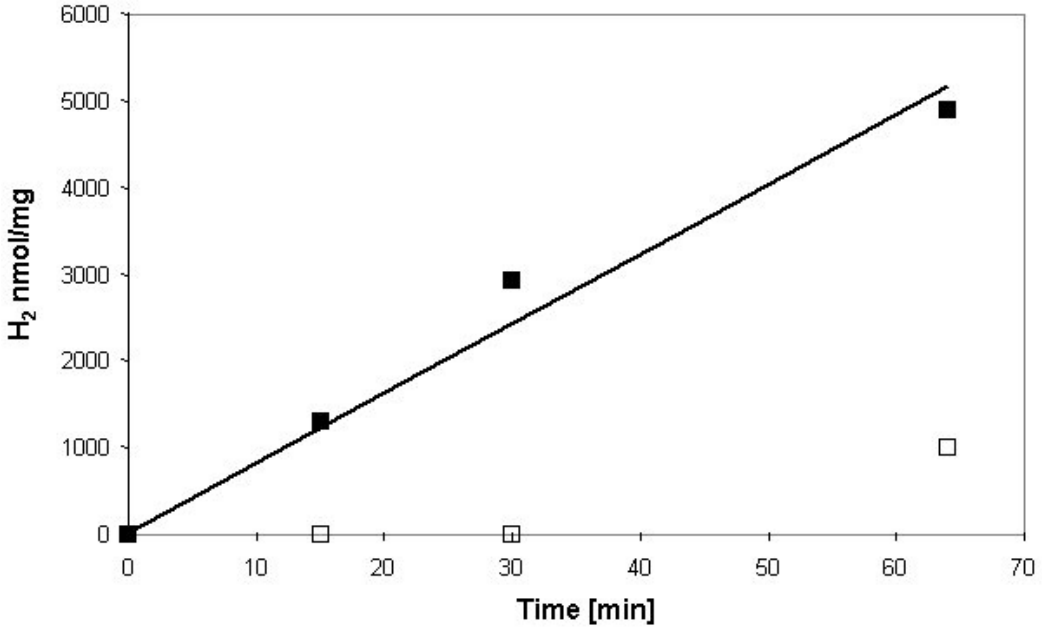

Figure 37: Generation of H_2 from Fd_{red} by membrane fractions of *Mm. luminyensis*. A specific activity of 80 nmol min^{-1} mg^{-1} was measured, which was probably due to the Ech hydrogenase. (■) H_2 formation by the membrane fraction of *Mm. luminyensis*. Fd_{red} was supplied via the IOR, H_2 was measured gaschromatographically; (□) negative control without Fd.

The question arose how Fd_{red} produced by HdrABC/MvhADG is re-oxidized and how ion translocation for the generation of a membrane potential is accomplished. An enzyme suitable for both tasks is the membrane-bound Ech hydrogenase. All subunits of the Ech hydrogenase as present in *Ms. mazei* and *Ms. barkeri* could be identified in two copies in *Mm. luminyensis*. The Ech hydrogenase belongs to the [NiFe] containing hydrogenases that couple Fd_{red}-oxidation to the translocation of protons (Künkel *et al.*, 1998; Meuer *et al.*, 1999; Welte *et al.*, 2010a). In the course of the reaction H_2 is produced, which easily diffuses outside the cell. In this study H_2 formation from Fd_{red} by the *Mm. luminyensis* membrane fraction was investigated (Figure 37).

For the generation of Fd_{red}, the indolpyruvate:ferredoxin oxidoreductase was employed. It oxidized phenylpyruvate and reduced Fd Mm1619 to guarantee a steady supply with Fd_{red}. H_2 was measured gaschromatographically and quantified according to a standard curve. With this test system H_2 formation rates of 80 nmol min^{-1} mg^{-1} were determined. No H_2 formation could be detected in the negative control without Fd. Thus, a membrane-bound Ech hydrogenase most probably is active in cells of *Mm. luminyensis*.

In summary, it could be shown here that the soluble HdrABC/MvhADG enzyme complex is active in cells of *Mm. luminyensis*. Furthermore, membrane fractions catalyzed Fd_{red}-dependent hydrogen production, which means that a membrane-bound Ech hydrogenase most probably is active in cells of *Mm. luminyensis*. This simple system of Fd reduction and re-oxidation with concomitant proton translocation could be sufficient to sustain cells of *Mm. luminyensis*. However, it remains to be investigated if other membrane-bound enzymes like the Fpo complex contribute to oxidation of Fd_{red} and generation of an ion gradient. Another question that has to be resolved is whether electron transfer reactions occur between the different membrane-bound enzymes. A prerequisite for that would be the presence of the lipid-soluble electron carrier MP, which has not yet been shown. However, in methanogenic archaea, membrane-bound electron transport chains so far have only been observed in the order Methanosarcinales. The presence of such a system in *Mm. luminyensis* would be contradictory to current knowledge about respiratory processes in methanogenic archaea and therefore is highly speculative.

All in all, different aspects of energy conservation mechanisms in methanogenic archaea have been investigated. The obligate aceticlastic *Mt. thermoacetophila* needs to spend two ATP equivalents for acetate activation, which is catalyzed by the AMP-forming ACS Mthe1194. PP_i built in the course of the reaction is subsequently hydrolyzed by the type II PPase Mthe0236. Consequently, more than two ATP equivalents per acetate molecule have to be synthesized by the ATP synthase. Therefore, at least seven ions have to be translocated by membrane-bound enzymes of the *Mt. thermoacetophila* respiratory chain. Ion translocation stoichiometry and a possible explanation for the survival of

Mt. thermoacetophila will be discussed in one of the following chapters (4.2.3).

Another organism used in this study was *Ms. mazei*, which is more versatile than *Mt. thermoacetophila* and can also use methylated compounds for methanogenesis. In the methylotrophic pathway, reducing equivalents are transferred to Fd and to F_{420}. $F_{420}H_2$ is re-oxidized via the membrane-bound Fpo complex. In the course of this study, a *Ms. mazei* deletion mutant, missing subunit FpoO (*Ms. mazei* Δ*fpoO*), was investigated in terms of growth parameters and enzymatic activity of the Fpo complex. The function of subunit FpoO is not known, however, in this study it could be shown that cultures of the mutant had a similar doubling time and final OD to the wild type. Furthermore, the $F_{420}H_2$-oxidizing activity was comparable as well. It was concluded, that FpoO is not involved in electron transport processes but might be a redox-sensitive regulator. While $F_{420}H_2$ is oxidized by the Fpo complex, the Ech hydrogenase was shown to be responsible for Fd_{red}-oxidation. However, a *Ms. mazei* Δ*ech* mutant retained 50 % Fd_{red}-oxidizing activity (Welte *et al.*, 2010b). It was proposed that the Fpo complex also catalyzed Fd_{red}-oxidation (Welte and Deppenmeier, 2011a, 2014). In the course of this study, electron transport from Fd_{red} to the heterodisulfide was measured in membrane fractions of the *Ms. mazei* Δ*ech* mutant. It could be demonstrated that an antibody, which specifically bound to subunit FpoI, could completely inhibit Fd_{red}-dependent thiol production. Therefore, the Fpo complex indeed is capable of Fd_{red}-oxidation. Since Fd is considered to be a very ancient electron carrier (George *et al.*, 1985), it seems feasible that Fd_{red} was the original electron donor of the Fpo complex, which is now replaced by $F_{420}H_2$.

The last part of this thesis dealt with the new isolate *Mm. luminyensis*, which consumes H_2 and methylated substrates. Bioinformatic analyses revealed an unusual combination of enzymes probably involved in energy conservation processes. On the one hand, the soluble HdrABC/MvhADG complex is present, which is typical of obligate hydrogenotrophic methanogens. On the other hand, the Fpo complex could be detected, which was so far only found in the order Methanosarcinales. Furthermore, an Ech hydrogenase was identified. The HdrABC/MvhADG complex could catalyze H_2-oxidation and concomitantly reduce Fd and the heterodisulfide as was also shown for *Mtb. marburgensis* (Kaster *et al.*, 2011). The Ech hydrogenase could transfer electrons from Fd_{red} to protons and translocate protons across the cytoplasmic membrane as was shown in *Ms. mazei* (Welte *et al.*, 2010b; Welte *et al.*, 2010a). The activity of HdrABC/MvhADG, as well as the activity of the Ech hydrogenase from *Mm. luminyensis* could be demonstrated in cytoplasmic and membrane fraction, respectively. Therefore, according to the current model, energy conservation in *Mm. luminyensis* relies on these enzymes. However, a detailed investigation of the role of the Fpo complex and the potential presence of an electron transport chain will be interesting targets for future studies.

4. DISCUSSION

Strictly anaerobic prokaryotes from the domain archaea that produce methane from products of bacterial anaerobic metabolism belong to the group of methanogenic archaea. They play an important role in global carbon cycling and since methane is a potent green house gas also contribute to global warming. Furthermore, they are part of every biogas plant, producing biogas, which is composed mainly of methane and CO_2. Thus, an in-depth understanding of methanogenic metabolism is crucial with respect to ecological as well as economical aspects.

Methanogenic archaea have been grouped into six orders, namely Methanobacteriales, Methanocellales, Methanococcales, Methanopyrales, Methanomicrobiales and Methanosarcinales (Liu and Whitman, 2008; Sakai *et al.*, 2008). Recently, a new methanogen was isolated from the human gut and named *Mm. luminyensis.* This organism belongs to a new order of methanogens, that is referred to as Methanomassiliicoccales (Iino *et al.*, 2013). Members of the Methanobacteriales, Methanocellales, Methanococcales, Methanopyrales and Methanomicrobiales use H_2+CO_2 and in some cases formate as substrates. Thus, the majority of methanogens depends on these compounds. Members of the genus *Methanosarcina* from the order of Methanosarcinales are more metabolically versatile and are able to use also methylated compounds like TMA or methanol as substrates. Moreover, acetate can be degraded, which is the methanogenic substrate with the lowest change in free energy with only -36 kJ mol^{-1} CH_4 under standard conditions. The second genus capable of acetate breakdown, *Methanosaeta*, likewise belongs to the Methanosarcinales. In contrast to members of the genus *Methanosarcina, Methanosaeta* species obligatory depend on acetate. About two-thirds of biologically produced methane are derived from acetate, thus species of *Methanosaeta* and *Methanosarcina* are of great ecological importance. *Mm. luminyensis* differs from most other methanogens by consuming a combination of H_2 and methylated compounds. It was isolated from the human gut where H_2 and methanol or TMA are products of bacterial metabolism (Dridi *et al.*, 2012). Consumption of those products makes *Mm. luminyensis* an important part of microbial degradation processes. Furthermore, it was postulated that depletion of TMA by *Mm. luminyensis* helps in prevention of trimethylaminuria or “fish-odor-syndrome” (Brugère *et al.*, 2014). Therefore, human health is another aspect where a detailed understanding of methanogenesis is needed.

4.1 Energy conservation in *Mt. thermoacetophila*

As mentioned above methanogenesis in *Mt. thermoacetophila* strictly depends on acetate. Acetate as inert molecule has to be converted to the more reactive acetyl-CoA, before it can

be disproportionated into methane and CO_2. It is thought that acetate activation in *Mt. thermoacetophila* is catalyzed by an acetyl-CoA synthetase (ACS), that generates acetyl-CoA, AMP and pyrophosphate (PP_i) from acetate, CoA and ATP (Jetten *et al.*, 1989).

The intracellular accumulation of PP_i inhibits biosynthesis of macromolecules and therefore has to be prevented. Hydrolysis of one phosphoanhydride bond by the ACS and subsequent hydrolysis of PP_i by a pyrophosphatase (PPase) would sum up to an expense of two ATP equivalents per acetate molecule. Under the assumption that for phosphorylation of ADP to ATP three ions are needed by the ATP synthase, a minimum of seven ions have to be translocated by the respiratory chain of *Mt. thermoacetophila*. Six protons would be needed for the production of ATP to activate acetate and the seventh translocated proton could be used for ion homeostasis and anabolism. Yet, according to current models, it is still a matter of debate whether this is possible. In this study different putative ACS genes and the gene encoding a soluble PPase were examined with regard to gene expression level and enzymatic activity, to investigate the acetate activation reaction in *Mt. thermoacetophila*. Special attention was paid to the question, if indeed two ATP equivalents are consumed by ACS and PPase.

4.1.1 Acetyl-CoA production in *Mt. thermoacetophila*

In the first part of this study, the acetate activation reaction in the obligate aceticlastic methanogen *Mt. thermoacetophila* was examined. In aceticlastic methanogens there are two possible ways of acetyl-CoA formation. The well studied *Methanosarcina* spp. employ acetate kinase and phosphotransacetylase (Reaction 5). The acetate kinase converts acetate and ATP to acetyl phosphate and ADP. Acetyl phosphate is further converted to acetyl-CoA by the phosphotransacetylase. The joint activity of these two enzymes forms acetyl-CoA at the expense of one ATP equivalent. However, both genes encoding the enzymes originate from bacteria and were probably acquired by lateral gene transfer (Deppenmeier *et al.*, 2002).

For the other genus of methanogens capable to use acetate as a substrate, *Methanosaeta*, there is evidence that ACS enzymes catalyze formation of acetyl-CoA (Reaction 6, (Kohler and Zehnder, 1984; Jetten *et al.*, 1989; Teh and Zinder, 1992)).

Reaction (5): acetate + ATP + CoA ↔ acetyl-CoA + ADP + P_i
Reaction (6): acetate + ATP + CoA ↔ acetyl-CoA + AMP + PP_i

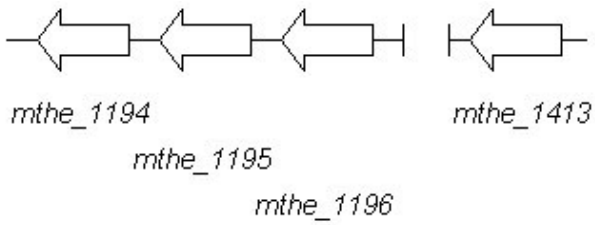

Figure 38: Genomic organization of putative ACS encoding genes. *Mthe_1194/95/96* are tandemly positioned and are interrupted by spacers of about 300 bp. *Mthe_1413* is located at a different chromosomal site.

The genome of *Mt. thermoacetophila* was sequenced in 2007 and revealed the presence of four ACS encoding genes (*mthe_1194/95/96, mthe_1413*) (Smith and Ingram-Smith, 2007). Three of these genes are tandemly positioned (*mthe_1194/95/96*), the fourth one is located further downstream ((Smith and Ingram-Smith, 2007), Figure 38). A closer inspection of the genome revealed a gene with high homology to a gene encoding an ADP-forming ACS from *Pyrococcus* (*P.*) *furiosus* (*mthe_0554*) (Mai and Adams, 1996b; Berger *et al.*, 2012). It does not share any homology with the other putative ACS encoding genes. RT-qPCR experiments were performed to investigate the expression level of *mthe_0554*. Yet, under the chosen conditions, expression of *mthe_0554* was near to the detection limit of the assay. It was concluded that the respective enzyme does not have an important role in acetate metabolism in *Mt. thermoacetophila.*

The question arose, whether the other putative ACS encoding genes are transcribed to the same extent, or if one of them is preferentially transcribed. Preferential transcription would be a hint for an important role of the respective enzyme in acetate metabolism. Furthermore, a possible operon structure of the clustered genes was investigated. RT-qPCR experiment revealed a high expression level of *mthe_1194.* In comparison, transcription of the single gene *mthe_1413* was slightly decreased. Transcript concentrations of *mthe_1195* and *mthe_1196* were significantly lower in comparison to *mthe_1194*. Thus, it was concluded that under the chosen conditions *mthe_1194* encodes the most important putative ACS enzyme. Additional RT-qPCR experiments were performed to investigate if *mthe_1194/95/96* were transcribed together, to form a single polycistronic mRNA. In the intergenic regions between all genes, stretches of about 300 bp could be found (Table 17, Figure 38). Primers were designed that spanned the whole intergenic region. In RT-qPCRs assays a product could only be generated if two genes and their intergenic region formed a contiguous transcript. No product was detected for the intergenic region between *mthe_1194* and *mthe_1195*. Thus, *mthe_1194* most likely represents an autonomous transcription unit. However, from the intergenic region between *mthe_1195* and *mthe_1196* a product was generated. The transcript concentration was in the same range as measured for the genes themselves.

Hence, *mthe_1195* and *mthe_1196* are co-transcribed and form a transcriptional unit, that is distinct from *mthe_1194*.

The 5' intergenic region between *mthe_1194* and *mthe_1195* was examined with respect to a potential transcription starting site for *mthe_1194* (Table 17). Likewise, the upstream region of *mthe_1196* was examined, since it should harbor a transcription starting site for the transcript of *mthe_1195/96*. Additionally, a closer look was taken at the intergenic region between *mthe_1195* and *mthe_1196*. Since both genes form a transcriptional unit, in their intergenic region a transcription starting site should not be required. Transcription initiation in archaea mostly relies on two well-known elements found in the upstream region of open reading frames (Palmer and Daniels, 1995). One is the TATA-box, which is also common in eukaryotes. However, consensus sequences differ depending on the organism. For methanogens the consensus sequence is TTTATATA (Soppa, 2001). The other important module is the BRE-box, which is less well conserved. Archaeal BRE-boxes usually consist of a GA-rich region in close proximity to the TATA-box (Soppa, 2001).

The archaeal transcription machinery in general shares similarities with eukaryotes, rather than with bacteria (Bell *et al.*, 2001). However, it is much less complicated. Only three transcription factors are needed. For transcription initiation the TBP (TATA-binding protein) binds the TATA-box, which is facilitated by TFE, a homolog of the eukaryal TFIIE. The TBP-DNA complex is bound by TFB, a TFIIB homolog that recognizes the BRE element. TFB is used to make contact with the RNA polymerase, which than starts mRNA synthesis (Bell *et al.*, 2001; Bjornsdottir and Myers, 2008).

Table 17: DNA-sequences of 5' intergenic regions between genes encoding putative ACS enzymes in *Mt. thermoacetophila* (*mthe_1194/95*, *mthe1195/96*) and the sequence upstream of *mthe_1196*.

ACS gene(s)	DNA sequence of intergenic regions/upstream region of *mthe_1196*
mthe_1196	AGAGTTTCTTAAATAATTTTATATAGTTTTGGAGCTATTCGATATAGACGACGATCC AACAAGATGTAATATTGTAAAATGAATTGTTTGCTTCGAGGTTACTTCAATGATTTT TCAATATCATTATTAAACATTAATTTCATTCAAACGTTAACTTTATAAACGAAAGAG ATAATTATCAATCGTAATAATGCCTCTGAGTCTCCACATCCTGATTTGTCTGCTGGG AGGGCAGATTCGCAACAGATCGGGATGGGCTGGAGGCAGAATGGCCGAGGAAACCGC AAAAACTGCGGTCCTTCTCGAGGAGAGGAGGTT

mthe_1195/ mthe_1196	AACGTCCGCAATTTTTATTTTTATTAAATTTCTATGCTGCGGATTTGTCTGCAGCCG AGAGTTTCTTAAATAATTTTATATAGTTTTGGAGCTATTCGATATAGACGACGATCC AACAAGATGTAATATTGTAAAATGAATTGTTTGCTTCGAGGTTACTTCAATGATTTT TCAATATCATTATTAAACATTAATTTCATTCAAACGTTAACTTTATAAACGAAAGAG ATAATTATCAATCGTAATAATGCCTCTGAGTCTCCACATCCTGATTTGTCTGCTGGG AGGGCAGATTCGCAACAGATCGGGATGGGCTGGAGGCAGAATGACTGTTGAGGAGTG TCACAAAATGGCTGAGGAAAAAGCTGCTA
mthe_1194/ mthe_1195	GCGGTCAACCTATTTTATTTGATTTTATGTGATACTCTGTTTTGGCCTGACTTCGTG TGTTTTCTTATCATGGTCCCTTCTGCTGGATATCGATATCGTTAATTTACATATAAT CTTTAACACTTTTATCACGAAAAATAATTATTACAAATTTTTGGTGACATTTCTATA TCGACAGCTTTATAAATACGGAATACGTATGGAATTATCGTGTTTCCGGAGTCTCCC AATGCTCATAGGTGATCGCGGCATGGCAGTTATGGTTTGGCAGGAGGACTTCTTGAC CCGCTTCTTCTCAGGAGGAGTTCTCGGGTGGAGCTCATGCCAGCGGCATCGTGGGAC GGAAGCACATTATCTAGATGAATGGAGGTATGTAAATGGCTGAGACTGCAAAGACTG CTGTTCTGCAGGAGGAGACCAGGAT

1) Highlighted in gray: possible BRE-elements

2) Marked in black: sequences identified as TATA-boxes

3) Underlined: gene sequence starting with ATG

In the 5' intergenic region of *mthe_1196* a sequence exactly matching the TATA-box consensus sequence could be identified as well as a potential BRE-element (Table 17). Surprisingly, also in the intergenic region between *mthe_1195* and *mthe_1196* both sequence elements could be detected. In RT-qPCR experiments it could be demonstrated that *mthe_1195* and *mthe_1196* form a single transcriptional unit, therefore the transcription starting site in the intergenic region between *mthe_1195* and *mthe_1196* might be silenced by an unknown regulatory mechanism. The TATA-box upstream of *mthe_1196* is probably used for transcription initiation for both *mthe_1195* and *mthe_1196*. The intergenic region between *mthe_1194* and *mthe_1195* contains a TATA-box sequence, which is very similar to the TTTATA consensus motive. Additionally, a convincing BRE-element consisting mainly of G and A can be found. Thus, the differential expression of putative ACS encoding genes is reflected in different transcription initiation sequences.

The consensus TATA-box sequence as found for the transcription unit *mthe_1195/96* would be expected to trigger a higher gene expression, than the slightly modified sequence in the 5' intergenic region of *mthe_1194*. However, at least in eukaryotes also sequences deviating from the consensus sequence were shown to be functional. Moreover, it could be demonstrated that affinity of the TATA-binding protein to the TATA-box sequence can be uncoupled from transcriptional activity (Hahn *et al.*, 1989; Bjornsdottir and Myers, 2008). Therefore, high expression of *mthe_1194* is feasible although the TATA-box sequence does not fully match the consensus sequence.

Apart from TATA-box and BRE-element long 5' intergenic regions might contain targets for posttranscriptional regulation on the mRNA level, such as regulatory proteins or stable RNAs. 5’ and 3’ untranslated regions (UTRs) have been investigated in the halophilic archaea *Halobacterium salinarum* and *Haloferax volcanii* (Brenneis *et al.*, 2007). Further studies have been performed with *Pyrobaculum aerophilum* and *Sulfolobus sulfataricus*. In all of them mRNA transcripts were shown to possess short 5’ UTR or no 5’ UTR at all. Therefore, mRNAs in these organisms are considered to be leaderless.

In contrast, analysis of the genomes of three different *Methanosarcina* species revealed an unexpectedly low proportion of coding regions. With 74.2 % coding region in *Ms. acetivorans*, 75.15 % coding region in *Ms. mazei* and 79.2 % coding region in *Ms. barkeri* only about three-quarters of the genomes of these methanoarchaea are actual coding sequences. In 2009 the transcriptome of the model organism *Ms. mazei* was investigated by RNA preparation with subsequent generation of a cDNA library, which was sequenced by the pyrosequencing technique (Jäger *et al.*, 2009). 521 mRNAs contained 5’ UTRs of 150-200 bp on average, with some transcripts having 5’ UTRs of up to 500 bp. Thus, in contrast to other archaea, methanoarchaea regularly produce mRNAs containing a leader sequence. This indicates considerable posttranscriptional regulation, which would make 5' UTRs an important part of the regulatory network of methanoarchaea. Therefore, the 5' intergenic region of ACS encoding genes in *Mt. thermoacetophila* might not only contain sequences for initiation of transcription, but also motives that are targets for posttranscriptional regulators. In this case, differential transcription could be complemented by posttranscriptional regulation.

The ADP-forming ACS was first discovered in the eukaryotic *Entamoeba (En.) histolytica* and later also in the likewise eukaryotic *Giardia lamblia* (Reeves *et al.*, 1977; Sanchez and Müller, 1996). Instead of working towards acetate activation, here the ACS enzymes are involved in acetate formation and ATP production in fermentative metabolism. Later it was shown that also in the domain archaea the ADP-forming ACS is commonly encountered: All acetate-producing species that were tested so far, used the ADP-forming ACS for acetate formation (Schäfer *et al.*, 1993; Schönheit and Schäfer, 1995). The AMP-forming ACS on the other hand generally seems to be involved in acetyl-CoA formation.

The halophilic archaeon *Haloarcula (H.) marismortui* possesses an AMP-forming ACS as well as an ADP-forming ACS enzyme. The activity of both enzymes can be tested with glucose as substrate. Glucose is degraded to acetate in cultures of *H. marismortui* and after glucose is consumed, acetate is taken up from the medium. Activity of an ADP-forming ACS could be demonstrated during acetate formation, but no AMP-forming ACS activity. During acetate utilization the situation turned to the opposite: AMP-forming ACS activity was measured but the ADP-forming ACS was no longer present. Thus, in *H. marismortui* the ADP-forming ACS was responsible for acetate formation, whereas the AMP-forming enzyme catalyzed acetate

activation (Bräsen and Schönheit, 2004).

Hence, it seems rather clear that ADP-forming ACS enzymes catalyze acetate formation whereas AMP-forming ACS enzymes catalyze the reverse reaction and thus produce acetyl-CoA. Yet, in principle both reactions are reversible and could proceed in either way. The ADP-forming ACS enzyme from the hyperthermophilic archaeon *P. furiosus* was shown to act in both directions in *in vitro* assays. The enzyme was isolated from the organism and catalyzed ATP-dependent acetyl-CoA formation as well as ADP-dependent acetate formation (Mai and Adams, 1996b).

For *Mt. thermoacetophila* it would be beneficial if acetate activation would be catalyzed by an ADP-forming ACS enzyme *in vivo*. Instead of two ATP equivalents spent by AMP-forming ACS enzymes only one ATP equivalent would be consumed. Therefore, in this study it was tested whether the heterologously produced Mthe1194 produced AMP or ADP from ATP. It could be demonstrated that ATP was converted to AMP, thus Mthe1194 is an AMP-forming ACS. Therefore, the highly homologous genes *mthe_1195/96* and *mthe_1413* most likely encode AMP-forming ACS enzymes as well. The non-homologous *mthe_0554* shares similarity with the ADP-forming ACS from *P. furiosus* and thus rather encodes an ADP-forming ACS enzyme. However, in this study *mthe_0554* was not expressed and thus does not have an important role in acetate metabolism.

AMP-forming ACS enzymes have been described in different organisms. Among others, the respective enzymes from *Mt. concilii* and *Mt. thermoacetophila* DSM 3870 were examined (Kohler and Zehnder, 1984; Jetten *et al.*, 1989; Teh and Zinder, 1992). Both organisms are close relatives of *Mt. thermoacetophila* DSM 6194 examined in this study.

In their studies Jetten and colleagues (Jetten *et al.*, 1989) measured a v_{max} of 55 U mg^{-1} for the ACS from *Mt. concilii*. The K_M value for acetate was 0.86 mM and the K_M value for CoA was 48 µM. In another study with *Mt. thermoacetophila* DSM 3870 Teh and Zinder (Teh and Zinder, 1992) found a v_{max} of 93 U mg^{-1}, K_M value for acetate of 2-4 mM, for ATP 5.5 mM and the K_M value for CoA was below 0.2 mM. In the course of this study, the ACS from *Mt. thermoacetophila* DSM 6194 was purified and the kinetic parameters were determined in an assay employing auxiliary enzymes, or with a chemical detection method for PP_i (2.7.1). In the assay with auxiliary enzymes v_{max} was 21.7 U mg^{-1} (linear regression) or 16.1 U mg^{-1} (non-linear regression, 2.7.2). With the PP_i detection method 28 U mg^{-1} (linear regression) or 31 U mg^{-1} (non-linear regression) were measured. The K_M value for acetate was determined with the enzymatic method and was 0.4 mM (linear regression) or 0.6 mM (non-linear regression). For ATP and CoA the PP_i detection method was used. K_M values for ATP were 20 µM (linear regression) and 24 µM (non-linear regression). For CoA and 14.5 µM (linear regression) and 20 µM (non-linear regression) were measured. Hence, kinetic parameters of Mthe1194 were in the same range compared to ACS enzymes from closely related

organisms. One exception was the K_M value for ATP of the ACS enzyme from *Mt. thermoacetophila* DSM 3870, which was 5.5 mM (Teh and Zinder, 1992). However, this value is above normal cellular ATP concentrations and therefore is not compatible with efficient acetyl-CoA formation. Thus, it might be that a repeated measurement might yield a value in the range of values measured for other ACS enzymes.

Furthermore, the substrate spectrum of Mthe1194 has been tested and it could be shown that acetate is the preferred substrate (Berger *et al.*, 2012). A strong preference for acetate has also been observed for the ACS enzyme from *Methanothermobacter* (*Mtb.*) *thermoautotrophicus*. It could be demonstrated that four residues in the substrate binding pocket influence substrate specificity (Ingram-Smith *et al.*, 2006). The first three residues are isoleucine, threonine and valine at positions 312, 313 and 388 in *Mtb. thermoautotrophicus*. All of them are conserved among the four homologous ACS from *Mt. thermoacetophila*. The fourth important residue is tryptophan, which is in position 416 in *Mtb. thermoautotrophicus*. It is conserved in Mthe1194, Mthe1195 and Mthe1196 but not in Mthe1413. In Mthe1413 phenylalanine is found in the respective position. The above-mentioned residues form a pocket, which is large enough for short chain fatty acids like acetate and propionate but not for longer molecules. Therefore, only acetate and propionate can be converted by the ACS of *Mtb. thermoautotrophicus*, by Mthe1194 and probably also by Mthe1195 and Mthe1196. Phenylalanine is slightly smaller than tryptophan, therefore Mthe1413 might be able to convert molecules slightly longer than propionate (Ingram-Smith and Smith, 2007; Smith and Ingram-Smith, 2007).

The presence of multiple ACS gene copies that are all transcribed at least to some extent, could provide enhanced acetate activation capacities to cells of *Mt. thermoacetophila*. However, it might also be that the ACS enzymes differ in affinity for acetate or ATP and are thus differentially expressed, in response to substrate availability or the energetic status of the cell. Furthermore, it has been shown that ACS enzyme activity is regulated by post-translational modifications. In *Salmonella* (*S.*) *enterica* the Pat acetyltransferase acetylates a conserved lysine residue and thus inactivates the enzyme. It is reactivated by deacetylation by the sirtuin Sir-2 ortholog CobB (Starai and Escalante-Semerena, 2004). In *Bacillus* (*B.*) *subtilis* in contrast the AcuA and AcuC proteins acetylate and deacetylate the respective ACS enzyme (Gardner *et al.*, 2006). In the genome of *Mt. thermoacetophila* three open reading frames could be identified, that share 28-30 % identity to the C-terminal GNAT functional domain of the *S. enterica* Pat acetyltransferase (*mthe_0619, mthe_0086, mthe_0336*). No homolog of the CobB deacetylase was identified. Yet, four putative deacetylases with >35% identity to the *B. subtilis* AcuC have been identified (*mthe_1425, mthe_0676, mthe_1405, mthe_0463*). It was postulated that *Mt. thermoacetophila* might be using parts of two different acetylation/deacetylation systems (Smith and Ingram-Smith, 2007). Therefore, regulation

might not only occur on the transcriptional and/or posttranscriptional level, but also by post-translational modification.

In summary, Mthe1194 is a typical AMP-producing ACS enzyme. Due to rather low K_M values it can efficiently bind its substrates acetate, ATP and CoA and produce acetyl-CoA that can be further converted during methanogenesis. The only known inhibitor is PP_i: 0.25 mM PP_i lead to 50 % inhibition of enzymatic activity (Berger *et al.*, 2012). Furthermore, it was shown that Mthe1194 specifically converts acetate. The only other substrate is propionate, which is converted to propionyl-CoA. However, the specific activity with propionate is strongly reduced in comparison to the specific reaction rate with acetate (Berger *et al.*, 2012). Therefore, it can be concluded that Mthe1194 is not involved in turnover of medium- or long-chain fatty acids that are used as biosynthetic precursors but instead catalyzes acetate activation.

4.1.2 Pyrophosphatase from *Mt. thermoacetophila*

The reaction catalyzed by Mthe1194 produces acetyl-CoA, AMP and PP_i. Acetyl-CoA is fed into the pathway of methanogenesis and AMP is used for the regeneration of ATP. PP_i generated in the course of the reaction could be hydrolyzed and the energy set free in this exergonic reaction could be dissipated as heat. PP_i is not only a byproduct of acetate activation, but is formed during many biosynthetic reactions like RNA and DNA synthesis, biosynthesis of proteins, in lipid metabolism and during synthesis of polysaccharides and nucleotides (Heinonen, 2001). The equilibrium in those biosynthetic reactions is shifted to the educts, meaning that product formation is an endergonic process. Therefore, the reactions are coupled to the exergonic hydrolysis of one phosphoanhydride bond of nucleosid triphosphates, like ATP, which shifts $\Delta G^{0'}$ of the reaction to near zero. This yields the desired product and PP_i. PP_i hydrolysis as well is an exergonic reaction, which renders $\Delta G^{0'}$ more negative, and thus guarantees efficient synthesis of macromolecules. Therefore, the PP_i concentration of living cells cannot exceed a certain level. For *E. coli* this has been shown to be 16 mM (Chen *et al.*, 1990). PP_i hydrolysis is accomplished by PPases. Two main types of the enzyme can be distinguished, which are the membrane-bound PPases on the one hand and soluble enzymes on the other hand.

Membrane-bound PPases hydrolyze PP_i and concomitantly translocate H^+ or Na^+ across the cytoplasmic membrane, generating an electrochemical ion gradient. H^+-translocating PPases can be found in plants and in many protists. Likewise, a membrane-bound PPase is encoded in a quarter of all fully sequenced bacterial and archaeal genomes (Jämsen *et al.*, 2007). In the purple nonsulfur bacterium *Rhodospirillum* (*R.*) *rubrum* studies revealed an important physiological role of the membrane-bound PPase. Upon a metabolic shift from respiratory to photosynthetic metabolism, a Δ*ppase* mutant of *R. rubrum* showed a considerably longer lag phase than the wild type (40 h in the mutant compared to 14 h in the wild type (Garcia-

Contreras *et al.*, 2004)). Upon the shift from respiratory to photosynthetic growth, components needed for photosynthesis such as chromatophores need to be synthesized. It was concluded, that in the *R. rubrum* Δ*ppase* mutant less energy for this metabolic shift was available, due to the lack of the membrane-bound PPase. Thus, the enzyme significantly contributed to the electrochemical ion gradient used for ATP synthesis.

Among the methanogenic archaea *Ms. mazei* was shown to encode two membrane-bound PPases, one of which is produced during growth with methanol (Bäumer *et al.*, 2002). Additionally, in the genome of *Ms. mazei* a soluble PPase is encoded, but preparation of the cytoplasmic fraction and subsequent enzymatic assays resulted in no PPase activity. Therefore, the soluble PPase was not produced under the chosen conditions (Bäumer *et al.*, 2002). The membrane-bound enzyme was investigated in vesicle preparations of *Ms. mazei*. It was found that protons served as coupling ions and that the hydrolysis of 1 mol of PP_i was equivalent to the translocation of 1 mol of protons. It was calculated, that the free energy change of PP_i hydrolysis in the cytoplasm was -27.3 kJ mol^{-1} (Davies *et al.*, 1993) and that for the translocation of 1 mol of protons at least 14.6 kJ are needed. It was concluded that PP_i hydrolysis by the membrane-bound PPase from *Ms. mazei* still is an exergonic process, even though part of the energy is conserved in the form of a proton gradient (Bäumer *et al.*, 2002). Therefore, biosynthesis of macromolecules is still driven towards product formation on the one hand. On the other hand, the membrane-bound PPase contributes to the formation of an electrochemical potential by proton translocation, and might therefore be part of the energy conservation system of *Ms. mazei* (Bäumer *et al.*, 2002).

While this might be the case in *Ms. mazei,* no membrane-bound PPases are encoded in the genomes of *Mt. thermoacetophila*, *Mt. harundinacea* and *Mt. concilii* (Smith and Ingram-Smith, 2007; Barber *et al.*, 2011; Zhu *et al.*, 2012). Instead, soluble PPases are encoded in the three genomes.

Soluble PPases are subdivided into families or types I and II. Type I soluble PPases can be found in prokaryotes as well as in plants, animals and fungi (Sivula *et al.*, 1999). Although the overall amino acid sequence is poorly conserved, the active site of type I PPases is very similar and can be used for classification (Cooperman *et al.*, 1992; Kankare *et al.*, 1994). It consists of 14 - 16 amino acid residues and 3 - 4 Mg^{2+} ions (Parfenyev *et al.*, 2001). Eukaryotic type I PPases are organized as dimers, with a subunit size of 30–35 kDa. Prokaryotic type I PPases typically are hexamers consisting of 20 kDa subunits (Young *et al.*, 1998; Parfenyev *et al.*, 2001). The k_{cat} value of all type I PPases typically is in the range of 200-400 s^{-1} (Avaeva, 2000).

The first type II PPase has been characterized in 1967 in *Bacillus subtilis* (Tono and Kornberg, 1967). At that time, the protein was not recognized as belonging to an evolutionary lineage that is distinct from type I PPases. They were identified as an independent enzyme

family about 15 years ago (Shintani *et al.*, 1998; Young *et al.*, 1998). Type II PPases are well-conserved, but share no sequence homology with type I PPases. They are classified as belonging to the DHH phosphoesterase superfamily. DHH stands for a conserved Asp-His-His motive, which is essential for binding of metal ions. Type II PPases can be found primarily in the genera *Bacillus* and *Clostridium* (Kajander *et al.*, 2013). Additionally, they are frequently encountered in human pathogens like *Vibrio cholerae, Streptococcus agalactiae* and *Streptococcus mutans* (Salminen *et al.*, 2006; Fabrichniy *et al.*, 2007). Their typical subunit molecular mass is about 34 kDa and for many type II PPases a homodimeric quarternary structure has been demonstrated (Ahn *et al.*, 2001; Merckel *et al.*, 2001; Halonen *et al.*, 2005; Rantanen *et al.*, 2007).

Mg^{2+} can be used as metal ion in the catalytic center, but transition metal ions like Mn^{2+} and Co^{2+} are bound with higher, nanomolar affinity (Fabrichniy *et al.*, 2007). With these transition metal ions, k_{cat} values of 1700-3300 s^{-1} are reached, which is one order of magnitude higher than in type I PPases (Parfenyev *et al.*, 2001).

Type II soluble PPases from archaea have been characterized in the methanogenic species *Mt. concilii* (Jetten *et al.*, 1992a) and *Methanocaldococcus* (*Mc.*) *jannaschii* (Kuhn *et al.*, 2000). The enzyme from *Mc. jannaschii* was heterologously produced in *E. coli* and catalyzed hydrolysis of PP_i at a rate of 8000 U mg^{-1} at 85 °C, which is the optimal growth temperature of *Mc. jannaschii*. This conferred to a k_{cat} of 14443 s^{-1} and was thus exceptionally high. Enzymatic assays revealed the presence of two metal binding sites. Both could be occupied by Mg^{2+}, however one site required high Mg^{2+} concentrations of up to 50 mM. In contrast, Mn^{2+} and Co^{2+} could be added at a concentration of 20 μM or 50 μM to support activity of the enzyme. Additionally, Mn^{2+} and Co^{2+} conferred resistance towards F^-, to which the enzyme otherwise was very sensitive. The molecular mass of a single subunit as investigated by mass spectrometry was 34.169 kDa. Chromatographic methods revealed a quarternary structure of 3 – 4 subunits in the native enzyme.

The type II soluble PPase from *Mt. concilii* was isolated from cell extract. SDS-PAGE analysis revealed two bands of comparable intensity, which were thought to be 33 kDa and 35 kDa subunits. Size exclusion chromatography was performed with the native enzyme and resulted in a molecular mass of 139 ± 7 kDa, which confers to a heterotetrameric $\alpha_2\beta_2$ structure (Jetten *et al.*, 1992a). However, only one gene homologous to other type II PPase genes can be found in the genome of *Mt. concilii* (Barber *et al.*, 2011). Therefore, it might be, that the preparation was contaminated by a protein of a similar subunit molecular mass. For accurate data concerning the quarternary structure of the *Mt. concilii* PPase it would be helpful to specifically target the respective gene and the corresponding protein. The preparation catalyzed PP_i hydrolysis with Mg^{2+} in the active center with a k_{cat} of 1400 s^{-1}. Addition of Mn^{2+} increased the activity by 160 % (Jetten *et al.*, 1992a).

In this study, the type II soluble PPase from *Mt. thermoacetophila* was heterologously produced and purified via Strep-tactin affinity chromatography. SDS-PAGE analysis revealed a single band of 35 kDa, representing the typical subunit size of type II PPases. The enzymatic activity was measured by detecting P_i in an assay modified after (Saheki *et al.*, 1985). A v_{max} of 726 ± 40 U mg^{-1} was measured after preincubation with Mn^{2+}. This corresponded to a k_{cat} of 1728 s^{-1} which accords with other type II PPases (Parfenyev *et al.*, 2001). The quarternary structure of the native enzyme was investigated by size exclusion chromatography. A molecular mass of 71.4 ± 5 kDa was determined, hence the enzyme was a homodimer. Therefore, in its subunit composition the *Mt. thermoacetophila* PPase resembled bacterial enzymes. Since the subunit composition of the *Mc. jannaschii* PPase was not totally clear and the preparation of the *Mt. concilii* PPase might have been contaminated, it is feasible that homodimers are the natural form also of archaeal type II PPases.

It remains to be answered, why type II PPases are strongly activated by transition metal ions like Mn^{2+} or Co^{2+}. The mechanism of PP_i hydrolysis has been studied in type I as well as in type II PPases. As far as it is understood, both employ metal ions to activate a water molecule. A hydroxide ion is formed that attacks the electrophilic phosphate moiety of PP_i. The differences in catalytic efficiency and preference of either Mg^{2+} or transition metal ions can be largely explained by differences in the overall structure and amino acid composition of the active site. Type I PPases have a simple single-domain structure and the conserved active site consists of a D-(S/G/N)-D-P-(C/I/L/M/V)-D-(C/I/L/M/V)-(C/I/L/M/V) motive (Kankare *et al.*, 1994). D117 was shown to be involved in activation of the water molecule and D120 binds metal ions at binding sites M1 and M2 (Heikinheimo *et al.*, 2001). In contrast, type II PPases have a N-terminal and a C-terminal domain, that are connected by a flexible hinge region (Ahn *et al.*, 2001; Merckel *et al.*, 2001). Upon substrate binding, the enzyme switches from an “open” to a “closed” conformation by an induced-fit mechanism. The catalytic center is at the domain interface, thus the conformational change is necessary for PP_i hydrolysis (Ahn *et al.*, 2001; Ilias and Young, 2006). Metal ions at M1 and M2 are coordinated not only by a single Asp but also by His ligands (Kajander *et al.*, 2013). This leads to a preference for transition metal ions because these prefer soft ligands like Cys and His. Transition metal ions further prefer a five-coordinated state, which is adopted in the open conformation, but are able to switch to a six-coordinated state in the closed conformation. In the type II PPase from *B. subtilis* adoption of the closed conformation changes the state of the metal ion bound at M2 from five-coordinated (D15, D75, H97, D149, and the nucleophilic OH^-) to six-coordinated. When being six-coordinated the metal ion is bound to the aforementioned residues and to P1 of PP_i (Fabrichniy *et al.*, 2007). Mg^{2+}, which is almost always six-coordinated, cannot undergo these changes (Harding, 2001). However, although transition metal ions can adopt a five-coordinated as well as a six-coordinated state they tend to return

to the preferred five-coordinated state. This may well drive removal of P_i from the active site and support the high catalytic activity of type II soluble PPases (Fabrichniy *et al.*, 2007).

Therefore, type II soluble PPases normally catalyze PP_i hydrolysis at a high rate and efficiently degrade PP_i. However, for the type II soluble PPase from *Moorella* (*Mo.*) *thermoacetica* strong inhibition by the adenine nucleotides AMP and ADP has been demonstrated (Jämsen *et al.*, 2007). *Mo. thermoacetica* additionally contains a H^+-translocating membrane-bound PPase. Hence, at low energy level of the cell with high AMP and ADP concentrations, PP_i hydrolysis by the soluble PPase will be strongly inhibited. Thus, the membrane-bound PPase could contribute to the formation of an electrochemical ion gradient for ATP synthesis.

The inhibition was due to a ~250 amino acid insert comprising two cystathionine β-synthase (CBS) domains. CBS domains were first identified in 15 different proteins from *Mc. jannaschii* and were homologous to a motive also found in the cystathionine β-synthase, which is involved in the metabolism of sulfur-containing amino acids (Bateman, 1997). By now, CBS domains were shown to be widespread in all domains of life and to occur in proteins with many different functions. They are frequently encountered in proteins involved in purine metabolism (39 %), active transport of solutes (12 %), selenoamino acid metabolism (6 %) and methionine metabolism (6 %) with the other 37 % distributed among various functional classes (Jämsen, 2011). Interestingly, the insertion of ~250 amino acids comprising two CBS domains can be found in approximately one quarter of all known type II PPases (Jämsen *et al.*, 2007).

CBS domains are thought to have mainly regulatory function binding metal ions (Hattori *et al.*, 2009), DNA (Aguado-Llera *et al.*, 2010) or, most common, adenosine ligands. Besides AMP and ADP in the *Mo. thermoacetica* PPase these are for example AMP and ATP in case of AMP-activated protein kinases, ATP in case of 5'-Inosine monophosphate dehydrogenases (IMPDH) and S-adenosyl methionine in case of cystathionine β-synthases (Scott *et al.*, 2004; King *et al.*, 2008).

A single CBS domain consists of ~60 amino acids. Yet, very often a tandem repeat consisting of two CBS domains called Bateman domain can be found. The crystal structure of a CBS domain was solved as part of the IMPDH of the Chinese hamster (Sintchak *et al.*, 1996). Three β-sheets and two α-helices form a β1-α1-β2-β3-α2 structure. Two CBS domains are intimately linked via β-sheets, composed of three strands from one domain and one from the other. Therefore, two domains are needed to maintain structural integrity (Scott *et al.*, 2004). Furthermore, it could be shown that the binding site for various ligands is formed by a cleft at the interface of two CBS domains. Thus, also in ligand binding two CBS domains are involved (Ereno-Orbea *et al.*, 2013; Jeong *et al.*, 2013).

A single CBS domain could be identified in the sequence of the type II soluble PPase from *Mt. thermoacetophila* (Berger *et al.*, 2012). In comparison to CBS-PPases from *Mo. thermoacetica* and *Cl. perfringens,* the protein is significantly shorter (Figure 39). CBS-PPases from both, *Mo. thermoacetica* and *Cl. perfringens,* contain two CBS domains, which are linked by a so-called DRTGG domain with unknown function (Jämsen *et al.*, 2007; Tuominen *et al.*, 2010). The second CBS domain and the DRTGG domain are missing in the *Mt. thermoacetophila* PPase and therefore the protein is 238 amino acids shorter than the *Cl. perfringens* PPase and 125 residues shorter than the *Mo. thermoacetica* PPase.

Inhibition of the soluble PPase in *Mt. thermoacetophila* by AMP and/or ADP would prevent PP_i hydrolysis and save PP_i that could be used to improve the energetic balance. As already mentioned above, no membrane-bound PPase in encoded in the genome of *Mt. thermoacetophila*. But it is also conceivable, that PP_i is used to phosphorylate intermediates of the central metabolism and thus at least part of the energy otherwise lost as heat could be conserved. Yet, the PPase from *Mt. thermoacetophila* is neither inhibited by AMP nor by ADP (Berger *et al.*, 2012). Most likely, this is due to the fact that since only one CBS domain is present the ligand binding site cannot be formed and AMP and/or ADP cannot be bound. Therefore, the enzyme is not regulated by adenine nucleotides and will not be inhibited by AMP and ADP in cells of *Mt. thermoacetophila*.

Yet, despite the high phosphorolytic activity the K_M value of the *Mt. thermoacetophila* PPase is relatively high (0.16 mM, 3.1.3). This might allow other enzymes to phosphorylate metabolic intermediates with consumption of PP_i, which could spare ATP and might thus improve the energy balance of *Mt. thermoacetophila*.

PP_i-dependent enzymes phosphorylating metabolic intermediates have already been described. Their number is quite limited, but nevertheless in some organisms PP_i seems to have a central role in energy metabolism. *Entamoeba hystolytica*, the causative agent of amebic dysentery, is devoid of enzymes of the citric acid cycle and oxidative phosphorylation. Therefore, the organism relies on glycolysis for ATP synthesis. The final product of amebal metabolism is acetate. For several enzymes that are in involved in glycolysis and normally consume ATP, PP_i-dependent counterparts have been identified (Reeves, 1968; Reeves *et al.*, 1974). For the phosphofructokinase (PFK), catalyzing phosphorylation of fructose-1-phosphate to yield fructose-1,6-bisphosphate, the presence of an ATP- and a PP_i-dependent enzyme has been demonstrated (Chi *et al.*, 2001). Yet, the enzymatic activity of the ATP-dependent isoenzyme was only about 10 % of that of the PP_i-dependent enzyme (Reeves *et al.*, 1974; Chi *et al.*, 2001). Furthermore, for the last step of glycolysis, dephosphorylation of phosphoenolpyruvate (PEP) to yield ATP and pyruvate, two enzymes possibly catalyzing the

```
Mt.thermoacetophila   MADNIYVVGHKSPDTDSVTSAITYANLKNQLGMKDVVPAAAGEINNETKYVLEYFKIAPP 60
Cl.perfringens        MKDVIYITGHKNPDSDSICAALAYAEFKNKTQDTPAIPVRLGNVSQETQYILDYFGVEAP 60
Mo.thermoacetica      MGKEILVIGHQRPDTDSIAAAIGYAALRNKTDGGGFQAARCGKLNGETEFVLSYFDVPVP 60
                      * . * : **: **:**: :*: ** ::*:       ..  *::. **:::*.** :  *
Mt.thermoacetophila   VVLN---------------------------------------------------------- 64
Cl.perfringens        QFLETVKLKVEDLEMDKIAPLAPEVSLKMAWNIMRDKNLKSIPVADGNNHLLGMLSTSNI 120
Mo.thermoacetica      PLVNDVRARVKDVLDGGLLFIQPGATVRQAGIFMRQHGVKTLAVVDENRHLLGLFTVGDL 120
                       .::
Mt.thermoacetophila   ----------------------------------------------------------
Cl.perfringens        TATYMDIWDSNILAKSATSLDNILDTLSAEAQNINEERKVFPGKVVVAAMQAESLKEFIS 180
Mo.thermoacetica      ARLLLEAWDTG---------------------------------------------- 131

Mt.thermoacetophila   ----------------------------------------------------------
Cl.perfringens        EGDIAIAGDRAEIQAELIELKVSLLIVTGGHTPSKEIIELAKKNNITVITTPHDSFTASR 240
Mo.thermoacetica      ----------------------------------------------------------

Mt.thermoacetophila   ----------------------------------------------------------
Cl.perfringens        LIVQSLPVDYVMTKDNLVAVSTDDLVEDVKVTMSETRYSNYPVIDENNKVVGSIARFHLI 300
Mo.thermoacetica      NVPMDEPVYKVMQSDNLVIFNQDDLITEVRRTMLETRYRNYPVVDDNHCLVGLIARYHLL 191

Mt.thermoacetophila   DATDKKVILVDHNEVGQAVDNIMKADILEIIDHHKIGDIQTGKPIFFHNEPVGATGTIIA 124
Cl.perfringens        STHKKKVIQVDHNERGQSVHGLEDAEVLEIIDHHRVADIQTGNPIYFRNEPLGSTSTIVA 360
Mo.thermoacetica      AMRGKRVILVDHNEKSQAVPGIEEAETVEIIDHHRVADIETAEPIMVRNEPVGSTATIIA 251
                          *:** ***** .*:* .: .*: :******::.**:*.:** .:***:*:*.**:*
Mt.thermoacetophila   SMYELNGVAISKEMAGLMMAAILSDTVLFKSPTCTDKDKATVEKLSKICGEDPQKFGMEM 184
Cl.perfringens        KRFFENGIRPSREAAGLLCGAIISDTLLFKSPTCTPQDVKMCRKLAEIAGIVPETFAKEM 420
Mo.thermoacetica      RMYKERGLDPDAAIAGVLCAAILSDTLLFKSPTTTQVDKELAAWLADIAGLDVANFGREM 311
                        :  .*:  .   **:: .**:***:****** *  *      *:.*.*    .*. **
Mt.thermoacetophila   LKAKSDIKSKTAKDILFGDFKKFDFSGVKAGVGQIEVMDLADLAPKREEILAEMRKALES 244
Cl.perfringens        FKAGTSLKGKSIEEIFNADFKPFTIEGVKVGVAQVNTMDIEGFMPLKGEMLDYMNQKAES 480
Mo.thermoacetica      FRAGSSLRGRSGREIILEDFKSFNFGSNRVGIGQIEIIDPDTLPVGRDELQAELEKLQAE 371
                      ::* :.::.:: .:*:  *** * : . :.*:.*:: :*   :   : *:   :.:   .
Mt.thermoacetophila   EKLDMIVLMLTDVIKEASDLLFVGTAAAKEGFEKAFGGKVTNNSIYKEKVLSRKKQVIPP 304
Cl.perfringens        MGLEMIMLLLTDIINEGSQILVAGRSPEIA--EEAFKVKLEDSTTFLPGVLSRKKQVVPP 538
Mo.thermoacetica      KQYDLVVLMVTDLMRNGTELLFAG--PQGRAVELAFNVTPGEKSVFLPGVMSRKKQVVPP 429
                         ::::*::**::.:.:::*..*  .     * **  .  :.: :   *:******:**
Mt.thermoacetophila   LESAFKK---- 311
Cl.perfringens        LTQIITTRVSK 549
Mo.thermoacetica      LRRLLQG---- 436
                      *   :
```

Figure 39: Alignment of CBS-PPases from *Mt. thermoacetophila*, *Cl. perfringens* and *Mo. thermoacetica*. The *Mt. thermoacetophila* PPase amino acid sequence is significantly shorter since one CBS domain and the DRTGG domain are missing. The other residues are well conserved among the three enzymes.

reaction have been identified. On the one hand, the classical pyruvate kinase (PK) that catalyzes the conversion of ADP and PEP to ATP and pyruvate is present in *En. histolytica*

(Saavedra *et al.*, 2004). On the other hand a pyruvate phosphate dikinase (PPDK) has been described (Reeves 1968). This enzyme catalyzes the reversible conversion between PEP, AMP and PP_i to pyruvate, ATP and phosphate. It can thus replace the PK in *En. histolytica*, which was not as active as the PPDK and inhibited at PEP concentrations between 1-5 mM (Saavedra *et al.*, 2004).

Finally, there is a PP_i-dependent acetate kinase in *En. histolytica* (Reeves and Guthrie, 1975). The enzyme catalyzes the conversion between acetyl-phosphate and P_i to acetate and PP_i. Although the reaction is reversible, the enzyme displayed a higher specific activity in the direction of acetate and PP_i formation. Since acetate is the final product of amebal metabolism, acetate production might be the physiological role of the enzyme.

Although the physiological impact of the enzymes mentioned above is not very well understood, it is conceivable that PP_i is used as a substitute for ATP. *En. histolytica* suffered a secondary loss of mitochondria, which is probably due to its lifestyle as a parasite, living under conditions of low oxygen supply (Clark and Roger, 1995). The remaining so-called mitosomes are not able to produce ATP (Dolezal *et al.*, 2010). Therefore, *En. histolytica* relies on glycolysis for ATP synthesis. Consumption of PP_i instead of ATP by glycolytic enzymes improves the ATP balance of glycolysis. E.g. if the PP_i-dependent PFK is used for the formation of fructose-1,6-bisphosphate one ATP equivalent per molecule is spared. Furthermore, if the PPDK catalyzes formation of pyruvate and ATP from PEP, AMP and PP_i, two ATP equivalents per molecule are synthesized in the course of the reaction instead of one, which is produced by the PK. Finally, *En. histolytica* apparently does not possess a PPase (Deng *et al.*, 1998). Thus, it seems reasonable that PP_i is regularly used by glycolytic enzymes and therefore PP_i could make a significant contribution to energy conservation in *En. histolytica*.

PP_i-dependent PFK and PPDK have also been described in *Caldicellulosiruptor saccharolyticus* from the class of Clostridia (Bielen *et al.*, 2010). Since PEP synthase and fructose-1,6-bisphosphatase are missing, they might have a rather anabolic function in this organism. PP_i-dependent PFK and PPDK are also present in the archaeon *Thermoproteus* (*T.*) *tenax* (Siebers and Hensel, 2001; Tjaden *et al.*, 2006). Hence, PP_i-dependent enzymes converting central carbon metabolites have been described in all three domains of life.

In *Mt. thermoacetophila* no such enzymes have been characterized until now. A PP_i-dependent PFK is not encoded in the genome. There is one gene, which is homologous to the gene encoding PPDK from *T. tenax* (Berger *et al.*, 2012). If *Mt. thermoacetophila* had a PPDK enzyme this could provide a cost-effective way for the interconversion of the central carbon metabolites pyruvate and PEP. However, the metabolic flux through the methanogenic pathway exceeds the need for biosynthetic carbon metabolites. Therefore, PPDK activity would not be sufficient to compensate PP_i production by ACS enzymes.

In summary, in this study the acetate activation reaction in the obligate aceticlastic methanogenic archaeon *Mt. thermoacetophila* was investigated. Therefore, the highly transcribed gene *mthe_1194,* which encodes a putative AMP-forming ACS enzyme was cloned and the corresponding enzyme was produced in *E. coli*. It could be demonstrated, that Mthe1194 catalyzes conversion of acetate, ATP and CoA to acetyl-CoA, AMP and PP_i. This was interesting, because there are also ADP-forming ACS enzymes, which could provide a less costly mode of acetate activation. Yet, Mthe1194 was a typical AMP-forming ACS enzyme, which was suitable to efficiently generate acetyl-CoA for methanogenesis. A byproduct of the reaction is PP_i. PP_i hydrolysis is an exergonic reaction, which if catalyzed by a soluble PPase produces P_i and heat. The gene *mthe_0236* annotated as soluble type II PPase was likewise highly transcribed. It was cloned and the respective enzyme produced and thoroughly characterized. It was interesting whether Mthe0236 was probably active *in vivo* because if PP_i hydrolysis was inhibited, at least part of the energy stored in PP_i could possibly be conserved. Inhibition by adenine nucleotides seemed feasible, since the protein contained a CBS domain known as potential regulator of enzyme activity (Scott *et al.*, 2004; Jämsen *et al.*, 2007). However, Mthe0236 turned out to be a typical type II PPase with high specific activity and no known inhibitors. The binding site for adenosine ligands is formed in a cleft located between two CBS domains. Since Mthe0236 contained only a single repeat, it could not bind adenine nucleotides and thus could not be regulated. Therefore, most likely two ATP equivalents are spent for acetate activation in *Mt. thermoacetophila*.

4.2 The Fpo complex from *Ms. mazei*

The $F_{420}H_2$ dehydrogenase, also known as Fpo complex (F_{420}:phenazine oxidoreductase), was shown to oxidize $F_{420}H_2$ produced in methylotrophic methanogenesis. In the model organism *Ms. mazei* it concomitantly translocates two protons (Bäumer *et al.*, 2002). Thus, it contributes to the formation of an electrochemical proton gradient, used for ATP synthesis. In *Ms. mazei* the whole complex comprises subunits FpoABCDFHIJ1J2KLMNO. There are hydrophobic subunits, which are membrane-integral and are according to comparison with homologous respiratory complex I involved in proton translocation (FpoAHJ1J2KLMN, (Welte and Deppenmeier, 2014)). Subunits FpoBCDI are associated to the membrane and are most likely responsible for electron transfer to the membrane-integrated subunits and finally to the lipophilic electron carrier methanophenazine (MP). The hydrophilic subunit FpoF functions as electron input module that oxidizes $F_{420}H_2$. However, FpoF can dissociate from the complex, which makes the membrane-associated subunits FpoBCDI accessible for Fd. In aceticlastic methanogenesis, reducing equivalents are transferred exclusively to Fd. In *Ms. mazei* Fd_{red} was thought to be re-oxidized by the Ech hydrogenase, yet, a *Ms. mazei* Δ*ech* mutant

retained approximately 50 % Fd_{red}-oxidizing activity as compared to the wild type (Welte *et al.*, 2010b). This meant, there had to be another protein catalyzing Fd_{red} oxidation. The Fpo complex seemed to be a possible candidate to accept electrons from Fd_{red}, probably via subunit FpoI. This hypothesis was corroborated in the course of this study. Fd_{red}-oxidation via the Fpo complex might also take place in *Mt. thermoacetophila*, where no genes encoding FpoF, Ech hydrogenase or Rnf complex are present. Instead, the *fpo* operon without *fpoO* can be found. Furthermore, the organism was shown to possess a highly active Fd:heterodisulfide oxidoreductase system (Welte and Deppenmeier, 2011b).

Subunit FpoO is the only subunit to which neither exact localization nor function of the protein could be assigned so far. In this study a *Ms. mazei* Δ*fpoO* mutant was used to investigate, if the lack of FpoO had an impact on growth rate or yield and if the $F_{420}H_2$-oxidizing activity of the Fpo complex was impaired, if FpoO was missing. According to the results presented here, energy conservation in the *Ms. mazei* Δ*fpoO* was not impaired, and thus FpoO appears not to be important for the overall functioning of the Fpo complex.

4.2.1 Subunit FpoO from the Fpo complex

The exact localization of subunit FpoO from the Fpo complex from *Ms. mazei* is not known. This is due to the fact that no FpoO homologs can be found in the well-studied complex I, or the Fqo complex from *Archaeoglobus fulgidus* (Brüggemann *et al.*, 2000). Furthermore, no function can be assigned, since FpoO shares no significant homology with any protein characterized to date.

Since the Fpo complex differs from its homologs, because it uses MP as electron acceptor instead of quinones, it seemed reasonable that FpoO might be involved in electron transfer to MP. Therefore, the function of FpoO was approached by growth experiments, with a *Ms. mazei* Δ*fpoO* mutant and with enzyme activity assays using membrane fractions of *Ms. mazei* wild type and Δ*fpoO* mutant.

Growth experiments with *Ms. mazei* Δ*fpoO* mutant and wild type were performed, using TMA and acetate as substrates. TMA oxidation results in formation of $F_{420}H_2$ and Fd_{red}. Whereas the Ech hydrogenase catalyzes Fd_{red} oxidation, $F_{420}H_2$ is oxidized by the Fpo complex (Abken and Deppenmeier, 1997). A different route of $F_{420}H_2$ oxidation is present in *Ms. barkeri*. Here, reducing equivalents from $F_{420}H_2$ are transferred to H^+ by the F_{420}-reducing hydrogenase, bypassing the Fpo complex (Kulkarni *et al.*, 2009). H_2 generated in the course of the reaction is oxidized by the membrane-bound Vho hydrogenase. However, in *Ms. mazei* the Fpo complex was shown to be much more important than in *Ms. barkeri* (Welte and Deppenmeier, 2011a). Mutants missing the whole complex or subunit FpoF had a considerably prolonged doubling time in comparison to the wild type. Therefore, the *Ms. mazei* Δ*fpoO* mutant should have a similar phenotype, if subunit FpoO was essential for

$F_{420}H_2$ oxidation. Yet, no significant differences between mutant and wild type could be measured. This indicated that FpoO was not important for $F_{420}H_2$ oxidation by the Fpo complex. This could be confirmed by measuring the enzymatic activity of the Fpo complex in membrane fractions of the *Ms. mazei* wild type and Δ*fpoO* mutant.

Using acetate as substrate, reducing equivalents are transferred to Fd. Therefore, if not only the Ech hydrogenase but also the Fpo complex catalyzes Fd_{red} oxidation and if FpoO was important for the reaction, this should become visible using acetate as substrate for growth. However, growth parameters measured for wild type and mutant were similar in the respective experiment. Finally, membrane fractions were used to measure electron transfer from the Fpo complex to the membrane-bound heterodisulfide reductase via MP. It was demonstrated that electron transfer was not impaired by the lack of FpoO.

Altogether, there was no evidence that FpoO was directly involved in oxidation of $F_{420}H_2$ or Fd_{red} and transfer of electrons from the Fpo complex to MP. It was therefore concluded, that FpoO was not directly contributing to energy conservation in *Ms. mazei*.

Nevertheless, FpoO might still have an important function. It is conceivable that it works as transcriptional regulator controlling transcription of the *fpo* operon and/or *fpoF*. This has been investigated by (Hofmann, 2003). Recombinant, purified FpoO protein and the amplified promoter region of the *fpo* operon or *fpoF* were used for mobility shift assays. In this experiment, FpoO and the DNA fragments were incubated together and afterwards applied to 2 % agarose gels or 5 % polyacrylamide gels. With this method, binding of FpoO to the respective DNA fragments could be investigated. However, FpoO did neither bind the promoter region of the *fpo* operon nor of *fpoF* (Hofmann, 2003). Therefore, FpoO most likely does not regulate transcription of the above-mentioned genes. It could still work as regulator for other genes but it might also have yet another function.

After FpoO did not participate in in electron transfer reactions and in transcriptional regulation of the *fpo* operon and *fpoF,* another possible function of FpoO is that of a redox sensor. A prerequisite is the presence of redox sensitive prosthetic group like iron sulfur clusters. For FpoO one [2Fe2S] cluster is predicted by Prosite. This is in agreement with 1.5 nmol of non-heme iron and 1.6 nmol of acid labile sulfur measured in purified FpoO protein (Hofmann, 2003). It seems feasible that FpoO measures the redox state of a cell and acts as signal transducer. A similar role has been demonstrated for LdpA from *Synechococcus elongatus* (Ivleva *et al.*, 2005). This protein is involved in the regulation of the circadian period of the cyanobacterial circadian clock. It contains two [4Fe4S] clusters, which help sensing the redox state of the plastoquinone pool. If the plastoquinone pool is rather oxidized, which is the case at low light intensities, LdpA submits a signal to the central oscillator, which lengthens the circadian period (Ivleva *et al.*, 2005). If the plastoquinone pool is reduced at high light intensities LdpA is degraded and the central oscillator is set to “short-period mode” (Ivleva *et*

al., 2005).

Homologs for FpoO from *Ms. mazei* can be found in *Ms. acetivorans*, *Ms. barkeri*, *Methanohalobium evestigatum*, *Methanolobus tindarius, Methanolobus psychrophilus*, *Methanococcoides methylutens*, *Methanococcoides burtonii*, *Methanohalophilus mahii*, *Methanomethylovorans hollandica* and *Methanosalsum zhilinae*. Additionally, in all of them, homologs of the $F_{420}H_2$-oxidizing module FpoF are present. This seems reasonable since all the above-mentioned organisms are able to perform methylotrophic methanogenesis, where reducing equivalents are transferred to F_{420}. Neither in the NCBI nor in the KEGG database methylotrophic methanogens missing FpoO could be identified. Species that do not convert methylated compounds but contain an Fpo complex consequently are lacking subunit FpoF but also FpoO. These are *Mt. thermoacetophila*, *Mt. concilii* and *Mt. harundinaceae* as well as *Mm. luminyensis* and "*Candidatus* Methanomassiliicoccus intestinalis". All of them do not reduce F_{420} during breakdown of methanogenic substrates. Therefore, there seems to be a connection between FpoO and FpoF and/or between FpoO and F_{420}. It is conceivable that FpoO is reduced by $F_{420}H_2$. However, the F_{420} binding motive GXhG (h, hydrophobic residue) as deduced from FpoF and FrhB (Mills *et al*., 2013; Welte and Deppenmeier, 2014) is not present in FpoO.

The second electron acceptor in methylotrophic methanogenesis is Fd, which is re-oxidized either by the Ech hydrogenase or the Rnf complex (Welte and Deppenmeier, 2014). Fd_{red}-oxidation has been thoroughly investigated in *Ms. mazei* (Welte *et al*., 2010b; Welte *et al*., 2010a) and is catalyzed by the Ech hydrogenase. In the other above-mentioned methylotrophic methanogens Fd_{red}-oxidation has not been investigated in such detail. However, it is known that the Ech hydrogenase is present in *Ms. barkeri* but not in *Ms. acetivorans,* that instead uses the Rnf complex for Fd_{red} oxidation (Wang *et al*., 2011a; Schlegel *et al*., 2012). According to genome sequence data of *Methanohalophilus mahii, Methanococcoides burtonii* and *Methanosalsum zhilinae,* no Ech hydrogenase is present in those methanogens but potential Rnf encoding genes could be identified (Spring *et al*., 2010).

Since there are enzymes catalyzing Fd_{red}-oxidation, it seems unnecessary that a second enzyme complex catalyzes the same reaction. Yet, it could be shown in this study that the Fpo complex in *Ms. mazei* has a double function. It catalyzes oxidation of $F_{420}H_2$ but it can likewise oxidize Fd_{red}, most probably via subunit FpoI (3.2.2). Fd_{red}-oxidation is considered to be an ancient trait of the Fpo complex, which obviously survived until today. In organisms that additionally contain Ech hydrogenase or Rnf complex, this might be important under conditions when Ech hydrogenase or Rnf complex are inhibited. In *Ms. mazei* subunit FpoI is probably blocked by subunit FpoF, but FpoF is able to dissociate from the complex (Welte and Deppenmeier, 2011a). It seems feasible that FpoO is involved in dissociation of subunit

FpoF to make FpoI accessible for Fd_{red}. Dissociation could be coupled to the redox state of the Fd pool via FpoO. Therefore, in *Ms. mazei* and other methylotrophic methanogens, subunit FpoO could be involved in fine tuning of $F_{420}H_2$ and Fd_{red}-oxidation by the Fpo complex. It is unlikely that FpoO is needed to stabilize the interaction of FpoF with the membrane-bound part of the complex, since the *Ms. mazei* Δ*fpoO* mutant was still able to catalyze oxidation of $F_{420}H_2$. In contrast, in *Mt. thermoacetophila* the Fpo complex is the only Fd_{red}-oxidizing enzyme complex known to date. Thus, there is no competition between different electron carrier molecules, hence regulation of alternative pathways is not necessary.

If FpoO was really needed to enable Fd_{red}-oxidation by the Fpo complex, the *Ms. mazei* Δ*fpoO* mutant could possibly have a phenotype, when acetate is used as substrate. This was not the case, indicating that the Ech hydrogenase oxidized the largest portion of Fd_{red} generated during methanogenesis, making the Fpo complex unnecessary.

4.2.2 Oxidation of Fd_{red} by the Fpo complex

Ms. mazei has a branched respiratory chain consisting of the membrane-bound heterodisulfide reductase (Hdr), the F_{420} non-reducing hydrogenase (Vho), the Fd_{red}-oxidizing Ech hydrogenase and the $F_{420}H_2$-oxidizing Fpo complex (Welte and Deppenmeier, 2014). Experiments with a *Ms. mazei* Δ*ech* mutant revealed, that although the Ech hydrogenase was missing, the membrane fractions could still catalyze oxidation of Fd_{red} (Welte *et al.*, 2010b). It was concluded that there was a second enzyme, that could oxidize Fd_{red}. The Fpo complex seemed to be a potential candidate. The [4Fe4S] clusters in FpoI could accept electrons from Fd_{red} and transfer them to iron sulfur clusters in subunit FpoB and further to MP.

In *Mt. thermoacetophila* the respiratory chain consists of the Fpo complex without subunit FpoF and the membrane-bound Hdr. Since *Mt. thermoacetophila* is an obligate aceticlastic methanogen without Ech hydrogenase or Rnf complex, this opens the question of Fd_{red}-oxidation. Interestingly, subunit FpoI of the Fpo complex from *Mt. thermoacetophila* shows a C-terminal stretch containing lysine residues, which could facilitate interaction with negatively charged Fd (Welte and Deppenmeier, 2011b).

The ability of the Fpo complex to oxidize Fd_{red} is supported by studies of the highly homologous complex I (Nuo complex). Functionally, complex I can be divided into the hydrophilic part, which comprises the electron input module NuoEFG. Electron transfer to ubiquinone is achieved by the membrane-associated part and the membrane-bound part of the enzyme is responsible for proton translocation.

The electron input module NuoEFG often is encoded in the same operon as the other *nuo*

genes. However, in the eubacterium *Aquifex aeolicus nouEFG* is located at a different chromosomal site (Deckert *et al.*, 1998). Furthermore, although complex I homologs can be found in many archaea homologs for *nuoEFG* genes are always missing (Moparthi and Hägerhäll, 2011). In some members of the Methanosarcinales and the closely related sulfate reducer *Archaeoglobus* NuoEFG has been replaced by $F_{420}H_2$-oxidizing FpoF and FqoF, respectively (Abken and Deppenmeier, 1997; Brüggemann *et al.*, 2000). This gave rise to the idea that the electron input module evolved independently and that the rest of the complex may function without a special input module.

Fd has been discussed as potential electron donor for the headless complex. Fd probably evolved very early when the Earth' atmosphere was anoxic and iron and sulfur were highly abundant (George *et al.*, 1985; Wächtershäuser, 1988). It seems feasible that when later the atmosphere became oxygenic, Fd was replaced by oxygen-stable NADH and the respective input module evolved (Imlay, 2006). However, also today many enzymes rely on Fd as electron acceptor or donor, often due to its low midpoint potential. In many organisms NAD/NADH-dependent oxidoreductases are replaced by Fd-dependent enzymes. These are e.g. pyruvate:Fd oxidoreductase, 2-oxoglutarate:Fd oxidoreductase, 2-ketoglutarate:Fd oxidoreductase, 2-oxoisovalerate:Fd oxidoreductase, indolepyruvate:Fd oxidoreductase in *Halobacterium halobium, Thermococcus litoralis, and Methanobacterium thermoautotrophicum* (Kerscher and Oesterhelt, 1981; Mai and Adams, 1996a; Tersteegen *et al.*, 1997). Also aldehyde:Fd oxidoreductases are present in *Pyrococcus furiosus, Thermococcus litoralis* and *Pyrobaculum aerophilum* (George *et al.*, 1992; Mukund and Adams, 1993; Hagedoorn *et al.*, 2005). Often also a glyceraldehyde:Fd oxidoreductase can be found such as in *Thermotoga maritima, Pyrococcus furiosus, Methanococcus maripaludis* and *Aeropyrum pernix* (Selig *et al.*, 1997; van der Oost *et al.*, 1998; Sakuraba and Ohshima, 2002; Reher *et al.*, 2007).

Another line of evidence for Fd_{red}-oxidation with or without a special input module is based on the fact that the membrane-integral and membrane-associated subunits NuoBCDIHL of complex I have a common ancestor with the family of energy-converting [NiFe] hydrogenases, to which also the Ech hydrogenase belongs (Künkel *et al.*, 1998; Friedrich, 2001). This type of enzyme has been shown to accept electrons from (poly)Fd_{red} (Sauter *et al.*, 1992; Fox *et al.*, 1996; Künkel *et al.*, 1998; Silva *et al.*, 2000; Soboh *et al.*, 2002; Sapra *et al.*, 2003; Soboh *et al.*, 2004).

In 2003 Sapra et al. demonstrated that the [NiFe] membrane-bound hydrogenase (Mbh) from *Pyrococcus furiosus* was able to couple Fd_{red}-oxidation to proton translocation. This has also been shown for the Ech hydrogenase from *Ms. mazei* (Welte *et al.*, 2010b; Welte *et al.*, 2010a). In complex I the original hydrogenase [NiFe] active site was lost and a quinone binding site was acquired.

In this study it could be demonstrated, that the Fpo complex from *Ms. mazei* indeed is able to catalyze Fd_{red}-oxidation. It was attempted to generate double knock-out mutants missing Ech hydrogenase and either the whole Fpo complex or parts thereof. Generation of double knock-outs was not possible, probably due to too severe damage of energy conservation mechanisms. Therefore, an antibody against subunit FpoI from the Fpo complex of *Ms. mazei* was produced and purified. The FpoI antibody was used for enzymatic assays with membrane fractions of a *Ms. mazei* Δ*ech* mutant. Fd_{red} was supplied via the indolpyruvate:ferredoxin oxidoreductase and electrons should be transferred to the heterodisulfide, which was measured by addition of Ellman's reagent. Since the Ech hydrogenase was absent, Fd_{red}-oxidation could be catalyzed by the Fpo complex. This should be inhibited by the FpoI antibody, which would specifically bind to FpoI and thus block electron transfer. Indeed, addition of the FpoI antibody led to partial or total inhibition of Fd_{red}-oxidation, depending on the amount of antibody. Various controls validated that the FpoI antibody specifically targeted the Fpo complex. Thus, the headless Fpo complex is able to accept electrons directly from Fd_{red}. Since the FpoI antibody could completely abolish Fd_{red}-oxidation, there was no further enzyme catalyzing oxidation of Fd_{red}.

4.2.3 Energy conservation via the Fpo complex

The Fpo complex is known to translocate protons across the cytoplasmic membrane and thus is involved in generation of an electrochemical gradient used for ATP synthesis. The revelation of the structure of highly homologous respiratory complex I in 2010 and the refinement of the structure in 2011 (Efremov *et al.*, 2010; Efremov and Sazanov, 2011) greatly facilitated the development of a model of the underlying mechanisms (Welte and Deppenmeier, 2014). In this study the *E. coli* nomenclature will be used (Nuo nomenclature). The whole complex I from *Thermus thermophilus* and the membrane-integral part of the complex from *E. coli* was crystallized and the structure solved to 3.9 Å and 3.0 Å resolution (Efremov *et al.*, 2010; Efremov and Sazanov, 2011). Almost all subunits of the highly homologous Fpo complex could be modeled onto the given structure (Welte and Deppenmeier, 2014). Only FpoJ1 and FpoJ2 could not be aligned. Also there were no counterparts for FpoF and FpoO, because there are no homologs for these subunits in complex I.

It is hypothesized, that after oxidation of soluble carriers by specific input modules, the electron transport in complex I and in the Fpo complex is very similar. In complex I electrons are transferred via the tetranuclear FeS clusters N6a and N6b in subunit NuoI to the terminal cluster N2 in NuoB. The conserved residues that coordinate the [4Fe4S] clusters are also conserved in subunits FpoI and FpoB, indicating the presence of a similar electron transfer pattern.

Lipid-soluble carrier molecules serve as electron acceptors, ubiquinone in case of complex I and MP in case of the Fpo complex. The ubiquinone binding pocket has been identified in NuoABCDH. The respective residues are conserved in FpoB and FpoH, however, some of the residues have smaller side chains and residues binding the hydrophilic part of the ubiquinone molecule are partially missing. This in accordance with the fact that MP is a larger molecule than ubiquinone and needs more space for accurate binding.

It is thought that the transfer of electrons from N2 to membrane-bound carrier molecules drives conformational changes, that eventually lead to proton translocation by the membrane-bound part of the complex. Subunits FpoAHJKLMN form more than 50 transmembrane helices and are thus membrane-integral. Subunits FpoLMN can be well aligned with NuoLMN, that comprise antiporter-like half channels responsible for proton translocation and a transversal helix acting like a piston. The transversal helix was identified in FpoL and is thought to mediate conformational changes between the site of quinone/methanophenazine reduction and the half channels. As a result, protons are translocated across the cytoplasmic membrane. Another structural element is the E-channel that is probably conserved in subunits FpoABHJK. It is responsible for translocation of one proton.

As already mentioned above, different electron carrier molecules are oxidized via different input modules. Complex I oxidizes NADH via subunits NuoEFG. In methylotrophic methanogenesis the Fpo complex oxidizes $F_{420}H_2$ via FpoF. However, it was shown in this study that in *Ms. mazei* the core complex is functional without a special input module. Fd_{red} was oxidized by membranes of a *Ms. mazei* Δ*ech* mutant and the reaction could be inhibited with an antibody masking subunit FpoI. Thus, no special input module is needed for interaction with Fd. In *Mt. thermoacetophila* so far no input module has been identified. The lack of FpoF is in accordance with the fact that $F_{420}H_2$ cannot serve as electron donor for membrane fractions of *Mt. thermoacetophila* (Welte and Deppenmeier, 2011b). Thus, it seems very likely that electron transfer from Fd_{red} directly to FpoI is also possible here. This is in accordance with the fact that a comparison of FpoI from *Methanosarcina* and *Methanosaeta* spp. revealed that FpoI from *Methanosaeta* spp. contains a C-terminal extension, where lysine residues are accumulated. Lysine as basic amino acid could trigger interaction with acidic Fd (Welte and Deppenmeier, 2011b).

In addition to the nature of the electron donor, also the stoichiometry of ion translocation has to be considered. A theoretical value can be calculated for the number of protons translocated across the membrane according to Equation 8.

Equation 8: $n = 2 \quad (\Delta E/\Delta p)$

n = number of protons translocated
ΔE = redox potential difference
Δp = membrane potential (ΔpH + ΔΨ)

The redox potential difference between $F_{420}H_2$ (-360 mV) and MP (-165 mV, (Tietze *et al.*, 2003)) is 195 mV. With a Δp value of -180 mV (Deppenmeier and Müller, 2008), theoretically the translocation of 2.2 protons per two electrons is possible. This has been experimentally confirmed (Bäumer *et al.*, 2000). Using Fd_{red} as electron donor the situation is different. Fd has a redox potential of around -500 mV (Thauer *et al.*, 2008). With MP as electron acceptor ($\Delta E^{0\prime}$ = –165 mV, (Tietze *et al.*, 2003)) the redox potential difference is 335 mV. Theoretically, this would allow translocation of 3.7 protons. Therefore, translocation of three protons per two electrons donated by Fd_{red} seems feasible.

Complex I contains enough coupling sites to translocate four protons upon oxidation of NADH (NADH -320 mV, ubiquinone +108 mV). The situation should be similar in the highly homologous Fpo complex. But besides the thermodynamic restrictions, in *Methanosarcina* spp. the transmembrane helix TM12 of subunit FpoL contains an insertion, which might render it dysfunctional. In *Methanosaeta* spp. no such insertion occurs and thus there might be an additional coupling site in comparison to *Methanosarcina* spp. (Welte and Deppenmeier, 2014).

It seems feasible, that the headless Fpo complex from *Methanosaeta* spp. accepts electrons from reduced Fd and concomitantly translocates three protons across the cytoplasmic membrane (Welte and Deppenmeier, 2014). In *Mt. thermoacetophila* the acetate activation reaction consumes two ATP equivalents (3.1.2 and 3.1.3). Under the assumption that the ATP synthase needs three ions to synthesize one ATP molecule at least seven ions per acetate molecule have to be translocated, in order to sustain cells of *Mt. thermoacetophila*. If ion translocation in *Mt. thermoacetophila* worked with the same stoichiometry as ion translocation in *Ms. mazei,* breakdown of one acetate molecule would result in translocation of six ions across the cytoplasmic membrane. This would result in no ATP net gain. But with Fd_{red} as electron donor and the translocation of three protons by the Fpo complex there would be a net gain of one proton per acetate molecule. This is the threshold that is needed to sustain life and a possible explanation how *Mt. thermoacetophila* makes a living.

4.3 *Mm. luminyensis* – a methanogen from the human gut

Methanogenic archaea are a normal part of the microbial flora, which resides in the intestinal tract of humans. *Methanobrevibacter* (*Mb.) smithii* is highly abundant and also

Methanosphaera (*Mp.*) *stadtmanae* can be frequently encountered (Miller and Wolin, 1982; Miller *et al.*, 1982; Dridi *et al.*, 2009). The impact of methanogenic archaea for human health is still a matter of debate. Yet, recently it was proposed that methanogenic archaea consuming TMA in the gut might relieve the symptoms of trimethylaminuria (TMAU, "fish-odor-syndrome", (Brugère *et al.*, 2014)). In any case the removal of H_2 produced by fermentative bacteria is important for the procedure of fermentative processes. Methanogenic archaea consuming H_2+CO_2 or H_2 and methylated compounds are thus a crucial part of microbial food chains in the gut.

Mm. luminyensis, which was part of this study belongs to a newly identified order of methanogens, that is related to the Thermoplasmatales and is referred to as Methanomassiliicoccales (Iino *et al.*, 2013). Members of the new order were shown to thrive with H_2 and methylated compounds and thus use a rather unusual combination of substrates. The characteristics of methanogenic archaea in the human gut and cultivation as well as energy metabolism of *Mm. luminyensis* will be discussed in the next chapters.

4.3.1 Methanogens and the human intestinal tract

While most parts of the human body are sterile others are densely colonized by microorganisms. Most microorganisms are harbored by the skin, the oral cavity and the intestine. Up to 100 trillion (10^{14}) microbes live in the human intestinal tract (Ley *et al.*, 2006), which is estimated to exceed the number of somatic and germ cells of the human body by 10-fold (Turnbaugh *et al.*, 2007). The colon is considered to be the most densely colonized habitat on Earth (Whitman *et al.*, 1998). The collective genomes of microbes in the intestine (microbiome) are thought to contain at least a 100 times more genes than the human genome does. Genes encoding enzymes involved in metabolism of amino acids, xenobiotics and biosynthesis of vitamins and isoprenoids are present. Therefore, humans can be seen as supraorganisms, whose metabolism is a synthesis of microbial and human characteristics (Gill *et al.*, 2006).

The majority of microorganisms in the intestinal tract are bacterial species. The phyla Firmicutes and Bacteroidetes are highly abundant. It was proposed that their representatives cluster in three enterotypes that are dominated either by species of *Bacteroides* (enterotype 1), *Prevotella* (enterotype 2) or *Ruminococcus* (enterotype 3, (Arumugam *et al.*, 2011)). Enterotype 1 has great saccharolytic potential and probably derives energy mainly from fermentation of carbohydrates and proteins. Enterotype 2 and 3 are dominated by mucin degraders (Arumugam *et al.*, 2011). Interestingly, for the establishment of an enterotype, parameters such as nationality, gender, age or body mass index seem to play a less important role than the long-term diet (Wu *et al.*, 2011).

A limited number of archaeal species has been identified with PCR and culture-dependent

methods. Members of the Halobacteriales could be identified but it is not yet clear whether they are transient or persistent inhabitants. A possible source of transient Halobacteriales are table salts and sea food (Gaci *et al.*, 2014).

Methanogenic archaea are frequently encountered, thus the predominant archaeal genus in the human gut is *Methanobrevibacter,* with the most prominent member *Mb. Smithii* (Miller and Wolin, 1982; Miller *et al.*, 1982). It belongs to the Methanobacteriales and hence consumes H_2+CO_2 as substrates for methanogenesis. The other important methanogen from the human intestine, *Mp.* s*tadtmanae,* likewise belongs to the order of Methanobacteriales. Surprisingly, *Mp. stadtmanae* requires methanol and H_2 as substrates for growth and depends on acetate as carbon source (Fricke *et al.*, 2006). To test the occurrence of methanogenic archaea in the intestinal tract, a breath test detecting methane gas can be performed. With this test exhalation of methane can be confirmed for approximately 40 % of individuals (Levitt *et al.*, 2006; Stewart *et al.*, 2006). However, the sensitivity of the test seems to be too low: In a PCR-based approach *Mb. smithii* and *Mp. stadtmanae* were detected in 95.7% and 29.4% of specimens, respectively (Dridi *et al.*, 2009).

Recently, a deep-branching lineage of Archaea distantly related to the Thermoplasmatales has been identified by analyses of 16S rRNA genes (Mihajlovski *et al.*, 2008; Mihajlovski *et al.*, 2010; Paul *et al.*, 2012). Sequences could be derived from environmental habitats like coastal marine environments (DeLong, 1992), marine plankton (Fuhrman *et al.*, 1992), rice field soil (Grosskopf *et al.*, 1998) and the sediment of fresh water lakes (Nüsslein *et al.*, 2001), but importantly also from the intestinal tract of various animals like termites (Shinzato *et al.*, 1999; Friedrich *et al.*, 2001), cockroaches (Hara *et al.*, 2002) and scarab beetle larvae (Egert *et al.*, 2003). In mammals the respective sequences were identified in cattle (Tajima *et al.*, 2001; Denman *et al.*, 2007; Wright *et al.*, 2007; Janssen and Kirs, 2008), sheep (Wright *et al.*, 2004), wallabies (Evans *et al.*, 2009) and in the subgingival pocket of humans (Li *et al.*, 2009).

Since these deep-routing archaeal phylotypes were detected by PCR-based assays, their nature remained unclear. Yet, based on the presence of *mcrA* gene sequences, which is a molecular marker for methanogenic archaea, it was hypothesized that they might be methanogens. Novel *mcrA* gene sequences were detected that formed a deep-routing cluster (Lueders *et al.*, 2001; Luton *et al.*, 2002). Interestingly, this novel cluster was distinct from *mcrA* gene sequences of the established orders of methanogens (Lueders *et al.*, 2001). Mihajlovski and colleagues (Mihajlovski *et al.*, 2008) obtained the respective *mcrA* and 16S rRNA gene sequences from human stool samples and hypothesized that they were derived from the same methanogenic organism. A putative new order of methanogens was postulated (Mihajlovski *et al.*, 2008). The presence of the novel *mcrA* gene sequence in the human gut was confirmed by Scanlan *et al.* (Scanlan *et al.*, 2008). In a later study a

comprehensive analysis of available *mcrA* and 16S rRNA gene sequences was performed and strongly supported the existence of a seventh order of methanogens (Paul *et al.*, 2012). Therefore, there was convincing evidence that methanogens in the human intestinal tract are not restricted to *Mb. smithii* and *Mp. stadtmanae.* but that the diversity is further increased by species of a new Thermoplasmatales-related lineage.

Final proof was given by the isolation of a methanogenic archaeon from a human stool sample (Dridi *et al.*, 2012). According to its 16S rRNA gene sequence the organism was part of the above-mentioned Thermoplasmatales-related lineage and produced methane using H_2 and methanol as substrates. Based on the phylogenetic data it was placed in the new genus *Methanomassiliicoccus.* Since it was isolated in Luminy, Marseille, France the full species name is *Methanomassiliicoccus* (*Mm.*) *luminyensis* B10 (Dridi *et al.*, 2012). With the enrichment of "*Candidatus* Methanogranum caenicola" from waste treatment sludge, the first methanogenic archaeon of the new lineage was placed in a new order, which was termed Methanomassiliicoccales (Iino *et al.*, 2013).

Several other methanogens belonging to the new order have been enriched from human feces. "*Candidatus* Methanomassiliicoccus intestinalis" was obtained using methanol and H_2 as substrates (Borrel *et al.*, 2013). The 16S rRNA gene sequence was 98 % identical with the sequence of *Mm. luminyensis*. However, the *Methanomassiliicoccus* clade is phylogenetically related to sequences from non-digestive environments, including representatives of the Rice Cluster III (Kemnitz *et al.*, 2005; Borrel *et al.*, 2013). Therefore, probably not all representatives of this clade are adapted to the conditions of the intestinal tract. Using the same isolation procedure as for "*Candidatus* Methanomassiliicoccus intestinalis" "*Candidatus* Methanomethylophilus alvus" was obtained from the human gut. It is distantly related to *Mm. luminyensis* with 87 % 16S rRNA gene sequence identity (Borrel *et al.*, 2012b). Yet, 16S rRNA gene sequences of uncultured archaea with more than 97% identity to "*Candidatus* Methanomethylophilus alvus" have been retrieved from various animals and form a part of the previously described rumen cluster C (Janssen and Kirs, 2008). Therefore, there might be numerous representatives of these archaea, which are specifically associated to gut environments.

Altogether, methanogenic archaea in the human gut seem to be much more diverse and their abundance is much greater than previously thought. This reflects their substantial role in the microbial food chain. Together with sulfate reducing bacteria and acetogenic bacteria they are responsible for removal of H_2 from the gut. Due to the large number of fermenting bacteria, H_2 is constantly produced and has to be removed in order to prevent inhibition of fermentative metabolism. Hydrogenotrophic methanogenesis is a feature typical of the Methanobacteriales, to which *Mb. smithii* belongs. Another member of the Methanobacteriales, which is also present in the human intestinal tract, is *Mp. stadtmanae*. In

contrast to *Mb. smithii* this methanogen consumes H_2 and methanol and thus was considered an exception (Fricke *et al.*, 2006). Few other organisms growing with H_2 and methylated compounds have been described. Among them are two other members of the Methanobacteriales, *Methanobacterium lacus* isolated from lake sediment (Borrel *et al.*, 2012a) and *Methanobacterium veterum* isolated from Siberian permafrost (Krivushin *et al.*, 2010). A methanogenic archaeon that belongs to the order Methanosarcinales and uses the respective substrates is *Methanomicrococcus* (*Mi.*) *blatticola* (Sprenger *et al.*, 2000). It was isolated from the hindgut wall of the cockroach *Periplaneta americana* and in the presence of H_2 methanol, MMA, DMA and TMA could be used as substrates for methanogenesis. It was postulated that *Mi. blatticola* is not capable of oxidation of methyl groups and therefore strictly depends on H_2 as electron donor (Sprenger *et al.*, 2005). A similar substrate spectrum was observed for members of the Methanomassiliicoccales. All isolates or enrichment cultures obtained so far were cultivated with H_2 and methanol as substrates. No growth could be observed using H_2+CO_2 or only methanol (Dridi *et al.*, 2012). Additionally, *Mm. luminyensis* was cultivated using H_2+TMA (Brugère *et al.*, 2014). Hence, methanogenic archaea from different orders were isolated from a digestive environment and were shown to use H_2 as electron donor and methylated compounds as electron acceptors. Therefore, this metabolic strategy might be an adaptation to the conditions of the intestinal tract. Yet, in case of the *Methanomassiliicoccus* clade sequencing of environmental samples revealed that numerous representatives, which probably likewise consume H_2 and methylated compounds, are present in many environmental sites (Borrel *et al.*, 2013). Thus, the current predominance of species from this clade isolated from the human gut is probably due to a sampling bias. Still, since methanogenesis from H_2 and methylated compounds seems to play a paramount role in the intestinal tract of humans and other animals it can be concluded, that this environment selects methanogens with this metabolic strategy.

At present it is rather unclear, how or to what extent methanogenic archaea influence the condition of their human host. Contradictory results have been obtained for several diseases. It has been speculated that methanogens may be associated with colorectal cancer since in the majority of colorectal cancer patients methane can be detected in their breath (Haines *et al.*, 1977) and the severity of the disease correlates with methane production (Piqué *et al.*, 1984). This correlation could not be confirmed in a study with 1016 individuals from rural to urban sites in South Africa (Segal *et al.*, 1988). Furthermore, methanogens could be affiliated with obesity. In a mouse model system the simultaneous presence of *Bacteroides thetaiotaomicron* and *Mb. smithii* led to significantly increased production of short chain fatty acids, which are resorbed by the host and lead to lipogenesis and body weight gain (Samuel *et al.*, 2008). In contrast, it was reported that cell numbers of *Mb. smithii* are decreased in obese patients (Million *et al.*, 2012; Million *et al.*, 2013). Finally, the presence of methanogens was studied in patients suffering from inflammatory bowel disease (IBD), which

is a general term for inflammatory processes in colon and small intestine. The two principal types of IBD are Crohn's disease and Ulcerative Colitis. It could be observed in several studies that according to breath test and PCR-based methods, the presence of methanogens in the gut was significantly reduced in patients suffering from either Crohn's disease or Ulcerative Colitis in comparison to a healthy control group (Mckay *et al.*, 1985; Pimentel *et al.*, 2003; Scanlan *et al.*, 2008). However, this might be due to accelerated gut passage under diarrheal conditions and subsequent loss of slowly growing methanogens (Scanlan *et al.*, 2008).

Recently, it was proposed that methanogenic archaea consuming TMA in the gut might be beneficial for their host (Brugère *et al.*, 2014). TMA is produced from dietary ingredients like choline by gut bacteria. It has an intense fishy smell, which is perceived as very unpleasant even in small doses. Normally, TMA produced in the gut is taken up into the bloodstream and converted to the oderless TMAO in the liver. The reaction is catalyzed by a flavin-containing monooxygenase 3. The function of this enzyme can be impaired either due to genetic defects or due to dietary or hormonal factors leading to so-called fish-odor-syndrome or trimethylaminuria (TMAU (D'Angelo *et al.*, 2013)). In these cases patients excrete TMA with their breath, sweat and urine, which puts them under considerable psychological stress. Their condition can be temporary but only in case of non-hereditary TMAU. However, even if the monooxygenase 3 is working normally, also enhanced levels of TMAO should be prevented. Studies with patients suffering from cardiovascular disease and with mice revealed, that TMAO triggers arteriosclerosis (Wang *et al.*, 2011b; Tang *et al.*, 2013). Therefore, depletion of TMA in the gut e.g. by *Mm. luminyensis* could help to reduce levels of TMAO in the bloodstream and/or levels of TMA in breath, sweat and urine and thus improve health and well-being in humans (“archaebiotics”, (Brugère *et al.*, 2014)).

4.3.2 Cultivation of *Mm. luminyensis*

Several representatives from the new order Methanomassiliicoccales have been enriched. One isolate, which was named *Mm. luminyensis*, is available in pure culture. The isolate was obtained using *Methanobrevibacter* medium (Dridi *et al.*, 2012), containing KH_2PO_4, $MgSO_4$, NH_4Cl, $CaCl_2$ and a relatively high amount of NaCl (0.5 % [w/v]). Complex components are yeast extract and tryptone. Acetate is added, which can be used as a biosynthetic precursor being converted to acetyl-CoA and further to the universal precursor molecule pyruvate. Trace element solution SL10 is added as well as cysteine as a reductant. Since the trace elements tungstate or selenite seem to be required (Dridi *et al.*, 2012), but are not contained in SL10 these are supplemented separately. Prior to autoclaving the pH is adjusted to 7.5 and the medium is boiled under N_2 and additionally sparged with N_2+CO_2 (80:20) to remove oxygen. Resazurin is used as redox indicator, which turns pink upon contamination with

oxygen. Upon inoculation $NaHCO_3$ is added as buffer, Na_2S as reductant and finally formate and vitamin solution are supplied. 40 mM methanol and H_2+CO_2 (80:20) at 1 bar are used as substrates. After inoculation with 10 % [v/v] fecal specimen of an 86-year old healthy man and incubation at 37 °C with shaking *Mm. luminyensis* could be obtained.

In this study the same medium was used to cultivate *Mm. luminyensis*, which was purchased from the DSMZ. *Mm. luminyensis* initially thrived in the medium but after several passages the final OD of cultures decreased, until no more growth could be observed (Figure 40). Cultivation in DSMZ medium 120, which also contains various salts, vitamins, trace elements and complex components and is routinely used for cultivation of *Ms. mazei* retrieved the same result. It was speculated, that an essential compound was not supplied in these media, which became diluted by passing of the original DSMZ culture and finally was concentrated too low to support growth of *Mm. luminyensis*.

Figure 40: Decrease in final OD_{600} in cultures of *Mm. luminyesis*. Growth medium was not supplemented with sludge fluid, which led to significantly reduced cell density after several passages.

Methanogenic archaea employ several unusual cofactors, one of which is 2-mercaptoethanesulfonate, also termed HS-CoM. In 1974 a *Methanobacterium ruminantium* strain was demonstrated to depend on external HS-CoM supply (Taylor *et al.*, 1974). In another study the minimum requirement of *Methanobacterium ruminantium* for HS-CoM was measured. The minimum threshold that could sustain growth in cultures of *Methanobacterium ruminantium* was 5 nM HS-CoM (Balch and Wolfe, 1976). Yet, in the

majority of methanogenic archaea HS-CoM is synthesized *de novo*. Two different biosynthetic pathways exist, which both consist of five steps (Graham *et al.*, 2009). In the first pathway L-phosphoserine is converted via dehydroalanine, L-cysteate, sulfopyruvate and sulfoacetaldehyde to HS-CoM. The other pathway starts from phosphoenolpyruvate and proceeds via phosphosulfolactate, sulfolactate, sulfopyruvate and sulfoacetaldehyde to HS-CoM. It could be shown that *comABCDE* genes are associated with HS-CoM biosynthesis. While *comDE* are present in all methanogenic archaea that synthesize HS-CoM, *comABC* participate in the second biosynthetic pathway and cannot be found in Methanomicrobiales, Methanocellales and Methanosarcinales. In these orders cysteate synthase and aspartate aminotransferase are used as functional replacements. The enzyme catalyzing reductive thiolation of sulfoacetaldehyde to yield HS-CoM is unknown for both pathways. The genes encoding ComDE and a cysteate synthase as well as an aspartate aminotransferase are present in *Mm. luminyensis* (Borrel *et al.*, 2014). Therefore, *Mm. luminyensis* most probably uses the same pathway of HS-CoM biogenesis like members of the Methanomicrobiales, Methanocellales and Methanosarcinales. Nevertheless, in this study it was tested whether the addition of HS-CoM was effective in restoring growth of *Mm. luminyensis* cultures. The growth medium was supplemented with 0.1 % HS-CoM, yet, no stimulatory effect could be observed.

Therefore, it was attempted to cultivate *Mm. luminyensis* in DSMZ medium 119, which is recommended for cultivation of the organism. In comparison to *Methanobrevibacter* medium it contains essentially the same salts (KH_2PO_4, $MgSO_4$, NH_4Cl, $CaCl_2$) albeit the amount of NaCl is significantly reduced (0.04 % [w/v]) and extra $FeSO_4$ is added. Trace element solution SL10, complex and organic compounds as well as vitamin solution, reductants, resazurin and the carbonate buffer are added as is described for *Methanobrevibacter* medium, except for tryptone, which is omitted. In contrast to *Methanobrevibacter* medium DSMZ medium 119 does not contain extra tungstate/selenite and other important differences are the addition of the so-called sludge fluid and a fatty acid mixture. The fatty acid mixture contains valeric acid, isovaleric acid, 2-methylbutyric acid and isobutyric acid (pH 7.5 with NaOH). To investigate the effect of the single components *Mm. luminyensis* was cultivated in DSMZ medium 119, prepared in three different ways: DSMZ medium 119 without sludge fluid, without fatty acids and without tungstate/selenite; DSMZ medium 119 without sludge fluid, without tungstate/selenite but with fatty acids and DSMZ medium 119 without sludge fluid, without fatty acids but with extra tungstate/selenite solution. For all conditions 75 mM methanol and H_2 were used as substrates. None of the different media was suitable for long-term cultivation of *Mm. luminyensis*.

Therefore, DSMZ medium 119 was prepared without fatty acids and without tungstate and selenite but with sludge fluid. In the original recipe sludge fluid is prepared by the addition of

0.4 % yeast extract to sludge from an anaerobic digester. After 24 h incubation at 37 °C, the sludge is centrifuged at 13000 g. The supernatant is called sludge fluid and after autoclaving under N_2, it can be stored at room temperature in the dark. In the course of this study, sludge fluid was prepared from sludge of a mesophilic biogas plant, which was stored for some days to several weeks at 4 °C. The incubation step prior to centrifugation was excluded since no benefit like a significantly increased density of methanogens can be expected from that.

The modified medium 119 containing 5 % [v/v] sludge fluid finally provided suitable conditions for long-term cultivation of *Mm. luminyensis.* Therefore, it was concluded that the sludge fluid contained a component, which is essential for growth of the organism, but cannot be synthesized *de novo*. This was confirmed by the fact that upon the addition of sludge fluid, *Mm. luminyensis* could also be cultivated in *Methanobrevibacter* medium, which was then routinely used. The successful isolation of *Mm. luminyensis* using *Methanobrevibacter* medium without sludge fluid might be due to the fact that 10 % [v/v] fecal specimen were used as inoculum.

However, as is shown in 3.3.2 also the addition of 5 % [v/v] sludge fluid supported exponential growth of cultures of *Mm. luminyensis* only during the first 72 h of incubation. After this period the growth rate was significantly decreased, although cultures had not yet reached the stationary phase. It was concluded, that the concentration of the growth factor(s) supplied by the addition of sludge fluid by then fell below the threshold, that could sustain exponential growth. To evaluate whether the missing compound could be a cofactor specific for methanogens, extract from a culture of *Ms. mazei* was produced and added in addition to the sludge fluid. Yet, no difference could be observed between the two conditions and thus the missing compound is no methanogenic cofactor.

The cultivation conditions might be improved, if more than 5 % [v/v] sludge fluid were added to the medium. Unfortunately, due to the presence of humic acids, sludge fluid has a dark brown color and high amounts impair the measurement of OD_{600}. Furthermore, for the production of sludge fluid considerable amounts of biogas sludge are needed and since the whole procedure is rather time-consuming, identification of the unknown factor would considerably simplify cultivation of *Mm. luminyensis*. Without addition of sludge fluid, growth of the organism was still possible for some passages. Hence, the unknown factor might be a trace element or an organic compound acting like a vitamin. According to Dridi *et al.* (Dridi *et al.*, 2012) *Mm. luminyensis* requires tungstate and selenite, which are not supplied by trace element solution SL10. However, medium containing 5 % [v/v] sludge fluid will contain more than sufficient amounts of every possible trace element. Yet, to avoid any risk of limited supply, the medium routinely used for cultivation of *Mm. luminyensis* was supplied with tungstate and selenite in addition to the sludge fluid. Therefore, a shortage in trace elements is highly unlikely. Thus, the identification of the unknown compound stimulating growth of

Mm. luminyensis probably requires a systematic scan of small organic molecules, which are contained in sludge fluid.

Despite the fact, that cultivation conditions of *Mm. luminyensis* can still be further improved, it could be demonstrated in the course of this study, that not only methanol and TMA (Dridi *et al.*, 2012; Brugère *et al.*, 2014) can be used as substrates, but also DMA and MMA. Bioinformatic analyses revealed the presence of permeases facilitating substrate uptake, substrate-specific methyltransferases and a pyrrolysine biosynthesis machinery (3.3.1). This already indicated the ability of the organism to use the respective substrates for growth. Accordingly, *Mm. luminyensis* could be cultivated with H_2 and 75 mM MMA or 37.5 mM DMA.

Despite the fact that the genome sequence of *Mm. luminyensis* is not yet properly assembled, clusters of methyltransferases could be inferred from annotated sequences (Figure 30). The corresponding genes potentially form operons, as is also the case in *Ms. acetivorans* and *Ms. mazei* (Pritchett and Metcalf, 2005; Bose *et al.*, 2006; Krätzer *et al.*, 2009). In *Ms. acetivorans* three operons containing methanol-specific methyltransferases have been identified. Studies with deletion mutants revealed that each operon is required for growth with methanol. Thus, each operon has a distinct role in methanol metabolism (Pritchett and Metcalf, 2005). In contrast, in *Ms. mazei* two operons containing TMA and DMA-specific methyltransferases exist (Krätzer *et al.*, 2009). It could be demonstrated, that the operon, which additionally contains a TMA permease is preferentially transcribed, if TMA is used as substrate. Additionally, an operon comprising DMA-specific methyl transferase and a DMA permease is encoded. If DMA is used as substrate, this operon is highly transcribed. Finally, there are two operons, which contain MMA-specific methyltransferases. One additionally contains a permease and similar to what was observed for TMA and DMA, during growth with MMA, the permease-containing operon is most intensely transcribed (Krätzer *et al.*, 2009). In *Mm. luminyensis*, multiple copies of MMA- and methanol-specific methyltransferases have been identified. They might be differentially transcribed, e.g. according to the concentration of substrates. However, only one copy of TMA- and DMA-specific methyltransferases is present, which cluster together with yet another copy of MMA-specific methyltransferases. Additionally, a TMA permease is part of the cluster. Hence it is feasible, that if TMA is used as a substrate, the degradation products DMA and MMA are not accumulated in the medium. Instead, they might be retained inside cells of *Mm. luminyensis* and stepwise demethylated. Thus, in this respect *Mm. luminyensis* might be different from *Ms. mazei*, where TMA degradation products are excreted and can be found in the medium (Krätzer *et al.*, 2009).

The evolutionary ancestry of the methyltransferase genes from *Mm. luminyensis* was the subject of a study performed by Borrel *et al.* (Borrel *et al.*, 2013). It has been proposed that the *mtaABC* gene cluster in *Mp. stadtmanae* was acquired from the Methanosarcinales by

lateral gene transfer (Fricke *et al.*, 2006). However, the Methanomassiliicoccales, to which also *Mm. luminyensis* belongs, comprise quite distantly related species and are probably also present at numerous environmental sites. It is a matter of debate whether methanogenesis from H_2 and methylated compounds represents an adaptation to the gut or if it is present in the whole lineage. Gene sequences encoding methanol-specific methyltransferases could be retrieved from *Mm. luminyensis,* from "*Candidatus* Methanomethylophilus alvus" and also from environmental sites. They cluster in a group, which is distinct from the sequences from other methyl group converting methanogens. Therefore, and because also environmental samples could be obtained, it was postulated that already the ancestor of the whole Methanomassiliicoccus lineage could use H_2 and methylated substrates for methanogenesis (Borrel *et al.*, 2013)

4.3.3 A tentative model of energy conservation mechanisms in *Mm. luminyensis*

The methanogenic archaeon *Mm. luminyensis* uses H_2 and methylated compounds like methanol and methylated amines as substrates for methanogenesis. This combination of substrates is rather unusual. Most methanogens thrive with H_2+CO_2, which are the substrates with the highest change in free energy under standard conditions ($\Delta G^{0'}$ = –130 kJ mol^{-1} CH_4, (Deppenmeier, 2002b). Members of the Methanosarcinales are able to use methylated compounds or acetate as sole substrates for methanogenesis. Biochemically, there are important differences between the obligate hydrogenotrophic methanogens and the more versatile members of the Methanosarcinales. Methanosarcinales, which are the evolutionary youngest lineage of methanogens, contain membrane-bound cytochromes. These cannot be found in obligate hydrogenotrophic methanogens (Thauer *et al.*, 2008). The presence of cytochromes and the membrane-integral electron carrier molecule methanophenazine (MP) enables membrane-bound electron transport processes (Welte and Deppenmeier, 2014). These allow efficient conservation of energy available from methanogenic substrates. This is also reflected in growth yields: for members of the Methanosarcinales growing with H_2+CO_2 yields of 6.4 -7.2 g per mol of methane have been reported. In contrast, in the obligate hydrogenotrophic methanogens without cytochromes the growth yield ranges from 1.3 to 3 g per mole of methane (Thauer *et al.*, 2008). The only ion-translocating enzyme in obligate hydrogenotrophic methanogens is the membrane-bound H_4MPT:HS-CoM methyltransferase (Mtr) that translocates 2 mol of Na^+ per 1 mol of CH_4. The Mtr is not encoded in the genome of *Mm. luminyensis* and thus certainly is not involved in energy conservation. Therefore, the question of proton translocation processes in *Mm. luminyensis* arises and was addressed in the course of this study.

In *Mm. luminyensis* methyltransferases catalyzing transfer of methyl groups from methanol, TMA, DMA and MMA to HS-CoM have been identified by blast search analyses. Methyl-CoM

derived from methylated compounds and HS-CoB serve as substrates for the methyl-CoM reductase, which forms methane and CoM-S-S-CoB. Bioinformatic analyses furthermore revealed, that genes encoding enzymes involved in CO_2 reduction/methyl group oxidation (formyl-MF dehydrogenase, Eha or Ehb, formylmethanofuran-H_4MPT formyltransferase, methenyl-H_4MPT cyclohydrolase, methylene-H_4MPT dehydrogenase and reductase, F_{420}-reducing hydrogenase) are not present. Similar results have been obtained for "*Candidatus* Methanomethylophilus alvus", another representative of the Methanomassiliicoccales with a similar substrate spectrum (Borrel *et al.*, 2012b). Hence, in *Mm. luminyensis* clearly methyl groups serve as electron acceptor.

Bioinformatic analyses indicated that *Mm. luminyensis* possesses a soluble heterodisulfide reductase in complex with the Mvh hydrogenase (HdrABC/MvhADG). In obligate hydrogenotrophic methanogens, this enzyme complex oxidizes H_2 and reduces Fd and the heterodisulfide CoM-S-S-CoB. Since one mol of Fd is reduced per mole CoM-S-S-CoB an electron bifurcation mechanism was proposed (Kaster *et al.*, 2011). In electron bifurcation, electrons are concomitantly used for an exergonic and an endergonic reaction, whereas the exergonic reaction drives the endergonic one. Electron bifurcation was first discovered for the butyryl-CoA dehydrogenase/Etf complex from *Clostridium kluyveri* (Li *et al.*, 2008). Later, it was demonstrated in methanogenic archaea by purification and characterization of the HdrABC/MvhADG from *Methanothermobacter marburgensis* (Kaster *et al.*, 2011). Thus, the enzyme complex employs the exergonic reduction of the heterodisulfide to generate Fd_{red}.

In the course of this study HdrABC/MvhADG activity was measured in the cytoplasmic fraction of *Mm. luminyensis*. Photometric assays were performed, which contained Fd naturally occuring in the cytoplasmic fraction, the heterodisulfide, which was supplied in non-limiting amounts and the artificial electron donor reduced benzylviologen. The heterodisulfide was reduced with 2500 mU mg^{-1}, which indicated the presence of a functional HdrABC/MvhADG complex. In another assay the natural electron donor H_2 was added and Fd reduction was measured via the ferredoxin:$NADP^+$ reductase (3.3.3). The activity was low but measurable and thus, functionality of the HdrABC/MvhADG in the cytoplasm of *Mm. luminyensis* could be demonstrated.

Since electrons cannot be used for CO_2 reduction, Fd_{red} has to be otherwise re-oxidized. Genes encoding a putative membrane-bound Ech hydrogenase could be identified in *Mm. luminyensis*. Interestingly, the genome harbors two copies of Ech hydrogenase genes. The Ech hydrogenase belongs to the energy-conserving hydrogenases and catalyzes the reversible transfer of electrons from Fd_{red} to protons. Concomitantly, protons are translocated across the cytoplasmic membrane, generating an electrochemical membrane potential. The Ech hydrogenase is also present in *Ms. mazei*, oxidizing Fd_{red} which is produced during methylotrophic and aceticlastic methanogenesis. A *Ms. mazei* Δ*ech* mutant was unable to

grow with acetate and had severe growth deficiencies, when TMA was used as a substrate (Welte *et al.*, 2010b). Thus, the Ech hydrogenase had an important role for energy conservation and obviously significantly contributed to the electrochemical membrane potential, which is used for ATP synthesis. It is conceivable that it plays a comparable role in *Mm. luminyensis*. In the course of this study, Fd_{red}-dependent H_2 production was measured with membrane fractions of *Mm. luminyensis*. H_2 was produced at a rate of 80 nmol min^{-1} mg^{-1}, which is more than was determined in vesicle preparations of *Ms. mazei (*32.8 nmol min^{-1} mg^{-1} (Welte *et al.*, 2010a)). It can be concluded that an active Ech hydrogenase is present in membranes of *Mm. luminyensis*, that transfers electrons from Fd_{red} to protons and probably significantly contributes to the generation of an electrochemical membrane potential used for ATP synthesis.

Yet, in the genome of *Mm. luminyensis* also genes encoding the Fpo complex ($F_{420}H_2$ dehydrogenase), have been identified. No homolog of the $F_{420}H_2$-oxidizing subunit FpoF was detected. The presence of the Fpo complex in *Mm. luminyensis* was surprising since until then it has been detected only in members of the Methanosarcinales. It was even more surprising because the HdrABC/MvhADG complex is considered as a typical feature of obligate hydrogenotrophic methanogens. Thus, *Mm. luminyensis* possesses an unusual combination of enzymes possibly involved in energy conservation. However, at present it is not clear, whether the Fpo complex contributes to the generation of an electrochemical membrane potential. It could be shown in the course of this study that the Fpo complex from *Ms. mazei* accepts electrons from Fd_{red}. It is conceivable that the Fpo complex from *Mm. luminyensis* catalyzes a similar reaction using Fd_{red} generated by HdrABC/MvhADG. Yet, the nature of the electron acceptor in this reaction is rather ambiguous.

In *Ms. mazei* electrons are transferred to the membrane-integral electron carrier MP. MPH_2 is oxidized by the heme *b* containing subunit HdrE of the membrane-bound heterodisulfide reductase (HdrDE) (Abken *et al.*, 1998; Murakami *et al.*, 2001). Subunit HdrE is not encoded in the genome of *Mm. luminyensis* and therefore this kind of electron transfer reaction is not possible. However, subunit HdrD, which combines the sequences of HdrB and HdrC and represents the catalytic subunit of the membrane-bound Hdr enzyme, could be identified in *Mm. luminyensis*. Very recently, it has been proposed that HdrD interacts with the Fpo complex to form a Fd:heterodisulfide oxidoreductase (Lang *et al.*, 2014).

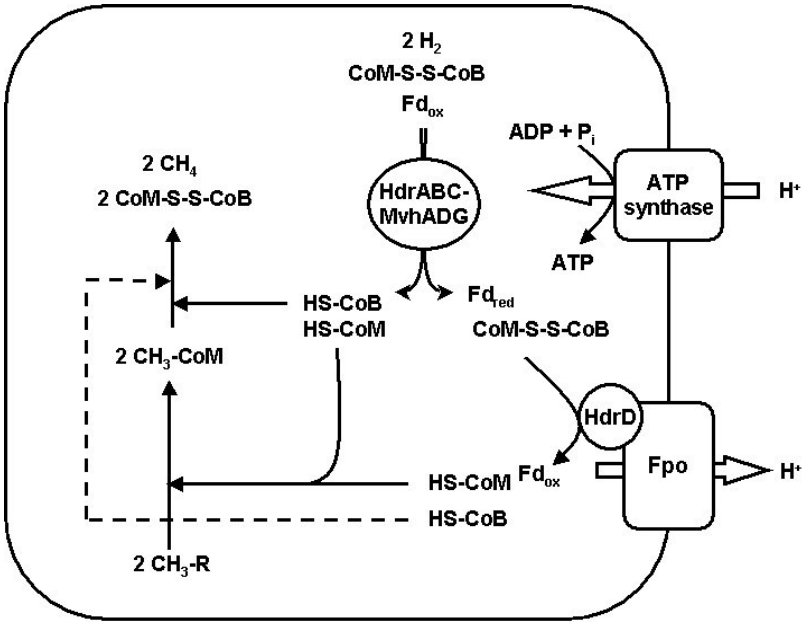

Figure 41: Model of energy conservation in *Mm. luminyensis* as proposed by Lang *et al.,* 2014. CoM-S-S-CoB: heterodisulfide; HdrABC/MvhADG: soluble heterodisulfide reductase with Mvh hydrogenase; HdrD: subunit D of the membrane-bound heterodisulfide reductase.

According to the model (Figure 41), electrons would be derived from H_2 and transferred to Fd and CoM-S-S-CoB by HdrABC/MvhADG. This yields the reduced cofactors HS-CoM and HS-CoB and, furthermore, Fd_{red}. Fd_{red} could be oxidized by the Fpo complex and electrons could be transferred to a second molecule of CoM-S-S-CoB. In the course of Fd_{red}-oxidation, protons could be translocated by the Fpo complex to build an electrochemical ion gradient across the cytoplasmic membrane. HS-CoM could be used as acceptor molecule for methyl groups and HS-CoB would be used for reduction. Thus, in one cycle, two moles of H_2 would be used for reduction of two moles of CoM-S-S-CoB. Accordingly, two moles of methyl groups would be reduced. The integration of the Fpo complex via Fd_{red} could account for the formation of an electrochemical ion gradient used for ATP synthesis. However, biochemical evidence is needed to support this hypothesis.

In the course of this study it was tested, whether membrane fractions of *Mm. luminyensis* could catalyze reduction of CoM-S-S-CoB with the artificial electron donor benzyl viologen. Yet, no heterodisulfide reductase activity was measured. Therefore, the Ech hydrogenase rather than the Fpo complex is the principal enzyme catalyzing Fd_{red}-oxidation and proton translocation in *Mm. luminyensis*.

All in all, in this study energy conservation mechanisms in three different methanogenic archaea have been investigated. Since methanogenic substrates yield a low change in free energy, methanogenic archaea had to develop efficient energy conservation systems. Yet, for

the obligate aceticlastic *Mt. thermoacetophila* until recently it could not be explained how an ATP net gain is achieved. In *Mt. thermoacetophila* acetate has to be activated at the expense of ATP. It could be shown here, that the reaction is catalyzed by an AMP-forming ACS enzyme. PP_i built in the course of the reaction is hydrolyzed by a soluble PPase. Thus, two ATP equivalents are consumed per acetate molecule. Based on the assumption that the ATP synthase works with a stoichiometry of three ions per one ATP, at least seven ions have to be translocated by the enzymes of the respiratory chain. Hence, the ATP expense for acetate activation would be compensated and the net gain would be one proton. This is the minimum threshold that is needed to sustain cell proliferation.

In the genome of *Mt. thermoacetophila* a membrane-bound Hdr is encoded, as well as an Mtr and the Fpo complex. In analogy to *Ms. mazei* the membrane-bound Hdr and the Mtr would translocate four ions. The Fpo complex from *Mt. thermoacetophila* is missing subunit FpoF, which is the $F_{420}H_2$-oxidizing electron input module. It has been hypothesized, that the truncated Fpo complex from *Mt. thermoacetophila* instead of $F_{420}H_2$ oxidizes Fd_{red} (Welte and Deppenmeier, 2014). In this study, oxidation of Fd_{red} by the Fpo complex from *Ms. mazei* has been tested. Therefore, an antibody binding to subunit FpoI was employed. It could be demonstrated, that the FpoI antibody inhibited oxidation of Fd_{red} in membrane fractions of a *Ms. mazei* Δ*ech* mutant. Thus, the Fpo complex from *Ms. mazei* is indeed able to accept electrons from Fd_{red}. Hence, also the Fpo complex from *Mt. thermoacetophila* could be responsible for oxidation of Fd_{red}. Since the redox potential difference between Fd and MP is higher than between F_{420} and MP, with Fd_{red} as electron donor three protons could be translocated by the Fpo complex instead of two, as was previously described (Bäumer *et al.*, 2000). This could explain, how *Mt. thermoacetophila* makes a living by consuming acetate for methanogenesis.

Furthermore, in this study the first isolate of the new order Methanomassiliicoccales, *Mm. luminyensis*, was investigated bioinformatically and biochemically. The organism uses methylated compounds and H_2 as substrates for methanogenesis. Bioinformatic analyses revealed that methyl groups are transferred to HS-CoM via substrate-specific methyltransferases. Methane is produced from methyl-CoM and HS-CoB via the methyl-CoM reductase. Electrons for the reduction of CoM-S-S-CoB are derived from H_2 via the soluble HdrABC/MvhADG complex. The activity of the complex could be demonstrated in the cytoplasmic fraction of *Mm. luminyensis*. Upon reduction of CoM-S-S-CoB, electrons derived from H_2 are also transferred to Fd in a bifurcation mechanism (Kaster *et al.*, 2011). Oxidation of Fd_{red} via a membrane-bound enzyme potentially involves ion translocation and may thus be associated with energy conservation. Membrane-bound enzymes encoded in the genome of *Mm. luminyensis* are the Ech hydrogenase and the Fpo complex. The Ech hydrogenase belongs to the family of energy-conserving [NiFe] hydrogenases, which are able to oxidize

Fd_{red} and to translocate ions across the cytoplasmic membrane. In the course of this study, Fd_{red}-dependent formation of H_2 was measured, that was catalyzed by membrane fractions of *Mm. luminyensis*. Thus, the organism possesses an active Ech hydrogenase, that probably contributes to the formation of an electrochemical ion gradient, which is used for ATP synthesis. Recently, it was proposed, that the Fpo complex in *Mm. luminyensis* together with HdrD oxidizes Fd_{red} and concomitantly translocates protons (Lang *et al.*, 2014). However, there is no biochemical evidence for this hypothesis. In this study, no Hdr activity could be detected in membrane fractions of *Mm. luminyensis*. Thus, Fd_{red}-oxidation via the Fpo complex is a rather theoretical possibility and it seems more likely that the Ech hydrogenase is used *in vivo*.

This study contributes to the understanding of energy conservation mechanisms in the obligate aceticlastic *Mt. thermoacetophila* and the versatile *Ms. mazei*. Oxidation of Fd_{red} via the Fpo complex was shown for *Ms. mazei* and is also a possible explanation for the survival of *Mt. thermoacetophila*. Furthermore, first evidence for possible energy conservation mechanisms in *Mm. luminyensis* is presented. The organism possesses an unusual combination of enzymes. In this study, Ech hydrogenase and HdrABC/MvhADG have been targeted. However, energy conservation mechanisms in *Mm. luminyensis* are an interesting target for future studies.

5. SUMMARY

1) In the first part of this study, the acetate activation reaction in the obligate aceticlastic methanogenic archaeon *Methanosaeta* (*Mt). thermoacetophila* was examined. Acetate breakdown requires activation of the otherwise inert molecule at the expense of ATP. As a first step to identify enzymes involved in the reaction, the transcription of genes encoding four putative acetyl-CoA synthetases (ACS) and a soluble pyrophosphatase (PPase) was examined by RT-qPCR analysis. Only *mthe_1194* encoding a putative AMP-forming ACS and *mthe_0236* encoding a soluble PPase were highly transcribed. Mthe1194 was heterologously produced in *E. coli*. The enzyme catalyzed the hydrolysis of ATP to AMP and PP_i. The other product of the reaction was acetyl-CoA, that was formed at a rate of 16.1 U mg^{-1}. The K_M values for acetate, ATP and CoA were 0.6 mM, 24 μM and 20.5 μM, respectively. These values indicate an efficient formation of acetyl-CoA *in vivo*.
2) Mthe0236 was likewise heterologously produced. Gel filtration chromatography revealed that the native enzyme is a homodimer. It catalyzed PP_i hydrolysis with Mn^{2+} as metal ion in the active center with a typically high rate of 1067 U mg^{-1}. The K_M value for PP_i was 0.16 mM, which allowed efficient PP_i hydrolysis within the cells. With the formation of AMP and PP_i by Mthe1194 and subsequent PP_i hydrolysis by Mthe0236, acetate activation in *Mt. thermoacetophila* consumes two ATP equivalents, that have to be regained in energy conservation processes.
3) In the second part of this study the $F_{420}H_2$ dehydrogenase, also termed Fpo complex, from *Methanosarcina* (*Ms.) mazei* was investigated. The Fpo complex is a membrane-bound enzyme, which is homologous to respiratory complex I. In *Ms. mazei* it catalyzes oxidation of $F_{420}H_2$ and concomitantly translocates protons across the cytoplasmic membrane. In the course of this study, a *Ms. mazei* Δ*fpoO* mutant was analyzed by growth experiments and enzyme activity assays. Until now, the exact localization and function of subunit FpoO is unclear. However, it was found that growth neither with methylated substrates nor with acetate was impaired in the *Ms. mazei* Δ*fpoO* mutant. Similarly, $F_{420}H_2$ oxidation rates in the mutant were comparable to those of the wild type. It was concluded that the Fpo complex was functional without subunit FpoO. Hence, the current hypothesis is that FpoO might be a redox sensor, which facilitates interaction of the membrane-bound complex with the soluble subunit FpoF.
4) There was evidence that the Fpo complex besides $F_{420}H_2$ might also oxidize Fd_{red}, which is formed during methylotrophic and aceticlastic methanogenesis. The Ech hydrogenase was shown to be responsible for Fd_{red}-oxidation in *Ms. mazei.* Yet, membrane fractions of a *Ms. mazei* Δ*ech* mutant retained about 50 % Fd_{red}-oxidizing activity, which might be due to the Fpo complex (Welte *et al.*, 2010a; Welte and Deppenmeier, 2011a). Since it

was not possible to generate double mutants missing the Ech hydrogenase and the Fpo complex or parts thereof, an antibody against subunit FpoI was generated and used for inhibition studies. In membrane fractions of the *Ms. mazei* Δ*ech* mutant the Fd_{red}-oxidation rate was 52 ± 6 nmol min^{-1} mg^{-1} without FpoI antibody and 31 ± 6 nmol $min^{-1}mg^{-1}$ with 0.5 µg of the FpoI antibody. Higher amounts of FpoI antibody completely abolished oxidation of Fd_{red}. Therefore, the Fpo complex indeed interacts with Fd_{red}. Fd_{red}-oxidation via the Fpo complex might also occur in *Mt. thermoacetophila*, which lacks other Fd_{red}-oxidizing enzymes. The reaction might enable the translocation of three protons across the cytoplasmic membrane instead of two as was previously described for the Fpo complex (Bäumer *et al.*, 2000). This provides a possible explanation how *Mt. thermoacetophila* can grow with acetate as substrate.

5) The last part of this thesis dealt with the newly discovered methanogen *Methanomassiliicoccus* (*Mm.) luminyensis,* which was isolated from the human gut (Dridi *et al.*, 2012). Interestingly, it consumes H_2 and methanol as substrates for methanogenesis. Bioinformatic analyses revealed the presence of methyltransferases specific for methylated amines. Consequently, growth with dimethylamine and monomethylamine was possible, but depended on the addition of sludge fluid prepared from biogas sludge. It was concluded, that the sludge fluid contained a component, which cannot be synthesized by *Mm. luminyensis*.

6) Bioinformatic analyses revealed the presence of a soluble heterodisulfide reductase (HdrABC) and the associated MvhADG hydrogenase. Furthermore, subunit HdrD of the membrane-bound heterodisulfide reductase was identified. Other membrane-bound enzymes encoded in the *Mm. luminyensis* genome are the Ech hydrogenase, which exists in two copies and the Fpo complex without subunits FpoF and FpoO. The activity of the soluble HdrABC/MvhADG could be demonstrated in the cytoplasmic fraction of *Mm. luminyensis*. With H_2 as electron donor, electrons were transferred to the heterodisulfide and to Fd at a rate of 4 mU mg^{-1}. No heterodisulfide reductase activity was measured in the membrane fraction. Fd_{red} is probably re-oxidized via the Ech hydrogenase. H_2 formation rates of 80 nmol min^{-1} mg^{-1} could be demonstrated with membrane fractions of *Mm. luminyensis*. Fd_{red}-oxidation via the Fpo complex might occur, but it is rather ambiguous which electron acceptor could be used. Therefore, energy conservation in *Mm. luminyensis* probably relies on the Ech hydrogenase.

REFERENCES

Abken, H.J., and Deppenmeier, U. (1997) Purification and properties of an $F_{420}H_2$ dehydrogenase from *Methanosarcina mazei* Go1. *FEMS Microbiol Lett* **154**: 231-237.

Abken, H.J., Tietze, M., Brodersen, J., Bäumer, S., Beifuss, U., and Deppenmeier, U. (1998) Isolation and characterization of methanophenazine and function of phenazines in membrane-bound electron transport of *Methanosarcina mazei* Gö1. *J Bacteriol* **180**: 2027-2032.

Aguado-Llera, D., Oyenarte, I., Martinez-Cruz, L.A., and Neira, J.L. (2010) The CBS domain protein MJ0729 of *Methanocaldococcus jannaschii* binds DNA. *FEBS Lett* **584**: 4485-4489.

Ahn, S., Milner, A.J., Futterer, K., Konopka, M., Ilias, M., Young, T.W., and White, S.A. (2001) The "Open" and "Closed" structures of the type-C inorganic pyrophosphatases from *Bacillus subtilis* and *Streptococcus gordonii*. *J Mol Biol* **313**: 797-811.

Arumugam, M., Raes, J., Pelletier, E., Le Paslier, D., Yamada, T., Mende, D.R. et al. (2011) Enterotypes of the human gut microbiome. *Nature* **473**: 174-180.

Ausubel, F.M., Brent, R., and Kingston, R. (1987) Current protocols in molecular biology. New York: Wiley & Sons Inc.

Avaeva, S.M. (2000) Active site interactions in oligomeric structures of inorganic pyrophosphatases. *Biochemistry (Mosc)* **65**: 361-372.

Balch, W.E., and Wolfe, R.S. (1976) New approach to cultivation of methanogenic bacteria - 2-mercaptoethanesulfonic acid (HS-CoM)-dependent growth of *Methanobacterium ruminantium* in a pressurized atmosphere. *Appl Environ Microbiol* **32**: 781-791.

Barber, R.D., Zhang, L., Harnack, M., Olson, M.V., Kaul, R., Ingram-Smith, C., and Smith, K.S. (2011) Complete genome sequence of *Methanosaeta concilii*, a specialist in aceticlastic methanogenesis. *J Bacteriol* **193**: 3668-3669.

Bateman, A. (1997) The structure of a domain common to archaebacteria and the homocystinuria disease protein. *Trends Biochem Sci* **22**: 12-13.

Bäumer, S., Lentes, S., Gottschalk, G., and Deppenmeier, U. (2002) Identification and analysis of proton-translocating pyrophosphatases in the methanogenic archaeon *Methansarcina mazei*. *Archaea* **1**: 1-7.

Bäumer, S., Ide, T., Jacobi, C., Johann, A., Gottschalk, G., and Deppenmeier, U. (2000) The $F_{420}H_2$ dehydrogenase from *Methanosarcina mazei* is a redox-driven proton pump closely related to NADH dehydrogenases. *J Biol Chem* **275**: 17968-17973.

Bell, S.D., Magill, C.P., and Jackson, S.P. (2001) Basal and regulated transcription in *Archaea*. *Biochem Soc Trans* **29**: 392-395.

Berger, S., Welte, C., and Deppenmeier, U. (2012) Acetate activation in *Methanosaeta thermophila*: characterization of the key enzymes pyrophosphatase and acetyl-CoA synthetase. *Archaea* **2012**: 315153.

Biegel, E., and Müller, V. (2010) Bacterial Na^+-translocating ferredoxin:NAD^+ oxidoreductase. *Proc Natl Acad Sci U S A* **107**: 18138-18142.

Bielen, A.A.M., Willquist, K., Engman, J., van der Oost, J., van Niel, E.W.J., and Kengen, S.W.M. (2010) Pyrophosphate as a central energy carrier in the hydrogen-producing extremely thermophilic *Caldicellulosiruptor saccharolyticus*. *FEMS Microbiol Lett* **307**: 48-54.

Bjornsdottir, G., and Myers, L.C. (2008) Minimal components of the RNA polymerase II transcription apparatus determine the consensus TATA box. *Nucleic Acids Res* **36**: 2906-2916.

Bock, A.K., Kunow, J., Glasemacher, J., and Schonheit, P. (1996) Catalytic properties, molecular composition and sequence alignments of pyruvate: ferredoxin oxidoreductase from the methanogenic archaeon *Methanosarcina barkeri* (strain Fusaro). *Eur J Biochem* **237**: 35-44.

Borrel, G., O'Toole, P.W., Harris, H.M.B., Peyret, P., Brugere, J.F., and Gribaldo, S. (2013) Phylogenomic data support a seventh order of methylotrophic methanogens and provide insights into the evolution of methanogenesis. *Genome Biol Evol* **5**: 1769-1780.

Borrel, G., Joblin, K., Guedon, A., Colombet, J., Tardy, V., Lehours, A.C., and Fonty, G. (2012a) *Methanobacterium lacus* sp. nov., isolated from the profundal sediment of a freshwater meromictic lake. *Int J Syst Evol Microbiol* **62**: 1625-1629.

Borrel, G., Harris, H.M., Tottey, W., Mihajlovski, A., Parisot, N., Peyretaillade, E. et al. (2012b) Genome sequence of "*Candidatus* Methanomethylophilus alvus" Mx1201, a methanogenic archaeon from the human gut belonging to a seventh order of methanogens. *J Bacteriol* **194**: 6944-6945.

Borrel, G., Parisot, N., Harris, H.M.B., Peyretaillade, E., Gaci, N., Tottey, W. et al. (2014) Comparative genomics highlights the unique biology of Methanomassiliicoccales, a Thermoplasmatales-related seventh order of methanogenic archaea that encodes pyrrolysine. *BMC Genomics* **15**.

Bose, A., Pritchett, M.A., and Metcalf, W.W. (2008) Genetic analysis of the methanol- and methylamine-specific methyltransferase 2 genes of *Methanosarcina acetivorans* C2A. *J Bacteriol* **190**: 4017-4026.

Bose, A., Pritchett, M.A., Rother, M., and Metcalf, W.W. (2006) Differential regulation of the three methanol methyltransferase isozymes in *Methanosarcina acetivorans* C2A. *J Bacteriol* **188**: 7274-7283.

Bradford, M.M. (1976) A rapid and sensitive method for the quantitation of microgram quantities of protein utilizing the principle of protein-dye binding. *Anal Biochem* **72**: 248-254.

Bräsen, C., and Schönheit, P. (2004) Regulation of acetate and acetyl-CoA converting enzymes during growth on acetate and/or glucose in the halophilic archaeon *Haloarcula marismortui*. *FEMS Microbiol Lett* **241**: 21-26.

Brenneis, M., Hering, O., Lange, C., and Soppa, J. (2007) Experimental characterization of Cis-acting elements important for translation and transcription in halophilic archaea. *PLoS Genet* **3**: e229.

Brugère, J.F., Borrel, G., Gaci, N., Tottey, W., O'Toole, P.W., and Malpuech-Brugere, C. (2014) Archaebiotics: proposed therapeutic use of archaea to prevent trimethylaminuria and cardiovascular disease. *Gut Microbes* **5**: 5-10.

Brüggemann, H., Falinski, F., and Deppenmeier, U. (2000) Structure of the $F_{420}H_2$: quinone oxidoreductase of *Archaeoglobus fulgidus* - Identification and overproduction of the $F_{420}H_2$-oxidizing subunit. *Eur J Biochem* **267**: 5810-5814.

Chen, J., Brevet, A., Fromant, M., Leveque, F., Schmitter, J.M., Blanquet, S., and Plateau, P. (1990) Pyrophosphatase is essential for growth of *Escherichia coli*. *J Bacteriol* **172**: 5686-5689.

Chi, A.S., Deng, Z., Albach, R.A., and Kemp, R.G. (2001) The two phosphofructokinase gene products of *Entamoeba histolytica*. *J Biol Chem* **276**: 19974-19981.

Clark, C.G., and Roger, A.J. (1995) Direct evidence for secondary loss of mitochondria in *Entamoeba histolytica*. *Proc Natl Acad Sci U S A* **92**: 6518-6521.

Cooperman, B.S., Baykov, A.A., and Lahti, R. (1992) Evolutionary conservation of the active site of soluble inorganic pyrophosphatase. *Trends Biochem Sci* **17**: 262-266.

Costa, K.C., Wong, P.M., Wang, T., Lie, T.J., Dodsworth, J.A., Swanson, I. et al. (2010) Protein complexing in a methanogen suggests electron bifurcation and electron delivery from formate to heterodisulfide reductase. *Proc Natl Acad Sci U S A* **107**: 11050-11055.

D'Angelo, R., Esposito, T., Calabro, M., Rinaldi, C., Robledo, R., Varriale, B., and Sidoti, A. (2013) FMO3 allelic variants in Sicilian and Sardinian populations: Trimethylaminuria and absence of fish-like body odor. *Gene* **515**: 410-415.

Davies, J.M., Poole, R.J., and Sanders, D. (1993) The computed free energy change of hydrolysis of inorganic pyrophosphate and ATP - apparent significance for inorganic pyrophosphate driven reactions of intermediary metabolism. *Biochim Biophys Acta* **1141**: 29-36.

Deckert, G., Warren, P.V., Gaasterland, T., Young, W.G., Lenox, A.L., Graham, D.E. et al. (1998) The complete genome of the hyperthermophilic bacterium *Aquifex aeolicus*. *Nature* **392**: 353-358.

DeLong, E.F. (1992) Archaea in coastal marine environments. *Proc Natl Acad Sci U S A* **89**:

5685-5689.

Deng, Z.H., Huang, M., Singh, K., Albach, R.A., Latshaw, S.P., Chang, K.P., and Kemp, R.G. (1998) Cloning and expression of the gene for the active PPi-dependent phosphofructokinase of *Entamoeba histolytica*. *Biochem J* **329**: 659-664.

Denman, S.E., Tomkins, N.W., and McSweeney, C.S. (2007) Quantitation and diversity analysis of ruminal methanogenic populations in response to the antimethanogenic compound bromochloromethane. *FEMS Microbiol Ecol* **62**: 313-322.

Deppenmeier, U. (2002a) Redox-driven proton translocation in methanogenic archaea. *Cell Mol Life Sci* **59**: 1513-1533.

Deppenmeier, U. (2002b) The unique biochemistry of methanogenesis. *Prog Nucleic Acid Res Mol Biol* **71**: 223-283.

Deppenmeier, U., and Müller, V. (2008) Life close to the thermodynamic limit: how methanogenic archaea conserve energy. *Results Probl Cell Differ* **45**: 123-152.

Deppenmeier, U., Johann, A., Hartsch, T., Merkl, R., Schmitz, R.A., Martinez-Arias, R. et al. (2002) The genome of *Methanosarcina mazei*: evidence for lateral gene transfer between bacteria and archaea. *J Mol Microbiol Biotechnol* **4**: 453-461.

Dolezal, P., Dagley, M.J., Kono, M., Wolynec, P., Likic, V.A., Foo, J.H. et al. (2010) The essentials of protein import in the degenerate mitochondrion of *Entamoeba histolytica*. *PloS Pathogens* **6**.

Dridi, B., Henry, M., El Khechine, A., Raoult, D., and Drancourt, M. (2009) High prevalence of *Methanobrevibacter smithii* and *Methanosphaera stadtmanae* detected in the human gut using an improved DNA detection protocol. *PLoS One* **4**: e7063.

Dridi, B., Fardeau, M.L., Ollivier, B., Raoult, D., and Drancourt, M. (2012) *Methanomassiliicoccus luminyensis* gen. nov., sp. nov., a methanogenic archaeon isolated from human faeces. *Int J Syst Evol Microbiol* **62**: 1902-1907.

Efremov, R.G., and Sazanov, L.A. (2011) Structure of the membrane domain of respiratory complex I. *Nature* **476**: 414-420.

Efremov, R.G., Baradaran, R., and Sazanov, L.A. (2010) The architecture of respiratory complex I. *Nature* **465**: 441-445.

Egert, M., Wagner, B., Lemke, T., Brune, A., and Friedrich, M.W. (2003) Microbial community structure in midgut and hindgut of the humus-feeding larva of *Pachnoda ephippiata* (Coleoptera: Scarabaeidae). *Appl Environ Microbiol* **69**: 6659-6668.

Ehlers, C., Weidenbach, K., Veit, K., Deppenmeier, U., Metcalf, W.W., and Schmitz, R.A. (2005) Development of genetic methods and construction of a chromosomal glnK1 mutant in *Methanosarcina mazei* strain Gö1. *Mol Genet Genomics* **273**: 290-298.

Ellman, G.L. (1958) A colorimetric method for determining low concentrations of mercaptans. *Arch Biochem Biophys* **74**: 443-450.

Ereno-Orbea, J., Majtan, T., Oyenarte, I., Kraus, J.P., and Martinez-Cruz, L.A. (2013) Structural basis of regulation and oligomerization of human cystathionine beta-synthase, the central enzyme of transsulfuration. *Proc Natl Acad Sci U S A* **110**: E3790-3799.

Evans, P.N., Hinds, L.A., Sly, L.I., McSweeney, C.S., Morrison, M., and Wright, A.D. (2009) Community composition and density of methanogens in the foregut of the Tammar wallaby (*Macropus eugenii*). *Appl Environ Microbiol* **75**: 2598-2602.

Fabrichniy, I.P., Lehtio, L., Tammenkoski, M., Zyryanov, A.B., Oksanen, E., Baykov, A.A. et al. (2007) A trimetal site and substrate distortion in a family II inorganic pyrophosphatase. *J Biol Chem* **282**: 1422-1431.

Ferry, J.G., and Lessner, D.J. (2008) Methanogenesis in marine sediments. *Ann N Y Acad Sci* **1125**: 147-157.

Fox, J.D., Kerby, R.L., Roberts, G.P., and Ludden, P.W. (1996) Characterization of the CO-induced, CO-tolerant hydrogenase from *Rhodospirillum rubrum* and the gene encoding the large subunit of the enzyme. *J Bacteriol* **178**: 1515-1524.

Fricke, W.F., Seedorf, H., Henne, A., Kruer, M., Liesegang, H., Hedderich, R. et al. (2006) The genome sequence of *Methanosphaera stadtmanae* reveals why this human intestinal archaeon is restricted to methanol and H_2 for methane formation and ATP synthesis. *J Bacteriol* **188**: 642-658.

Friedrich, M.W., Schmitt-Wagner, D., Lueders, T., and Brune, A. (2001) Axial differences in community structure of Crenarchaeota and Euryarchaeota in the highly compartmentalized gut of the soil-feeding termite *Cubitermes orthognathus*. *Appl Environ Microbiol* **67**: 4880-4890.

Friedrich, T. (2001) Complex I: a chimaera of a redox and conformation-driven proton pump? *J Bioenerg Biomembr* **33**: 169-177.

Fuhrman, J.A., McCallum, K., and Davis, A.A. (1992) Novel major archaebacterial group from marine plankton. *Nature* **356**: 148-149.

Gaci, N., Borrel, G., Tottey, W., O'Toole, P.W., and Brugere, J.F. (2014) Archaea and the human gut: new beginning of an old story. *World J Gastroenterol* **20**: 16062-16078.

Garcia-Contreras, R., Celis, H., and Romero, I. (2004) Importance of *Rhodospirillum rubrum* H^+-pyrophosphatase under low-energy conditions. *J Bacteriol* **186**: 6651-6655.

Gardner, J.G., Grundy, F.J., Henkin, T.M., and Escalante-Semerena, J.C. (2006) Control of acetyl-coenzyme A synthetase (AcsA) activity by acetylation/deacetylation without NAD^+ involvement in *Bacillus subtilis*. *J Bacteriol* **188**: 5460-5468.

Gaston, M.A., Jiang, R., and Krzycki, J.A. (2011) Functional context, biosynthesis, and genetic encoding of pyrrolysine. *Curr Opin Microbiol* **14**: 342-349.

George, D.G., Hunt, L.T., Yeh, L.S., and Barker, W.C. (1985) New perspectives on bacterial ferredoxin evolution. *J Mol Evol* **22**: 20-31.

George, G.N., Prince, R.C., Mukund, S., and Adams, M.W.W. (1992) Aldehyde ferredoxin oxidoreductase from the hyperthermophilic archaebacterium *Pyrococcus furiosus* contains a tungsten oxo-thiolate center. *J Am Chem Soc* **114**: 3521-3523.

Gill, S.R., Pop, M., Deboy, R.T., Eckburg, P.B., Turnbaugh, P.J., Samuel, B.S. et al. (2006) Metagenomic analysis of the human distal gut microbiome. *Science* **312**: 1355-1359.

Gorlas, A., Robert, C., Gimenez, G., Drancourt, M., and Raoult, D. (2012) Complete genome sequence of *Methanomassiliicoccus luminyensis*, the largest genome of a human-associated *Archaea* species. *J Bacteriol* **194**: 4745.

Graham, D.E., Taylor, S.M., Wolf, R.Z., and Namboori, S.C. (2009) Convergent evolution of coenzyme M biosynthesis in the Methanosarcinales: cysteate synthase evolved from an ancestral threonine synthase. *Biochem J* **424**: 467-478.

Grosskopf, R., Janssen, P.H., and Liesack, W. (1998) Diversity and structure of the methanogenic community in anoxic rice paddy soil microcosms as examined by cultivation and direct 16S rRNA gene sequence retrieval. *Appl Environ Microbiol* **64**: 960-969.

Hagedoorn, P.L., Chen, T., Schröder, I., Piersma, S.R., de Vries, S., and Hagen, W.R. (2005) Purification and characterization of the tungsten enzyme aldehyde:ferredoxin oxidoreductase from the hyperthermophilic denitrifier *Pyrobaculum aerophilum*. *J Biol Inorg Chem* **10**: 259-269.

Hahn, S., Buratowski, S., Sharp, P.A., and Guarente, L. (1989) Yeast TATA-binding protein TFIID binds to TATA elements with both consensus and nonconsensus DNA sequences. *Proc Natl Acad Sci U S A* **86**: 5718-5722.

Haines, A., Dilawari, J., Metz, G., Blendis, L., and Wiggins, H. (1977) Breath-methane in patients with cancer of large bowel. *Lancet* **2**: 481-483.

Halonen, P., Tammenkoski, M., Niiranen, L., Huopalahti, S., Parfenyev, A.N., Goldman, A. et al. (2005) Effects of active site mutations on the metal binding affinity, catalytic competence, and stability of the family II pyrophosphatase from *Bacillus subtilis*. *Biochemistry* **44**: 4004-4010.

Hanahan, D. (1983) Studies on transformation of *Escherichia coli* with plasmids. *J Mol Biol* **166**: 557-580.

Hara, K., Shinzato, N., Seo, M., Oshima, T., and Yamagishi, A. (2002) Phylogenetic analysis of symbiotic archaea living in the gut of xylophagous cockroaches. *Microbes and Environments* **17**: 185-190.

Harding, M.M. (2001) Geometry of metal-ligand interactions in proteins. *Acta Crystallogr D Biol Crystallogr* **57**: 401-411.

Hattori, M., Iwase, N., Furuya, N., Tanaka, Y., Tsukazaki, T., Ishitani, R. et al. (2009) Mg^{2+}-dependent gating of bacterial MgtE channel underlies Mg^{2+} homeostasis. *EMBO J* **28**: 3602-3612.

Heiden, S., Hedderich, R., Setzke, E., and Thauer, R.K. (1993) Purification of a cytochrome *b* containing H_2:heterodisulfide oxidoreductase complex from membranes of *Methanosarcina barkeri*. *Eur J Biochem* **213**: 529-535.

Heikinheimo, P., Tuominen, V., Ahonen, A.K., Teplyakov, A., Cooperman, B.S., Baykov, A.A. et al. (2001) Toward a quantum-mechanical description of metal-assisted phosphoryl transfer in pyrophosphatase. *Proc Natl Acad Sci U S A* **98**: 3121-3126.

Heinonen, J.K. (2001) Biological role of inorganic pyrophosphate. Norwell, MA: Kluver Academic Publishers Group.

Hofmann, K. (2003) Charakterisierung und Kristallisation der Elektronen-einspeisenden Module der $F_{420}H_2$-Dehydrogenase. Georg-August-Universitaet Goettingen.

Hovey, R., Lentes, S., Ehrenreich, A., Salmon, K., Saba, K., Gottschalk, G. et al. (2005) DNA microarray analysis of *Methanosarcina mazei* Gö1 reveals adaptation to different methanogenic substrates. *Mol Genet Genomics* **273**: 225-239.

Iino, T., Tamaki, H., Tamazawa, S., Ueno, Y., Ohkuma, M., Suzuki, K. et al. (2013) *Candidatus* Methanogranum caenicola: a novel methanogen from the anaerobic digested sludge, and proposal of *Methanomassiliicoccaceae* fam. nov and *Methanomassiliicoccales* ord. nov., for a methanogenic lineage of the class Thermoplasmata. *Microbes and Environments* **28**: 244-250.

Ilias, M., and Young, T.W. (2006) *Streptococcus gordonii* soluble inorganic pyrophosphatase: an important role for the interdomain region in enzyme activity. *Biochim Biophys Acta* **1764**: 1299-1306.

Imlay, J.A. (2006) Iron-sulphur clusters and the problem with oxygen. *Mol Microbiol* **59**: 1073-1082.

Ingram-Smith, C., and Smith, K.S. (2007) AMP-forming acetyl-CoA synthetases in *Archaea* show unexpected diversity in substrate utilization. *Archaea* **2**: 95-107.

Ingram-Smith, C., Woods, B.I., and Smith, K.S. (2006) Characterization of the acyl substrate binding pocket of acetyl-CoA synthetase. *Biochemistry* **45**: 11482-11490.

Ivleva, N.B., Bramlett, M.R., Lindahl, P.A., and Golden, S.S. (2005) LdpA: a component of the circadian clock senses redox state of the cell. *Embo J* **24**: 1202-1210.

Jäger, D., Sharma, C.M., Thomsen, J., Ehlers, C., Vogel, J., and Schmitz, R.A. (2009) Deep sequencing analysis of the *Methanosarcina mazei* Gö1 transcriptome in response to nitrogen availability. *Proc Natl Acad Sci U S A* **106**: 21878-21882.

Jämsen, J. (2011) Functional studies on bacterial nucleotide regulated inorganic pyrophosphatases. Turun Yleopisto University Turku.

Jämsen, J., Tuominen, H., Salminen, A., Belogurov, G.A., Magretova, N.N., Baykov, A.A., and Lahti, R. (2007) A CBS domain-containing pyrophosphatase of *Moorella thermoacetica* is regulated by adenine nucleotides. *Biochem J* **408**: 327-333.

Janssen, P.H., and Kirs, M. (2008) Structure of the archaeal community of the rumen. *Appl Environ Microbiol* **74**: 3619-3625.

Jeong, B.C., Park, S.H., Yoo, K.S., Shin, J.S., and Song, H.K. (2013) Change in single cystathionine beta-synthase domain-containing protein from a bent to flat conformation upon adenosine monophosphate binding. *J Struct Biol* **183**: 40-46.

Jetten, M.S., Stams, A.J., and Zehnder, A.J. (1989) Isolation and characterization of acetyl-

coenzyme A synthetase from *Methanothrix soehngenii*. *J Bacteriol* **171**: 5430-5435.

Jetten, M.S., Fluit, T.J., Stams, A.J., and Zehnder, A.J. (1992a) A fluoride-insensitive inorganic pyrophosphatase isolated from *Methanothrix soehngenii*. *Arch Microbiol* **157**: 284-289.

Jetten, M.S.M., Stams, A.J.M., and Zehnder, A.J.B. (1992b) Methanogenesis from acetate - a comparison of the acetate metabolism in *Methanothrix soehngenii* and *Methanosarcina* spp. *FEMS Microbiol Rev* **88**: 181-197.

Kajander, T., Kellosalo, J., and Goldman, A. (2013) Inorganic pyrophosphatases: one substrate, three mechanisms. *FEBS Lett* **587**: 1863-1869.

Kankare, J., Neal, G.S., Salminen, T., Glumoff, T., Glumhoff, T., Cooperman, B.S. et al. (1994) The structure of *E.coli* soluble inorganic pyrophosphatase at 2.7 Å resolution. *Protein Eng* **7**: 823-830.

Kaster, A.K., Moll, J., Parey, K., and Thauer, R.K. (2011) Coupling of ferredoxin and heterodisulfide reduction via electron bifurcation in hydrogenotrophic methanogenic archaea. *Proc Natl Acad Sci U S A* **108**: 2981-2986.

Kemnitz, D., Kolb, S., and Conrad, R. (2005) Phenotypic characterization of Rice Cluster III archaea without prior isolation by applying quantitative polymerase chain reaction to an enrichment culture. *Environ Microbiol* **7**: 553-565.

Kerscher, L., and Oesterhelt, D. (1981) Purification and properties of two 2-oxoacid:ferredoxin oxidoreductases from *Halobacterium halobium*. *Eur J Biochem* **116**: 587-594.

King, N.P., Lee, T.M., Sawaya, M.R., Cascio, D., and Yeates, T.O. (2008) Structures and functional implications of an AMP-binding cystathionine beta-synthase domain protein from a hyperthermophilic archaeon. *J Mol Biol* **380**: 181-192.

Kohler, H.P.E., and Zehnder, A.J.B. (1984) Carbon monoxide dehydrogenase and acetate thiokinase in *Methanothrix soehngenii*. *FEMS Microbiol Lett* **21**: 287-292.

Krätzer, C., Carini, P., Hovey, R., and Deppenmeier, U. (2009) Transcriptional profiling of methyltransferase genes during growth of *Methanosarcina mazei* on trimethylamine. *J Bacteriol* **191**: 5108-5115.

Krivushin, K.V., Shcherbakova, V.A., Petrovskaya, L.E., and Rivkina, E.M. (2010) *Methanobacterium veterum* sp. nov., from ancient Siberian permafrost. *Int J Syst Evol Microbiol* **60**: 455-459.

Krzycki, J.A. (2004) Function of genetically encoded pyrrolysine in corrinoid-dependent methylamine methyltransferases. *Curr Opin Chem Biol* **8**: 484-491.

Kuang, Y., Salem, N., Wang, F., Schomisch, S.J., Chandramouli, V., and Lee, Z. (2007) A colorimetric assay method to measure acetyl-CoA synthetase activity: application to woodchuck model of hepatitis virus-induced hepatocellular carcinoma. *J Biochem Biophys Methods* **70**: 649-655.

Kuhn, N.J., Wadeson, A., Ward, S., and Young, T.W. (2000) *Methanococcus jannaschii* ORF *mj0608* codes for a class C inorganic pyrophosphatase protected by Co^{2+} or Mn^{2+} ions against fluoride inhibition. *Arch Biochem Biophys* **379**: 292-298.

Kulkarni, G., Kridelbaugh, D.M., Guss, A.M., and Metcalf, W.W. (2009) Hydrogen is a preferred intermediate in the energy-conserving electron transport chain of *Methanosarcina barkeri*. *Proc Natl Acad Sci U S A* **106**: 15915-15920.

Künkel, A., Vorholt, J.A., Thauer, R.K., and Hedderich, R. (1998) An *Escherichia coli* hydrogenase-3-type hydrogenase in methanogenic archaea. *Eur J Biochem* **252**: 467-476.

Laemmli, U.K. (1970) Cleavage of structural proteins during assembly of head of bacteriophage T4. *Nature* **227**: 680-685.

Lang, K., Schuldes, J., Klingl, A., Poehlein, A., Daniel, R., and Brune, A. (2014) Comparative genome analysis of "*Candidatus* Methanoplasma termitum" indicates a new mode of energy metabolism in the seventh order of methanogens. *Appl Environ Microbiol.*, in press

Levitt, M.D., Furne, J.K., Kuskowski, M., and Ruddy, J. (2006) Stability of human

methanogenic flora over 35 years and a review of insights obtained from breath methane measurements. *Clin Gastroenterol Hepatol* **4**: 123-129.

Ley, R.E., Peterson, D.A., and Gordon, J.I. (2006) Ecological and evolutionary forces shaping microbial diversity in the human intestine. *Cell* **124**: 837-848.

Li, C.L., Liu, D.L., Jiang, Y.T., Zhou, Y.B., Zhang, M.Z., Jiang, W. et al. (2009) Prevalence and molecular diversity of Archaea in subgingival pockets of periodontitis patients. *Oral Microbiol Immunol* **24**: 343-346.

Li, F., Hinderberger, J., Seedorf, H., Zhang, J., Buckel, W., and Thauer, R.K. (2008) Coupled ferredoxin and crotonyl coenzyme A (CoA) reduction with NADH catalyzed by the butyryl-CoA dehydrogenase/Etf complex from *Clostridium kluyveri*. *J Bacteriol* **190**: 843-850.

Li, Q., Li, L., Rejtar, T., Lessner, D.J., Karger, B.L., and Ferry, J.G. (2006) Electron transport in the pathway of acetate conversion to methane in the marine archaeon *Methanosarcina acetivorans*. *J Bacteriol* **188**: 702-710.

Lin, C., and Miller, T.L. (1998) Phylogenetic analysis of *Methanobrevibacter* isolated from feces of humans and other animals. *Arch Microbiol* **169**: 397-403.

Liu, Y., and Whitman, W.B. (2008) Metabolic, phylogenetic, and ecological diversity of the methanogenic archaea. *Ann N Y Acad Sci* **1125**: 171-189.

Lueders, T., Chin, K.J., Conrad, R., and Friedrich, M. (2001) Molecular analyses of methyl-coenzyme M reductase alpha-subunit (*mcrA*) genes in rice field soil and enrichment cultures reveal the methanogenic phenotype of a novel archaeal lineage. *Environ Microbiol* **3**: 194-204.

Luton, P.E., Wayne, J.M., Sharp, R.J., and Riley, P.W. (2002) The *mcrA* gene as an alternative to 16S rRNA in the phylogenetic analysis of methanogen populations in landfill. *Microbiology* **148**: 3521-3530.

Mai, X., and Adams, M.W. (1996a) Characterization of a fourth type of 2-keto acid-oxidizing enzyme from a hyperthermophilic archaeon: 2-ketoglutarate ferredoxin oxidoreductase from

Thermococcus litoralis. *J Bacteriol* **178**: 5890-5896.

Mai, X., and Adams, M.W. (1996b) Purification and characterization of two reversible and ADP-dependent acetyl coenzyme A synthetases from the hyperthermophilic archaeon *Pyrococcus furiosus*. *J Bacteriol* **178**: 5897-5903.

Mckay, L.F., Eastwood, M.A., and Brydon, W.G. (1985) Methane excretion in man - a study of breath, flatus, and feces. *Gut* **26**: 69-74.

Meng, Y., Ingram-Smith, C., Cooper, L.L., and Smith, K.S. (2010) Characterization of an archaeal medium-chain acyl coenzyme A synthetase from *Methanosarcina acetivorans*. *J Bacteriol* **192**: 5982-5990.

Merckel, M.C., Fabrichniy, I.P., Salminen, A., Kalkkinen, N., Baykov, A.A., Lahti, R., and Goldman, A. (2001) Crystal structure of *Streptococcus mutans* pyrophosphatase: a new fold for an old mechanism. *Structure* **9**: 289-297.

Meuer, J., Bartoschek, S., Koch, J., Kunkel, A., and Hedderich, R. (1999) Purification and catalytic properties of Ech hydrogenase from *Methanosarcina barkeri*. *Eur J Biochem* **265**: 325-335.

Meuer, J., Kuettner, H.C., Zhang, J.K., Hedderich, R., and Metcalf, W.W. (2002) Genetic analysis of the archaeon *Methanosarcina barkeri* Fusaro reveals a central role for Ech hydrogenase and ferredoxin in methanogenesis and carbon fixation. *Proc Natl Acad Sci U S A* **99**: 5632-5637.

Mihajlovski, A., Alric, M., and Brugere, J.F. (2008) A putative new order of methanogenic *Archaea* inhabiting the human gut, as revealed by molecular analyses of the *mcrA* gene. *Res Microbiol* **159**: 516-521.

Mihajlovski, A., Dore, J., Levenez, F., Alric, M., and Brugere, J.F. (2010) Molecular evaluation of the human gut methanogenic archaeal microbiota reveals an age-associated increase of the diversity. *Environ Microbiol Rep* **2**: 272-280.

Miller, T.L., and Wolin, M.J. (1982) Enumeration of *Methanobrevibacter smithii* in human

feces. *Arch Microbiol* **131**: 14-18.

Miller, T.L., Wolin, M.J., Demacario, E.C., and Macario, A.J.L. (1982) Isolation of *Methanobrevibacter smithii* from human feces. *Appl Environ Microbiol* **43**: 227-232.

Million, M., Angelakis, E., Maraninchi, M., Henry, M., Giorgi, R., Valero, R. et al. (2013) Correlation between body mass index and gut concentrations of *Lactobacillus reuteri, Bifidobacterium animalis, Methanobrevibacter smithii* and *Escherichia coli*. *Int J Obes (Lond)* **37**: 1460-1466.

Million, M., Maraninchi, M., Henry, M., Armougom, F., Richet, H., Carrieri, P. et al. (2012) Obesity-associated gut microbiota is enriched in *Lactobacillus reuteri* and depleted in *Bifidobacterium animalis* and *Methanobrevibacter smithii*. *Int J Obes (Lond)* **36**: 817-825.

Mills, D.J., Vitt, S., Strauss, M., Shima, S., and Vonck, J. (2013) De novo modeling of the F_{420}-reducing [NiFe]-hydrogenase from a methanogenic archaeon by cryo-electron microscopy. *eLife* **2**: e00218.

Mondorf, S., Deppenmeier, U., and Welte, C. (2012) A novel inducible protein production system and neomycin resistance as selection marker for Methanosarcina mazei. *Archaea* **2012**: 973743.

Moparthi, V.K., and Hägerhäll, C. (2011) The evolution of respiratory chain complex I from a smaller last common ancestor consisting of 11 protein subunits. *J Mol Evol* **72**: 484-497.

Mukund, S., and Adams, M.W. (1993) Characterization of a novel tungsten-containing formaldehyde ferredoxin oxidoreductase from the hyperthermophilic archaeon, *Thermococcus litoralis*. A role for tungsten in peptide catabolism. *J Biol Chem* **268**: 13592-13600.

Mullis, K., Faloona, F., Scharf, S., Saiki, R., Horn, G., and Erlich, H. (1986) Specific enzymatic amplification of DNA *in vitro* - the polymerase chain reaction. *Cold Spring Harbor Symposia on Quantitative Biology* **51**: 263-273.

Murakami, E., Deppenmeier, U., and Ragsdale, S.W. (2001) Characterization of the

intramolecular electron transfer pathway from 2-hydroxyphenazine to the heterodisulfide reductase from *Methanosarcina thermophila*. *J Biol Chem* **276**: 2432-2439.

Nüsslein, B., Chin, K.J., Eckert, W., and Conrad, R. (2001) Evidence for anaerobic syntrophic acetate oxidation during methane production in the profundal sediment of subtropical Lake Kinneret (Israel). *Environ Microbiol* **3**: 460-470.

Palmer, J.R., and Daniels, C.J. (1995) *In vivo* definition of an archaeal promoter. *J Bacteriol* **177**: 1844-1849.

Parfenyev, A.N., Salminen, A., Halonen, P., Hachimori, A., Baykov, A.A., and Lahti, R. (2001) Quaternary structure and metal ion requirement of family II pyrophosphatases from *Bacillus subtilis, Streptococcus gordonii*, and *Streptococcus mutans*. *J Biol Chem* **276**: 24511-24518.

Paul, K., Nonoh, J.O., Mikulski, L., and Brune, A. (2012) "Methanoplasmatales," Thermoplasmatales-related archaea in termite guts and other environments, are the seventh order of methanogens. *Appl Environ Microbiol* **78**: 8245-8253.

Pflüger, K., Ehrenreich, A., Salmon, K., Gunsalus, R.P., Deppenmeier, U., Gottschalk, G., and Müller, V. (2007) Identification of genes involved in salt adaptation in the archaeon *Methanosarcina mazei* Gö1 using genome-wide gene expression profiling. *FEMS Microbiol Lett* **277**: 79-89.

Pimentel, M., Mayer, A.G., Park, S., Chow, E.J., Hasan, A., and Kong, Y. (2003) Methane production during lactulose breath test is associated with gastrointestinal disease presentation. *Dig Dis Sci* **48**: 86-92.

Piqué, J.M., Pallares, M., Cuso, E., Vilarbonet, J., and Gassull, M.A. (1984) Methane production and colon cancer. *Gastroenterology* **87**: 601-605.

Poulsen, M., Schwab, C., Jensen, B.B., Engberg, R.M., Spang, A., Canibe, N. et al. (2013) Methylotrophic methanogenic Thermoplasmata implicated in reduced methane emissions from bovine rumen. *Nat Commun* **4**: 1428.

Pritchett, M.A., and Metcalf, W.W. (2005) Genetic, physiological and biochemical

characterization of multiple methanol methyltransferase isozymes in *Methanosarcina acetivorans* C2A. *Mol Microbiol* **56**: 1183-1194.

Rantanen, M.K., Lehtio, L., Rajagopal, L., Rubens, C.E., and Goldman, A. (2007) Structure of the *Streptococcus agalactiae* family II inorganic pyrophosphatase at 2.80 Å resolution. *Acta Crystallogr D Biol Crystallogr* **63**: 738-743.

Rasi, S., Veijanen, A., and Rintala, J. (2007) Trace compounds of biogas from different blogas production plants. *Energy* **32**: 1375-1380.

Reeves, R.E. (1968) A new enzyme with glycolytic function of pyruvate kinase. *J Biol Chem* **243**: 3202.

Reeves, R.E., and Guthrie, J.D. (1975) Acetate kinase (pyrophosphate) - 4th pyrophosphate-dependent kinase from *Entomoeba histolytica*. *Biochem Biophys Res Commun* **66**: 1389-1395.

Reeves, R.E., South, D.J., Blytt, H.J., and Warren, L.G. (1974) Pyrophosphate-D-fructose 6-phosphate 1-phosphotransferase - new enzyme with glycolytic function of 6-phosphofructokinase. *J Biol Chem* **249**: 7737-7741.

Reeves, R.E., Warren, L.G., Susskind, B., and Lo, H.S. (1977) An energy-conserving pyruvate-to-acetate pathway in *Entamoeba histolytica*. Pyruvate synthase and a new acetate thiokinase. *J Biol Chem* **252**: 726-731.

Reher, M., Gebhard, S., and Schonheit, P. (2007) Glyceraldehyde-3-phosphate ferredoxin oxidoreductase (GAPOR) and nonphosphorylating glyceraldehyde-3-phosphate dehydrogenase (GAPN), key enzymes of the respective modified Embden-Meyerhof pathways in the hyperthermophilic crenarchaeota *Pyrobaculum aerophilum* and *Aeropyrum pernix*. *FEMS Microbiol Lett* **273**: 196-205.

Rother, M., and Krzycki, J.A. (2010) Selenocysteine, pyrrolysine, and the unique energy metabolism of methanogenic archaea. *Archaea* **2010**.

Rouvière, P.E., and Wolfe, R.S. (1989) Component A3 of the methylcoenzyme M

methylreductase system of *Methanobacterium thermoautotrophicum* delta H: resolution into two components. *J Bacteriol* **171**: 4556-4562.

Saavedra, E., Olivos, A., Encalada, R., and Moreno-Sanchez, R. (2004) *Entamoeba histolytica*: kinetic and molecular evidence of a previously unidentified pyruvate kinase. *Exp Parasitol* **106**: 11-21.

Saheki, S., Takeda, A., and Shimazu, T. (1985) Assay of inorganic phosphate in the mild pH range, suitable for measurement of glycogen phosphorylase activity. *Anal Biochem* **148**: 277-281.

Sakai, S., Imachi, H., Hanada, S., Ohashi, A., Harada, H., and Kamagata, Y. (2008) *Methanocella paludicola* gen. nov., sp nov., a methane-producing archaeon, the first isolate of the lineage 'Rice Cluster I', and proposal of the new archaeal order Methanocellales ord. nov. *Int J Syst Evol Microbiol* **58**: 929-936.

Sakuraba, H., and Ohshima, T. (2002) Novel energy metabolism in anaerobic hyperthermophilic archaea: a modified Embden-Meyerhof pathway. *J Biosci Bioeng* **93**: 441-448.

Salminen, A., Ilias, M., Belogurov, G.A., Baykov, A.A., Lahti, R., and Young, T. (2006) Two soluble pyrophosphatases in *Vibrio cholerae*: transient redundancy or enduring cooperation? *Biochemistry (Mosc)* **71**: 978-982.

Samuel, B.S., Shaito, A., Motoike, T., Rey, F.E., Backhed, F., Manchester, J.K. et al. (2008) Effects of the gut microbiota on host adiposity are modulated by the short-chain fatty-acid binding G protein-coupled receptor, Gpr41. *Proc Natl Acad Sci U S A* **105**: 16767-16772.

Sanchez, L.B., and Müller, M. (1996) Purification and characterization of the acetate forming enzyme, acetyl-CoA synthetase (ADP-forming) from the amitochondriate protist, *Giardia lamblia*. *FEBS Lett* **378**: 240-244.

Sapra, R., Bagramyan, K., and Adams, M.W. (2003) A simple energy-conserving system: proton reduction coupled to proton translocation. *Proc Natl Acad Sci U S A* **100**: 7545-7550.

Sauter, M., Böhm, R., and Böck, A. (1992) Mutational analysis of the operon *hyc* determining hydrogenase 3 formation in *Escherichia coli*. *Mol Microbiol* **6**: 1523-1532.

Scanlan, P.D., Shanahan, F., and Marchesi, J.R. (2008) Human methanogen diversity and incidence in healthy and diseased colonic groups using *mcrA* gene analysis. *BMC Microbiol* **8**: 79.

Schäfer, T., Selig, M., and Schönheit, P. (1993) Acetyl-CoA synthetase (ADP forming) in archaea, a novel enzyme involved in acetate formation and ATP synthesis. *Arch Microbiol* **159**: 72-83.

Schlegel, K., Welte, C., Deppenmeier, U., and Muller, V. (2012) Electron transport during aceticlastic methanogenesis by Methanosarcina acetivorans involves a sodium-translocating Rnf complex. *FEBS J* **279**: 4444-4452.

Schmehl, M., Jahn, A., Meyer zu Vilsendorf, A., Hennecke, S., Masepohl, B., Schuppler, M. et al. (1993) Identification of a new class of nitrogen fixation genes in *Rhodobacter capsulatus*: a putative membrane complex involved in electron transport to nitrogenase. *Mol Gen Genet* **241**: 602-615.

Schönheit, P., and Schäfer, T. (1995) Metabolism of hyperthermophiles. *World Journal of Microbiology & Biotechnology* **11**: 26-57.

Scott, J.W., Hawley, S.A., Green, K.A., Anis, M., Stewart, G., Scullion, G.A. et al. (2004) CBS domains form energy-sensing modules whose binding of adenosine ligands is disrupted by disease mutations. *J Clin Invest* **113**: 274-284.

Segal, I., Walker, A.R.P., Lord, S., and Cummings, J.H. (1988) Breath methane and large bowel-cancer risk in contrasting african populations. *Gut* **29**: 608-613.

Selig, M., Xavier, K.B., Santos, H., and Schönheit, P. (1997) Comparative analysis of Embden-Meyerhof and Entner-Doudoroff glycolytic pathways in hyperthermophilic archaea and the bacterium *Thermotoga*. *Arch Microbiol* **167**: 217-232.

Shintani, T., Uchiumi, T., Yonezawa, T., Salminen, A., Baykov, A.A., Lahti, R., and Hachimori,

A. (1998) Cloning and expression of a unique inorganic pyrophosphatase from *Bacillus subtilis*: evidence for a new family of enzymes. *FEBS Lett* **439**: 263-266.

Shinzato, N., Matsumoto, T., Yamaoka, I., Oshima, T., and Yamagishi, A. (1999) Phylogenetic diversity of symbiotic methanogens living in the hindgut of the lower termite *Reticulitermes speratus* analyzed by PCR and in situ hybridization. *Appl Environ Microbiol* **65**: 837-840.

Siebers, B., and Hensel, R. (2001) Pyrophosphate-dependent phosphofructokinase from *Thermoproteus tenax*. *Hyperthermophilic Enzymes, Pt B* **331**: 54-62.

Silva, P.J., van den Ban, E.C., Wassink, H., Haaker, H., de Castro, B., Robb, F.T., and Hagen, W.R. (2000) Enzymes of hydrogen metabolism in *Pyrococcus furiosus*. *Eur J Biochem* **267**: 6541-6551.

Sintchak, M.D., Fleming, M.A., Futer, O., Raybuck, S.A., Chambers, S.P., Caron, P.R. et al. (1996) Structure and mechanism of inosine monophosphate dehydrogenase in complex with the immunosuppressant mycophenolic acid. *Cell* **85**: 921-930.

Sivula, T., Salminen, A., Parfenyev, A.N., Pohjanjoki, P., Goldman, A., Cooperman, B.S. et al. (1999) Evolutionary aspects of inorganic pyrophosphatase. *FEBS Lett* **454**: 75-80.

Smith, K.S., and Ingram-Smith, C. (2007) *Methanosaeta*, the forgotten methanogen? *Trends Microbiol* **15**: 150-155.

Soboh, B., Linder, D., and Hedderich, R. (2002) Purification and catalytic properties of a CO-oxidizing:H2-evolving enzyme complex from Carboxydothermus hydrogenoformans. *Eur J Biochem* **269**: 5712-5721.

Soboh, B., Linder, D., and Hedderich, R. (2004) A multisubunit membrane-bound [NiFe] hydrogenase and an NADH-dependent Fe-only hydrogenase in the fermenting bacterium *Thermoanaerobacter tengcongensis*. *Microbiology* **150**: 2451-2463.

Soppa, J. (2001) Basal and regulated transcription in archaea. *Adv Appl Microbiol* **50**: 171-217.

Sprenger, W.W., Hackstein, J.H., and Keltjens, J.T. (2005) The energy metabolism of *Methanomicrococcus blatticola*: physiological and biochemical aspects. *Antonie Van Leeuwenhoek* **87**: 289-299.

Sprenger, W.W., van Belzen, M.C., Rosenberg, J., Hackstein, J.H., and Keltjens, J.T. (2000) *Methanomicrococcus blatticola* gen. nov., sp. nov., a methanol- and methylamine-reducing methanogen from the hindgut of the cockroach *Periplaneta americana*. *Int J Syst Evol Microbiol* **50 Pt 6**: 1989-1999.

Spring, S., Scheuner, C., Lapidus, A., Lucas, S., Glavina Del Rio, T., Tice, H. et al. (2010) The genome sequence of *Methanohalophilus mahii* SLP(T) reveals differences in the energy metabolism among members of the Methanosarcinaceae inhabiting freshwater and saline environments. *Archaea* **2010**: 690737.

Starai, V.J., and Escalante-Semerena, J.C. (2004) Identification of the protein acetyltransferase (Pat) enzyme that acetylates acetyl-CoA synthetase in *Salmonella enterica*. *J Mol Biol* **340**: 1005-1012.

Stewart, J.A., Chadwick, V.S., and Murray, A. (2006) Carriage, quantification, and predominance of methanogens and sulfate-reducing bacteria in faecal samples. *Lett Appl Microbiol* **43**: 58-63.

Tajima, K., Nagamine, T., Matsui, H., Nakamura, M., and Aminov, R.I. (2001) Phylogenetic analysis of archaeal 16S rRNA libraries from the rumen suggests the existence of a novel group of archaea not associated with known methanogens. *FEMS Microbiol Lett* **200**: 67-72.

Tang, W.H.W., Wang, Z.E., Levison, B.S., Koeth, R.A., Britt, E.B., Fu, X.M. et al. (2013) Intestinal microbial metabolism of Phosphatidylcholine and Cardiovascular Risk. *N Engl J Med* **368**: 1575-1584.

Taylor, C.D., Mcbride, B.C., Wolfe, R.S., and Bryant, M.P. (1974) Coenzyme M, essential for growth of a rumen strain of *Methanobacterium ruminantium*. *J Bacteriol* **120**: 974-975.

Teh, Y.L., and Zinder, S. (1992) Acetyl-coenzymeA synthetase in the thermophilic, acetate utilizing methanogen *Methanothrix* sp strain CALS-1. *FEMS Microbiol Lett* **98**: 1-8.

Tersteegen, A., Linder, D., Thauer, R.K., and Hedderich, R. (1997) Structures and functions of four anabolic 2-oxoacid oxidoreductases in *Methanobacterium thermoautotrophicum*. *Eur J Biochem* **244**: 862-868.

Thauer, R.K., Kaster, A.K., Seedorf, H., Buckel, W., and Hedderich, R. (2008) Methanogenic archaea: ecologically relevant differences in energy conservation. *Nat Rev Microbiol* **6**: 579-591.

Tietze, M., Beuchle, A., Lamla, I., Orth, N., Dehler, M., Greiner, G., and Beifuss, U. (2003) Redox potentials of methanophenazine and CoB-S-S-CoM, factors involved in electron transport in methanogenic archaea. *Chembiochem* **4**: 333-335.

Tindall, B.J. (2014) The genus name *Methanothrix* Huser et al. 1983 and the species combination *Methanothrix soehngenii* Huser et al. 1983 do not contravene Rule 31a and are not to be considered as rejected names, the genus name *Methanosaeta* Patel and Sprott 1990 refers to the same taxon as *Methanothrix soehngenii* Huser et al. 1983 and the species combination *Methanothrix thermophila* Kamagata et al. 1992 is rejected: Supplementary information to Opinion 75. *Int J Syst Evol Microbiol* **64**: 3597-3598.

Tjaden, B., Plagens, A., Dorr, C., Siebers, B., and Hensel, R. (2006) Phosphoenolpyruvate synthetase and pyruvate, phosphate dikinase of *Thermoproteus tenax*: key pieces in the puzzle of archaeal carbohydrate metabolism. *Mol Microbiol* **60**: 287-298.

Tono, H., and Kornberg, A. (1967) Biochemical studies of bacterial sporulation. 3. Inorganic pyrophosphatase of vegetative cells and spores of *Bacillus subtilis*. *J Biol Chem* **242**: 2375-2382.

Tuominen, H., Salminen, A., Oksanen, E., Jamsen, J., Heikkila, O., Lehtio, L. et al. (2010) Crystal structures of the CBS and DRTGG domains of the regulatory region of *Clostridium perfringens* pyrophosphatase complexed with the inhibitor, AMP, and activator, diadenosine tetraphosphate. *J Mol Biol* **398**: 400-413.

Turnbaugh, P.J., Ley, R.E., Hamady, M., Fraser-Liggett, C.M., Knight, R., and Gordon, J.I. (2007) The human microbiome project. *Nature* **449**: 804-810.

van der Oost, J., Schut, G., Kengen, S.W.M., Hagen, W.R., Thomm, M., and de Vos, W.M.

(1998) The ferredoxin-dependent conversion of glyceraldehyde-3-phosphate in the hyperthermophilic archaeon *Pyrococcus furiosus* represents a novel site of glycolytic regulation. *J Biol Chem* **273**: 28149-28154.

Veit, K., Ehlers, C., Ehrenreich, A., Salmon, K., Hovey, R., Gunsalus, R.P. et al. (2006) Global transcriptional analysis of *Methanosarcina mazei* strain Gö1 under different nitrogen availabilities. *Mol Genet Genomics* **276**: 41-55.

Wächtershäuser, G. (1988) Before enzymes and templates: theory of surface metabolism. *Microbiol Rev* **52**: 452-484.

Wang, M., Tomb, J.F., and Ferry, J.G. (2011a) Electron transport in acetate-grown *Methanosarcina acetivorans*. *BMC Microbiol* **11**: 165.

Wang, Z.N., Klipfell, E., Bennett, B.J., Koeth, R., Levison, B.S., Dugar, B. et al. (2011b) Gut flora metabolism of phosphatidylcholine promotes cardiovascular disease. *Nature* **472**: 57-U82.

Welte, C., and Deppenmeier, U. (2011a) Re-evaluation of the function of the F_{420} dehydrogenase in electron transport of *Methanosarcina mazei*. *FEBS J* **278**: 1277-1287.

Welte, C., and Deppenmeier, U. (2011b) Membrane-bound electron transport in *Methanosaeta thermophila*. *J Bacteriol* **193**: 2868-2870.

Welte, C., and Deppenmeier, U. (2011c) Proton translocation in methanogens. *Methods Enzymol* **494**: 257-280.

Welte, C., and Deppenmeier, U. (2014) Bioenergetics and anaerobic respiratory chains of aceticlastic methanogens. *Biochim Biophys Acta* **1837**: 1130-1147.

Welte, C., Krätzer, C., and Deppenmeier, U. (2010a) Involvement of Ech hydrogenase in energy conservation of *Methanosarcina mazei*. *FEBS J* **277**: 3396-3403.

Welte, C., Kallnik, V., Grapp, M., Bender, G., Ragsdale, S., and Deppenmeier, U. (2010b) Function of Ech hydrogenase in ferredoxin-dependent, membrane-bound electron transport

in *Methanosarcina mazei*. *J Bacteriol* **192**: 674-678.

Whitman, W.B., Coleman, D.C., and Wiebe, W.J. (1998) Prokaryotes: the unseen majority. *Proc Natl Acad Sci U S A* **95**: 6578-6583.

Wright, A.D., Auckland, C.H., and Lynn, D.H. (2007) Molecular diversity of methanogens in feedlot cattle from Ontario and Prince Edward Island, Canada. *Appl Environ Microbiol* **73**: 4206-4210.

Wright, A.D., Williams, A.J., Winder, B., Christophersen, C.T., Rodgers, S.L., and Smith, K.D. (2004) Molecular diversity of rumen methanogens from sheep in Western Australia. *Appl Environ Microbiol* **70**: 1263-1270.

Wu, G.D., Chen, J., Hoffmann, C., Bittinger, K., Chen, Y.Y., Keilbaugh, S.A. et al. (2011) Linking long-term dietary patterns with gut microbial enterotypes. *Science* **334**: 105-108.

Yamamoto, Y., Aiba, H., Baba, T., Hayashi, K., Inada, T., Isono, K. et al. (1997) Construction of a contiguous 874-kb sequence of the *Escherichia coli* -K12 genome corresponding to 50.0-68.8 min on the linkage map and analysis of its sequence features. *DNA Res* **4**: 91-113.

Young, T.W., Kuhn, N.J., Wadeson, A., Ward, S., Burges, D., and Cooke, G.D. (1998) *Bacillus subtilis* ORF *yybQ* encodes a manganese-dependent inorganic pyrophosphatase with distinctive properties: the first of a new class of soluble pyrophosphatase? *Microbiology* **144 (Pt 9)**: 2563-2571.

Zhu, J., Zheng, H., Ai, G., Zhang, G., Liu, D., Liu, X., and Dong, X. (2012) The genome characteristics and predicted function of methyl-group oxidation pathway in the obligate aceticlastic methanogens, *Methanosaeta* spp. *PLoS One* **7**: e36756.